DEVELOPMENT OF A TIME EFFICIENT METHOD FOR THE DETERMINATION OF ^{210}Pb, ^{210}Bi AND ^{210}Po ACTIVITIES IN SEAWATER BY LIQUID SCINTILLATION SPECTROMETRY.

Colin David Biggin

Scottish Universities Research and Reactor Centre

Presented as a thesis for the degree of
Doctor of Philosophy
in the University of Glasgow

September 2001

Table of contents

List of Tables

List of Figures

Acknowledgements

I would firstly like to thank my supervisors Dr Gordon Cook and Dr Jackie Pates for their support throughout the course of this research. I also wish to thank Chuck Passo and the Packard Instrument Company for their support in this project. Formally, I thank both NERC and Packard Instrument Company for financial support of this project.

The staff at SURRC have also been a great help in this project. Special thanks to Gus MacKenzie, Bob Anderson, Phil Naysmith, Alison Stewart and Caroline Donnelly who were a constant source of information and jokes. I also wish to thank Ernie Bennet and the crew of the Seascan for their help in sampling the Irish Sea.

Many thanks to Jock Thomson, Chuck Passo (and family) and the staff at Packard Instrument Company for their assistance and making me most welcome on my visit to the US.

I also wish to thank the students at SURRC for a making the whole experience a bit more bearable. Special thanks to Louise Brown and Elaine Higney for providing a constant source of amusement! Thanks to my family for their constant support throughout my studies and to my friends for putting up with my moaning (and shandy drinking) over the last 12 months.

Finally, a special thanks to Caroline Donnelly who put the field into field work!

Declaration

Except where specific reference is made to other sources, the work presented in this thesis is the original work of the author. It has not been submitted, in part or in whole, for any other degree

Colin David Biggin

Abstract

A time efficient method has been developed for the determination of the natural decay series radionuclides, ^{210}Pb, ^{210}Bi and ^{210}Po in dissolved and particle associated phases of the marine water column. The disequilibria between parent-daughter pairs of natural decay series radionuclides can provide information on the rates of particle scavenging in the marine environment. The rates of removal of particle reactive radionuclides can be used, by analogy, to determine the rates of removal of particle reactive pollutants in the marine environment.

The method utilises state of the art liquid scintillation spectrometry to directly determine ^{210}Pb. Traditional methods rely on the ingrowth of ^{210}Bi ($t_{½}$ 5.013 days) or ^{210}Po ($t_{½}$ = 138.378 d) to determine Pb indirectly. The direct determination of ^{210}Pb allows the whole procedure to be carried out in under 10 days, a significant time saving on the traditional methods.

Various techniques for the pre-concentration and purification were investigated during this research. Much of the difficulty in the method development was as a result of trying to obtain a suitable matrix for liquid scintillation spectrometry. The pre-concentration stage was carried out using $Fe(OH)_3$ to scavenge the dissolved metals from solution but the variation in recoveries required yield tracers to be applied. ^{212}Pb ($t_{½}$ = 10.6 hours) was utilised as a tracer for ^{210}Pb and ^{207}Bi was used as a tracer for ^{210}Bi. Liquid scintillation

spectrometry was used to determine ^{210}Pb and ^{210}Bi activities. However the requirement of ^{208}Po as a tracer for ^{210}Po meant that ^{210}Po determination had to be carried out using α spectrometry as liquid scintillation spectrometry could not resolve the α peaks of ^{208}Po and ^{210}Po to a sufficient degree.

With these problems overcome, the method was applied to a study of nearshore scavenging processes in the Irish Sea. The results obtained from this study were similar to other reported values of ^{210}Pb and ^{210}Po in the nearshore environment. Modelling of the data using a steady-state box model which accounted for atmospheric ^{210}Po inputs allowed dissolved residence times to be determined.

The method has the potential for future development to allow ^{234}Th and ^{238}U to be determined in the same sample which would allow rates of processes occurring on a range of timescales to be measured. However, the sample size should be increased for future applications to allow greater sensitivity due to the very low activities of ^{210}Pb, ^{210}Bi and ^{210}Po present in the nearshore marine environment.

Glossary of Abbreviations

AAS	atomic absorption spectrometry
ADC	analogue to digital converter
APDC-MIBK	ammonium pyrrolidine dithiocarbamate - methyl isobutyl ketone
BBL	benthic boundary layer
BBOT	2,5-bis-2-(tert-Butylbenzoxazoly)-Thiophene
BCC	burst count circuitry
bis-MSB	p-bis-(o-methylstyryl)-benzene
BGO	bismuth germanate oxide
butyl-PBD	2(4'-tert-Butylphenyl)-5-(4"-Biphenyl)-1,3,4-Oxadiazole)
DBB	delay before burst
DIN	di-isopropylnapthalene
DIPE	di-isopropyl ether
DOC	dissolved organic carbon
DVB	divinylbenzene
FWHM	full width half maximum
GPC	gas proportional counting
H#	Horrocks number
HPGe	high purity germanium
ICP-AES	inductively coupled plasma-atomic emission spectrometry
ICP-MS	inductively coupled plasma-mass spectrometry
K_d	distribution coefficient

LLCM	low level count mode
LLD	lower limit of detection
LSS	liquid scintillation spectrometry
MCA	multi channel analyser
MDA	minimum detectable activity
MOR	mid ocean ridge
NCM	normal count mode
NDS	natural decay series
PBBO	2-(4'-biphenylyl)-6-phenylbenzoxazole
PDA	pulse decay analysis
PDD	pulse decay discriminator
PERALS	photon/electron rejecting alpha liquid scintillation
PIPS	passivated ion implanted planer silicon
PMT	photo multiplier tube
POPOP	1,4-bis-2(5-phenyloxazolyl)-benzene
PPO	2,5-diphenyl oxazole
PSA	pulse shape analysis
PSD	pulse shape discrimination
PXE	phenylxylyethane
QIP	quench indicator parameter
RPH	relative pulse height
SCR	sample channels ratio

SML	surface mixed layer
SPQ(E)	sample quench parameter (external)
SURRC	Scottish Universities Research and Reactor Centre
TOPO	trioctyl phosphine oxide
TR-LSC	time resolved liquid scintillation counting
tSIE	transformed spectral index of the external standard
UG-LLT	Ultima Gold-Low Level Tritium

Chapter One: Introduction

This research was concerned with the development of a novel and time efficient method for the determination of ^{210}Pb, ^{210}Bi and ^{210}Po in the marine system by way of state of the art liquid scintillation spectrometry. In this section, the concept of natural decay series geochemistry and disequilibrium will be discussed. After a brief explanation of the processes of radioactive decay, the remainder of the introduction will discuss the principles of liquid scintillation spectrometry.

1.1 Natural Decay Series radionuclides

The largest ionizing radiation dose to the human population is not from nuclear power generation but instead from natural radionuclides, which have both cosmogenic and primordial sources (BEIR, 1990). They have been present on this planet since its creation but their existence was unknown until the late 19th century. The first detection of radioactivity was in 1896 when Henri Bequerel discovered that potassium uranyl salts would cause a darkening of photographic plates without their exposure to light (Senior, 1998). Marie and Pierre Curie furthered the work of Bequerel using pitchblende and found more intense radiation from another, yet unknown source. Exhaustive chemical separations isolated the new active substance in the bismuth fraction, which was named polonium in honour of Marie Curie's homeland (Vladimirova, 1998). Further work led to the discovery of radium by the Curies. Meanwhile, the field of radiochemistry was expanding and in 1908 Rutherford and Soddy characterized the three forms of radiation (alpha, beta and gamma). By now, the initial discovery by Bequerel was changing the world of chemistry forever and

its effect on mankind was permanent.

There are three categories of naturally occurring radionuclides: (i) primordial nuclides which have been present since the formation of the Earth; (ii) the daughters of these primordial nuclides; and (iii) cosmogenic nuclides such as ^{14}C, ^{3}H and ^{7}Be, which are formed by reactions in the atmosphere and the earth surface, induced by bombardment from cosmic rays from space. Natural Decay Series (NDS) radionuclides include both primordial nuclides and their progeny and belong to one of the three NDS that begin with ^{238}U (4n + 2 series), ^{235}U (4n + 3 series) or ^{232}Th (4n + 0 series). The end members of all three NDS is a stable Pb isotope, with ^{206}Pb, ^{207}Pb and ^{208}Pb being the end members for the ^{238}U, ^{235}U and ^{232}Th chains, respectively (Fig. 1.1). Another series that was once present on the Earth is the ^{237}Np (neptunium series). However, the half life of ^{237}Np is relatively short (2.14×10^{6} y) (Lederer and Shirley, 1978) compared to the age of the Earth, and it has decayed away completely (although members of its chain can be produced artificially).

U is primarily found in pitchblende (U_3O_8), a black uranium oxide found in hydrothermal veins or as carnotite ($K(UO_2)_2(VO_4)_2.3H_2O$), a complex hydrated oxide found as encrustations in sedimentary rocks (Plummer and McGeary, 1991). U can also be found in association with organic phosphorite deposits of marine origin. The principal economic sources of U are pitchblende and uraninite (UO_2). The most important economic source of thorium is monazite (ThO_2), as it frequently occurs as a placer deposit in detrital sands and is therefore easier and cheaper to extract (Jensen and Bateman, 1979).

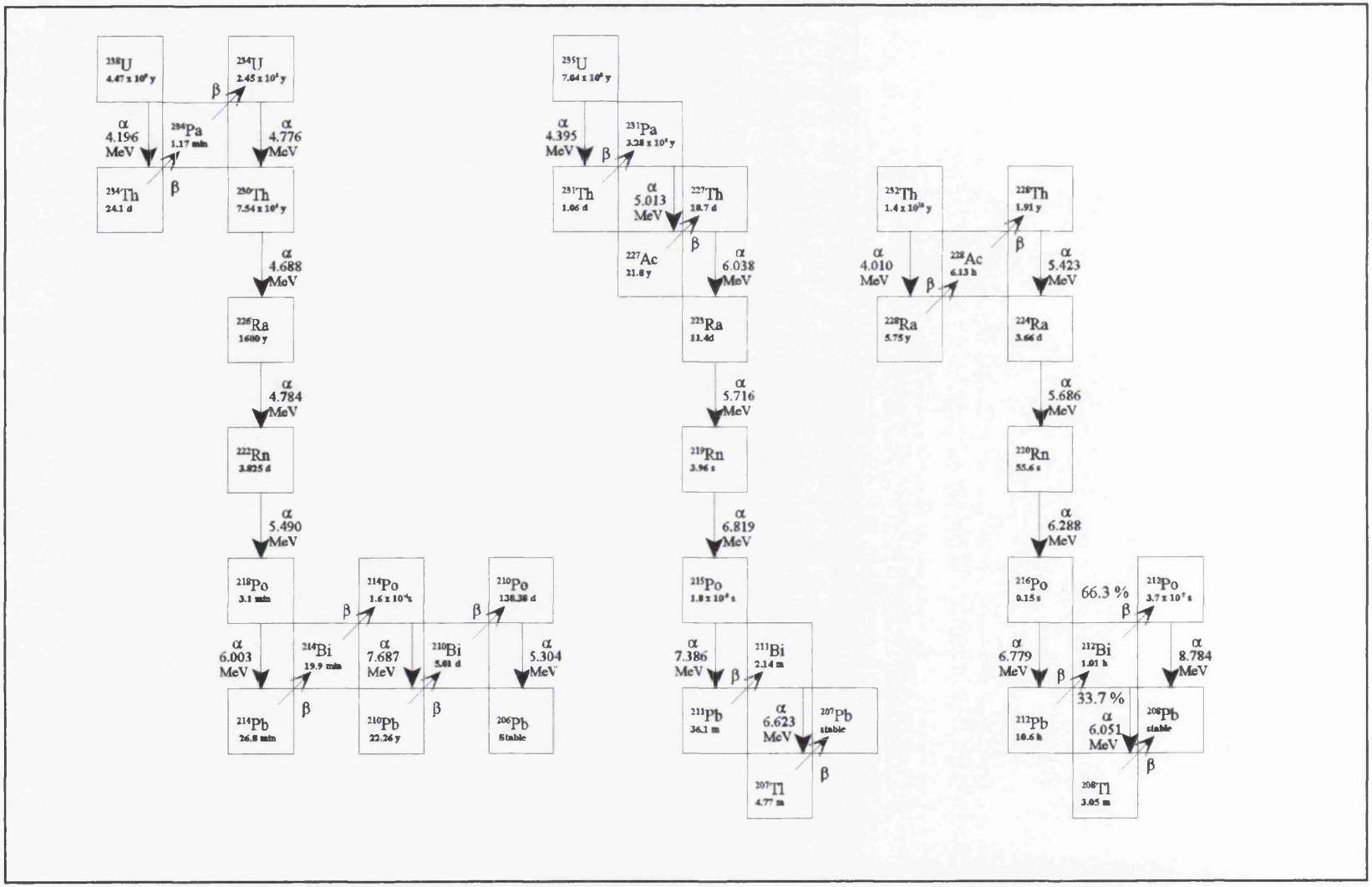

Figure 1.1: ^{238}U, ^{235}U and ^{232}Th decay series.

The ratio of Th:U in igneous rocks is generally 3.5 to 1, and this ratio holds for many igneous rock types due to the lack of fractionation during magmatic processes (Gascoyne, 1992). However, the differences in physio-chemical properties between NDS nuclides results in major differences in their behaviour in the environment, including their mobilisation, transport, deposition and burial. This may create fractionation or disequilibrium between the parent-daughter pairs. The daughter can be more, or less, soluble than its parent and this can lead to a state of radioactive disequilibrium between the parent and daughter radionuclides.

1.1.1 ^{238}U Natural Decay Series radionuclides

Before discussing marine disequilibrium it is first important to understand the equilibrium situation. A closed system in which a parent nuclide decays (A), producing a daughter nuclide (B) which itself is decaying, can be expressed as:

$$A \xrightarrow{\lambda_A} B \xrightarrow{\lambda_B} C$$

where λ_A and λ_B represent the decay constants of nuclides A and B respectively.

The rate of change of the number of atoms of the parent is given by equation 1.1:

$$-\frac{dN_A}{dt} = \lambda_A N_A \qquad (1.1)$$

where N_A is the number of atoms of nuclide A, and t is time.

The daughter product (B) is being formed from the decay of the parent (A), at a rate given by equation 1.2:

$$\frac{dN_B}{dt} = \lambda_A N_A \qquad (1.2)$$

However, the daughter is also decaying according to its half life (equation 1.3):

$$-\frac{dN_B}{dt} = \lambda_B N_B \qquad (1.3)$$

Therefore, the net change in the number of atoms of nuclide B is the sum of its rate of formation from the decay of nuclide A and the rate of decay of nuclide B (equation 1.4):

$$\frac{dN_B}{dt} = \lambda_A N_A - \lambda_B N_B \qquad (1.4)$$

If amount of nuclide A present at time = 0 is known, (N_A^0) it is possible to determine the amount remaining after time t from equation 1.5:

$$N_A^t = N_A^0 e^{-\lambda_A t} \qquad (1.5)$$

If equation 1.5 is then substituted into equation 1.4 then:

$$\frac{dN_B}{dt} = \lambda_A (N_A^0 e^{-\lambda_A t}) - \lambda_B N_B \qquad (1.6)$$

Equation 1.6 can be integrated and expressed as the number of atoms of nuclide B, allowing the number of atoms of the daughter to be calculated at any time (t):

$$N_B = \left(\frac{\lambda_A}{\lambda_B - \lambda_A}\right) . N_A^0 (e^{-\lambda_A t} - e^{-\lambda_B t}) + N_B^0 e^{-\lambda_B t} \qquad (1.7)$$

The activity of nuclide B can then be derived from:

$$A_B = N_B.\lambda_B \qquad (1.8)$$

If the half life of the parent nuclide is significantly greater than the half life of the daughter nuclide then secular equilibrium can be established. The difference in half life between parent-daughter nuclides required for secular equilibrium can be written as (equation 1.9):

$$\frac{\lambda_A}{\lambda_B} \leq 10^{-4} \qquad (1.9)$$

In this instance, the decay of the parent is insignificant compared to the ingrowth of the daughter. Thus λ_A is small relative to λ_B and $e^{-\lambda(A)t}$ tends to 1. If the parent and daughter are chemically separated then, at t = 0, $N^o_B = 0$. Thus equation 1.7 can be re-written as (equation 1.10):

$$N_B = \frac{\lambda_A N_A^0}{\lambda_B} (1\text{-}e^{-\lambda_B t}) \qquad (1.10)$$

When t becomes sufficiently large then equation 1.7 can be converted from number of atoms (N) to activity (A) and be simplified to:

$$\frac{A_A}{A_B} = 1 \qquad (1.11)$$

This condition is called secular equilibrium.

Another equilibrium situation arises if the parent is longer lived than the daughter but the requirements of equation 1.9 are not fulfilled. This is known as transient equilibrium and when t becomes sufficiently large, $N^{o}_{d}e^{-\lambda(B)t}$ tends to zero and $e^{-\lambda(B)t}$ becomes negligible relative to $e^{-\lambda(A)t}$ which tends to 1. This allows equation 1.7 to be expressed as a ratio of activity as shown in equation 1.12:

$$\frac{A_A}{A_B} = \frac{(\lambda_B - \lambda_A)}{\lambda_B} \qquad (1.12)$$

This work will focus on NDS radionuclides from the ^{238}U decay chain in the marine environment. It is possible to separate the nuclides of the uranium series into two distinct groups, namely those which remain dissolved in oxic aqueous solutions (U and Ra), and those which bind to particles (Th, Pa, Pb, Bi and Po). The exception is ^{222}Rn, an unreactive noble gas. The different solubilities of NDS radionuclides in the marine environment can create a state of radioactive disequilibrium between NDS radionuclides. This is due to preferential uptake onto sinking particles by the more particle reactive nuclides. The ratio of the specific activities of the nuclides is often termed the activity ratio. If the nuclides are in radioactive equilibrium the activity ratio will be unity. If the daughter is preferentially removed the activity ratio will be less than one and the activity ratio can be used to determine the extent of the removal of the particle reactive nuclide.

The degree of disequilibrium observed in the water column can provide information on rates of uptake onto particles and subsequent removal from the water column by settling of

particle associated radionuclides to the underlying sediments. Therefore, by analogy, corresponding information can be derived for particle reactive contaminant metals in the water column.

NDS radionuclides, especially those in the ^{238}U decay chain, have been widely employed as tracers of the rates and mechanisms of many marine processes and offer several major advantages over directly studying these process because: (a) radioactive decay allows rates of processes to be derived as the nuclide utilised will decay according to its specific half life; (b) decay of the parent nuclide allows the input of the daughter to be defined which allows inputs and outputs to the system to be included in models; and (c) radionuclides are relatively easy to measure at very low concentrations and can be easier to measure than the processes under investigation (Wu and Boyle, 1997).

Several parent-daughter pairs within the ^{238}U natural decay series have been employed successfully in the study of marine processes. These include: (a) $^{234}Th/^{238}U$ to estimate particle fluxes and reworking at the deep sea floor (Aller and De Master,1984; Murray *et al.*, 1996) and euphotic zone production (Coale and Bruland, 1985; Dunne *et al.*, 1997); (b) $^{230}Th/^{234}U$ to estimate sediment fluxes (Bacon and Anderson, 1982; Thomson *et al.*, 1993a); (c) $^{226}Ra/^{230}Th$ to study seawater circulation patterns and rates (Cochran and Krishnaswami, 1980); (d) $^{210}Pb/^{234}Th$ to determine the importance of lateral advection in the nearshore environment (DeMaster *et al.*, 1986); and (e) $^{210}Po/^{210}Pb$ to estimate biological productivity and nutrient cycling (Tanaka *et al.*, 1983; Smith and Ellis, 1995; Swarzenski *et al.*, 1999;

Sarin *et al.*, 1992, 1994, 1999), as tracers of particle scavenging processes (Bacon *et al.*, 1976, 1988; Chung and Craig, 1983; Cochran, 1983; Zuo and Eisma, 1993) and tracers of particle transport on the continental shelf and slope (Radakovitch *et al.*, 1998; Radakovitch *et al.*, 1999; Stavrakakis *et al.*, 2000).

The important factor in choosing parent-daughter pairs is the half life of the daughter nuclide which determines the time-scales of processes that can be measured. NDS parent-daughter pairs are useful for measuring rates of process on the time-scale of four to five times the daughters half life. For example, $^{210}Pb/^{226}Ra$ disequilibrium provides information on 100 year time-scale processes (Craig *et al.*, 1973) while $^{210}Po/^{210}Pb$ is applied to short time-scale (1 to 2 years) processes (Smoak *et al.*, 1996).

1.1.2 Introduction of ^{210}Pb and progeny to the marine system

Before the dynamics of ^{210}Pb, ^{210}Bi and ^{210}Po in the water column are discussed it is important to describe how these nuclides are introduced to the water column. The processes which introduce ^{210}Pb and its progeny to the marine system are shown in Figure 1.2 and are described below.

^{222}Rn is produced from decay of its parent, ^{226}Ra, in the geosphere. ^{222}Rn is a gas and can escape to the atmosphere by way of cracks, faults and fissures in the bedrock. Decay of ^{222}Rn in the atmosphere will produce ^{210}Pb, which in turn decays to produce ^{210}Bi and ^{210}Po.

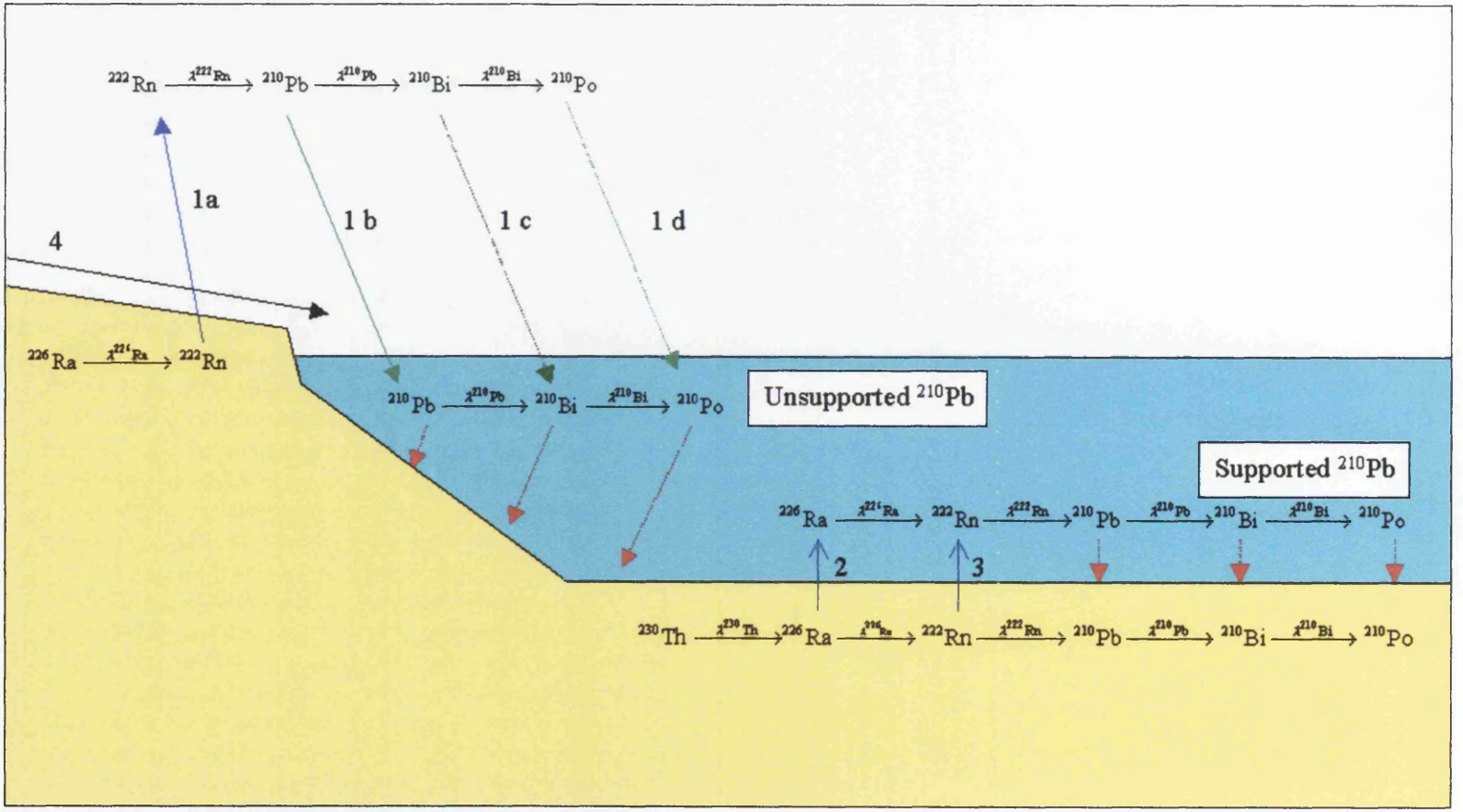

Figure 1.2: Inputs and removal processes of ^{210}Pb and progeny to and from the marine water column.

The residence time of ^{210}Pb in the atmosphere varies from a few days to around one month (Francis *et al.*, 1970). Therefore the activity of ^{210}Bi and ^{210}Po in the atmosphere is directly related to the atmospheric residence time of ^{210}Pb. Removal of ^{210}Pb from the atmosphere (Fig. 1.2: Input 1b) can occur through both wet and dry deposition. If sufficient time has elapsed for ^{210}Bi and ^{210}Po to be produced in the atmosphere the same processes (Fig. 1.2: Inputs 1c and 1d) can remove them. These inputs provide fluxes of unsupported ^{210}Pb to the surface oceans. The term unsupported describes a situation where the daughter nuclide has been separated from its parent and is decaying according to its own half life without being produced by its parent. The main input of ^{210}Po to the oceans is from in-situ production from ^{210}Pb. The inputs of ^{210}Bi may be from either atmospheric deposition or in-situ production in the water column. The short half life of ^{210}Bi (5.013 days) allows it to gain equilibrium rapidly with its parent.

NDS nuclides found within the oceanic sediment can also introduce NDS daughter products to the ocean. Decay of ^{230}Th in the sediments will produce ^{226}Ra which can enter into solution in the sediment interstitial waters and undergo diffusive movement in response to concentration gradients (Moore, 1981) (Fig. 1.2: Input 2). This introduces supported ^{222}Rn and progeny to the water column. Another input of ^{222}Rn to the water column is gaseous diffusion from the sediments, hence introducing a further source of ^{210}Pb and progeny (Fig. 1.2: Input 3).

A further input of NDS nuclides to the marine system is from dissolved U and Ra in river

water (Input 4). Direct inputs of ^{210}Pb from river systems to the oceans are thought to be considerably less than the atmospherically supplied ^{210}Pb (Benninger, 1978; Cochran, 1992; Bacon *et al.*, 1988). Although, in certain nearshore locations, lithogenic material introduced to the marine water column via rivers may be an important source (Carvalho *et al.*, 1997; Radakovich *et al.*, 1999).

1.1.3 Removal of NDS radionuclides from the marine system

The two main processes for the removal of NDS nuclides from the marine system are settling of particle-bound radionuclides to the underlying sediment and radioactive decay. Each nuclide has its dominant removal process depending on its geochemical behaviour. Conservative nuclides (U and Ra) remain in the dissolved phase in oxic marine conditions and their removal is due to radioactive decay or their re-distribution due to physical oceanographic processes such as vertical and lateral water movements (Nozaki *et al.*, 1998).

Non-conservative nuclides may be removed from the marine system by particles in the water column. Particle scavenging of NDS radionuclides describes the removal (or transfer) of an NDS radionuclide from the dissolved phase onto sinking particulate material. Discrimination between particulate and dissolved phases is determined by the pore size of the material used to separate the phases and is therefore a user defined term. 0.45 μm has often been used in studies to define the two phases but recently the importance of microbiological particles in scavenging processes has led to changes in the convention. Niven and Moore (1988) have shown the importance of colloidal particles in Th uptake. By using smaller pore size filter

papers (0.22 μm), smaller particles can be retained and this allows improved resolution between dissolved and particulate phases, although colloids and marine bacteria will still pass through this pore size.

1.1.3.1 Prediction of geochemical behaviour in the marine system

The behaviour of many elements in the aquatic environments can be predicted using Goldschmidt's concept of ionic potential. The ionic potential is the ratio of the charge of an ion to its radius (equation 1.13) and can be used to predict the partitioning of ions between solid and aqueous phases.

$$\text{Ionic Potential } (pm^{-1}) = \frac{\text{charge on ion}}{\text{ionic radius (pm)}} \qquad (1.13)$$

The size and charge of an ion in an aqueous system will influence its interaction with water molecules and hence its stability in the aqueous phase. It also predicts that different ions which have similar size and charge will show similar geochemical behaviour in aqueous media. Cations with low ionic potentials (< 0.025 pm^{-1}) will attract water molecules around them with the formation of a hydration sphere and therefore give the ion soluble behaviour. As the ionic potential increases, there is an increase in the repulsion between the hydrogen ions of the water molecules and the cation, resulting in the expulsion of an H+ ion from the water molecule and subsequent precipitation of an insoluble hydroxide (if sufficient concentration is present) in the process of hydrolysis. At ionic potentials greater than 0.056 pm^{-1}, two H+ ions may be lost from water molecules interacting with the cation, resulting

in the formation of a stable complex ion that is generally quite soluble.

The solubility of an ion is not based solely on its ionic potential. Other factors such as pH, Eh, salinity, microorganisms and certain ligands will also affect solubility, but the use of ionic potential does offer a useful method for the prediction of solubility of ions in solution (Table 1.1). The solubility characteristics of Bi^{3+} and Po^{4+} fit the pattern observed in Table 1.1. That is, they hydrolyse and form particle reactive species which favours their removal onto particles in the marine water column. However, this is not true for Pb^{2+}. On the basis of charge density, Pb^{2+} would be predicted to be soluble (Table 1.1). However, the electron configuration of Pb^{2+} causes it to be involved in covalent bonding due to its filled outer shell (Van Loon and Duffy, 2000), the net result being the particle reactivity of Pb in water (Cotton *et al.*, 1987).

In the marine water column, particle reactive nuclides are those which should exhibit insoluble behaviour, but do not occur in sufficiently large concentrations to precipitate out of solution. Instead, they bind to particles to gain stability (e.g. Th, Pb, Bi and Po). The particle reactive nuclides are found at concentrations substantially below their solubility product and the dominant processes controlling aqueous phase concentrations is uptake on the surface of particles. The particles can be of detrital origin (both organic and inorganic), insoluble hydroxides and oxides, biogenic particles (faecal pellets) and clay minerals (Carpenter *et al.*, 1981). The nuclides can form hydrolyzates, become absorbed into, adsorbed onto, or precipitate onto the surface of the particle; processes which are

	Charge	Ionic radius (pm)	Ionic potential (pm^{-1})
Bi	1+	98	0.0102
Ra	2+	143	0.0140
Pb	2+	120	0.0167
Ac	3+	118	0.0254
Pa	3+	113	0.0265
Bi	3+	96	0.0313
Th	4+	102	0.0392
Pa	4+	98	0.0408
U	4+	97	0.0412
Po	4+	94	0.0426
Pb	4+	84	0.0476
Bi	5+	74	0.0676
U	6+	80	0.0750
Po	6+	67	0.0896

Table 1.1: Ionic potential of NDS radionuclides. The ionic potential (pm^{-1}) is the charge of the ion divided by the ionic radius (pm). The ions in red are predicted to exhibit particle reactive behaviour in water. Cations with a low ionic potential (< 0.025 pm^{-1}) exhibit soluble behaviour. Cations with an ionic potential > 0.056 pm^{-1} are also soluble. Ionic Radii from CRC Handbook of Chemistry and Physics, 69th Edition 1988-89.

collectively termed "scavenging". Also, included in this general term are uptake by microorganisms and scavenging by marine colloids in the water column.

The removal of particle reactive trace metals from the water column is a complex process and specific computer codes have been developed for modelling such systems. The overall process is that the metals are scavenged from the dissolved phase onto particles in the water column which ultimately sink to the sediment surface, which is effectively the final sink for particle reactive contaminants released to the aquatic environment.

1.1.4 Scavenging models

Models have been constructed to calculate removal rates of particle reactive radionuclides in the marine system. The most basic of these models is a simple steady-state box model (Fig. 1.3). This model can be applied to a parent-daughter pair of radionuclides and incorporates first order kinetic terms to account for radioactive decay of the parent and removal, by scavenging, of the daughter. The model assumes the system to be in steady-state (i.e. inputs = outputs) The rate of production of the daughter nuclides is balanced by its rate of removal by radioactive decay and the scavenging component $k\,N_d$, where k = rate constant for removal. The assumptions in this model are that there is no horizontal advection and that the scavenging is irreversible.

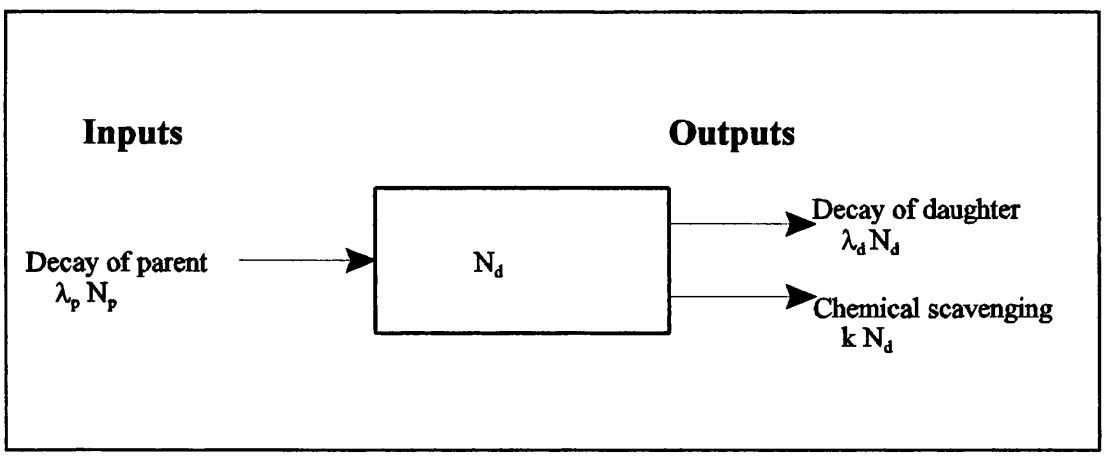

Figure 1.3: The steady-state box model for calculating residence times of particle reactive radionuclides in the water column (after Cochran, 1992). λ = decay constant, N = number of atoms and k = rate constant for removal. Sub-script p and d refer to parent and daughter nuclides respectively

The box model calculation can be written as:

$$\lambda_p N_p = \lambda_d N_d + k N_d \qquad (1.14)$$

where λ represents the radioactive decay constant, N the number of atoms and subscripts p and d refer to parent and daughter nuclides.

The activity (A) can be substituted for N and the equation expressed in terms of k as,

$$k = \lambda_d \left(\frac{A_p}{A_d} - 1 \right) \qquad (1.15)$$

Equation 1.15 allows the first order rate of chemical scavenging to be derived, and, by taking the reciprocal of k, allows the residence time, τ, to be calculated. This model has been applied in surface seawater studies of $^{210}Po/^{210}Pb$ disequilibrium where ^{210}Po is removed by scavenging and particle settling (Nozaki *et al.*, 1997, 1998) and calculating the residence time of ^{210}Pb in the deep oceans (Nozaki and Tsunogai, 1976). However, the model is now known to be oversimplified as the removal of Po onto particles has been shown to be reversible (Thomson and Turekian,1976; Bacon *et al.*, 1976; Sarin *et al.*,1992).

For modelling of ^{210}Pb behaviour in the Surface Mixed Layer (SML) of the oceanic water column it has long been realised that the atmospheric input is the main source of ^{210}Pb (Rama *et al.*, 1961) with only 2 to 4 % of the ^{210}Pb activity being derived from in-situ decay of ^{226}Ra

(Sarin *et al.*, 1992). Therefore, models must take account of this influx of ^{210}Pb to the oceans. Shannon *et al.* (1970) used a simple box model to determine the residence times of ^{210}Po and ^{210}Pb in seawater. They assumed, at steady-state, that the input from the atmosphere and the decay of ^{226}Ra (I) would be balanced by the radioactive decay and the removal by scavenging.

$$\frac{dN_{Pb}}{dt} = 0 = I_{Pb} - \lambda N_{Pb} - kN_{Pb} \qquad (1.16)$$

where I = total input rate from atmosphere and decay of parent

Similarly, for ^{210}Po,

$$\frac{dN_{Po}}{dt} = 0 = I_{Po} - \lambda N_{Po} - kN_{Po} \qquad (1.17)$$

However, the atmospheric input of ^{210}Po is assumed to be smaller (10 % that of ^{210}Pb) due to the relatively short residence time of ^{210}Pb in the atmosphere relative to the time required for ^{210}Po ingrowth.

Assuming that the SML was 100 m deep and that there was no vertical mixing below the SML, Shannon *et al.* (1970) obtained residence times of 5 years and 0.6 years for ^{210}Pb and ^{210}Po respectively. The in-situ production rate of ^{210}Pb from ^{222}Rn was calculated on the basis of ^{222}Rn/^{226}Ra activity ratios to be between 0.4 and 0.8 (Broecker *et al.*, 1967). Nozaki and Tsunogai (1976) used a similar model for calculating residence times of ^{210}Po and ^{210}Pb in the SML, but pointed out that variations in the thickness of the SML and the atmospheric

flux will introduce large uncertainties into the predictions. Bacon *et al.* (1976) carried out extensive $^{210}Po/^{210}Pb$ measurements as part of the GEOSECS programme and examined the activity ratio of $^{210}Po/^{210}Pb$ in both dissolved and particulate matter (using 0.45 μm filters). Previous workers had examined zooplankton $^{210}Po/^{210}Pb$ activity ratios but Turekian *et al.* (1974) showed that these were unreliable as indicators of SML fluxes. By examining the partitioning between particulate and dissolved ^{210}Po and ^{210}Pb, Bacon *et al.* (1976) were able to calculate the residence times of both particle-bound and dissolved ^{210}Po and ^{210}Pb by modelling each component separately. Bacon *et al.* (1976) found the residence time of particulate Po to be shorter than for dissolved Po residence times (0.11 y compared to 0.61 y) and estimates the recycling efficiencies of Pb and Po in the SML to be 5 % and 65 %, respectively. Residence times for dissolved ^{210}Pb in the SML were ~2 y. For ^{210}Po in the deep ocean, the residence time was estimated at 4 y. Reported dissolved ^{210}Pb deep ocean residence times vary from 50 to 200 years but these estimates are strongly affected by other processes such as enhanced scavenging at the sea floor by Fe and Mn and topographic effects such as boundary scavenging (Bacon *et al.*, 1976; Chung and Craig, 1983; Cochran *et al.*, 1983; Nozaki *et al.*, 1997).

The processes responsible for removal of particle reactive species from the water column are more complex than the simple box model suggests. Figure 1.4 is thought to be a more accurate interpretation of the processes involved. This model accounts for a reversible scavenging process in which particle-bound nuclides can be released back into the dissolved phase. Furthermore, it contains a second reversible process in which small particles

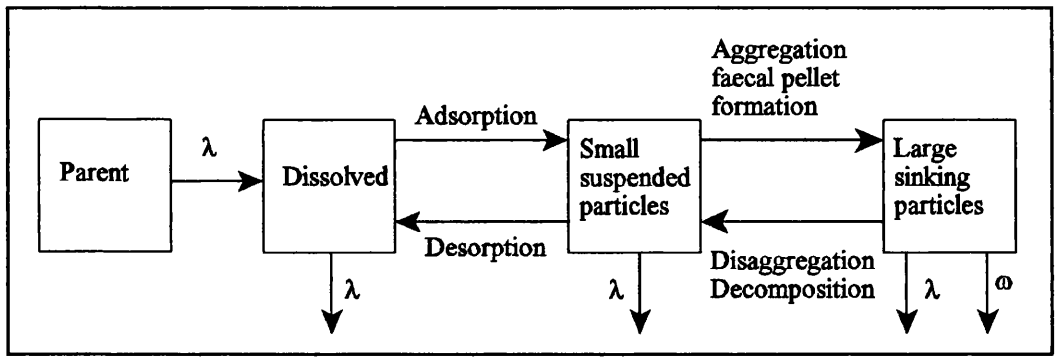

Figure 1.4: Advanced scavenging box model of particle reactive radionuclides in the water column (after Cochran, 1992). λ = radioactive decay constant and ω = sinking velocity of larger particles

aggregate to form larger particles which have a higher sinking velocity than the smaller particles, represented by ω in Figure 1.4. Adsorption and desorption processes allow for the recycling of ^{210}Po observed in the SML. This type of model is rarely applied to ^{210}Po/^{210}Pb disequilibrium as the steady-state box model can account for most of the observed disequilibria.

1.1.5 Distribution of ^{210}Pb and ^{210}Po activities in the surface oceans

^{210}Pb and ^{210}Po are not uniformly distributed in the surface oceans. Their activities are related to primary production, such that areas with high productivity will have lower surface concentrations of both ^{210}Pb and ^{210}Po (Sarin *et al.*, 1999). Nozaki *et al.* (1976) have demonstrated that total (aqueous + particle associated) ^{210}Pb and ^{210}Po concentrations are highest in the oceanic gyres, while their lowest total concentrations are found at the continental margins and equatorial zone where they are more effectively removed from the surface ocean. Nozaki *et al.* (1976) identify six dominant factors controlling the distribution of ^{210}Pb in the surface oceans, with the two most important being (i) the atmospheric flux of

^{210}Pb, and (ii) the ^{210}Pb scavenging efficiency. Thomson and Turekian (1976) examined ^{210}Po and ^{210}Pb in two stations off the coast of Peru. They observed lower ^{210}Po and ^{210}Pb activities but a higher ^{210}Po/^{210}Pb ratio in the upwelling site. They attributed the lower ^{210}Po and ^{210}Pb activities to enhanced scavenging due to increased production in the nutrient rich waters, and the higher ^{210}Po/^{210}Pb ratio to low ^{210}Pb activity water being brought to the surface by the upwelling of the deep ocean waters.

Thus the vertical distribution of ^{210}Po and ^{210}Pb in the water column is not always constant. Differences in the efficiency of particle scavenging between ^{210}Po and ^{210}Pb cause differences in their solid phase/aqueous phase distributions in the water column. For simplicity, the oceans can be split into three vertical sections and, although this is a generalisation of a highly complex system, this distribution has been observed in the Indian, Atlantic and Pacific Oceans (Cochran *et al.*, 1983; Bacon *et al.*, 1976; Nozaki *et al.*, 1976). The topmost layer is termed the surface mixed layer (SML) and varies in thickness from 100 to 500 m. In this layer, ^{210}Pb is found in excess of its parent ^{226}Ra due to the input of unsupported ^{210}Pb from the atmosphere. Dissolved ^{210}Po activities are usually lower than dissolved ^{210}Pb activities due to faster rates of Po scavenging and a larger atmospheric input of ^{210}Pb. Bacon and Elzerman (1980) found that the top 30 μm (micro) layer of the surface ocean was enriched in ^{210}Po and suggested that this may introduce ^{210}Po to the atmosphere as aerosols. Kim *et al.* (2000) observed excess ^{210}Po in the coastal air of Chesapeake and Delware Bay. The excess ^{210}Po is thought to originate from the top 30μm layer of the ocean and the higher ^{210}Po excess was observed at times of high wind speed which suggest gas exchange from the

oceans is responsible.

At the base of the SML, dissolved ^{210}Po activities can exceed those of ^{210}Pb due to dissolution of biogenic particles and subsequent recycling of ^{210}Po. This was observed in the Atlantic and Indian Oceans but not in the Pacific (Bacon *et al.*, 1976; Cochran *et al.*, 1983; Sarin *et al.*, 1992; Nozaki *et al.*, 1997). Generally, particle associated ^{210}Po activities are higher than particle associated ^{210}Pb activities due to higher particle reactivity of Po compared with Pb. The rate of removal of dissolved ^{210}Po is dependent on the level of productivity, with areas of high productivity showing a higher rate of ^{210}Po removal from the SML (Sarin *et al.*, 1999). Residence times for dissolved ^{210}Pb and ^{210}Po in the SML are estimated to be 2 years and 0.61 years respectively while particle bound ^{210}Po has a much shorter residence time of 0.08 years (Bacon *et al.*, 1976).

Below the SML there is a deficiency of ^{210}Pb with respect to ^{226}Ra due to particle scavenging. Bacon *et al.* (1976) observed dissolved ^{210}Po to be deficient relative to dissolved ^{210}Pb by around 12 % below the SML with a corresponding enrichment of particulate ^{210}Po and suggested that the distribution of ^{210}Po and ^{210}Pb between the dissolved and particulate phases is dependent on the particle flux. Sarin *et al.* (1992) observed a similar deficiency of ^{210}Po relative to ^{210}Pb in the Arabian Sea, yet Turekian and Nozaki (1980) found ^{210}Po and ^{210}Pb to be in equilibrium at depth in the Eastern Pacific. This suggests that deep water disequilibrium is dependent on the localised conditions. The deep ocean residence times for ^{210}Pb and ^{210}Po are estimated to be 50 to 200 years and 4 years

respectively (Bacon *et al.*, 1976).

The bottom layer of the ocean is the Benthic Boundary Layer (BBL). Lower observed $^{210}Pb/^{226}Ra$ activity ratios towards the seabed (Craig *et al.*, 1973) indicate that higher rates of particle scavenging occur in this region. This may be due to resuspension of particles from the sea floor or redox cycling of Fe and Mn in the water column. This is especially relevant at ocean margins and Mid Ocean Ridges (MORs) and will be discussed in the context of the nearshore environment (Section 1.1.6). Intensified scavenging of ^{210}Po and ^{210}Pb at the sediment-water interface appears to be ubiquitous throughout the aquatic system in both marine and non-marine environments (Bacon *et al.*, 1976; Chung and Craig, 1983; Cochran *et al.*, 1983; Benoit and Hemmond, 1987).

1.1.6 The nearshore marine environment

^{210}Po and ^{210}Pb provide a powerful tracer capability for establishing information on metal residence times which is of fundamental importance in understanding the biogeochemical cycling of heavy metals and modelling the behaviour of particle reactive pollutants in both marine and terrestrial water bodies.

The nearshore marine environment is of major importance with respect to geochemical cycling of contaminant metals since (a) they are the zones of maximum contaminant input and (b) they are highly active areas, both biologically and geochemically. Most low solubility contaminants are removed from the aqueous phase in these zones, where the dominant

removal process is scavenging by particulate matter, with subsequent removal from the water column by settling of the particles. Characterising the rates of these processes is fundamental in developing an understanding of biogeochemical cycling of particle reactive contaminant metals in the marine environment, however, they are difficult to quantify directly. In this context, NDS radionuclides can be used as tracers of the mechanisms which govern the removal of particle reactive metals from the marine water column.

The rates of particle scavenging of ^{210}Pb are affected by a number of variables, including proximity to land (McCartney *et al.*, 1990), particle concentrations, the concentration of dissolved ^{210}Pb, depth of the water column, upwelling and the presence of Fe/Mn oxyhydroxides (Carpenter *et al.*, 1981).

In the nearshore environment, Pb and Po residence times are shorter than in the surface ocean. Tanaka *et al.* (1983) reported dissolved ^{210}Po and ^{210}Pb residence times of 0.1 to 0.4 years in the nearshore environment. Schell (1977) observed increasing dissolved ^{210}Pb residence times in samples progressively further from the coast. Moving from the Juan de Fuca Strait to a station 5 miles from the coast saw the ^{210}Pb residence time increase from 58 days to 128 days, with a further increase to 163 days at a distance of 12 miles from shore.

Mn and Fe oxyhydroxides are effective scavengers of particle reactive pollutants and this is particularly important in nearshore studies (Kadko *et al.*, 1987). Terrigeneous inputs from rivers can supply significant quantities of Mn and Fe oxyhydroxides to the nearshore

environment (Overnell *et al.*, 1996). Mn and Fe are often major constituents of marine sediments. In oxic conditions, Fe and Mn exist as Fe^{3+} and Mn^{4+} which are insoluble. In reducing conditions, Fe and Mn exist as Fe^{2+} and Mn^{3+} which are soluble. Decomposition of organic matter within the sediments can result in reducing conditions in the sediment. Fe and Mn become soluble and diffuse through the sediment until they reach the oxic zone and form insoluble oxyhydroxides. This creates a redox front in the sediments in which an accumulation of Fe and Mn is observed (Chester, 1990). If suitably reducing conditions exist in the overlying water column, the redox front migrates from the sediment into the water column. Under these conditions particle reactive species are rapidly scavenged as Fe and Mn oxyhydroxides. Spencer *et al.* (1981) suggest that this process plays a key role in ^{210}Pb scavenging at the sediment water interface. This is a well accepted process, observed by many researchers, and although especially relevant to the nearshore environment (Swarzenski *et al.*, 1999), it has also been observed at the sediment-water interface in the deep sea (Nozaki *et al.*, 1997; Wei and Murray, 1994) and in freshwater environments (Benoit and Hemmond, 1987; Talbot and Andren, 1984).

Nearshore sediments show a larger inventory of unsupported ^{210}Pb than would be expected from the atmospheric flux and the dominant source of this excess is thought to be from deep water ^{210}Pb brought into shallower zones of intense scavenging by lateral advection. For example, Smoak *et al.* (1996) estimate that 67 % of the excess ^{210}Pb inventory on the Amazon continental shelf is supplied by this processes. However, by determining ^{210}Pb via ^{210}Po they assume equilibrium between parent and daughter. Thus, their analytical procedure

may be subject to significant error. Lateral advection would appear to act as the transport mechanism responsible for a great deal of the sedimentary excess ^{210}Pb observed in the nearshore environment (Krishnaswami *et al.*, 1975; Carpenter *et al.*, 1981; DeMaster *et al.*, 1986).

Similar studies have also been carried out in lake systems as they also receive atmospherically deposited ^{210}Pb. Benoit and Hemmond (1987) observed scavenging rates of ^{210}Pb to be faster than ^{210}Po in an oligotrophic lake. The dissolved residence time for ^{210}Pb was around 40 days while ^{210}Po dissolved residence time averaged 85 days. They also observed that only half the ^{210}Pb supplied to the lake (through atmospheric deposition and stream input) was lost as stream outflow. Finally, when reducing conditions were prevalent in the bottom waters, they found much higher activities of particulate ^{210}Po and ^{210}Pb in the bottom water suggesting mobilization of these nuclides in response to Fe/Mn redox cycling. Balistrieri *et al.* (1995) observed similar findings in Lake Sammamaish and suggest that sulphur cycling may be important in controlling ^{210}Pb and ^{210}Po distributions in anoxic conditions. Harada *et al.* (1989) found levels of ^{210}Po in Florida ground water reaching activities up to 16 Bq l^{-1} in a sulphide rich aquifer and suggested that the remobilisation of these nuclides may occur through sulphate reducing bacteria destroying the Fe/Mn oxyhydroxide coatings found on particles.

1.1.7 Tracer applications

^{210}Po/^{210}Pb activity ratio measurements have been used to study biological productivity and

boundary scavenging (Nozaki *et al.*, 1976, 1997, 1998; Bacon *et al.*, 1976; Thomson and Turekian 1976; Sarin *et al.*, 1992; Smith and Ellis, 1995). Bacon *et al.* (1988) noted that ^{210}Pb is a key analogue for studying atmospherically delivered contaminant inputs to the ocean and in particular, stable Pb, which is one of the most significant heavy metal contaminants in the environment. Wu and Boyle (1997) utilised ^{210}Pb as a proxy for anthropogenic Pb in the oceans to observe the dynamic response of the oceans to changing Pb sources. McCartney *et al.* (1990) used ^{210}Pb measurements in the Irish Sea to help predict the geochemical behaviour of other particle reactive pollutants (Pu and Am) in the same environment. Benninger (1978) used ^{210}Pb to examine the retention of heavy metals in Long Island Sound. ^{210}Po and ^{210}Pb have been utilised as tracers of particle transfer (Radakovitch *et al.*, 1999; Stavarakakis *et al.*, 2000) and ^{210}Po is though to be linked to sulphur cycling and strong evidence exists for this association (Harada *et al.*, 1989; Wei and Murray, 1994; Balistrieri *et al.*, 1995; Swarzenski *et al.*, 1999). This highlights the application of NDS nuclides as analogues of natural processes. By using NDS radionuclides as tracers of natural processes allows rates of processes derived which could not be derived from simply measuring the contaminant itself. NDS disequilibrium data can allow predictions of behaviour of pollutants introduced to the marine environment, their residence times and fate. The dilute and disperse practises of waste disposal introduces a great deal of waste to the marine system. Particle reactive pollutants and metals are being scavenged rapidly in the nearshore environment and not being dispersed to the deep sea. It is therefore imperative to have a clear understanding of the biogeochemical cycling in the nearshore environment in order to regulate and control the pollution of these highly productive areas.

1.2 Radioactive decay and interaction with matter

Radioactive decay is a spontaneous nuclear transformation involving a transition from one nuclear energy level to another. The difference between these two energy levels is known as the decay energy and the form and time of this decay characterises the transition. The main modes of decay are briefly discussed below.

1.2.1 Radioactive decay

Alpha particles are produced from the radioactive decay of heavy nuclei which have an excess of protons relative to neutrons. α emission is the ejection of two protons and two neutrons bound together in the equivalent of a helium nucleus. α decay occurs in heavier, unstable elements (atomic number > 80) and the emission of an α particle is in an attempt to gain stability.

For example:

$$^{238}_{92}U \rightarrow {}^{234}_{90}Th + {}^{4}_{2}He \qquad (1.18)$$

The helium nucleus has a mass of 4 amu and a +2 charge. The result of α emission of ^{238}U is that the atomic number is reduced by 2 and the mass number by four. The daughter occurs two places to the left hand side of the parent in the periodic table. The α particle is emitted in one or more groups of mono-energetic particles which have energies ranging from 1.8 MeV (^{144}Nd) to 10 MeV (^{262}Ns). The energy of the emitted α particle is characteristic of the radionuclide undergoing decay, therefore permitting identification of the decaying species. Several radioactive decay processes are associated with beta decay: electron emission (β^-),

positron emission (β^+) and electron capture (EC). Only β^- decay will be discussed as β^+ and EC are of less importance in this study. β^- decay occurs in nuclides which have an excess of neutrons relative to protons. In β^- decay a neutron is changed to a proton with the emission of an electron (β^-particle) and an antineutrino.

$$ {}^{1}_{0}n \rightarrow {}^{1}_{1}p + e^{-} + \bar{\nu} \qquad (1.19) $$

For example:

$$ {}^{210}_{83}Bi \rightarrow {}^{210}_{84}Po + e^{-} + \bar{\nu} \qquad (1.20) $$

The energy released by β^- decay is shared randomly between the β^- particle and the antineutrino in varying amounts and, as a result, the beta spectrum covers a wide range of energies up to the maximum energy released for the specific nuclide, which is termed the E_{max}. Thus, β^- energies range from zero to the E_{max}. For ^3H, the E_{max} is 18.6 keV while for ^{210}Bi the E_{max} is 1161 keV. As a result, the ^{210}Bi spectrum covers a much larger energy range than ^3H. Theoretically, the β^- particle can contain all the decay energy (in which case it would be emitting at the E_{max} of that nuclide) or all the energy can be transferred to the antineutrino (thus the beta energy would be zero).

In the strictest sense, the emission of γ photons is not a form of decay. Often, the daughter product from α or β decay is produced in an excited state. The newly formed nucleus can release this excitation energy in the form of a γ photon. γ photons are a form of

electromagnetic radiation with extremely short wavelengths and have energies ranging from 10 keV to 7 MeV. The energy released from γ decay is characteristic of the nuclide undergoing decay (for example ^{210}Pb can be measured by its 46.5 keV γ photon peak). This is because the de-excitation occurs between two defined energy levels, so the released energy is quantised.

In some cases, the nucleus may remain in an excited state for a measurable length of time, (more than one second) before decaying to its ground state by γ-emission. This is known as a meta-stable state or isomer.

For example:

$$^{137}_{55}Cs \rightarrow {}^{137m}_{56}Ba \rightarrow {}^{137}_{56}Ba + \gamma\ (661.7\ keV) \qquad (1.21)$$

where the superscript m indicates a meta-stable state.

The gamma intensity is a measure of the fraction of the total numbers of decays that occur by that particular transition at the specific γ energy. 5.4 % of ^{137}Cs decays to ^{137}Ba by β^- decay (E_{max} = 1173 keV) and 94.6 % of ^{137}Cs decays to ^{137m}Ba by β^- decay (E_{max} = 1176 keV). ^{137m}Ba then decays by γ emission to ^{137}Ba. Five γ-transitions take place between ^{137m}Ba and ^{137}Ba, but approximately 90 % of the γ emissions occur at 661.7 keV.

1.2.2 Interaction of radiation with matter

It is also important to consider the various ways in which α, β^-, and γ radiation interact with

matter. α, β^- and γ radiation all behave differently and it is these different modes of interaction which allow them to be discriminated. The properties of α and β^- particles are shown in Table 1.2. α particles have a larger mass relative to β^- particles, which causes them to travel more slowly than β^- particles. The result of this is that α particles have a higher specific ionization than β^- particles but lose their energy of excitation over a shorter path length.

	Mass (amu)	Charge	Ion pairs per mm of air for a 1 MeV particle	LET in water (keV μm^{-1})	Range in air (cm)
α	4	+2	10^4	^{210}Po 136	^{210}Po 3.6
β^-	0.0005435	-1	10	^{32}P 0.07	^{32}P 770

Table 1.2: Various properties of α and β^- particles highlighting the higher specific ionisation of α particles compared to β^- particles. The LET (linear energy transfer) describes the energy deposited per unit length of track (from Choppin, 1994).

Gamma radiation is high energy electromagnetic radiation. There are three principle ways in which γ radiation interacts with matter, namely the photoelectric effect, Compton scattering and pair production. The probability of each type of interaction is dependent on the energy of the γ photon and the z value of the absorbing material. The photoelectric effect dominates up to 0.02 MeV, Compton scattering predominates between 0.1 MeV and 3 MeV. Pair production has a threshold energy of 1.022 MeV.

1.3 Liquid scintillation spectrometry

The remainder of this section will discuss the theory and workings of liquid scintillation spectrometers. This is the main instrument used in this research from the method development, to the application of the method to study ^{210}Pb, ^{210}Bi and ^{210}Po in the nearshore marine environment. This section will first introduce the fundamentals of liquid scintillation spectrometry (LSS) before discussing some of the background reducing features that allow LSS to measure very low levels of activity. Other considerations for the measurement of low levels of activity include the preparation of the sample, the vial in which the sample is measured and the effects of quench in LSS.

The technique of LSS is based on the observation of Ageno *et al.* (1950) that certain organic liquids emit fluorescent light when excited by radiation. The fluorescence (or photons) emitted by the organic compounds (fluors) from the excitation can be converted to a burst of electrons by photo-multiplier tubes (PMTs) and subsequently measured as an electrical pulse by a LS spectrometer.

1.3.1 The spectrometer

The instrument used to measure these pulses is called a liquid scintillation spectrometer. It is comprised of two diametrically opposed PMTs, each with its own pre-amplifier, a coincidence circuit, a summation circuit, an amplifier, an analog to digital converter (ADC) and a multi-channel analyser (MCA). The basic components of a modern LS spectrometer are shown in Figure 1.5.

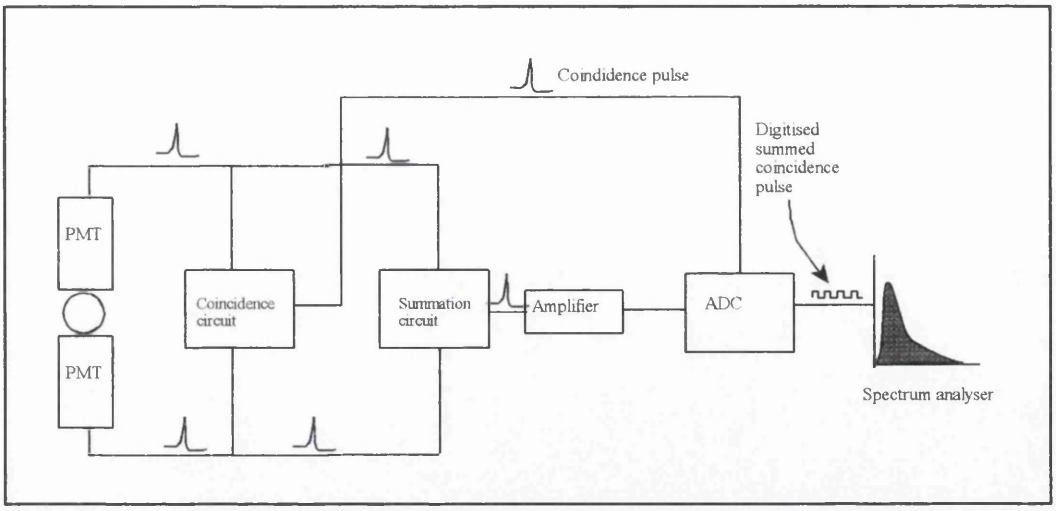

Figure 1.5: Schematic diagram of the principle components of liquid scintillation spectrometers (from Kessler, 1989).

During the scintillation counting process, the sample vial is held in a light-tight enclosure (the detection chamber), and the emitted light is detected by the PMTs which measure the photon intensity. Each PMT is housed in an opaque container and consists of an evacuated glass tube, with a photo-sensitive material at one end, termed the photo-cathode. The photo-cathode in modern PMTs is usually made of K_2CsSb (bi-alkali PMTs) while older photo-cathodes were made of CsSb (Rapkin, 1970). When a photon impinges upon the photo-cathode it produces photo-electrons which pass through the tube by way of a series of dynodes at increasing potential difference. There are usually ten to twelve dynodes in a PMT and these are coated either with a CsSb mixture or a Mg-Ag alloy activated by oxygen or Cs vapour (Gilmore and Hemmingway, 1995). When photo-electrons strike the dynodes they produce secondary electrons which impinge upon the next dynode in the chain. This continues down all twelve dynodes, each multiplying the number of electrons emitted (Fig. 1.6). The net result is an amplification of the original signal received at the photo-cathode (Kessler, 1989).

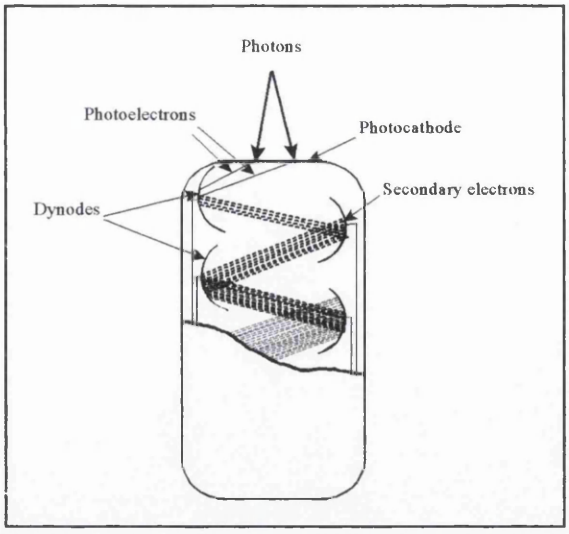

Figure 1.6: Cross section of a photo multiplier tubes used in LSS (after Kessler, 1989).

The amplification is linear, and the avalanche of electrons arriving at the final electrode is, therefore, representative of the original event and the number of photons that impinge upon the photo-cathode (Horrocks, 1974). The emitted photons are now registered as an electronic pulse by the LS spectrometer.

However, even in the absence of light, the PMT will produce random electrical pulses (noise) which must be discriminated against to prevent them being registered as background. To overcome this problem all LS spectrometers contain a coincidence circuit. For a pulse to be registered as a true event it must register in both PMTs within a specified time, usually 18 ns. The coincidence circuit therefore eliminates any pulses that originate within either of the individual PMTs. If the pulse is detected at both PMTs within 18 ns then it is accepted as a true event and is sent to the summation circuit.

The summation circuit is designed to allow for differences in pulse intensity caused by the position at which the pulse originated in the vial. For example, if an event occurred close to the edge of a vial then the response may be greater in one PMT than the other. The application of summation circuitry to LSS has long been standard for several reasons: it sharpens peaks, allowing better separation of α and β^- events and it allows more low energy events to be recorded. ^3H counting efficiency increased from ~ 30 % without summation, to ~ 45 % with summation (Kessler, 1989).

The signal, which has successfully passed through both the coincidence and summation circuitry, is amplified and fed into an ADC and then to a MCA. In instruments built before the 1980s the output of the LS counter was to predefined counting windows (usually three). This had the disadvantage that the operator could not change these counting windows once counting had begun. If changes to the counting windows were required, the sample had to be re-counted. The advent of affordable ADC and MCA technology started the revolution into so called windowless counting. As the amplification of photons by the PMTs is linear, the amplitude of the pulse is representative of the event energy. For example, a β^- particle will produce around 10 photons per keV of energy released into the cocktail, so a 50 keV particle will produce about 500 photons, and a 500 keV particle will produce around 5000 photons. The relationship between pulse height and energy is still retained after digitisation (L'Annunziata and Kessler, 1998).

The digitised pulses are passed to a MCA, which classifies the pulses into discrete energy

units representative of the amplitude of the original pulse. MCAs typically utilise 4000 channels, each representing an energy band 0.5 keV wide over the range 0 - 2000 keV. This can then be displayed visually as a spectrum showing number of counts against energy.

Beckman Instruments and Wallac Oy use logarithmic amplification of the pulse instead of the linear amplification applied in Packard spectrometers, and these spectra are displayed on a basis of channel number rather than energy. Apart from the amplification method, all LS spectrometers have the same basic detection system (Fig. 1.5). It is their additional features which differ between manufacturers, such as background reduction and determination of quench.

1.3.2 The liquid scintillation cocktail

The liquid scintillation cocktail is the matrix in which a radioactive sample is placed for its measurement by LSS. A scintillation cocktail requires several features essential to the mixing of the sample and the production of light from the decay. A conventional cocktail will contain a solvent, surfactants and fluors.

1.3.2.1 The solvent

The role of the primary solvent is to convert the kinetic energy of the radioactive decay into excitation energy. Primary solvents are the initial energy transfer agent, therefore, the correct choice of primary solvent is as crucial as the sample being placed in it. Primary solvents are aromatic hydrocarbons, the de-localised π electrons of which are effective in

converting the energy of the radiation into excitation energy. Solvent excitation can be written as:

$$P + s \rightarrow p + s^* \qquad (1.22)$$

where P and p represents the radioactive particle before and after decay (α, β or γ), s represents the solvent and * denotes an excited solvent molecule.

The properties of the solvent are important in LSS. The magnitude of anode pulses obtained using a single PMT and an external γ source for a range of different solvents allows pulses obtained from different solvents to be compared against each other. The pulse height from toluene is given an arbitrary value of 1, and the pulse heights obtained from other solvents can be compared. This is known as the Relative Pulse Height (RPH). The higher the RPH, the better the solvent. The ideal solvent should have a high RPH, be liquid at room temperature (low melting point), have a low flash point and have a high solubility for the scintillator to ensure maximum light output (Gibbs *et al.*, 1976). The properties of a range of common LS solvents are shown in Table 1.3. In the early days of LSS, toluene and xylene were the main solvents used by analysts and the development of emulsifying cocktails in the 1960s further enhanced their use. Dioxane and p-xylene have high RPHs but their freezing points are ~12 °C and 13-14 °C, respectively, and hence require room temperature counters. In older LS spectrometers, counting at room temperature resulted in higher background count rates than when the counter was temperature controlled. The effect of temperature control on background count rates with modern PMTs is negligible and temperature control is now used to minimise phase separation between the sample and the cocktail. Toluene is

	Relative Pulse Height (RPH)	Melting Point °C	Flash Point ° C	Vapour Pressure mm Hg @ 25°C	Biodegradable?	International Classification
1, 4-Dioxane	0.65	11.8	12	40	No	Flammable
p-Xylene	1.10	12 to 13	30	8	No	Flammable
toluene	1.00	-95	5	28	No	Flammable
benzene	0.85	5.5	-11	-	No	Flammable
pseudocumene	1.12	-60.5	52	2	No	Flammable
phenyl-ortho-xylylethane	1.14	-	150	-	No	Harmless
linear-alkyl benzene	0.91	-	150	0.76	No	Harmless
di-isopropyl naphthalene	1.14	-	148	1	Yes	Harmless

Table 1.3: The chemical and physical properties of common liquid scintillation cocktails. The RPH is a measure of pulse height relative to toluene (=1.0). The melting point signifies the minimum counter temperature (data from: Gibbs *et al.*, 1976; Kessler, 1989; Thomson 1991).

easily obtainable at a reasonable cost and has a low freezing point, but it poses a hazard in the laboratory as its flash point is below room temperature and it is now a suspected carcinogen. In addition, the disposal of toluene based cocktails represents a significant cost component of an analysis. Safety concerns drove analysts to find higher flash point cocktails. In the 1970s pseudocumene was introduced (Nibeck *et al.*, 1980), which has a high energy conversion factor (light produced per unit decay), and fewer safety restrictions. Although it has a higher toxicity than toluene, its higher flash point makes it safer in terms of both transportation and storage.

In the 1980s further advances were made in terms of cocktail safety with the development of polyalkylbenzenes, di-isopropyl naphthalene (DIN) and phenyl-o-xylylethene (PXE) as LS solvents (Thomson, 1991). The advantage of these solvents was their low vapour

pressures which allowed them to be dispensed in the open laboratory. DIN and PXE were the preferred solvents as polyalkylbenzenes have a lower energy conversion factor and still have toxicity problems.

Thomson (1991) reported that DIN was the ideal solvent for LSS. It is a high performance solvent with a low vapour pressure, low flammability, low toxicity and low plastic permeability. This latter feature allows DIN-based cocktails to be used in plastic vials instead of glass, which represents an advantage in terms of cost and background. Classical cocktails, such as those based on toluene and xylene, are steadily lost from plastic vials as the solvent permeates through the plastic. The biodegradability of DIN based cocktails also allows drain disposal, but it affects its long term stability as, over the course of a few months, the cocktail can be oxidised and become yellow. Although this is not a problem for most samples it may be of concern with regard to the long term stability of standards. However, some of the early-developed solvents are still the most popular choice today. In most radiometric radiocarbon applications benzene is both the sample and primary solvent.

1.3.2.2 Fluors

The next stage in the scintillation process is the transfer of the excitation energy from the solvent to the fluor. The fluor then exists in an excited state, when it loses this excitation energy, it returns to a ground state and emits a photon of light. The excitation of the fluor via the solvent can be written as:

$$S^* + F \rightarrow S + F^* \qquad (1.23)$$

where S represents the solvent molecule, F denotes the fluor and * denotes an excited state.

A scintillation cocktail may also contain a secondary fluor. In the early days of LSS, secondary fluors were required to ensure that the emitted light was at a wavelength detectable by the PMTs, but they are still used today for reasons described later in this section. Important properties of secondary fluors are light transmission, their peak fluorescence wavelength, the decay time of the light emission and their resistance to quenching. Light transmission describes the effectiveness in which the fluor converts the radiation energy into photons of light, while the peak fluorescence wavelength must be of suitable wavelength to ensure that the light produced registers with the photocathode. The decay time, in nanoseconds, describes how quickly the light pulse is produced. In the 1950s, there was intense investigation into many different types of fluor (Swank *et al.*, 1958), but today there are only a handful of primary and secondary fluors in common use, the properties of which are summarised in Table 1.4.

	Decay time (ns)	**Fluorescence Maximum (nm)**	**Solubility in Toluene (g l^{-1})**
PPO	1.6	364	451
butyl-PBD	1.2	367	67
BBOT	1.2	438	48
naphthalene	110	325	350
bis-MSB	1.3	412	4.5
POPOP	1.5	418	0.9
dimethyl POPOP	1.5	429	2.6

Table 1.4: The properties of fluors commonly used in LS cocktails. PPO and butyl-PBD are the most widely used primary and secondary fluors respectively. The fluors with low solubilities in toluene may be added only as secondary scintillators (from Gibbs *et al.*, 1976).

PPO (2,5-diphenyl oxazole) is a commonly used fluor, which has a good scintillation efficiency, a good solubility in primary solvents and is available at a reasonable price. Butyl-PBD (2(4'-tert-butylphenyl)-5-(4"-biphenyl)-1,3,4-oxadiazole) is also a very efficient fluor. However, to achieve this effectiveness it is necessary to use double the concentration of PPO, and this adds to the cost of the analysis as the cost of butyl-PBD is double that of PPO (S. Temple, personal communication, 2001). Furthermore, butyl-PBD can react with acids, bases, amines and other compounds, the effect of which is to reduce its scintillation efficiency. BBOT (2,5-bis-2-(tert-butylbenzoxazoly)-thiophene) is only 80 % as efficient in producing light as PPO. It does, however, emit light in the visible region which makes it more resistant to quenching. Unfortunately BBOT suffers the same drawbacks as butyl-PBD, namely; its cost compared to PPO, its chemical reactivity and its lower solubility. Although not a secondary fluor, naphthalene is often added to LS cocktails, since its long decay time leads to an improved energy transfer to the triplet state. This leads to an improvement in the resolution of α/β LSS (Kaihola and Oikari, 1991).

More common secondary fluors include bis-MSB (p-bis-(o-methylstyryl)-benzene), POPOP (1,4-bis-2(5-phenyloxazolyl)-benzene and dimethyl POPOP (1,4-bis-2-(4-methyl-5-phenyloxazolyl)-benzene). Often, secondary fluors are better scintillators than the primary fluors, but for reasons of solubility, reactivity with sample and cost, they are often added in a smaller concentration.

1.3.3 Pulse shape analysis

As stated earlier, β^- decay produces β^- particles with a range of energies, whereas α particles are approximately mono-energetic for a given nuclide. This difference explains the characteristic spectral shapes observed for α and β^- emitters. The β^- spectrum covers the range from 0 keV to the E_{max}, while α particles have a Gaussian distribution. When a β^- particle interacts with the scintillation cocktail, the ionization causes the fluors to be raised to an excited singlet state (S_1, S_2, S_3 etc). There are several processes by which this energy can be lost from the fluor molecule, returning it to the ground state, S_0. An excited singlet state results in the transition of a de-localised π electron (from the fluor) to a higher energy level, the direction of spin of this electron remains opposite to the electron in the ground state (Fig. 1.7). A photon is produced when the excited singlet state returns to its ground state. The probability of an excited triplet state forming from β^- induced excitation is small due to the relatively low specific ionization of β^- particles in the cocktail.

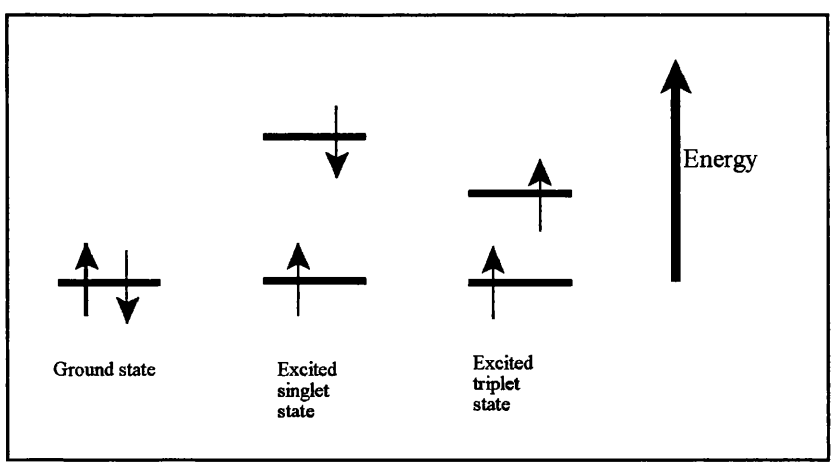

Figure 1.7: Electron distribution and spin in ground, excited singlet and excited triplet states (from Spinks and Wood, 1964).

An excited triplet state cannot form directly from the ground state, as this involves both transfer of an electron to a higher orbit and an inversion in the direction of spin in the excited electron (Spinks and Wood, 1964). Instead, excited triplet states form by inter-system crossing from an excited singlet state to an excited triplet state. α particles have a much higher specific ionization than β^- particles, which leads to more ion recombination, and as a result, a larger proportion of electrons can be raised to an excited triplet state. Excited triplet states, (T_2, T_3 etc) rapidly de-excite to their lowest excited triplet state by internal conversion (Spinks and Wood, 1964). However, triplet states cannot directly lose their energy radiatively as this is a forbidden process (due to the parallel spin of electrons). Triplet states are lower energy than singlet states so they cannot transfer their energy to singlet states by internal conversion (Fig. 1.7). Instead, triplet states de-excite by a process known as triplet-triplet annihilation. In this diffusion-based process, two excited triplet states collide to form an excited singlet, a molecule in the ground state and a photon. The excited singlet can then de-excite and produce an additional photon. The time taken for triplet-triplet annihilation to occur causes α particles to have a longer scintillation decay time than β^- particles, as will be discussed in Section 1.3.5.

The higher specific ionization of α particles causes them to ionize nearly every molecule they encounter, which results in a counting efficiency very close to 100 %. Their relatively short range means that α particles produce only $1/10^{th}$ the number of photons as a β^- particle of the same energy. This occurs as the shorter path length of an α particle compared to a β^- particle results in less efficient excitation energy transfer from solvent to fluor (McKlveen

and McDowell, 1984). For example, a β^- particle with an E_{max} of 500 keV will produce photons whose energy is dispersed from 0 to 500 keV. An α particle with an energy of 5 MeV will have its energy spread in a Gaussian distribution centred at 500 keV. The Full Width Half Maximum value (FWHM) is measure of the width of a peak at half of its maximum amplitude. For α particles measured by LSS this is approximately 200 to 300 keV. Hence it is therefore not possible to resolve multiple α emitters in the same sample unless their energies are significantly different. Sanchez-Cabeza *et al.* (1996) were able to resolve the peaks from ^{214}Po (7.69 MeV) from the composite α peak of ^{226}Ra, ^{222}Rn and ^{218}Po in analysis of drinking water radioactivity. Many α emitters cannot be resolved by LSS and this is one of the few disadvantages of LSS compared to α spectrometry and is discussed more in Section 2.7.

1.3.4 Considerations in LSS

The technique of LSS can be applied to samples of almost any activity. In nuclear power generation they are used for a wide range in nuclides where activities can be measured in M Bq. In contrast, LSS is becoming increasing important in environmental measurements where activities in mBq are determined (Benitez-Nelson and Buesseler, 1997; Pates *et al.*, 1996). In the determination of low levels of activity it is important to optimize the instrument to minimise the detection limit.

1.3.4.1 Background

Counts that register on a radiation detector but do not originate from the sample being

analysed are termed background counts. When the activity of the analyte is very high, the background count rate becomes insignificant in terms of the total count rate. However, an accurate determination of background count rate is critical for the correct determination of low sample activities. In terms of environmental analysis, LSS was originally used for ^{3}H and ^{14}C measurements and the main driving force behind background reduction has been the measurement of ^{14}C for dating applications. Reductions in background count rates give lower detection limits and reduce the errors associated with the ^{14}C measurements, thus extending the range of ^{14}C dating. As background count rates have fallen, the huge potential for LSS determination of a wide range of natural and anthropogenic nuclides at very low activities has been realised.

The background of an LS spectrometer can be divided into two categories, quenchable and unquenchable. Unquenchable background events occur outside of the scintillation cocktail and are the result of external radiation entering the counting chamber (Horrocks, 1985). It accounts for around two-thirds of the total background count rate and includes cosmic interactions with the PMTs, the vial material and the natural radiation in the vial material. Unquenchable background events are essentially low photon yield Cerenkov events which dominate the low energy region (0 - 18.6 keV). Quenchable background counts originate within the cocktail and account for around one-third of total background (Horrocks, 1985; Passo and Cook, 1994). The name quenchable background is used because these counts can be affected by quenching within the vial. Quenchable background results from interaction of cosmic rays with the cocktail, chemiluminescence or photoluminescence.

Chemiluminescence results from light-producing chemical reactions within the vials, and can be controlled by allowing the sample to sit in the counter for several hours prior to counting. This cools the vial to the temperature of the counter, usually around 13 °C, and thereby slows down the rate of any chemical reactions occurring in the vial. Monitoring the count rate of the samples is often the best way to deal with severe chemiluminescence. For example, monitoring radioactivity in oil requires the samples to be left several days before counting begins. Photoluminesence is the result of excitation of the vials, caps or cocktail by light. Again this can be reduced by leaving the sample in the counter (dark adapting) prior to counting and by storage of the vials, caps and cocktail in the dark to limit excitation in the first instance. In modern LS spectrometers, the percentage of counts originating from luminescence can be determined, allowing the analyst to decide when counting can begin. Quenchable background covers a wide range of energies and will increase with increasing cocktail volume and decrease with increasing quenching agent (Horrocks, 1985).

Any technique that can reduce either component of background is highly beneficial to the LSS user. The simplest way to reduce background is to reduce the amount of cosmic radiation reaching the counter. There have been some rather dramatic solutions to this problem such as placing the counter beneath a dam (Alessio *et al.*, 1976) or in an underground counting chamber (Polach *et al.*, 1988). These solutions are not practical for most analysts and are also very costly to set up. This has led both users and manufacturers to develop alternative background reduction techniques.

Homemade background reducing steps usually involve increasing the lead shielding that surrounds the detector, decreasing the voltage across the PMTs and masking the PMTs to minimise crosstalk between the two PMTs. γ-photons and the soft cosmic muon component of background can be removed by increasing the Pb shielding that surrounds the LS detector, however, increasing the Pb shielding will not prevent the high energy component of cosmic rays from penetrating the shielding. As the Pb shielding slows down these cosmic rays, Pb X-rays are emitted at 75 and 85 keV. The shielding has then to be lined with Cu and Cd. The Cd will absorb the Pb X-rays and the Cu will absorb the Cd X-rays.

Researchers looked towards active shielding to lower backgrounds and the first generation of cosmic guards were developed by the users (Alessio *et al.*, 1976; Jiang *et al.*, 1983). One type of active shielding can be seen today on the Wallac Quantulus. This instrument features a scintillating guard that surrounds the sample PMTs and has a further two guard PMTs which operate in anti-coincidence with the sample PMTs. This allows photons which strike both the vial and the guard to be rejected as a background event.

To address the problems associated with unquenchable background, the Packard Instrument Company pioneered the use of a background reducing feature based on pulse shape analysis (PSA). Each pulse that is detected is examined, and on the basis of the number of afterpulses, the pulse is either rejected as a background event, or accepted as a true event. This novel background reduction technique is based on the different pulse shapes produced by a β^- particle and a background event. A typical β^- pulse will comprise a prompt pulse

lasting 2 to 8 ns (singlet de-excitation) followed by the delayed component (the length of delayed component of a true β^- induced pulse varies depending on the energy of the β^- particle). A typical background pulse will have a similar prompt pulse but will contain more afterpulses, lasting up to 5 μs (Roodenberg *et al.*, 1972; Van Cauter, 1986) (Fig. 1.8).

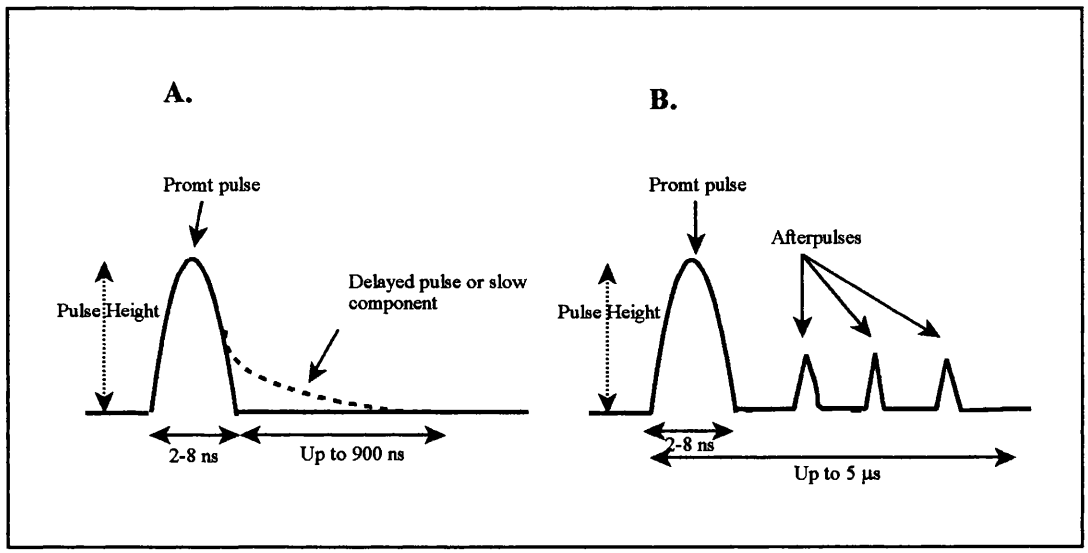

Figure 1.8: Graphical representation of a typical β^- induced pulse (A) and a background induced pulse (B) from an unquenchable event (afterpulses are not to scale) (from Passo and Cook, 1994).

When a coincident pulse is registered by the counter it activates the "burst counting circuitry" (BCC) which records the number of afterpulses occurring after the coincident pulse. The number of afterpulses is summed and termed the pulse index. If the pulse index is greater then the pre-set maximum, the event is rejected as background. Initially, the user had no control of this pulse index setting as the default setting was based on the β^- pulse length from a ^{14}C source. This had a detrimental effect on the counting efficiencies of long delay pulses, which resulted from high energy β^- emitters, de-oxygenated samples (oxygen

acts as quenching agent and shortens the pulses lengths) or solid scintillators which have a long delay time. Currently, Packard LS spectrometers have a modified feature which allows the analyst to select the time delay before burst counting begins. This is termed the Delay Before Burst (DBB), and has a range of delay settings from 75 to 800 ns. The lower the DBB setting, the smaller the background count rate but consequently, the lower the counting efficiency of high energy radiation (Passo and Roberts, 1996). Conversely, with the DBB set at is maximum time of 800 ns, much higher counting efficiencies are achieved, but at the cost of higher background count rates compared to the lower settings. The optimum setting is one which gives a balance between the highest counting efficiency and the lowest background.

The optimum DBB setting can be derived by calculating the Figure of Merit (E^2/B, where E = efficiency and B = background) at a range of DBB settings. By calculating the E^2/B for each setting, the highest figure of merit value can be found, providing the optimum counting conditions. This setting is entirely dependent upon the nuclide of interest and characteristics of the cocktail.

Another background reducing feature on the Packard 3170 TR/SL used in the present research is a quasi-active guard which acts to increase the discrimination between true and background events (Noakes and Valenta, 1996). The guard is made of bismuth germanate oxide ($Bi_4Ge_3O_{12}$) (BGO). Its high density (7.13 g cm^{-3}) makes it extremely effective at interacting with high energy cosmic radiation. The BGO does not stop cosmic rays reaching

the PMTs but its long fluorescence lifetime causes a stretching of the pulses passing through it, which gives the electronic pulse a long delayed component This can be discriminated by BCC (Noakes and Valenta, 1996). Caution should be exercised when β/γ-emitting nuclides are being assayed by a BGO-LS spectrometer due to reduction in γ counting efficiency from interaction with the guard, and in some cases a non-BGO LSS may give higher counting efficiencies. If the γ emission is coincident with the β^- and is sufficiently energetic then the interaction of the γ induced photon with the BGO guard may cause rejection of true events by the BCC. The choice of cocktail is also important in LS spectrometer which feature PSA. Cook *et al.* (1991) found that bis-MSB was crucial as a secondary scintillator in conjunction with a butyl-PBD scintillator. The bis-MSB acts to minimise afterpulsing and therefore bring more true β^- events within the cut off threshold of the burst counter.

1.3.4.2 The sample

It is important in LSS to have the sample in a form which will allow it to become homogeneously mixed with the cocktail. In most applications of LSS, the sample is in a liquid form, allowing the sample and the cocktail to become intimately mixed into a homogeneous matrix. In some cases this is not possible and solid samples have been counted by LSS, including ^{90}Sr and ^{241}Am on filter papers and wipe assays (Cooper *et al.*, 1998) and ^{241}Pu on stainless steel disks (Cook and Anderson, 1991). In some cases the sample may be prepared as a precipitate, such as ^{35}S (as $BaSO_4$), ^{90}Sr (as $SrCO_3$) (Friedrich and Schönhoffer, 1996) and ^{226}Ra (as $RaSO_4$) (Chalupnik and Lebecka, 1990), and suspended in a gelling cocktails. Although this method of sample preparation may introduce a degree

of sample self absorption, it offers a quick and reliable way to incorporate the nuclide of interest into the scintillation vial.

1.3.4.3 The vial

The vial is the container which holds the sample while it is counted in the LS spectrometer, therefore it is vital to chose the correct interface between the sample and the PMTs to ensure the best counting efficiency. Vials are available in a range of sizes manufactured from a variety of materials. The choice of material for the LS vial can have a significant effect on the counting efficiency. The material used should exhibit a low background count rate, have minimum absorbance of the emitted light, be chemically inert to the sample and the cocktail, be uniformly manufactured to minimize any variation between vials, have a reliable method of closure (and re-opening) and be available at low cost (Gibbs *et al.*, 1976). The two main materials routinely used to manufacture LS vials are low-K borosilicate glass and polyethylene. Polyethylene vials are perhaps more commonly used today since the development of DIN based cocktails. Before the advent of these environmentally safe cocktails, many of the solvents were able to diffuse into the polyethylene. Since the polyethylene is manufactured from a low background source (petroleum distillates), the background count rates from polyethylene vials are lower than those of glass vials. In terms of cost, plastic vials are cheaper than their glass equivalents and their opacity results in improved transmission of light as the matt surfaces minimise the chance of any light being reflected off the insides of the vial (Oikari *et al.*, 1987; Pates, 1996).

Glass vials were the main counting vessel for LSS until the cheaper alternative of plastic became a viable option. The glass used in their construction is low-K borosilicate which has lower background count rates due to its lower potassium content, ^{40}K being the main background component of glass vials. Glass vials still have advantages in a wide range of LSS applications. One of their main uses is in ^{14}C dating due to the permeability of benzene through plastic vials. They also allow visual inspection for any heterogeneity in the sample due to phase separation, colour formation or precipitation of sample from the cocktail. These problems are not readily detectable in plastic vials. Furthermore, they allow sample volume to be reduced in-situ on a hotplate which is important in certain applications. Several other types of materials have been experimented with to allow lower background count rates in ^{14}C dating, including synthetic quartz (Hogg, 1993) and Teflon (Polach *et al.*, 1983). Teflon vials require a rigorous cleaning procedure before their re-use and although synthetic quartz vials require only minimal washes, their use is restricted to a handful of samples which require the highest sensitivity, due to the cost of such vials.

The size of the vial also plays an important role in terms of background and detection limit. Plastic vials are available in a wide range of geometries, the most popular being 20 ml and 7 ml. Glass vials are also available in a range of sizes but again, the two main geometries are 20 ml and 7 ml. In the simplest terms, the 7 ml geometry contains less vial material, and hence, gives a lower background count rate. Furthermore, the quenchable component of background is related to cocktail volume (Horrocks, 1985). In certain applications the limits of detection depends on the size of sample that can be incorporated into the vial and larger

vials offer improved detection limits (Ingenco, unpublished data, 2001). For example, in direct ^{3}H measurements, the sample cannot be evaporated to a smaller size without losses of ^{3}H as $^{3}H_2O$. Therefore, not only is the correct choice of vial important but also the correct vial size for the activity being measured.

1.3.4.4 Quenching

LSS measurements are subject to their own type of interference called quenching. If not controlled, quenching may severely influence the results. Quenching is the reduction in light output by the sample itself. In the simplest form, any reduction in the number of photons reaching the PMTs is termed a quench process.

There are three types of quenching processes that can occur in a LS sample. Absorption quench occurs when a solid material is present in the vial which attenuates any emitted radiation before it excites the solvent molecules. This type of quenching is particularly relevant when counting filter papers or any undissolved sample such as the direct counting of soils (Adu and Oades, 1974). The overall result is a decrease in counting efficiency. Chemical quench occurs when an excited solvent molecule transfers its energy to a non-light producing impurity. The impurity emits no photons and/or disrupts the energy transfer process to the fluor, again a reduced number of photons are observed at the PMT. The net result is a reduction in counting efficiency and shifting of the spectrum to lower energies. Finally, the term colour quench is used when the excited fluor molecules emit photons but these are absorbed by a coloured species in the sample. The coloured species either loses

this energy non-radiatively (without the production of light) or emits it at inappropriate frequencies. Again, the net effect is a decrease in counting efficiency. These three processes are summarised in Figure 1.9.

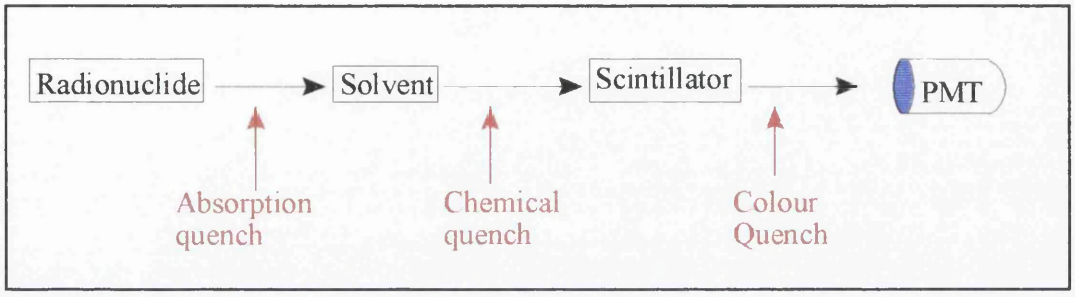

Figure 1.9: Schematic diagram of the three main types of quench occurring in LS cocktails (from Passo and Kessler, 1992).

It is therefore imperative to have a measurement of the degree of quench that affects each sample to allow corrections to be made to compensate for any reduction in counting efficiency. There have been various methods for quench determination in LS samples. The earliest technique was known as internal standardisation. This involved adding a known activity of the same radionuclide to the sample and recounting with the known activity present to allow the counting efficiency to be determined (Hayes, 1956). However, this changed the chemical composition of the sample and therefore changed the degree of quenching into the vial. In addition, this technique required accurate pipetting of the spike, the sample had to be counted twice and the original sample could not be recounted.

To overcome the problems with internal standardisation, quench corrections based on the sample spectrum were developed. The Sample Channels Ratio (SCR) technique was

developed when instruments with two or more counting windows became available. It relied on the spectral shift that could be observed with increasing quench and measured the ratio of the counts in the two windows (one low energy and the other high energy) to quantify the quench conditions in the vial. The method relies on having sufficient activity to record enough counts in the two channels for the ratio and hence the efficiency to be determined accurately and is therefore not suitable for low activity measurements. Quench indicator parameters (QIPs) based on the end point of the sample spectrum have also been applied. The QIP of a sample is derived from the activity of the sample by integrating the total counts observed over the whole spectrum. It is independent of sample volume, wall effects and cocktail density, but because it relies on the count rate of the sample, is subject to low count rate uncertainties.

The most accurate method of determining quench is termed the external standard method. It uses an external γ emitting source to induce Compton electrons in the sample (Rapkin, 1970). The γ source (^{133}Ba, ^{137}Cs or ^{226}Ra) is brought close to the sample vial. The γ photons interact with the sample to produce lower energy γ photons and Compton electrons. A Compton electron is similar to a β^- particle and is detected similarly. Thus, a Compton energy spectrum is collected. As this QIP is based on the spectrum obtained from an external standard, it is independent of sample activity and is therefore suitable for low activity samples. Originally the external standard method of quench correction was affected by different vial thicknesses, which introduced a degree of uncertainly into quench measurements. Nowadays, the Compton energy spectrum is manipulated mathematically to

compensate for the effect of vial types and the main instrument manufacturers use different mathematical techniques to derive a QIP from the external standard method.

The external standard QIP used by Wallac Oy is based on the spectrum obtained from a ^{152}Eu source and is called the spectral quench parameter of the external standard, abbreviated to SPQ(E). Beckman Instruments utilise ^{137}Cs as the external standard and base their quench determination on the Horrocks number (H#) (Horrocks, 1976). Packard Instruments external standard QIP is called the transformed spectral index of the external standard (tSIE) (De Filipis and Van Cauter, 1985) and is based on a ^{133}Ba source. The instruments used in this research are Packard LS spectrometers and the QIP was the tSIE. This has a scale of 0 to 1000 units, where 1000 representing a completely unquenched sample while 0 would signify no light output (i.e. opaque).

All these QIPs use quench curves to determine the counting efficiency. A series of quenched standards, comprising of a number of vials with the same sample activity but quenched to different degrees is counted, allowing the counting efficiency for each standard to be derived and plotted against QIP. This allows the counting efficiency to be calculated for a range of quench conditions and allows count rates to be converted into activities.

1.3.5 α/β LSS

Modern LS spectrometers are now capable of simultaneous α and β measurements in the same sample. In conventional LS spectrometers there is significant spectral overlap between

α and β/γ spectra. This makes determination of α emitters difficult due to the interference of β/γ spectrum and high background count rates. Thorngate *et al.* (1974) applied PSA to the measurement of ^{239}Pu. Background count rates of 1 cpm were reduced to 0.01 cpm by applying PSA. McKlveen and Johnson (1975) were able to discriminated between ^{90}Sr(^{90}Y) and ^{210}Po spectrum using a single PMT and PSA. Much of the research into PSA was carried out by McDowell and co-workers and forms the basis of the PERALS system (McDowell and McDowell, 1991). As discussed in earlier sections, the way in which α and β events interact with the cocktail are different. Fundamentally, this is due to the higher specific ionization of α events compared to β events. The pulse shape of α events is longer than β events, and in the same way as PSA can be used to differentiate between true events and background, PSA can accurately discriminate between pulse produced by α and β events by analysis the pulse lengths (Oikari *et al.*, 1987). There are several ways in which α and β pulses can be separated by LS spectrometers but they are all based on the different pulse shapes obtained from the PMT's. Pates *et al.* (1995) utilised α/β LSS in a study of ^{234}Th/^{238}U disequilibrium in the marine water column. This application allowed simultaneous determination of the β^- emitting ^{234}Th and an α emitting ^{230}Th yield tracer.

State of the art LSS offers the analyst a unique instrument capable of measuring α, β and γ activity in samples with very low activity. Compared to more conventional counting techniques such as α spectrometry and gas proportional counting (GPC) it offers shorter counting times due to the increased counting efficiencies. Although the resolution of α

events is not as sharp as α spectrometry it is better than GPC. In terms of β analysis it does not suffer from sample self adsorption and allows even low energy nuclides such as ^{3}H to be accurately measured. The remainder of this thesis will now focus on a novel and time efficient method developed to determine the natural decay series radionuclides ^{210}Pb, ^{210}Bi and ^{210}Po in the marine water column using LSS.

1.4 Aims

The primary aim of this research is to develop a more time efficient method for the measurement of the NDS radionuclides ^{210}Pb and ^{210}Po in aquatic matrices using LSS.

The method will then be applied in a study of nearshore marine scavenging processes. This will provide information on the rates of particle removal and biological production in a highly dynamic coastal region. In these environmental settings the rates of removal are thought to be fast but there is still a paucity of data on $^{210}Po/^{210}Pb$ disequilibria. Therefore, a more time efficient method of $^{210}Po/^{210}Pb$ disequilibrium is highly attractive as it will allow results to be obtained faster than currently available and reduce the time required for counting which will allow more samples to be processed.

Finally, the possibility of a simultaneous measurement of ^{210}Bi will also be investigated. If successful, this will allow processes occurring on shorter timescales to be examined and will also provide data on the biogeochemical cycling of ^{210}Bi in the marine environment.

Chapter Two: Methodologies

2.1 Introduction

This chapter will cover analytical techniques investigated during the course of this research. Much of this work focusses on separation and purification techniques required to successfully analyse the isobaric radionuclides ^{210}Pb, ^{210}Bi and ^{210}Po. To provide a framework for the attempted methodologies, a flow diagram of successful and less successful methods is shown in Figure 2.1. This chapter will begin with a brief introduction to the current methods of analysis before discussing the methodologies investigated.

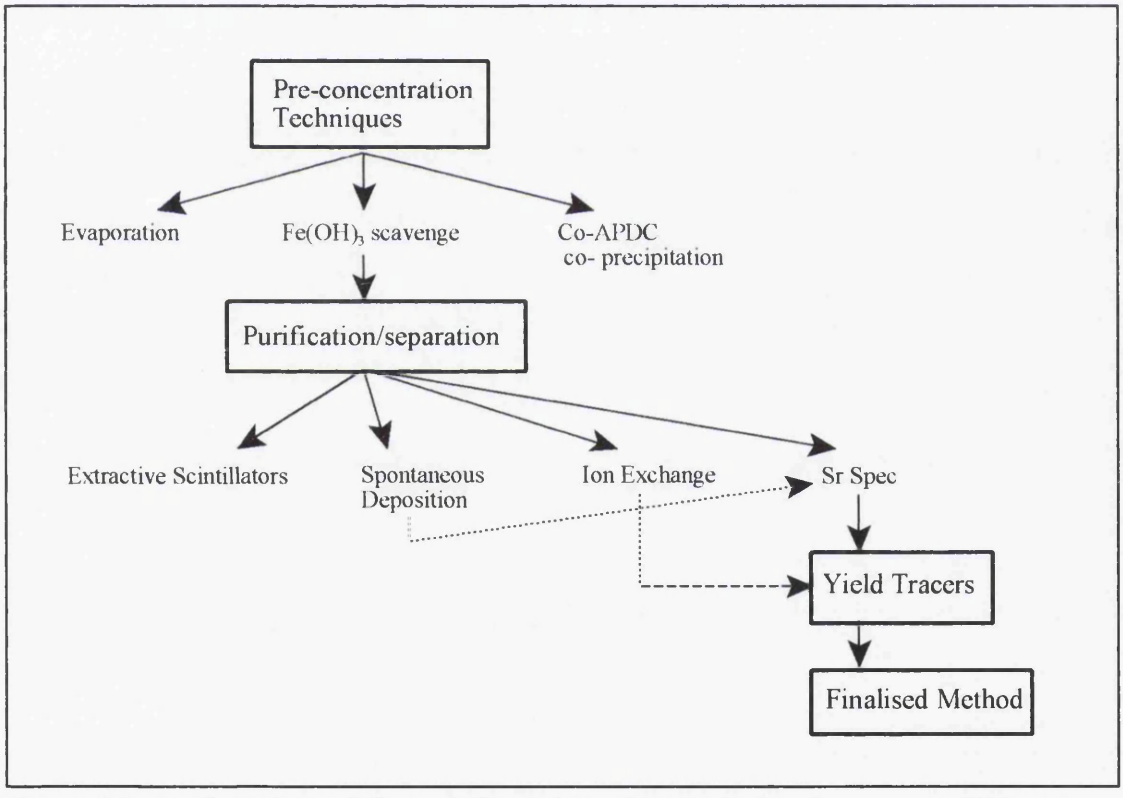

Figure 2.1: Overview of the techniques investigated during the course of this research and the route to the finalised methodology.

2.1.1 Current methodologies

The aim of this work has been to develop a more accurate and time efficient method for the determination of the NDS radionuclides ^{210}Pb, ^{210}Bi and ^{210}Po in marine waters. At the outset, only ^{210}Pb and ^{210}Po were to be measured but during the course of this research it was realized that ^{210}Bi determination could also be carried out. The current methods examined all have their own individual advantages and disadvantages. There is, however, a framework which is common to all of these methods. Firstly, there is an initial pre-concentration of the nuclides, the samples then undergo a variable number of purification stages and finally there is the method of measurement (Fig. 2.2).

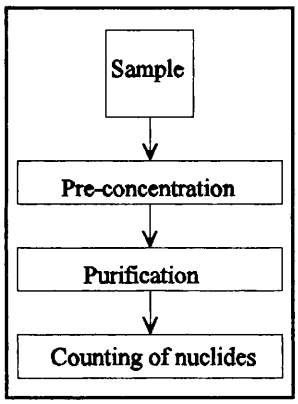

Figure 2.2: General framework for radiochemical analysis of environmental samples.

This framework is required because, firstly, the activities of ^{210}Pb, ^{210}Bi and ^{210}Po present in seawater are extremely low and pre-concentration is required to allow large sample volumes to be processed. Purification is required to remove any radionuclides (NDS or anthropogenic) which may interfere with counting procedures. Purification can also remove

the non-radioactive contaminants, which is especially relevant in the context of seawater analysis, because the matrix has a high dissolved ion content.

2.1.2 Counting techniques

^{210}Pb ($t_{½}$ = 22.3 years) decays via combined β^- emission (E_{max} = 61 keV), γ emission ($E\gamma$ = 46.5 keV) and internal conversion to the β^- emitting ^{210}Bi ($t_{½}$ = 5.1 days, E_{max} = 1161 keV). In turn, ^{210}Bi decays to the α emitting ^{210}Po ($t_{½}$ = 138.4 days, $E\alpha$ = 5.3 MeV). ^{210}Po is the last radioactive nuclide of the ^{238}U decay chain before the stable ^{206}Pb end member (Fig. 2.3).

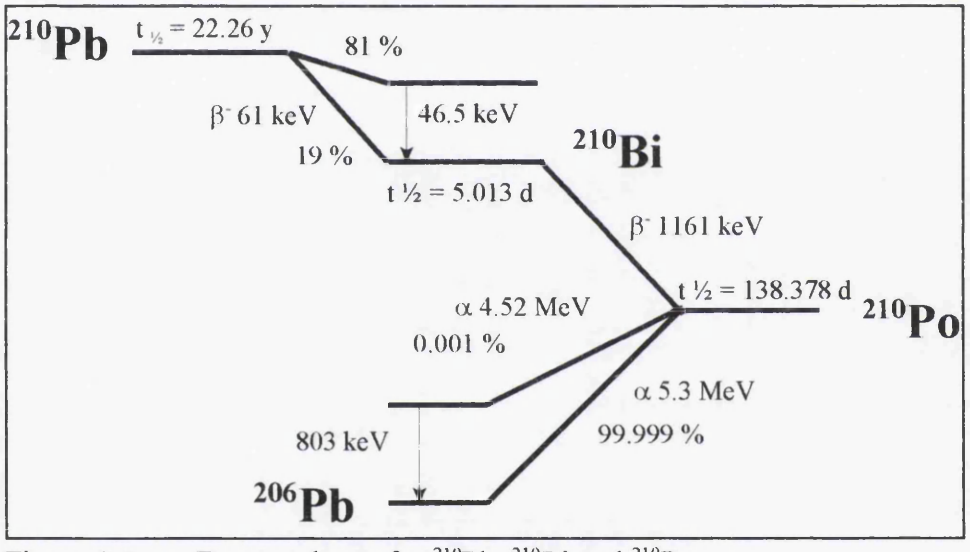

Figure 2.3: Decay scheme for ^{210}Pb, ^{210}Bi and ^{210}Po.

There are three ways by which ^{210}Pb is typically determined: direct counting of ^{210}Pb via its γ emissions, or indirectly by measurement of its β^- emitting daughter (^{210}Bi) or its α emitting grand-daughter, ^{210}Po. ^{210}Pb is not directly determined by β spectrometry due to the difficulty of measuring the soft beta emissions.

Direct measurement of the 46.5 keV γ photons of ^{210}Pb can be accomplished using an N-type HPGe γ photon detector with a thin beryllium or carbon-epoxy thin window. The difficulty in this technique is that large activities of ^{210}Pb are needed because of its low absolute intensity of the 46.5 keV γ photon (~4 % intensity) and the intrinsically low counting efficiency of HPGe detectors. Calibration of γ photon detectors for low energy γ photons is more complicated than measurement of high energy γ photons due to problems of self-absorption of low energy γ photons by the sample itself. To overcome this problem the sample must be in as small a counting geometry as possible. Obviously this prohibits direct counting of large volume water samples such as seawater. The counting efficiency is often as low as 0.5 % (Section 2.9.2.1) and would require the use of extremely low background counters combined with long count times for the low activities observed in seawater (0.48 - 2.35 mBq l^{-1}) (Nozaki *et al.*, 1998).

The main method employed for the determination of ^{210}Pb in marine samples is by measuring ^{210}Pb via its grand-daughter, ^{210}Po. In sediments, it is often assumed that ^{210}Po and ^{210}Pb are in equilibrium, and the activity of ^{210}Pb can be estimated from that of its grand-daughter, ^{210}Po (*e.g.* Sanchez-Cabeza *et al.*, 1999). In the upper water column, equilibrium is rarely achieved and a separate determination of ^{210}Pb is required. After an initial pre-concentration, ^{210}Po is plated from the solution by spontaneous deposition onto silver foils, the plating solution containing the original ^{210}Pb is then stored. During this storage period the second generation of ^{210}Po will be produced from the decay of ^{210}Pb (Fig. 2.4).

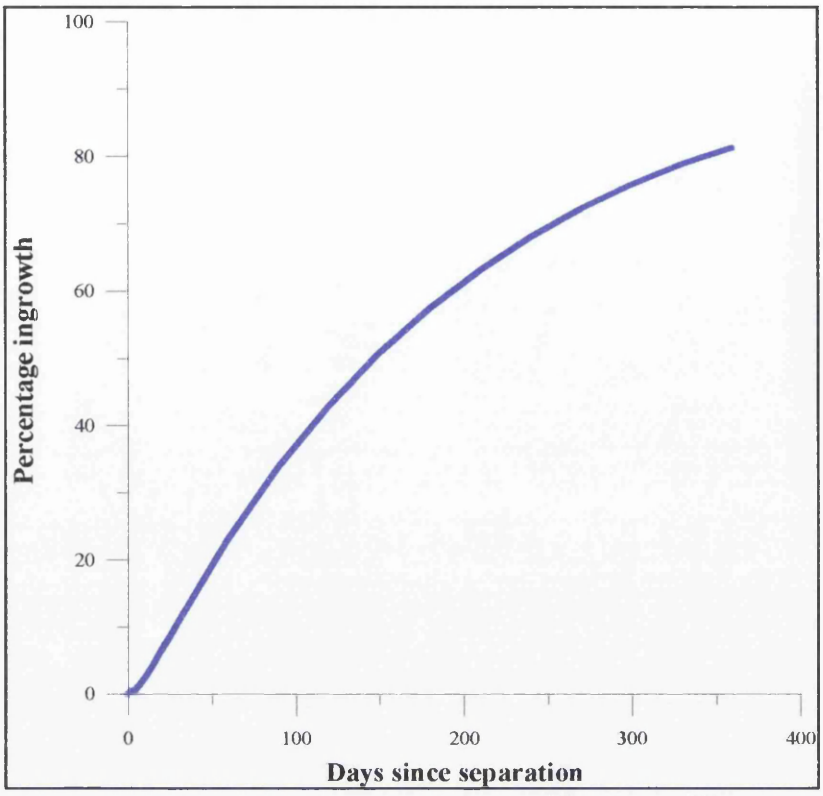

Figure 2.4. The ingrowth of supported ^{210}Po from ^{210}Pb after initial removal of ^{210}Po by spontaneous deposition.

By performing a second spontaneous deposition onto silver, after allowing sufficient time for ingrowth, it is assumed that any ^{210}Po plated in this second stage is a result of the decay of ^{210}Pb during storage. ^{210}Po can be counted by α spectrometry and the activity of ^{210}Pb can be derived by applying the Bateman equation (equation 1.7). This method of determining ^{210}Po and ^{210}Pb has been used by numerous workers, including Thomson and Turekian (1976), Schell (1977), Benninger (1978), Fleer and Bacon (1984), Holtzman (1987), Benoit and Hemond (1987), Thomson *et al.* (1993b) and Skwarzec (1997), amongst many others. The technique of spontaneous deposition used to remove ^{210}Po from solution

will be discussed in detail in Section 2.4. There are some obvious disadvantages to this general procedure:

1. The large time lag between the initial plating and the second plating, which is necessary for sufficient ^{210}Po ingrowth ($t_{½}$ = 138.378 d). Some workers leave their plating solutions only a few months (Thomson *et al.*, 1993b; Bacon *et al.*, 1976; Shannon and Orren, 1970), while others, including Tanaka *et al.* (1983), Nozaki *et al.* (1997) and Wei and Murray (1994) allow more than one year of ingrowth before replating. The ingrowth of supported ^{210}Po from ^{210}Pb is illustrated in Figure 2.4.

2. The initial polonium plating is not always 100 % efficient, which will cause an under-estimation in the ^{210}Pb activity resulting from un-plated Po remaining in solution after this initial plating. To rectify this problem requires either an anion exchange procedure to separate ^{210}Pb from its daughters (Joshi and Ku, 1979; Benninger, 1978) or necessitates storage of the sample with silver for a short period to remove the last traces of ^{210}Po before starting the ingrowth period (Benoit and Hemmond, 1987; Schell, 1977).

3. ^{210}Bi can also partially plate onto silver foils (Section 2.4.2.1) and the ingrowth of ^{210}Po from the decay of ^{210}Bi can introduce a significant error if counting times are long. Furthermore, ^{210}Bi cannot be determined separately.

4. The plated ^{210}Po is counted by α spectroscopy. Although the α counting efficiency

of ^{210}Po is greater than the γ photon counting efficiency of ^{210}Pb (20 % cf. 0.5 %), the samples have to be counted for long periods of time (up to two weeks) due to the very low activities present in seawater.

The logical progression of this method is to indirectly measure ^{210}Pb by the ingrowth of its daughter ^{210}Bi ($t_{½}$= 5.013 days). Figure 2.5 displays the ingrowth of ^{210}Bi after purification of ^{210}Pb. After 30 days, ^{210}Bi has reached equilibrium with its parent. The measurement of ^{210}Pb via ^{210}Bi is not as common as the ^{210}Po ingrowth method but is sometimes applied in the marine system (Craig *et al.*, 1973; Chung and Craig, 1983). Pb is purified by ion exchange techniques, precipitated as $Pb(SO_4)$, stored for 1 month then analysed for the β^--emitting daughter ^{210}Bi. The high energy β^- emission of ^{210}Bi is relatively easy to detect and its short half life makes the wait for ingrowth faster than the ^{210}Po ingrowth method. Furthermore, it may also allow a faster sample throughput as some GPC systems can count multiple samples during one run. However, measurement of ^{210}Bi ingrowth by GPC produces backgrounds that are higher than those obtained with α spectrometry, resulting in poorer detection limits (Holtzman, 1987). Joshi and Ku (1979) recommend a further purification of the $Pb(SO_4)$ precipitate to remove any contaminants adsorbed onto the $Pb(SO_4)$ crystals but this procedure has not been regularly applied. Nozaki *et al.* (1976) show the inter-comparison of the ^{210}Po (Yale) and ^{210}Bi (Scripps Institute) derived ^{210}Pb data from the GEOSECS program to yield similar values within analytical error. The β^- counting efficiency by GPC is usually around 30 % (the same nuclide counted by LSS offers close to 100% counting efficiency).

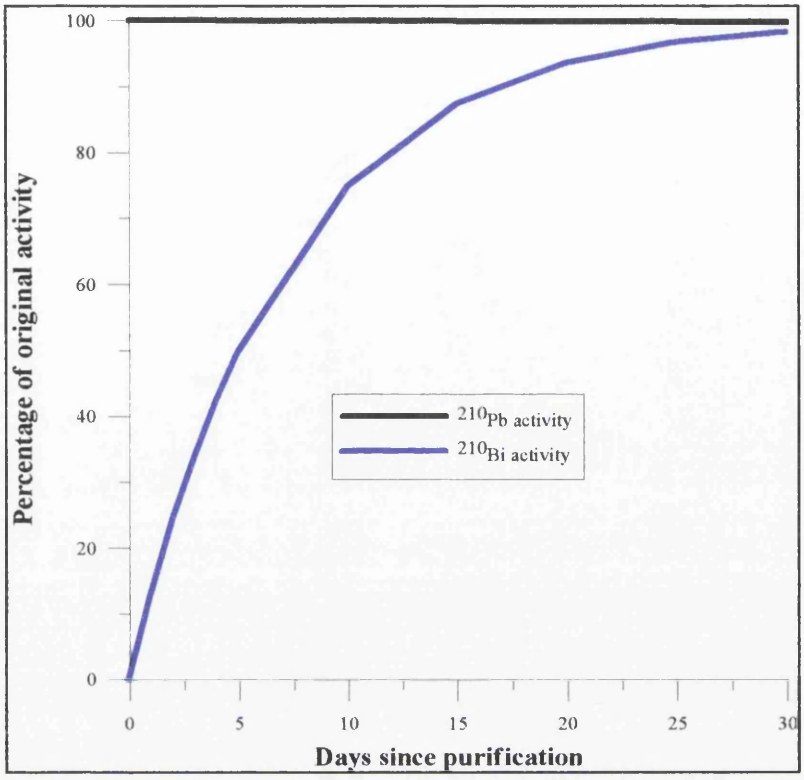

Figure 2.5. The ingrowth of supported ^{210}Bi from ^{210}Pb after the stripping of ^{210}Bi.

Wallner (1997) used a liquid/liquid extraction technique to purify ^{210}Bi then counted the β^- emitting nuclide by LSS. It was this logical progression through the method that drove the research into extractive scintillators and this will be discussed in Section 2.3.

2.1.3 LSS counting procedures for method development

Much of the method development discussed in this chapter utilises LSS as the main instrument of detection. Two spectrometers were used in this research: (i) a Packard 2250 CA; and (ii) a Packard 2770 TR/SL which had the software package upgraded to run on the Windows operating platform during this research. The upgraded spectrometer became a

Packard 3170 TR/SL although there were no changes to the actual instrumentation. Unless stated otherwise, all counting was carried out on the 3170 TR/SL using NCM for a 100 minutes count time in 20 ml low K borosilicate glass vials after allowing the samples to sit in the counter for at least one hour. Background vials were always made using the same acid molarity and acid/cocktail ratio and counted with the samples. Spectral analysis was carried out using the SpectraWorks software package (Packard).

2.2 Pre-concentration of Natural Decay Series nuclides

The dissolved activities of ^{210}Pb, ^{210}Bi and ^{210}Po found in seawater are too low to be measured directly. Virtually every method for analysis of the dissolved ^{210}Pb and ^{210}Po activities in aquatic samples requires a pre-concentration stage. Pre-concentration reduces the sample volume and may also be used to remove interferences from major ions present in the original sample. There are several common techniques available for pre-concentration of ^{210}Pb, ^{210}Po and other NDS nuclides, which are discussed below.

Direct analysis of ^{210}Po has been carried out by Othman *et al.* (1994) who plated ^{210}Po directly from a 1 litre sample of filtered seawater. α spectrometry is sufficiently sensitive to detect ^{210}Po plated without concentration of the sample, but long count times are required to achieve suitable measurement precision and it is more usual to employ significantly greater volumes. No detection limits or count times are quoted in the paper.

2.2.1 Evaporation techniques

The most obvious way of volume reduction of aquatic samples is by evaporation of the sample on a hot-plate. Swarzenski *et al.* (1999) used an evaporation technique on 10 litre water samples from the Framvaren fjord. The procedure was carried out at 60 °C under an array of heat lamps to prevent any volatilisation of Po and in a clean room to minimise any contamination from ^{210}Pb produced from ^{222}Rn in the laboratory. The solution was evaporated close to dryness and Po isotopes (^{210}Po and a ^{209}Po tracer) were spontaneously deposited onto silver foil. The ^{210}Pb activity was determined by storing the plating solution

for 8 months and re-plating the second generation of ^{210}Po as a measure of ^{210}Pb. Clearly, this technique is time consuming and requires large clean room facilities to carry out the evaporation, especially if multiple samples are being analysed.

This technique does allow determination of ^{210}Pb and ^{210}Po in marine samples without the need for a chemical concentration stage but highlights the difficulty in the evaporation technique. Direct measurement of ^{210}Pb by evaporation of marine water samples is hindered by the mass of salts in the sample. Typically, 10 litres of seawater will produce around 350 grams of salts but the self-absorption of the ^{210}Pb γ emissions by these salts presents a considerable difficulty for its measurement by γ spectrometry. Evaporation was not chosen for this method due to the length of time required for evaporation, the presence of a large mass of salts and the large clean room facilities that would be required.

2.2.2 Pre-concentration by organic extraction

Shannon and Orren (1970) developed a method for the concentration of ^{210}Pb and ^{210}Po from seawater by APDC-MIBK (ammonium pyrrolidine dithiocarbamate - methyl isobutyl ketone) solvent extraction. 4 % w/v APDC was added to a 1.5 litre sample of acidified seawater and the solution was mixed for 5 minutes. Then 75 ml of MIBK were added and the APDC (together with complexed ^{210}Pb and ^{210}Pb) was extracted into the organic phase. The organic phase was separated, oxidised and evaporated close to dryness on a hot-plate. The residue was dissolved in HCl and Po was plated onto silver foils using the standard technique of Flynn (1968). ^{210}Pb was determined by ^{210}Po ingrowth (Section 2.1). The disadvantage

of this method is that solvent extraction techniques are not suitable for large sample volumes. In addition, Shannon and Orren (1970) reported that MIBK is slightly soluble in the aqueous sample and as a result, not all the APDC complex is removed into the organic phase. They also reported some problems with the phase separation. Despite the problems in this method, recoveries of ^{210}Po and ^{210}Pb added as spikes were 92 % and 85 %, respectively.

Boyle and Edmund (1975) refined this method for the concentration of trace metals using an APDC chelate co-precipitation. If an excess of a transition metal is added to a sample containing APDC it will result in precipitation of a metal-APDC. At very low metal concentrations, APDC forms a colloid in water (which was extracted by MIBK by Shannon and Orren, 1970). If the metal concentration is sufficiently high, a metal chelate precipitate forms. The precipitation is non-selective because the scavenged metals are shielded by the APDC and, thus, any metals present in the sample will be precipitated. By adding an excess of Co^{2+}, they reported high yields (> 90 %) of co-precipitated metals. The Co-APDC precipitate can be collected by filtration and the APDC chelate oxidised. Bacon *et al.* (1976) used this technique to pre-concentrate dissolved ^{210}Pb and ^{210}Po from seawater. Again, ^{210}Pb is determined via the ingrowth of ^{210}Po in the original plating solution. This technique has been applied in oceanic samples (Fleer and Bacon, 1984), brackish waters (Young, 1996) and non-saline (lake and river) water (Benoit and Hemmond, 1987).

2.2.2.1 Trial pre-concentration using Co-APDC

An experiment was carried out to assess the Co-APDC co-precipitation technique on an artificial seawater sample using the method of Fleer and Bacon (1984). The artificial seawater comprised 20 litres of reverse osmosis water with 70 g NaCl (equivalent to 35 ‰ salinity), spiked with ^{210}Pb (with ^{210}Bi and ^{210}Po in equilibrium) and left overnight. The following day, 1.0 g APDC (equivalent to 50 mg l^{-1}) was added, and co-precipitated with 0.042 grams $CoCl_2$ (equivalent to 0.5 mg Co l^{-1}). The green precipitate was collected by filtration through 0.22 μm membrane filters and the filtrate reserved for a second experiment (see below).

Fleer and Bacon (1984) oxidised the filters in a solution of 15 M HNO_3 and 12 M $HClO_4$ but the use of $HClO_4$ is prohibited in our laboratory. Instead, the filter and precipitate were re-fluxed overnight with a mixture of 15 M HNO_3 and 12 M HCl. Problems arise when the solution is brought close to dryness as an explosive reaction can (and did) occur due to the incomplete oxidation of the cellulose nitrate filter. The volatility of Po has been previously reported (Bagnall, 1957) and heating the sample during oxidation with acid can lead to losses of Po by volatilisation. The solution was eventually re-dissolved in 2M HCl and transferred to a scintillation vial where it was again taken to dryness. The residue was dissolved in 1 ml 0.1 M HCl and 4 ml 7 M H_3PO_4. 2 ml of POLEX extractive scintillator were added. POLEX is a specialised organic LS cocktail that was used to extract ^{210}Bi and ^{210}Po from a HCl/H_3PO_4 aqueous phase into an organic phase which is also a LS cocktail (discussed in detail in Section 2.3). Once the separation was complete the POLEX fraction

(containing ^{210}Bi and ^{210}Po) was counted by LSS (Section 2.1.3).

The scavenging efficiency of Co-APDC was assessed by repeating the precipitation on the filtrate. Similar problems arose with the oxidation of the re-extracted sample. The LS spectra obtained for the two POLEX extractions are shown in Figure 2.6. The recoveries were calculated by comparing the ^{210}Bi and ^{210}Po counts from the Co-APDC extraction to a spike extraction. The relative recoveries of ^{210}Bi and ^{210}Po from the first extraction were 86 % and 42 % respectively. This technique is reported to be non-selective and roughly equal recoveries would be expected. The relative recoveries measured from the second extraction were around 3 % for both ^{210}Bi and ^{210}Po. The 20 litre container in which the Co-APDC precipitation was performed was left with a significant coating of the green precipitate on the inside. This could not be removed easily and required soaking in acid for several weeks followed by scrubbing to remove it.

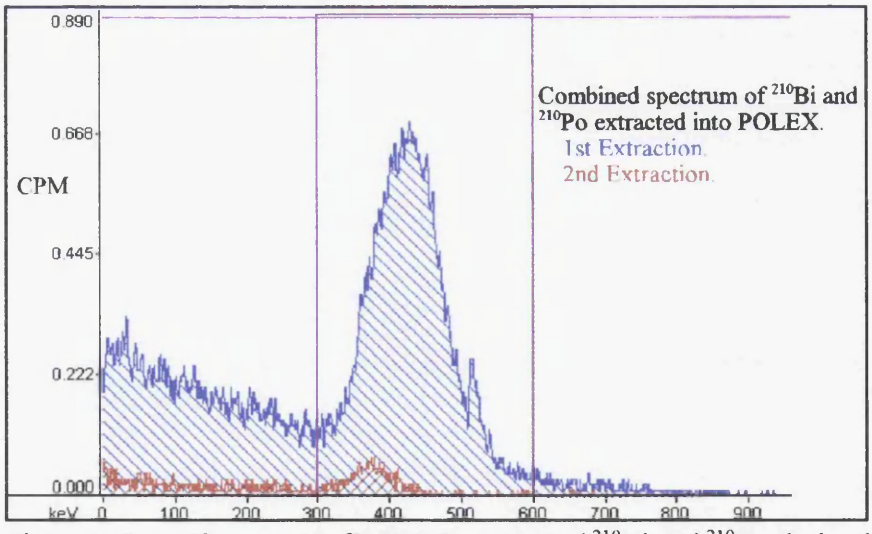

Figure 2.6. Spectrum of POLEX-extracted ^{210}Bi and ^{210}Po derived from Co-APDC extraction from seawater. The second extraction shows that not all ^{210}Bi and ^{210}Po are removed in first Co-APDC precipitation.

Disadvantages of Co-APDC

1. The method requires the destruction of the filter paper to allow the Co-APDC precipitate to be oxidised. Oxidation without $HClO_4$ is a time consuming process. Furthermore, there is a risk of explosion which may volatilise ^{210}Po.

2. The Co-APDC is difficult to remove from the sample containers and the filtering apparatus. This could lead to lower chemical recoveries and cross-contamination of samples.

2.2.3 Pre-concentration using inorganic scavengers

It was decided to investigate other pre-concentration techniques that might be more suitable for ^{210}Pb, ^{210}Bi and ^{210}Po determination. Inorganic precipitation has also been utilised to "*scavenge*" dissolved metals from solution into a precipitate. Mn impregnated cartridges have been used to concentrate dissolved NDS nuclides from seawater. Moore (1976) impregnated acrylic fibres with MnO_2 and used the technique to pre-concentrate Ra and Th isotopes from 1000 litre seawater samples. Wei and Murray (1994) used this technique to determine the behaviour of ^{210}Pb and ^{210}Po in the Black Sea, however, Thomson *et al.* (1993b) reported that MnO_2 absorber columns have a poor efficiency for ^{210}Pb. With two MnO_2 columns in series, the second column should act as a guard column which allows the extraction efficiency of the first column to be calculated. However, they found that the second column occasionally contained a higher activity than the first column, meaning that it was impossible to quantify losses. Pates (1995) found a similar failing with MnO_2

cartridges and called their validity into question.

Co-precipitation of NDS radionuclides has also been achieved using Mn, which is precipitated as $MnOH_4$ when the pH of the solution is raised by the addition of 18 M NH_4OH. Bojanowski *et al.* (1983), Skwarzec (1997), Carvalho (1997) and Peck and Smith (2000) all report success with this technique. Peck and Smith (2000) report Pb and Bi recoveries of 97 ± 4 % and 90.3 ± 3.4 % respectively. Another co-precipitation reaction was used by Wu and Boyle (1997), in a study of Pb concentrations in the ocean, where they used $Mg(OH)_2$ to co-precipitate Pb.

2.2.3.1 Pre-concentration with $Fe(OH)_3$

$Fe(OH)_3$ has been used to pre-concentrate a range of NDS nuclides from seawater, including ^{238}U, ^{234}Th, ^{210}Pb and ^{210}Po (Kim *et al.*, 1999) and has also been applied in methods involving LSS (Pates *et al.*, 1996). In this technique, an Fe^{3+} carrier solution is added to the sample. The pH is raised by addition of NH_4OH, causing an $Fe(OH)_3$ precipitate to form. Because the Fe^{3+} is added in excess to other dissolved metals it can co-precipitate other metals from solution. This technique has been applied in both radiochemical and non-radiochemical analysis. A review of applications of the $Fe(OH)_3$ precipitation technique can be found in Crompton (1993).

The $Fe(OH)_3$ precipitation has been used to co-precipitate ^{210}Pb and ^{210}Po in a wide variety of aquatic matrices. Sarin *et al.* (1992), Benninger (1978), Craig *et al.* (1973), Nozaki *et*

al. (1998) and many other workers have successfully applied it to seawater analysis. Hussain and Krishnaswami (1980, 1982), Church *et al.* (1994) and Harada *et al.* (1989) have applied the technique to groundwater. In a study of Florida ground water, Harada *et al.* (1989) found differences between the "$Fe(OH)_3$-scavengeable ^{210}Po" and "total ^{210}Po." They found between 30 and 80 % of the natural ^{210}Po failed to co-precipitate with the $Fe(OH)_3$. It may be that the chemical and geochemical conditions in the aquifer caused ^{210}Po to be in a form that was not able to co-precipitate with the iron. Harada *et al.* (1989) suggest that this may be a result of the high sulphide concentration (> 10 μM H_2S), the low pH (< pH 5) or simply a result of the very high ^{210}Po levels reported in that aquifer (~17 Bq l^{-1}). This study suggested that $Fe(OH)_3$ precipitation may not be suitable for some groundwater samples. Chakravarty and Van Grieken (1982) examined the co-precipitation behaviour of $Fe(OH)_3$ and Pb in a range of water types to examine the effect of the sample matrix on the overall recovery. They observed 100 % recovery in bi-distilled water, 3 % NaCl and North Sea water, which indicates the $Fe(OH)_3$ scavenging efficiency not influenced by the sample matrix.

The Fe^{3+} carrier was prepared using the method of Pates (1995) to remove any U or Th contamination. 11 g of analytical grade $Fe(NO_3)_3.9H_2O$ were dissolved in 50 ml 9 M HCl with gentle heating. Fe^{3+} was then extracted into 3 successive 50 ml aliquots of di-isopropyl ether (DIPE). The aqueous phase was discarded and Fe^{3+} was back-extracted into 150 ml of 1.2 M HCl. This creates an Fe^{3+} carrier solution of around 10 mg ml^{-1} which can be stored without the risk of hydrolysis due to the acidification in 1.2 M HCl. Pates (1995)

suggests that the Fe^{3+} concentration in the sample should be around 10 mg l^{-1} to achieve optimum co-precipitation yields for Th. Thus, for a 20 litre sample, 20 ml of the Fe^{3+} solution were added.

The precipitation of Fe^{3+} as $Fe(OH)_3$ is achieved by adding sufficient 18 M NH_4OH to raise the pH of the solution to pH 9. Various Fe^{3+} concentrations, equilibration times and precipitation pH values can be found in the literature. Chakravarty and Van Grieken (1982) examined the pH dependence of Mn, Ni, Cu, Zn and Pb co-precipitation with $Fe(OH)_3$ from a 10 mg l^{-1} Fe solution. With the exception of Mn, a pH of 9 gave the optimum recovery (Pb was fully precipitated at pH 6). Sarin *et al.* (1992) also used a pH value of 9 for co-precipitation of U, Th, Pb and Po. Harada *et al.* (1989) used a pH value of 8 when measuring ^{210}Pb, ^{210}Bi and ^{210}Po. A pH value of 9 was chosen for this work as it will allow full precipitation of ^{210}Pb, ^{210}Bi and ^{210}Po. If too high a pH value is reached, Ca and Mg may co-precipitate, and interfere with the subsequent chemistry. Table 2.1 illustrates the various Fe^{3+} concentrations, spike equilibration times and $Fe(OH)_3$ equilibration times found in the literature. Chung *et al.* (1983) found that Pb spike equilibration times had no discernable effect on the Pb recovery. Therefore, the procedure for this study was based on speed of sample processing. The concentration of Fe^{3+} carrier that was employed is higher than several other methods where ^{234}Th measurements were also carried out (Sarin *et al.*, 1992; Harada *et al.*, 1983; Kim *et al.*, 1999). Lower Fe^{3+} concentrations were used in these experiments to minimise ^{238}U co-precipitation and consequently minimise the activity of ^{234}Th resulting from decay of ^{238}U.

Author	Sample Volume	Fe^{3+} concentration	Spike equilibration	pH for precipitation	Equilibration time
Kim *et al* (1999)	20 l	3.5 mg l^{-1}	3 hours	8	4 -5 hours
Wei and Murray (1994)	18 l	2.8 mg l^{-1}	12 hours	8	*
Craig *et al* (1973)	20 l	10 mg l^{-1}	*	*	*
Sarin *et al* (1992)	25 l	2.8 mg l^{-1}	3 hours	7	3 hours
Harada *et al* (1989)	4 l	5 mg l^{-1}	*	8	*
Tanaka *et al* (1983)	50 l	2 mg l^{-1}	6 hours	*	*
Chung and Craig (1983)	20 l	15 mg	36 hours	8.5	*
This study	20 l	10 mg l^{-1}	12 hours	9	2 hours

Table 2.1: Various Fe^{3+} concentrations, spike equilibration and $Fe(OH)_3$ equilibration times found in the literature and in this study (* = not reported).

2.2.3.2 Trial pre-concentration with $Fe(OH)_3$

A 20 litre seawater sample was filtered through 0.22 μm cellulose nitrate filters. The filtrate was acidified to pH 2 with 15 M HNO_3. 20 ml of Fe^{3+} carrier (10 mg ml^{-1} Fe^{3+}) and ^{210}Pb were added and the sample was shaken and left for 12 hours to allow the spike and Fe^{3+} carrier to equilibrate with the sample (Benninger, 1978). After this time, approximately 50 ml of 18 M NH_4OH were added to raise the pH to 9. The sample was shaken vigorously for 2 minutes and the solution was bubbled with air for 20 minutes to ensure that full precipitation and thus maximum scavenging efficiency were achieved. The sample was then left for two hours to allow the precipitate to fully form and settle out.

The filtering apparatus used in this work changed throughout the research as larger diameter filtering apparatus became available. Much of the initial work had to be carried out using 47 mm diameter filters (0.22 μm pore size). This resulted in filtering operations taking close to five days and hence it was time efficient to store the precipitate for at least one day to allow settling of the precipitate. A floating filtering apparatus was designed to allow the

surface waters to be filtered without disturbing the settling precipitate (Fig. 2.7) but the process was still very time consuming.

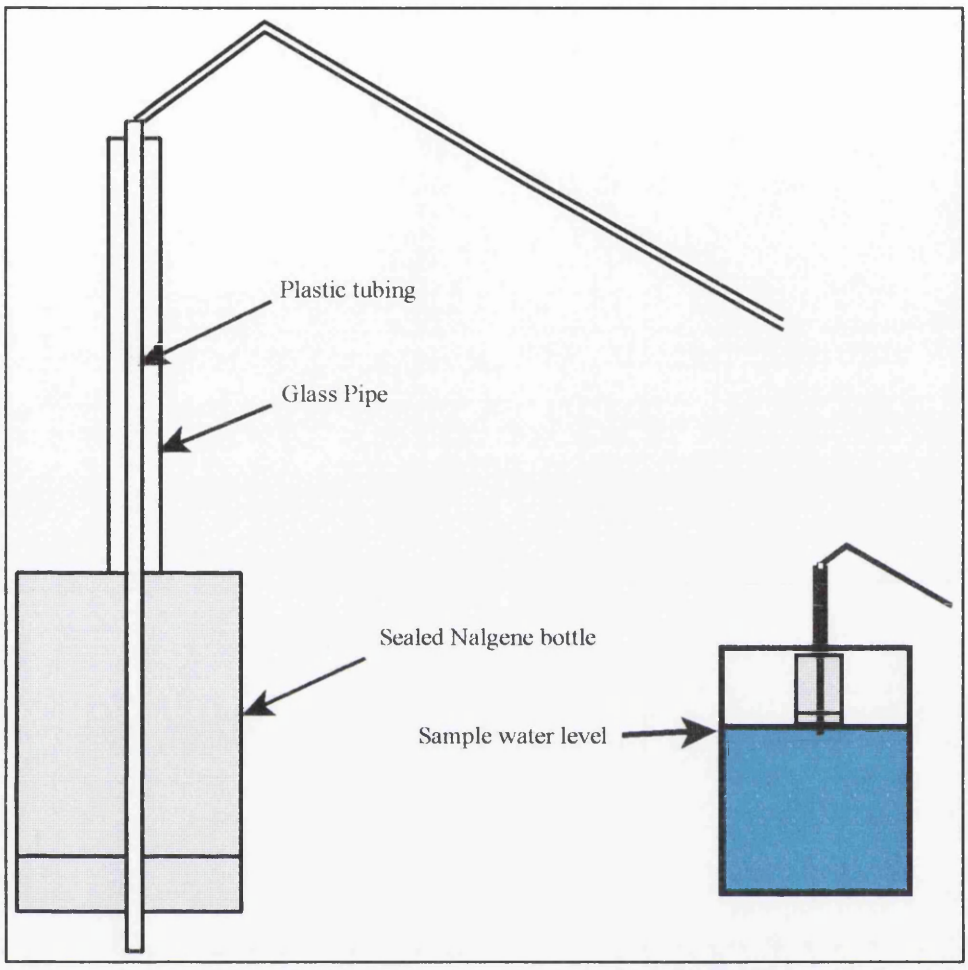

Figure 2.7 Ballcock filtering apparatus designed to filter the surface water without disturbing the $Fe(OH)_3$ precipitate. The plastic tubing was sealed into both ends of a 100 ml Nalgene bottle with epoxy resin. The glass pipe (in conjunction with a guide on top of the sample container) kept the device vertical.

At the beginning of 1999, a larger diameter filtering rig which accepted142 mm diameter filters became available. This reduced the filtering time to around 6 hours. In April 2000 an even larger filtering rig, which held 293 mm diameter filter papers, was constructed. This allowed the filtering to be carried out in 20 minutes.

The big advantage of this technique over the Co-APDC method is the ease of removal of the $Fe(OH)_3$ precipitate from the filter paper and apparatus, as $Fe(OH)_3$ is easily dissolved in dilute HCl. A range of different HCl molarities were examined. Although the HCl molarity had no effect on the removal of the precipitate, it was found that washing the paper with stronger than 6 M HCl began to degrade the filter papers. This had implications for the subsequent separation chemistry and several samples were found to contain a white colloidal material. However, to use large volumes of weaker HCl to dissolve the $Fe(OH)_3$ is also not ideal as it leaves a much larger sample to be processed. To overcome both of these problems, the large cellulose nitrate filters were simply placed in the base of large evaporating dishes and 10 ml of 2 M HCl were added. The acid was swirled around, allowing contact with all the precipitate. Once the majority of the precipitate was dissolved, the filter paper was removed with tweezers and further washed into the basin with 2 M HCl until the yellow colouration was no longer visible on the filter. In this way, the $Fe(OH)_3$ precipitate could be re-dissolved without dissolving any of the filter paper. This is an important time saving as the sample requires less oxidation if there is no cellulose nitrate present to destroy. This is especially important when short half life nuclides are being determined.

The recoveries of ^{210}Pb, ^{210}Bi and ^{210}Po using the $Fe(OH)_3$ technique are somewhat variable. Table 2.2 shows the recoveries of samples collected from the Irish Sea.

Sample	^{210}Pb % recovery	^{210}Po % recovery
IS 1	39.5 ± 5.0 %	52.4 ± 4.7 %
IS 2	66.9 ± 3.4 %	49.2 ± 3.8 %
IS 3	76.5 ± 3.0 %	56.3 ± 2.8 %
IS 4	49.7 ± 3.8 %	35.9 ± 2.1 %
IS 5	51.7 ± 4.1 %	64.1 ± 2.1 %
IS 6	78.8 ± 3.6 %	42.3 ± 4.1 %
IS 7	76.3 ± 4.4 %	53.1 ± 1.7 %

Table 2.2. Recoveries of ^{210}Pb and ^{210}Bi from 20 litre seawater samples scavenged with $Fe(OH)_3$.

Previous experiments are ignored as much of the variability resulted from other factors (ion exchange problems, POLEX problems etc). There were some disadvantages to the $Fe(OH)_3$ precipitation technique. Namely, the variable yield highlighted the need for chemical yield tracers in this methodology. Also, if Fe^{3+} is not removed from the sample, it will have a quenching effect in the LS cocktail (Section 1.3). The advantages of this technique lie in the ease of dissolution of the $Fe(OH)_3$ precipitate. It can be easily removed from the filter without the need for lengthy oxidation of the cellulose nitrate filters. This allows the sample to be processed quicky and decreases the losses by volatilisation. The filtering equipment and sample containers are easily cleaned in a weak acid solution which minimises sample cross-contamination. The precipitate can be washed to remove any co-precipitated salts from the sample which may interfere with the subsequent chemistry. Finally, it is a simple and inexpensive technique suitable for many sample matrices. For these reasons $Fe(OH)_3$ was chosen as the method of pre-concentration.

Without the time constraints of this project it would have been beneficial to examine the $Mn(OH)_4$ and $Mg(OH)_2$ scavenging techniques. The advantage of the $Mg(OH)_2$ method for Pb scavenging is that a divalent scavenging ion has more likelihood of scavenging a larger percentage of dissolved Pb than with Fe^{3+}.

2.3 Extractive scintillators

One method for the separation and measurement of polonium uses an extractive scintillator. An extractive scintillator is a specialized scintillation cocktail that contains both a selective extraction agent and the solvent and fluors necessary for the radioactive decay to be detected by the PMTs in the LS spectrometer.

Extractive scintillators were developed in the 1970s by McDowell and co-workers (McDowell and Coleman, 1974; McDowell *et al.*, 1980) to determine a range of α emitting nuclides in the PERALS (Photon/Electron Rejecting Alpha Liquid Scintillation) spectrometer. The PERALS spectrometer has a single PMT and uses pulse shape analysis to separate α from β/γ induced pulses (Thorngate *et al.*, 1974). The system was developed to obtain the best α/α resolution, and the rejection of β/γ induced pulses makes PERALS unsuitable for β spectrometry. This discrimination allows very low α activity to be determined without interference from β/γ induced pulses which would otherwise underlie the α spectrum. In addition to their selectivity, extractive scintillators also reduce the amount of quenching and the background count rate in a sample since almost nothing is transferred into the scintillator except the analyte nuclide. Quenching agents, such as acids and salts, remain in the aqueous phase, and therefore the α resolution is maximised. Furthermore, the samples are de-oxygenated with a dry, oxygen free gas, which further improves the energy resolution by removing any oxygen dissolved in the scintillator, and the associated quenching effect. There now exists a range of extractive scintillators for the commonly analysed α emitters (Table 2.3). Although the extractants are different, the same

chemical principals hold for all the extractive scintillators.

Extractive Scintillator	Elements extracted
ALPHAEX	Th, Pa, U, Np, Pu, Am, Cm, Bk, Cf, Es, Fm, Md and No. *Does not extract Ra*
URAEX	Selectively extracts uranium.
THOREX	Extracts thorium and uranium.
POLEX	Selectively extracts polonium.
RADEX	Selectively extracts radium
RADONS	Selectively extracts radon from water and aqueous solutions
STRONEX	Strontium selectivity

Table 2.3: The range of commercially available extractive scintillators and the elements they can extract.

The use of extractive scintillators combined with the PERALS system has been applied to a number of transuranic elements in range of sample matrices, from waste material from the phosphate industry to low level environmental studies. The studies include: U on cellulose air filters (McDowell and Case, 1986); gross α activity in environmental materials (McDowell, 1986); U and Th in phosphate materials by sequential extraction into URAEX followed by THOREX (McDowell *et al.*, 1980); Pu on filters and smears (Shaw, 1991); ^{226}Ra in groundwater and ocean water samples (Burnett and Tai, 1992); and Po in U tailings (Case and McDowell, 1982). However, extractive scintillators are not limited to use in PERALS spectrometry (α/α LSS). They have also been applied in standard α/β LSS (Dazhu *et al.*, 1991; Kaihola and Oikari, 1991; Möbius *et al.*, 1993), which is also able to differentiate α from β^- events and therefore reduce the effect of co-extracted β^-s on the α background. Combining α/β LSS with extractive scintillators is becoming increasingly important as it allows determination of any co-extracted β^- or γ emitters in the sample.

Although, unlike the PERALS spectrometer, resolution of individual α peaks is much more limited.

2.3.1 Polonium specific extractive scintillators

The extractive scintillator, POLEX is, as the name suggests, a polonium specific extractive scintillator. The extractive scintillator is composed of 77 g l^{-1} trioctylphosphine oxide (TOPO), 180 g l^{-1} scintillation grade naphthalene and 4 g l^{-1} 2-(4'-biphenylyl)-6-phenylbenzoxazole (PBBO) dissolved in toluene. The extractive agent, TOPO, is an excellent extractant for Po in hydrochloric media (White and Ross, 1961). 100 % polonium extraction is easily obtained and a distribution co-efficient of over 1000 can be obtained (representing partitioning into the organic phase) (Case and McDowell, 1982). Po is extracted from a matrix of H_3PO_4 and HCl. In this matrix Po can be extracted as $PoCl_4.2$(TOPO) into the scintillation cocktail.

Case and McDowell (1982) successfully applied this method to the determination of ^{210}Po in ores, mill tailings and environmental samples. By extraction from an aqueous solution of 7.4 M H_3PO_4 - 0.01 M HCl into POLEX it was possible to obtain a detection limit of 0.141 mBq using PERALS spectrometry. In HCl solutions, Bi can also be extracted by TOPO and this makes it necessary to count the samples within 8 hours of extraction to prevent any significant ingrowth of ^{210}Po from its parent ^{210}Bi. Momoshima *et al.* (1994) used the extraction properties of TOPO to determine ^{210}Bi and ^{210}Po on pine needles. The co-extraction of Bi^{3+} (β^--emitter) with Po^{4+} (α-emitter) was utilised by Wallner (1997) and

Wallner and Irlweck (1997) who combined the extractive scintillator, POLEX, with α/β LSS to simultaneously determine ^{210}Pb and ^{212}Pb progenies in aerosol samples. POLEX extracts ^{210}Bi and ^{210}Po into the organic phase while ^{210}Pb remains entirely in the aqueous phase. After an initial extraction of Bi and Po, the sample is stored for two weeks and the extraction is performed again. This time the scintillator only contains ^{210}Bi, which has been produced from the decay of ^{210}Pb that remained in the aqueous phase. The ingrowth of ^{210}Bi is then used to determine the ^{210}Pb activity in the sample. The methods employed by Case and McDowell (1982), Wallner (1997) and Wallner and Irlweck (1997) were tracer free methods because of the high levels of reproducibility that were achieved.

The use of extractive scintillators in the development of this method was beginning to look favourable, because the method did not necessarily have to provide absolute activities. In marine disequilibrium studies, it is the ratio of daughter/parent that is important and not the actual activity. Extractive scintillators offered a fast, highly reproducible method, which would reduce the time of analysis from over six months to around two weeks.

2.3.2 Experiments with extractive scintillators

2.3.2.1 Choice of vials and purging

Two issues had to be addressed before attempting to extract ^{210}Bi and ^{210}Po into POLEX:

(i) What is the best method to count a 1 ml aliquot of POLEX?

(ii) Is purging to remove O_2 suitable for samples counted by α/β LSS?

The effect of purging the extractive scintillator was examined in conjunction with an examination of the best vial types to use. Three vial types were chosen:

1. a 2 ml low potassium borosilicate glass vial placed in a 7 ml plastic vial (Packard)
2. a 7 ml plastic vial (Packard).
3. a 7 ml low potassium borosilicate glass vial (Packard).

A 1 ml aliquot of POLEX (no spikes or extraction) was pipetted into each vial type in triplicate. The vials were counted fifteen times for 1 minute on a Packard 2770 TR/SL LS spectrometer. The same vials were then purged for two minutes with nitrogen gas and capped as quickly as possible. The vials were then recounted under the same conditions to examine the effect of purging on the quenching of each sample in the three vial types by examining the tSIE factor. The 15 tSIE factor for each vial were averaged and the data for purged and unpurged vials are presented in Table 2.4.

		Replicate 1	SD 1	Replicate 2	SD2	Replicate 3	SD3
Type 1	unpurged	**809.1**	16.31	**809.0**	11.98	**802.1**	12.36
Type 2	unpurged	**802.1**	12.36	**792.6**	15.02	**809.3**	13.90
Type 3	unpurged	**731.6**	11.08	**742.6**	8.25	**745.9**	7.05
Type 1	N_2 purged	**946.8**	27.43	**997.3**	17.47	**997.7**	11.87
Type 2	N_2 purged	**959.6**	15.18	**996.5**	16.80	**984.5**	16.72
Type 3	N_2 purged	**897.3**	7.51	**897.8**	7.38	**900.0**	6.32

Table 2.4: The effect of vial choice and N_2 purging on the tSIE values obtained from 1 ml aliquots of neat POLEX counted on a Packard 2770 TR/SL. Three vial types were investigated (all Packard). Type 1: a 2 ml low potassium borosilicate glass vial placed inside a 7 ml plastic vials. Type 2: a 7 ml plastic vials. Type 3: a 7 ml low potassium borosilicate vial. Each vial type was measured in triplicate and counted 15 times each. The results for each vial type were averaged and the standard deviation calculated.

Clearly, the tSIE factors afterN_2 purging show a reduction in quenching (higher tSIE) than unpurged samples for all vial types, due to the removal of O_2 from the cocktail. The average tSIEs of glass vials were lower than for the plastic vials, but the difference in counting efficiency between plastic and glass vials resulting from slightly lower tSIE values would be small. The variation in tSIE over the 15 measurements was also examined. The variation in purged vials is larger for plastic vials, suggesting that the closure mechanism is not as effective as that of the glass vials. The 7 ml glass vials showed the least variability in both unpurged and purged samples and it was decided to use these for future work. If α/β LSS is to be carried out on a $^{210}Bi/^{210}Po$ mixture, variable quench would affect the α/β separation (Pates *et al.*, 1998), therefore, the vials which offer the most stable tSIE values are required.

2.3.2.2 Extraction of ^{210}Bi and ^{210}Po

Next, the extraction of ^{210}Bi and ^{210}Po into the extractive scintillator had to be examined. Although the extraction of ^{210}Po is stable over a wide range of HCl molarities, the extraction of ^{210}Bi is dependent on the HCl molarity of the aqueous phase. Two extractions were performed to examine this effect, one with 0.01 M HCl and the other with 0.1 M HCl. 7 M H_3PO_4 was used for all extractions and ^{210}Pb activity remained constant (8 Bq). 1 ml of either 0.1 M or 0.01 M HCl containing the ^{210}Pb spike was mixed with 4 ml of 7 M H_3PO_4 and 2 ml POLEX were added. This procedure was carried out in triplicate. The vials were shaken end-over-end for 30 minutes and left to stand a further 20 minutes for complete phase separation. A 1 ml aliquot of the extractive scintillator was pipetted into a 7 ml glass scintillation vial. The vial was then placed in a Packard 2770 TR/SL LS spectrometer for

at least 1 hour prior to counting to allow the sample to cool and any chemiluminescence to die out and counted on NCM for 100 minutes. Once the count was complete, the extracted POLEX was then purged for 2 minutes with N_2 and recounted. A mathematical solution was used to allow the composite spectra to be examined for ^{210}Bi and ^{210}Po activity by manipulating the spectra with the SpectraWorks software package (Packard). Five channels either side of the ^{210}Po peak were selected and the counts of ^{210}Bi either side of the ^{210}Po peak used to calculate the counts of ^{210}Bi underlain by ^{210}Po. The ^{210}Po activity could then be estimated by subtracting the ^{210}Bi counts from the total counts in that area. 100 % counting efficiencies were assumed for both ^{210}Po and ^{210}Bi. Relative recoveries were calculated for the 1 ml aliquots and the results are presented in Table 2.5.

	Unpurged		**N_2 purged**	
Acid type	^{210}Bi extraction (%)	^{210}Po extraction (%)	^{210}Bi extraction (%)	^{210}Po extraction (%)
0.01M HCl	8.1 ± 1.8 %	49.2 ± 1.8 %	9.2 ± 2.1 %	20.3 ± 2.4 %
0.1 M HCl	88.4 ± 6.0 %	98.3 ± 6.0 %	89.7 ± 5.4 %	45.2 ± 3.4 %

Table 2.5. The mean relative recovery (%) of ^{210}Bi and ^{210}Po into POLEX using 1 ml 0.1 M or 0.01 M HCl and 4 ml 7 M H_3PO_4 as the sample matrix. The same vials were purged with N_2 and recounted. The relative recovery represents both chemical recovery and counting efficiency.

The averaged spectra obtained are shown in Figure 2.8. Purging samples with N_2 prior to counting removes any dissolved oxygen within the scintillator which can cause quenching. However, the net effect was a lowering of α counting efficiencies for both HCl molarities. The removal of dissolved oxygen increases the delayed component on the scintillation pulse. This longer pulse width results in the rejection of true events as background by the BCC that must exist in the NCM on the 2770 TR/SL LS spectrometer. This effect is mainly confined

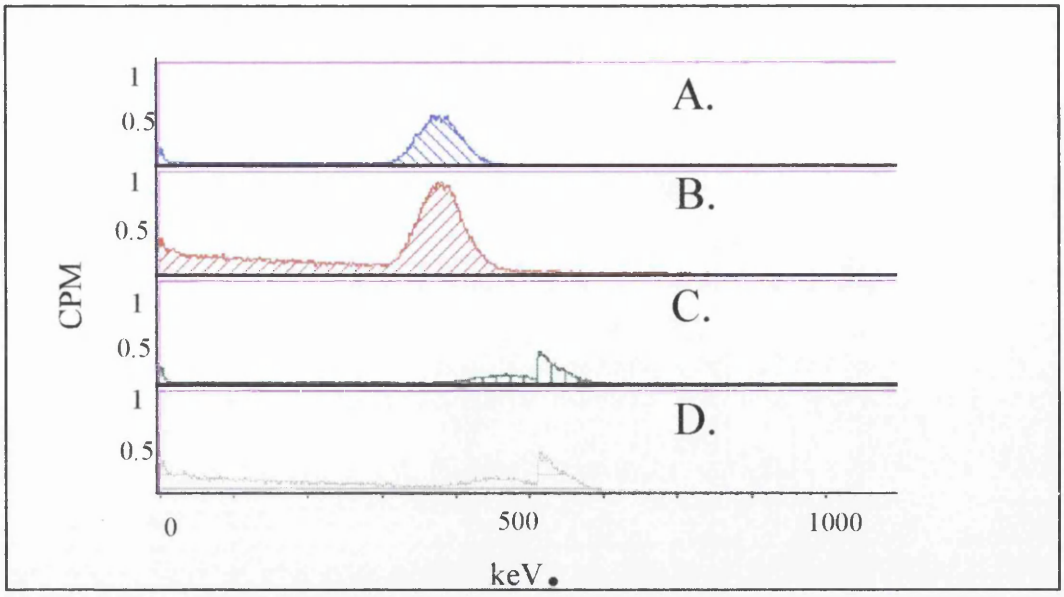

Figure 2.8. Averaged spectra of purged and unpurged extractions with 0.01 M and 0.1 M HCl in a Packard 2770 TR/SL LS spectrometer. A: 0.01 M HCl (unpurged). B: 0.1 M HCl (unpurged). C: 0.01 M HCl (purged). D: 0.1 M HCl (purged).

to α induced scintillation pulses due to their larger delayed component (Section 1.3.3). Generally, purging of extractive scintillators for analysis by α/β LSS utilising PSD should be avoided. In the PERALS system, the circuitry and optics are optimized to measure only the very long pulses, while in α/β LSS, the circuitry is less specialized towards α analysis. However, when the same vial was counted on a Packard 2250 CA LS spectrometer there was no obvious degradation of the α peak (Fig. 2.9). The difference between the spectrometers must be related to the background reducing circuitry on the 2770 TR/SL.

Extraction of ^{210}Bi with 0.1 M HCl looked to be a highly selective extraction but to find the optimum molarity of HCl, a series of extractions was performed. White and Ross (1961) established that no extraction of ^{210}Bi occurs in more than 4 M HCl systems and because 0.1 M HCl gave such good results it was decided to focus around that region. If ^{210}Pb was

extracted into POLEX, its presence would be observed in the 0 to 40 keV region.

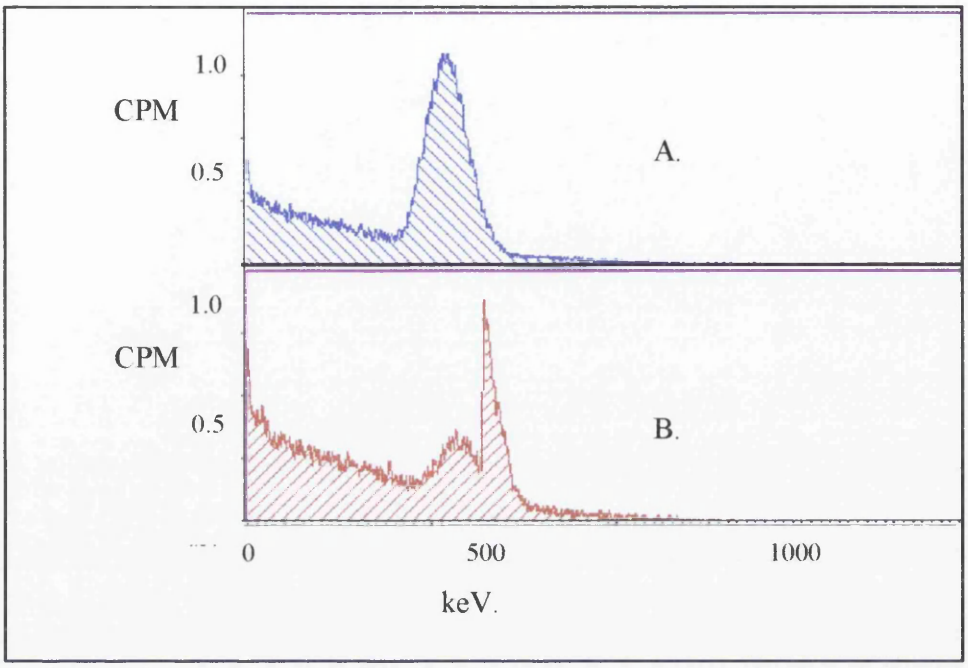

Figure 2.9. Comparison of spectra of purged samples in Packard 2250 CA and 2770 TR/SL liquid scintillators. A = 2250 CA spectrum and B = 2770 TR/SL spectrum.

Hydrochloric acid solutions spiked with 8 Bq of ^{210}Pb (in equilibrium with ^{210}Bi and ^{210}Po) were made up in the following HCl molarities: 0.01 M, 0.05 M, 0.075 M, 0.1 M, 0.25 M, 0.5 M, 1.0 M. 4 ml 7 M H_3PO_4 and 2 ml POLEX were added to 1 ml of spiked HCl. Triplicate extractions were carried out as before, but without N_2 purging. The vials were counted on NCM for 100 minutes on a Packard 2770 TR/SL and the relative recoveries of ^{210}Po and ^{210}Bi determined by the mathematical technique described previously. The results are presented in Figure 2.10. The maximum extraction of ^{210}Bi and ^{210}Po occurred with HCl molarities above 0.1 M while no ^{210}Pb extraction was observed below 0.25 M HCl. From the results obtained it was decided to use 0.1 M HCl and 7 M H_3PO_4 as the extraction matrix

for Bi and Po. This molarity would ensure a high extraction of Bi and Po into the TOPO based scintillator but that no ^{210}Pb was co-extracted in the first extraction.

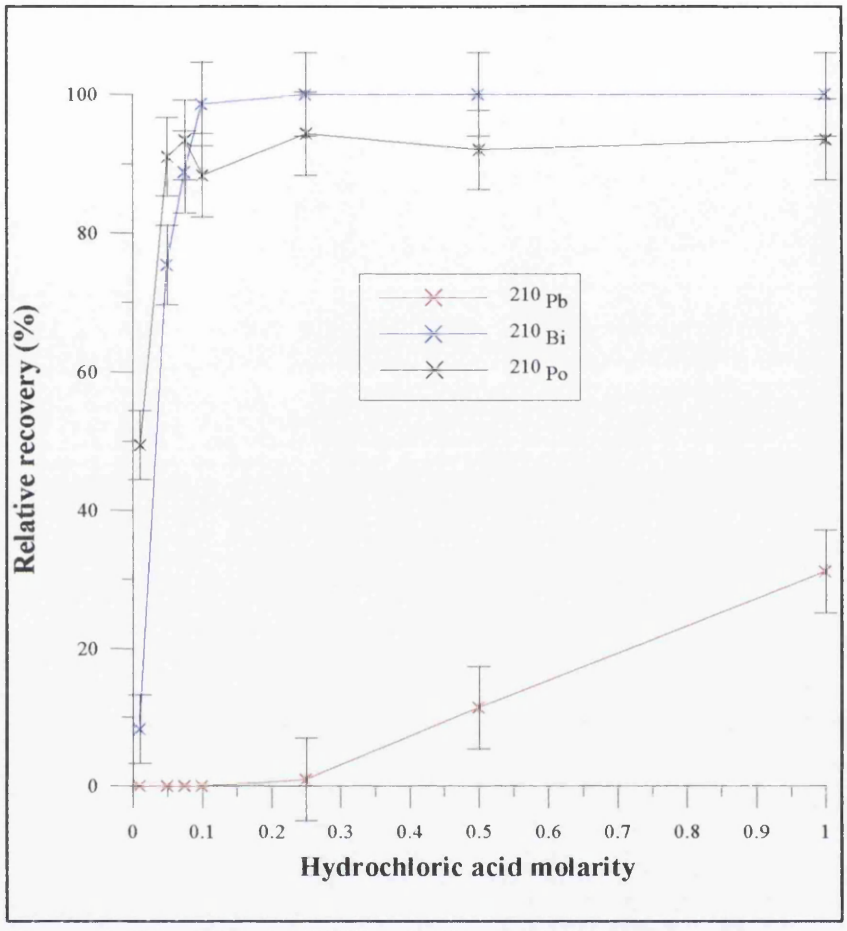

Figure 2.10: Effect of HCl molarity on Pb/Bi/Po extraction with POLEX.

Before any experimental based work was carried out, the reproducibility of the TOPO extraction was investigated using ten replicate extractions on the chosen extraction matrix (Fig. 2.11). The TOPO extraction of Bi and Po seemed to be highly reproducible with mean efficiencies of 85.9 ± 4.9 % and 99.6 ± 6.4 % for ^{210}Po and ^{210}Bi. The degree of quenching also remained constant in the unpurged samples (mean tSIE = 695.3 ± 4.6). The Po extraction (assuming 100 % efficiency) is only 85 % efficient but an immediate re-extraction

from the aqueous phase yielded no more Po. A possible source of error could have been the mathematical method used to determine ^{210}Po and ^{210}Bi activities.

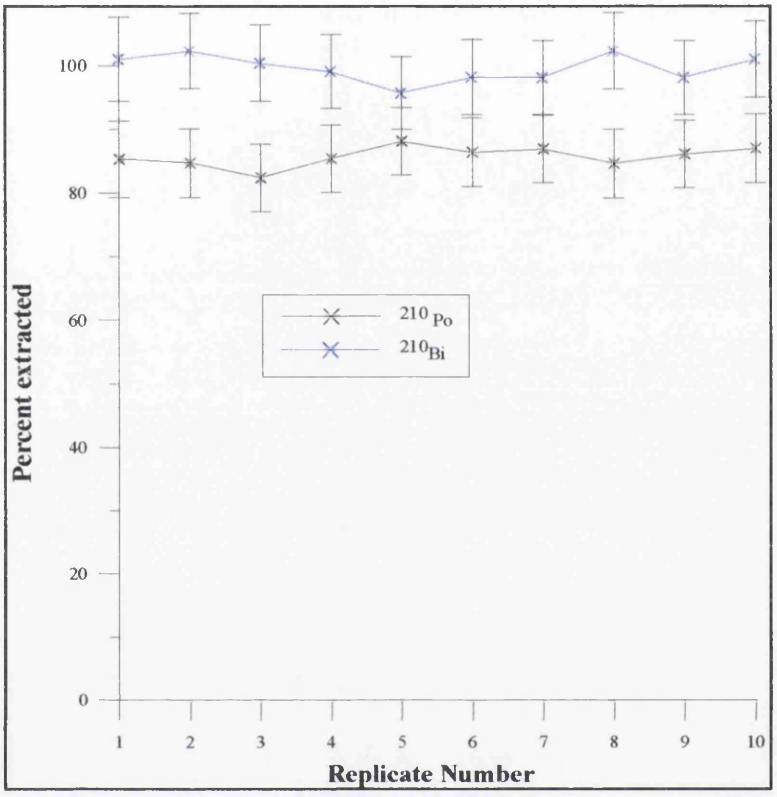

Figure 2.11: Reproducibility of POLEX extraction of ^{210}Bi and ^{210}Po.

At this stage, the samples were not counted using α/β LSS, as purified aliquots of ^{210}Bi and ^{210}Po could not yet be achieved to find the optimum time discriminator setting to allow an accurate determination.

2.3.2.3 α/β separation of ^{210}Bi/^{210}Po in POLEX

α/β LSS was investigated to simultaneously determine ^{210}Po and ^{210}Bi and to overcome the

possible errors introduced when ^{210}Po and ^{210}Bi were calculated mathematically. To find the optimum PDD setting requires purified individual aliquots of ^{210}Po and ^{210}Bi. The first POLEX extraction will produce a vial containing ^{210}Bi (pure β^- emitter) and ^{210}Po (pure α emitter). At this stage, no suitable technique was available to separate ^{210}Bi and ^{210}Po successfully. However, a virtually pure source of ^{210}Po is available by recounting a previous extraction after the decay of ^{210}Bi (to ^{210}Po). Counting ^{210}Po on a range of PDD settings in NCM for 100 minutes on the 2770 TR/SL allowed an estimate to be made of the optimum PDD setting (Fig. 2.12). Then a mixture of ^{210}Bi and ^{210}Po was counted at PDD settings close to the optimum setting and misclassification into either MCA was monitored visually from the spectrum obtained and the PDD adjusted manually. The percentage spill was calculated from each PDD setting. Misclassified α events in the β MCA can be observed as an α peak over a β continuum, while any misclassified β events in the α MCA can be observed below the main α peak. Although not an ideal technique for separation of ^{210}Bi and ^{210}Po, it offers an improvement of earlier techniques whereby the amount of ^{210}Bi underlying the ^{210}Po peak was calculated from the counts of ^{210}Bi either side of it. The optimum PDD for α/β LSS was found to be 191. When α/β LSS was applied to POLEX extracted ^{210}Bi and ^{210}Po it was found that the relative recoveries of ^{210}Po and ^{210}Bi were 95.3 $\pm$ 3.1 % and 94.1 $\pm$ 3.2 %. The associated counting errors using α/β LSS rather than conventional LSS are around half those obtained using the mathematical method of calculating recoveries. This suggests that the previously used method, combined with the greater errors may have led to lower ^{210}Po recoveries being reported.

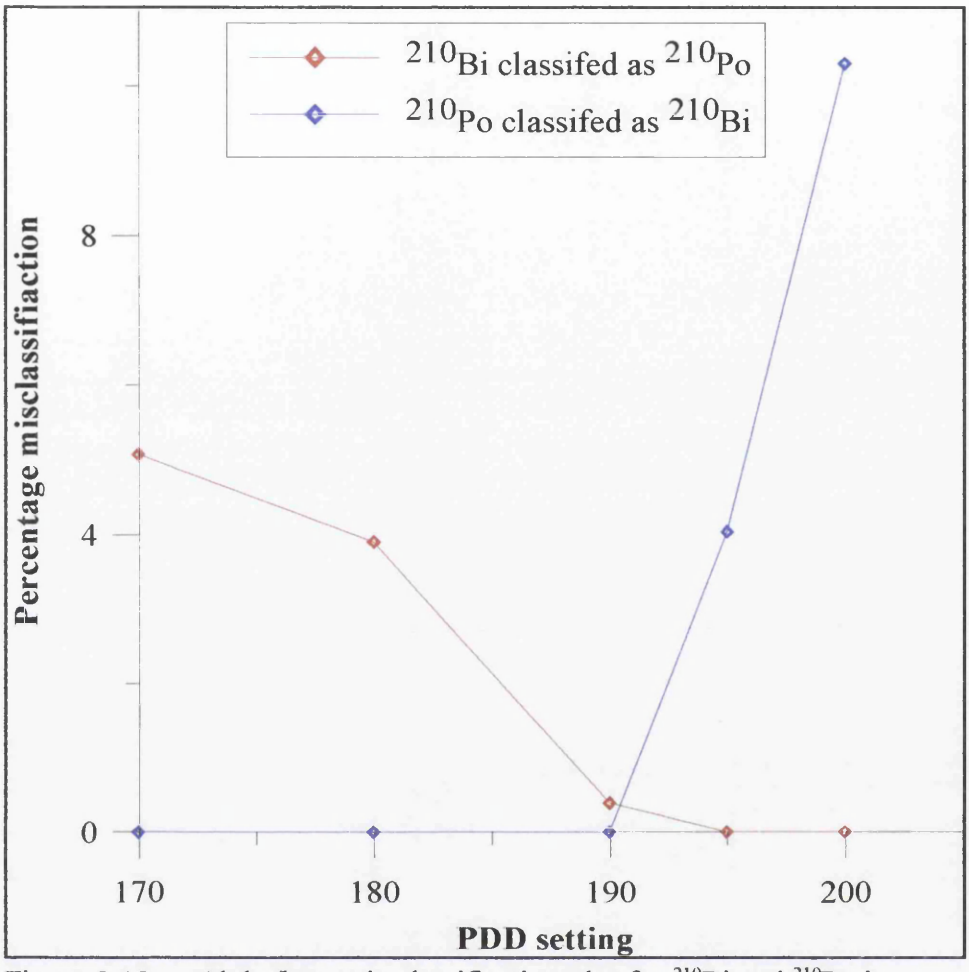

Figure 2.12: Alpha/beta mis-classification plot for ^{210}Bi and ^{210}Po in POLEX.

2.3.3 Freeze drying of samples

In early development of the method, the sample was taken to dryness in a 7 ml vial on a hotplate to evaporate the final traces of acid prior to re-dissolution in 1 ml of 0.1 M HCl and 4 ml of 7 M H_3O_4. If the vial was over heated at this stage, the residue in the vial would bake onto the vial wall and not be totally dissolved in 1 ml 0.1 M HCl. The resulting chemical recovery would be lower due to the presence of these undissolved particles

suspended in the extraction medium. This undissolved material could also have a quenching effect on the sample. On the other hand, if the sample is not dried sufficiently, there is a danger of acid remaining in the vial before the addition of 1 ml 0.1 M HCl and 4 ml 7 M H_3PO_4. The effect of this would be to raise the HCl molarity above 0.1 M and therefore cause partial extraction of ^{210}Pb alongside ^{210}Bi and ^{210}Po extraction (Fig. 2.10). Co-extraction of ^{210}Pb must be avoided. The presence of ^{210}Pb in the vial can be determined from visual inspection of the spectrum (a peak from 0 to 40 keV). Alternatively, the presence of co-extracted ^{210}Pb can monitored by recounting the vial after two weeks. Unsupported ^{210}Bi will decay according to its 5.013 day half-life, but ^{210}Bi supported by ^{210}Pb will remain. The method of Wallner (1997) relies on the determination of ^{210}Pb by the ingrowth of its daughter after around two weeks, but co-extraction of Pb at the first extraction would invalidate the results. The hotplate evaporation method is susceptible to losses either by volatilisation of ^{210}Po or by baking the sample onto the vial.

Freeze drying was proposed as a method for the removal of the final traces of acid from the sample. A conventional freeze drier could not be used as the acids that were removed from the sample would corrode the pump and other components. Instead, a freeze drying apparatus was constructed by connecting a large desiccator to a cold trap which was in turn connected to a vacuum pump (Fig. 2.13). This system allowed the acidic vapours to be frozen in the cold trap surrounded by a dewar of liquid nitrogen (LN_2), and prevented any acid being taken into the pump. This provided a method for drying samples without time consuming monitoring of the hotplate evaporation process.

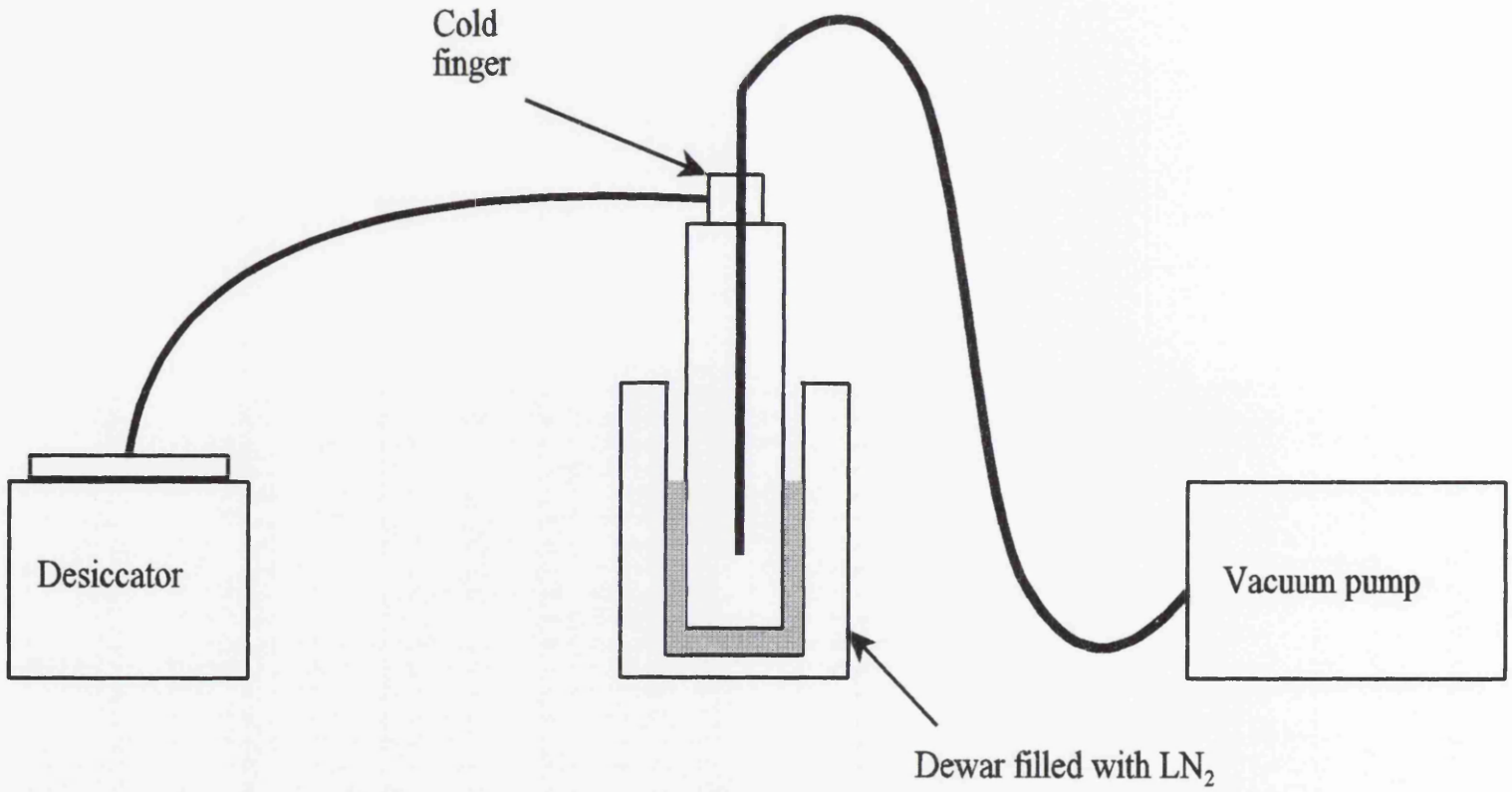

Figure 2.13: Diagram of the apparatus constructed to freeze dry the sample prior to uptake into POLEX extraction medium.

To check the recovery of ^{210}Bi and ^{210}Po using the freeze drying technique, 8 Bq of ^{210}Pb spike (with ^{210}Bi and ^{210}Po in equilibrium) was pipetted into a vial and freeze dried. In conjunction with this, an identical vial of ^{210}Pb spike in 0.1 M HCl was prepared at the same time. Once the first vial had been freeze dried, the residue was re-dissolved in 1 ml 0.1 M HCl and left overnight. ^{210}Bi and ^{210}Po were extracted out of both vials into POLEX 24 hours later and counted by LSS (Section 2.1.3). The results showed that the relative recovery of both samples was identical which shows that freeze drying and re-dissolution had no effect on the recovery as the residue was totally re-dissolvable (Table 2.6).

	^{210}Bi relative recovery	**^{210}Po relative recovery**
Control vial	96.1 ± 3 %	95.5 ± 3 %
Freeze dried vial	94.9 ± 3 %	95.2 ± 3 %

Table 2.6: Comparison between ^{210}Bi and ^{210}Po extracted into POLEX from a control vial (containing ^{210}Pb in 1 ml 0.1 M HCl) and a freeze dried ^{210}Pb spike re-dissolved in 1 ml 0.1 M HCl.

Once set up, the freeze drier can be left unattended until the process is complete, the only requirement being that the analyst maintains the level of LN_2 in the dewar. Hotplate evaporation needs virtually constant monitoring to prevent the sample spluttering or being over heated in the vial. However, a sample carefully evaporated on a hotplate can also be re-dissolved giving full recovery. Hotplate evaporation is a much faster technique and can be carried out in a few hours while the freeze-drying process requires around 12 hours to remove 1 ml of acid (this will vary depending on the degree of vacuum that can be obtained). If measurements of ^{210}Bi ($t_{½}$ = 5.013 days), or more importantly, ^{212}Pb ($t_{½}$ = 10.6 hours) are

required where the latter is used as a tracer for ^{210}Pb (Section 2.8.1), then the emphasis must be on preparing the purified sample for counting as quickly as possible. Freeze drying is therefore not ideal for this type of work but it does represent a useful technique for the careful removal of liquid from a sample.

2.3.4 Problems in POLEX extraction

A twenty litre seawater sample was filtered through 0.22 μm cellulose nitrate papers, and acidified with 50 ml of 12 M HCl. 20 ml of Fe^{3+} carrier (10 mg ml^{-1} Fe^{3+}) and 1 ml of ^{210}Pb spike in 0.1 M HCl (activity = 8 Bq) were added, the sample shaken vigorously and left overnight to allow the spike and carrier to equilibrate with the sample. The following day, 50 ml of 18 M NH_4OH were added and Fe was precipitated as $Fe(OH)_3$. The $Fe(OH)_3$ was collected by filtration through 0.22 μm cellulose nitrate paper and subsequently removed from the filter by dissolving in 50 ml of 6 M HCl. Fe^{3+} carrier was removed from the aqueous phase by shaking three times with an equal volume of DIPE. Not all the Fe^{3+} could be removed from the aqueous phase at this point and the sample was evaporated close to dryness and transferred to a 7 ml scintillation vial. The sample was freeze dried, the residue oxidised with 15 M HNO_3 and again freeze dried. The residue was this time re-dissolved in 6 M HCl and an in-vial DIPE extraction was performed to remove the last traces of Fe^{3+}. Again, the remaining liquid was removed by freeze drying and the residue was dissolved in 1 ml of 0.1 M HCl and 4 ml 7 M H_3O_4. There was a considerable mass of salts in the vial, which must have been co-precipitated with the $Fe(OH)_3$. ^{210}Bi and ^{210}Po were extracted into the TOPO based extractive scintillator as described earlier. The sample was counted by LSS

as described in section 2.1.3. Several problems were observed as a result of the above methodology:

-The tSIE of the sample indicated quenching of the sample, this was probably Fe which had not been removed by the DIPE extraction, this may be in part due to the presence of salts in the final sample which had inhibited the complete removal of Fe^{3+} by DIPE.

-The spectrum of the TOPO bases scintillator also contained co-extracted ^{210}Pb, this suggests that not all the acid was removed by the freeze drying and further that the presence of salts may have required the freeze drying process to have been carried out for longer.

-The residual salts may have influenced the extraction of Pb by POLEX.

This highlighted two important points in the method, namely that the salts should be removed and the vial must be freeze dried until the sample is completely dry. It is possible that other major ions may be responsible for the quenching (Ca, Na or Mg) but Fe seems the most likely due to the yellow colouration of $FeCl_3$. Furthermore, Mg and Ca should not be precipitated with $Fe(OH)_3$ at a pH of 9.

Several more samples were run but the recovery of ^{210}Pb, ^{210}Bi and ^{210}Po varied from sample

to sample. The different yields were most probably caused by variations in the efficiency of the $Fe(OH)_3$ scavenge, and unless this technique could be highly reproducible there would be significant errors in the proposed tracer free method. In a tracer-free method, Wallner and Irlweck (1997) measured ^{210}Pb and ^{210}Po in aerosols where there was minimal chemical manipulation prior to the POLEX separation. At this stage the use of yield tracers was beginning to look important. However, if a Po yield tracer was to be applied to the Po analysis then its determination by LSS would not be possible, as LSS would not be able to differentiate between the α peaks. Therefore, the POLEX technique offered little benefit to the Po extraction as α spectrometry would be required to resolve ^{210}Po from its α emitting tracer.

2.3.4.1 Salt interferences

A visual inspection of the sample prior to the addition of POLEX indicated the presence of salts. When the Fe^{3+} is precipitated as $Fe(OH)_3$ salts may become entrained into the $Fe(OH)_3$ precipitate and their presence may interfere with the POLEX extraction. The method had to be refined to remove these salts. To achieve this, the following methodology was employed.

Once the $Fe(OH)_3$ had been removed from the filter paper with 2 M HCl, 18 M NH_4OH was added to re-precipitate $Fe(OH)_3$. This was transferred to a 50 ml centrifuge tube and spun in a centrifuge for 5 minutes at 3000 rpm. The supernatant was carefully removed and the precipitate washed with 30 ml of reverse osmosis water. The tube was shaken to mix the

water with the $Fe(OH)_3$ precipitate and dissolve the salts into the reverse osmosis water. The sample was re-centrifuged and the supernatant (containing reverse osmosis water and dissolved salts) was discarded, leaving the $Fe(OH)_3$ without the interfering salts. This was repeated twice to ensure all salts had been removed. This technique enabled removal of the salts from the sample and allowed a clearer phase separation of the organic cocktail. As a result, the problems of ^{210}Pb co-extraction into POLEX were eliminated.

2.3.4.2 Coloured samples

Any colouration of the sample will result in quenching of the light output and therefore reduce the counting efficiencies and change the optimum PDD for α/β separation. It is therefore essential to have either a sample which contains no colouration, or a constant degree of colouration (constant tSIE). This means that the counting efficiencies and optimum PDD will be constant for each sample. Frequently, the POLEX cocktail had varying degrees of a yellow colouration which was thought to be the result of incomplete removal of Fe^{3+} carrier prior to the organic extraction. This colouration was transferred from the aqueous phase into the POLEX cocktail and resulted in highly variable tSIE measurements. Despite rigorous and repeated extraction with DIPE it proved extremely difficult to remove this contaminant.

Colour quench curves have previously been used for efficiency corrections in conventional LSS and Cerenkov LSS (L'Annunziata, 1998). Quench curves are commonly used in LSS applications to account for changes in counting efficiency with varying quench. For

example, in ^{3}H measurements, a series of quenched standards are counted and the resultant quench curve of efficiency versus QIP is derived. A quench series is a number of spiked samples which all have the same activity of spike added, but have different amounts of quench agents added (nitromethane being the most popular). This enables the operator to correct for changes in counting efficiency in variably quenched samples. A colour quench curve is based on the same principle, but uses different amounts of a coloured species to vary the counting efficiency.

When an attempt was made to create these colour quench curves for Fe^{3+} in POLEX, it was found that Fe^{3+} was complexed by the H_3PO_4 and was not transferred to the organic phase. This finding ruled out the colouration being the result of Fe^{3+} contamination. Another possibility was residual dissolved organic compounds (DOC), either directly quenching the POLEX, by their partitioning into the organic phase, or indirectly by competing with H_3PO_4 for the complexation of Fe^{3+} and allowing it to cross into the organic phase. Although the sample is well oxidised prior to its extraction into POLEX, residual DOC is the most probable cause of the quenching. Tracer free application of $^{210}Po/^{210}Pb$ via POLEX have been carried out on solid samples such as U tailings (Case and McDowell, 1982) or aerosol particles (Wallner, 1997). These matrices required no sample pre-concentration chemistry and the samples were simply digested in strong acids including HF and $HClO_4$. It maybe that such precise extractions using the POLEX cocktail are not best suited to seawater samples (for α/β LSS measurements) as the variability in the pre-concentration suggests that yield tracers were required.

2.3.4.3 Phase separation

The original applications of extractive scintillators were for the PERALS system. The extractive scintillator can be removed by pipette or counted directly if the extraction matrix is in a small volume. Small volumes (< 10 ml) of aqueous and organic phase can be added to a specially designed culture tube which permits direct counting of the sample without the requirement for phase separation. These tubes are not compatible with conventional LSS and hence the organic phase must be removed to a standard vial. The advantage of the culture tubes is that the entire organic phase is being counted and not a fraction (e.g 1 ml from 2 ml or 1.5 ml from 2 ml) which has implications for the detection limits. Also, care must be taken not to include any of the aqueous phase during the removal.

Experiments were carried out whereby the whole sample was placed in the LSS. High extraction efficiencies were obtained with ^{210}Po and ^{210}Bi recoveries being 98.3 ± 6.1 % and 104 ± 6.4 % respectively. Although the whole sample could be measured, the technique had its drawbacks. The background count rate is susceptible to Cerenkov events from the aqueous phase which interfere with the scintillation events from the cocktail. This is not a problem in PERALS spectrometry as the system is designed to reject these events. However in conventional LS measurements they may introduce variations in the sample count rate as they are not rejected as background events.

2.3.4.4 Background problems

When the TOPO based scintillator was first used, the background count rates were

consistently around 6 cpm for a 7 ml glass vial (June 1998). However, through time these background count rates were slowly increasing and were around 13 cpm (March 1999). Wallner (1998) had noticed that the background count rates using POLEX increased by an order of magnitude when a new H_3PO_4 solution was used, and the background varied for different brands of H_3PO_4. Phosphoric acid is produced from phosphate rock which can have significant amounts of U associated with it (Section 1.1.1). Therefore, the phosphoric acid itself may be a significant source of background with ^{210}Pb, ^{210}Bi and ^{210}Po present. To check the acid as a possible source of the background, several brands of H_3PO_4 were examined for background count rate along with old and new 0.1 M HCl solutions. This change in background count rate was independent of both HCl and H_3PO_4 (Table 2.7) and therefore must have been related to the background in the extractive scintillator. This could have been the result of a combination of two main factors. One cause of the increased background could have been ^3H contamination of the extractive scintillator. ^3H levels in the ambient water vapour in this building were high during this period. This ^3H most likely resulted from activation of Li in the concrete of the research reactor on site. ^3H is a low

H_3PO_4 manufacturer	BDH HCl	Acros HCl
Hopkin and Williams	9.25 ± 0.30 cpm	9.18 ± 0.30 cpm
Fisons	9.40 ± 0.31 cpm	9.30 ± 0.30 cpm
Merck	9.09 ± 0.30 cpm	9.25 ± 0.30 cpm

Table 2.7: The background count rate (0 to 2000 keV) obtained using various H_3PO_4 and HCl brands in the POLEX extraction matrix. Samples were counted on a Packard 2770 TR/SL LS spectrometer in NCM for 100 minutes. All reagents were analytical grade and errors quoted at the 1σ significance.

energy β^- emitter (E_{max} = 18.6 keV) which would be unseen in the lower end of the spectrum where the majority of the background events occurred. Secondly, ^{222}Rn has a strong affinity for toluene and although ^{222}Rn levels were not thought to be high at SURRC, it represents another potential source of this increase in background. Similar evaporative losses can occur in the aliquots of extractive scintillator being counted despite the cooling unit on the LS spectrometer. If samples are to be recounted, the evaporation of toluene will result in changes to the counting conditions of the cocktail and create non-uniform effects in the vial with respect to counting geometry and degree of quenching. As the volume of the sample decreases it would be expected that the counting efficiency of the sample may decrease. Evaporation of the solvent from the LS cocktail may affect the energy transfer processes in the cocktail and result in further reduction of counting efficiency. The relative increase in TOPO concentration may also influence the quench conditions in the sample.

2.3.5 Summary of technique

There were several factors that suggested POLEX was more suited to less complex materials that would not require significant pre-concentration or pre-treatment. Apart from the problems of quenching by salts, removal of colour and variable background, the main failing in the application of this technique was its requirement to have yield tracers for Pb, Bi and Po. Po measurements would require a Po yield tracer but the α energies are too similar to allow their resolution by LSS. Only ^{208}Po and ^{209}Po isotopes are suitable in terms of half life (Section 2.8.3), these are α emitting nuclides and although the PERALS system could resolve the two α peaks, counting on an α/β LS spectrometer would not have suitable

resolution to differentiate these two peaks. This meant that Po would have to be counted by conventional α spectrometry instead of α/β LSS. This would require its separation prior to ^{210}Pb and ^{210}Bi determination by POLEX extraction. Furthermore, if a ^{212}Pb tracer was used it would have implications for the determination of Bi recovery. It was hoped to utilise ^{212}Pb as a tracer for ^{210}Pb, but decay of ^{212}Pb produces ^{212}Bi (Fig. 1.1) which will be partitioned into the organic phase and contribute to the counts from ^{210}Bi. To maximise the MDA for the low activities of ^{210}Pb observed in seawater the direct counting of ^{210}Bi and ^{210}Pb (without phase separation) was desirable. This would require the sample to be stored until the unsupported ^{212}Pb tracer had decayed. This would introduce a significant time delay in the Bi determination, during which there would have been significant ingrowth of ^{210}Bi from ^{210}Pb. Despite the work carried out on POLEX as an extractant for Pb, Bi and Po, it was decided to investigate other separation techniques that had already been successfully applied to complex matrices like seawater and that would be suitable for a method which utilised chemical yield tracers for Pb, Bi and Po.

2.4 Deposition onto metal foils

Almost every method for the determination of ^{210}Po activity relies on its deposition onto a metal foil, either by spontaneous deposition or by electro-deposition. Electro-deposition involves passing an electric current through an aqueous solution, causing the nuclide of interest to be removed onto the cathode. Spontaneous deposition requires no electrical currents, but is restricted to a few nuclides.

The spontaneous deposition of ^{210}Po has been used for preparation of ^{210}Po sources for the last 90 years. Marckwald (1905) first discovered that ^{210}Po could be deposited from acidic solutions onto silver discs while Curie and Debierne (1910) used this technique to separate ^{210}Po from ^{210}Pb. Since its discovery, this phenomenon has been well studied. Bagnall (1957) reviews work carried out on various metal types, much of which is subsequently reported in Figgins (1961). It is the simplicity of spontaneous deposition techniques that has limited research into other methods of Po purification. There is, however, a risk of plating impure sources since the potential between the metal in solution and the metal foil is fixed. Electro-deposition allows variable potential and thus control over the deposition processes.

2.4.1 Electro-deposition techniques

Narita *et al.* (1989) developed a technique which electrochemically separates ^{210}Pb, ^{210}Bi and ^{210}Po. ^{210}Po is removed by spontaneous deposition onto silver, ^{210}Bi is then electrodeposited onto a platinum gauze cathode and ^{210}Pb is then deposited from a fluoroborate medium onto the same platinum gauze used as the anode. They state that the whole procedure can be

carried out in 6 hours, but the technique appears long and labour intensive. Electro-deposition is used in U and Th analysis to produce a thin source for α spectrometry, free of any possible interferences. There may be three or more isotopes present (with multiple α emissions) so the purity of plating is essential for maximum resolution of the α peaks. In ^{210}Po analysis, the α spectrometry measurement is only to determine ^{210}Po (5.3 MeV) and either ^{208}Po (5.1 MeV) or ^{209}Po (4.88 MeV) as a yield tracer. These are all mono-energetic α emissions and the plating obtained by spontaneous deposition (regardless of the foil type) is adequate for their successful resolution and therefore makes electro-deposition techniques over-complicated and time consuming. Cowan *et al.* (1977) used a direct electro-deposition method to deposit ^{210}Po from seawater without the need for pre-concentration. However, to achieve a comparable yield to a pre-concentrated sample required a deposition time of 48 hours.

2.4.2 Spontaneous deposition methods

The simplicity of the spontaneous deposition method has resulted in its popularity, but some of the techniques employed may suffer from contamination from other metals, hence, the choice of metal foil and the conditions in the plating solution are vital for obtaining pure sources. Much research has gone into the choice of metal foil to deposit ^{210}Po onto. The three main metals are silver, copper and nickel and the behaviour of the these metals will be described below.

2.4.2.1 Silver foils

Many of the methods applied today utilise the deposition of ^{210}Po onto silver foils (Fleer and Bacon, 1984; Sarin *et al.*, 1992) which are adapted from the method of Flynn (1968). Marckwald (1905) found that ^{210}Po plates onto silver foils and the deposition is enhanced if the plating solution contains HCl rather than HNO_3. Furthermore, he found that the rate of deposition is increased by raising the temperature of the solution. At a temperature of 97 °C it is reported that 99 % of the ^{210}Po can be removed from solution. Holtzman (1987) reported that 92 % of ^{210}Po can be deposited in six hours of plating. However, as early as 1928, the co-deposition of ^{210}Bi and ^{210}Pb onto silver foils was observed (Erbacher and Philip, 1928). This has also been observed by Ehinger *et al.* (1986), but is often over looked in the development of methods. There is a great deal of conflicting information on the purity of ^{210}Po plated onto silver foils but most workers agree that 100 % deposition is rare and other techniques are required to purify the residual plating solution prior to the start of ^{210}Po ingrowth from ^{210}Pb (Section 2.1).

2.4.2.2 Nickel foils

Blanchard (1966) found recoveries of 96 ± 4 % and 94 ± 3 % of ^{210}Po and ^{210}Bi deposited onto nickel foils. Ehinger *et al.* (1986) reported that ^{210}Bi and ^{210}Po can be separated from ^{210}Pb by their deposition onto nickel foils. As with deposition onto silver foils, HCl solutions offer an improved deposition compared to HNO_3 solutions. Church *et al.* (1994) used a silver foil to remove ^{210}Po from solution and then plated ^{210}Bi onto nickel foil in a helium environment, to prevent removal of ^{210}Bi from the nickel. They found it necessary to bubble

helium through the solution during plating to prevent oxidation and subsequent removal of ^{210}Bi. Even washing the foil after removal from the solution is carried out in water which has been freshly boiled to remove oxygen.

2.4.2.3 Copper foils

The spontaneous deposition onto copper was first described by Curie and Debierne (1910). Figgins (1961) reported that ^{210}Bi is also deposited onto copper, which has led to silver foils being used to remove ^{210}Po in many of the methods in the literature. The study of copper foils to remove ^{210}Po was re-investigated in 1979 by MacKenzie and Scott. They found that both ^{210}Bi and ^{210}Po did deposit onto copper foils, but that ^{210}Bi could then be removed from the copper foil by rinsing it with water heated to the temperature of the plating solution. They detailed the separation technique providing optimum conditions for temperature, pH and stirring speed for both the adsorption of ^{210}Po and ^{210}Bi onto copper and the subsequent desorption of ^{210}Bi back into solution. Ehinger *et al.* (1986) was unable to reproduce the results and obtained 30 % lower ^{210}Po recoveries with copper compared to silver foils and suggested that ^{210}Pb may be deposited onto copper. However, MacKenzie and Scott (1979) utilised ^{212}Pb as a tracer and found that Pb remained in solution.

2.4.3 Experiments on spontaneous deposition onto copper foils

The problems associated with plating onto silver foils have been described earlier (Section 2.1.1). Furthermore, copper is much less expensive than silver and foils do not need to be reused. Thus, plating onto copper foils appears to be a more attractive technique. Although

^{210}Bi may partially plate onto copper, it has been shown that co-deposited ^{210}Bi can be removed from the foil, back to the plating solution leaving a purified source of ^{210}Po. This technique was investigated after the POLEX extraction was found to be un-suitable for seawater samples. The aim of the work on spontaneous deposition was to allow ^{210}Po to be determined by α spectrometry and to utilise a ^{208}Po yield tracer which would compensate for the variable yields occurring from the pre-concentration stage (Section 2.2.3.2).

Copper foils were prepared from BDH copper sheet using a method previously used at SURRC (C.Donnelly, personal communication, 1998). A strip of copper foil (approximately 10 cm by 10cm) was unrolled and one side roughened with coarse sandpaper. This was then covered with epoxy resin to prevent ^{210}Po plating onto both sides of the copper. The coated foil was then cut into 1cm^2 pieces before the epoxy had fully set. The individual foils were placed epoxy side upwards on a clean tray, and left to cure for around one week. If the epoxy is not allowed to fully cure, the epoxy layer can separate from the copper during plating and allow Po isotopes to deposit on both sides.

MacKenzie and Scott (1979) suggested that a plating time of 3 hours at a temperature of 95 °C should be sufficient for 100 % removal of Po onto copper foils. Before any plating was carried out, the temperature setting of the hot-plate was adjusted to give 95° C and checked for stability. The magnetic stirrer was also set to give maximum stirring without excess vortexing.

2.4.3.1 Spontaneous deposition of ^{208}Po onto Cu foil

An aliquot of ^{208}Po spike (activity = 1.3 Bq) was added to 50 ml of reverse osmosis water with 5 ml $NH_2OH.HCl$. A magnetic stirrer was added and the solution was heated to 95° C. A copper foil was briefly immersed in 2 M HNO_3 to remove any oxide coating, and then rinsed thoroughly with reverse osmosis water to remove all traces of HNO_3 which could hinder the spontaneous deposition. Another beaker containing reverse osmosis water was placed on the hotplate and this was used to wash down the sides of the sample beaker during plating. If this is not carried out Po isotopes may bond onto the side of the beaker and introduce uncertainty into the determination (Feldman and Frish, 1956). This also acts to keep the plating solution at constant volume and maintain the same conditions in the plating solution.

Once the plating was complete, the copper foil was removed from the solution with tweezers and rinsed with reverse osmosis water. By rinsing the foil back into the original plating solution any co-deposited ^{210}Bi can be returned to the beaker. The foil was then left for 24 hours with periodic washing. No Bi will be present in a pure ^{208}Po spike, but by following the Bi removal method, any Po removal would be observed. The plating solution was then evaporated to dryness on a hotplate and the residue oxidised with 15 M HNO_3 and 35 % H_2O_2 to destroy any $NH_2OH.HCl$ remaining from the plating. The plating solution was then transferred to a 20 ml scintillation vial and evaporated to dryness. The residue was dissolved in 1 ml of 0.1 M HCl and 5 g of Ultima Gold-LLT cocktail were added. The vial was counted by LSS in NCM for 100 minutes alongside a background vial comprised of 1 ml of

0.1 M HCl and 5 g of UG-LLT (Table 2.8). The Cu foil was placed in a 20 ml glass vial and 3 g UG-LLT added. The vial was counted by LSS (Section 2.1.3) alongside a background vial containing an un-plated Cu foil and 3 g UG-LLT.

	cpm			cpm
^{208}Po on Cu-foil (in 3 g UG-LLT)	47.81 ± 0.69		Plating solution in 1 ml 0.1 M HCl and 5 g UG-LLT	14.32 ± 0.38
Blank Cu-foil (in 3 g UG-LLT)	12.08 ± 0.35		0.1 M HCl and 5 g UG-LLT background	14.06 ± 0.37
Net cpm	35.73 ± 0.77		Net cpm	0.26 ± 0.53
Counting efficiency	44.59 ± 5.44 %			

Table 2.8: Results of plating a ^{208}Po spike (activity = 1.34 ± 0.07 Bq) onto Cu foils. The foils were counted by LSS after addition of 3 g UG-LLT. The plating solution was also analysed by LSS after being evaporation close to dryness and transferred to a 20 ml scintillation vial and evaporated to dryness before re-dissolution in 1 ml 0.1 M HCl and 5 g UG-LLT. All vials were counted on NCM for 100 minutes on a Packard 2770 TR/SL LS spectrometer. Errors quoted at the 1σ significance.

No counts were observed above background, indicating that full removal of Po onto copper foils was achieved after a 3 hour plating. The LSS spectrum obtained for the copper foil (Fig. 2.14) could suggest that there was contamination of the foil with a β emitter. However, the spectral shape must be a function of the 2π geometry obtained from LSS of a copper foil as only ^{208}Po was present. It was decided to use LSS to determine ^{210}Po activities in the method development stages although α spectrometry would be applied in the final method. The α spectrometry method of ^{210}Po and ^{208}Po had already been successfully applied to determination of ^{210}Po activities in sediment (Chapter 4). There were several reasons for using LSS to determine the ^{210}Po activity instead of the conventional α

spectrometry technique. Firstly, a counting efficiency close to 50 % can be achieved with LSS compared to ~20 % with α spectrometry which allows faster counting times. LSS

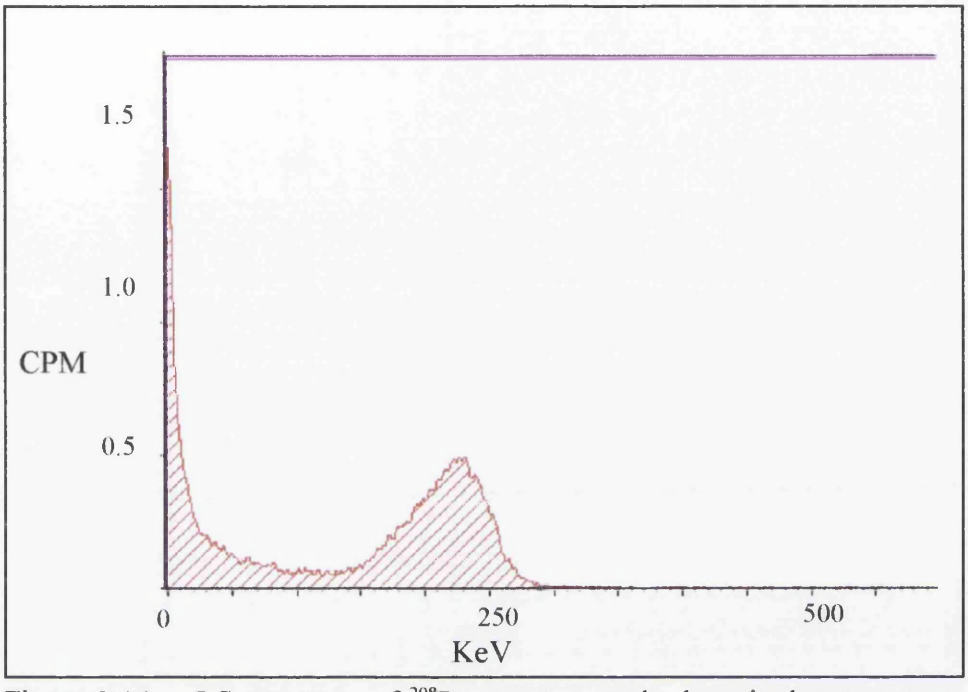

Figure 2.14. LS spectrum of ^{208}Po spontaneously deposited onto copper foil.

automatically changes the samples allowing faster throughput. Using LSS instead of α spectrometry prevents any possible contamination of the α spectrometer as freshly deposited ^{210}Po may volatilise (White and Ross, 1961) and much higher activities of spike would be used in the method development than would be expected in aquatic samples. Finally, and perhaps most importantly, LSS allows a spectrum to be produced for each sample which records all activity on the copper foil, which allows the partial plating of ^{210}Pb and ^{210}Po to be monitored.

2.4.3.2 Spontaneous deposition of ^{210}Po onto Cu foil

A similar experiment was carried out using ~8 Bq of ^{210}Pb spike (with ^{210}Bi and ^{210}Po in equilibrium). Following the plating procedure described above, the copper foil was placed in a 20 ml scintillation vial and 3 g of UG-LLT were added. The plating solution was also analysed as described in the above experiment. Furthermore, the vial containing the plating solution was also counted on a HPGe γ photon detector to ensure that no ^{210}Pb was removed from solution to the Cu foil. The count rate of the ^{210}Pb γ photon peak was compared to a control vial containing an identical aliquot of ^{210}Pb spike and indicated no ^{210}Pb was removed by spontaneous deposition onto Cu during the plating process (Table 2.9).

	cpm			cpm
^{210}Po on Cu-foil (in 3 g UG-LLT)	267.98 ± 1.64		Recount of ^{210}Po on Cu-foil (in 3 g UG-LLT).	266.39 ± 1.63
Blank Cu-foil (in 3 g UG-LLT)	12.25 ± 0.35			
Net cpm	255.73 ± 1.68		^{210}Pb γ (net) -sample (cps)	0.044 ± 2.66%
Counting efficiency	47.80 ± 5.65 %		^{210}Pb γ (net)-control (cps)	0.045 ± 1.83%
			^{210}Pb recovery	97.7 ± 3.23 %

Table 2.9: Results of plating a ^{210}Pb spike (activity = 8.83 ± 0.5 Bq) onto Cu foils. The foils were counted by LSS after addition of 3 g UG-LLT. The plating solution was also analysed by LSS after being evaporation close to dryness and transferred to a 20 ml scintillation vial and evaporated to dryness before re-dissolution in 1 ml 0.1 M HCl and 5 g UG-LLT. All vials were counted on NCM for 100 minutes on a Packard 2770 TR/SL LS spectrometer. Errors quoted at the 1σ significance. The plating solution was also counted on an HPGe γ photon detector to measure the recovery of ^{210}Pb and ensure no ^{210}Pb was deposited onto Cu foil.

If any ^{210}Bi deposited onto the copper foil, it would decay according to its 5.013 day half-life, as the complete recovery of ^{210}Pb had been established by γ spectrometry. The vial was

recounted after one week and no change in the count rate was observed indicating the absence of ^{210}Bi on the copper foil. With no change in the activity of the foil, it was assumed that the counts observed were a result of ^{210}Po only (Table 2.9). The vial containing the remaining plating solution was counted by LSS for 100 minutes in NCM and no α activity could be observed overlying the ^{210}Bi spectra. This indicates that copper foils are effective at plating ^{210}Po and, if ^{210}Bi is plated it can be completely removed from the copper surface back into solution. Furthermore, in the ion exchange procedure described in section 2.5, recoveries of ^{210}Pb and ^{210}Bi in the plating solution were 100 and 95 % respectively after spontaneous deposition of ^{210}Po. This is further evidence suggesting that ^{210}Bi can be completely removed from copper foils.

This series of experiments highlights the benefit of using LSS for radiochemical method development. Much of the data on the spontaneous deposition of ^{210}Bi and ^{210}Po onto different metal types was carried out using techniques which offered no spectral analysis (Holtzman, 1987; Ehinger *et al.*, 1986). The ability of LSS to measure α, β and γ emitters and provide a spectrum for each sample offers an advantage over other techniques.

2.5 Ion exchange chromatography

This section is based on the ion exchange experiments carried out to purify Pb, Bi and Po from seawater samples. The original aims of the method development were to achieve a tracer free method of ^{210}Pb, ^{210}Bi and ^{210}Po determination. However, the very low activities present in seawater require a pre-concentration stage in the methodology. The variations in yields obtained with this pre-concentration stage required application of chemical yield tracers to the analysis. The requirement of yield tracers makes chemical purification of Pb, Bi and Po necessary to allow calculation of chemical recovery and sample activity for each. One such technique suitable for such requirements is ion exchange chromatography. Ion exchange separation methods are popular in NDS radionuclide measurements and it was decided to investigate the possibilities of using such methods in this study. The possibility of an ion exchange technique would allow improved separation of Pb, Bi and Po from interfering ions (such as Fe^{3+}) and nuclides (such as ^{238}U). Such a method would also allow yield tracers to be employed without the problems that would be encountered with POLEX separation (Section 2.3.4).

2.5.1 Principles of ion exchange

An ion exchanger is essentially an insoluble matrix support which has exchangeable ions on its surface. These are held in a network of cross-linked charge groups and it is onto these charged groups that ions can be adsorbed. The cross-linking is achieved by divinylbenzene (DVB) and the degree of cross-linking has an influence on the behaviour of the resin. Ions can be exchanged for a stoichiometrically equivalent amount of other ions initially present

in an electrolyte solution brought into contact with it. These are known as counter ions and are exchangeable, equivalent per equivalent, with other ions of the same charge type. Neutral molecules (and those with the same charge as the functional groups) flow through the column and are separated from the ions which are sorbed onto the resin. Another ion may then displace and elute the sorbed ions or they may be sequentially de-sorbed from the resin starting with the weakest bound ion.

Originally, ion exchangers were natural materials such as wool, cellulose and clays, but their non-uniform behaviour made it difficult to predict separations performed using them. Today virtually all applications of ion exchange chromatography are carried out using synthetic materials.

2.5.1.1 Cation exchangers

Cation exchange resins are cross-linked polyelectrodes consisting of a three dimensional network of hydrocarbon chains which contain functional groups. Depending on the functional groups, the resins can be described as strongly or weakly acidic. Strongly acidic cation exchangers are produced by the sulphonation of polystyrene or poly-DVB and contain sulphonate ($-SO_3^-$) as the functional group. Weakly acidic cation exchange resins are produced from the polymerisation of methacrylic acid and have functional groups such as carboxylate ($-COO^-$) or phosphinate ($-HPO_2^-$). The negative charge on the functional group reacts with the positive charged metal ions (cations) and it is this behaviour which permits the exchange of ions on and off the surface of the resins. A simple cation exchange reaction

is shown in equation 2.1, * is either SO_3^- for strongly acidic resins or COO^- for weakly acidic resins.

$$\text{Resin*-H} + \text{NaCl} \rightarrow \text{Resin*-Na} + \text{HCl} \qquad (2.1)$$

2.5.1.2 Anion exchangers

As with cation exchange, anion exchange reins can be either strongly basic or weakly basic. Both types of anion resins contain amines as the functional group. Strongly basic resins are manufactured by chloromethylation of sulphonated polystyrene followed by reaction with a tertiary amine. Weakly basic resins are manufactured by the same processes as above but are reacted with either primary or secondary amines. The amines are fixed on the resin structure and exert a positive charge. It is the basis of this positive charge that allows the interaction of the counter ions.

If an anion exchange resin is in the chloride form then the counter ions bound to the positively charged amine are Cl^-. These can be displaced by the sample ions (as negatively charged complexes) that have the same charge, which in turn become bound to the functional group. Because many metals can form negatively charged complexes, anion exchange techniques are also often used for metal separations.

2.5.1.3 Measurements of adsorbability.

It is vital to have knowledge of the adsorbabilities of the metals that require separation before beginning any work with ion exchange. The pioneering work in this field was carried

out by Kraus and Nelson (1956). They produced charts for the adsorbability of many elements in a wide range of different acids, over a broad range of molarities and calculate the distribution coefficient (K_d) (i.e. the partitioning of the element between the solid and liquid phase). Thus, a high K_d factor suggests that the element is held tightly by the resin, and conversely, a low K_d factor signifies little adsorption by the resin of that element in that particular acid and at that specific concentration. The distribution coefficient can be written as either a weight factor or as a volume factor but are interchangeable due to their shared relationship with bed density.

2.5.1.4 Column and batch techniques

There are two techniques available when using ion exchange resins, they are the column and batch techniques. The column technique is probably the better known of the two. It involves adding the resin as a slurry to a glass column. Once the column has been made, the sample is introduced to the top and the separated fractions can be eluted at the base. The column technique is more often used for several reasons.

1. The results obtained can be more easily reproduced.
2. It is easier to control for multi-element analysis.
3. Less resin is required so it is therefore cheaper both in terms of purchase cost and disposal cost (if the resin is contaminated after the experiment).

However, the batch technique also has its advantages. In essence, the batch technique

involves adding a quantity of the resin directly to the sample vessel. After allowing time for equilibration, the resin and the liquid can be separated by filtration or sieving. It is frequently used for the removal of ions from solution where quantitative exchange is not crucial. It is also a useful technique for ions strongly held on the resin (high K_d) which would require very large liquid volumes to elute them by column techniques. After adsorption onto the resin, the resin and the un-adsorbed ions can be separated by centrifugation and decanting the supernatant liquid. Indeed, despite the advantages of the column method, Kraus and Nelson (1956) used the batch technique for the majority of their work as it is less time-consuming than running large numbers of columns.

Some specific points regarding the resins used in the course of this research are noted as follows: Ion exchange resins are available from several companies (Dowex, BioRad, EiChrom, Rohm and Hass plus others). However, all are based on the Dowex product but specific manufacturers have their own purification processes. Indeed, during the course of this study, the anion exchange resin was changed from Bio-Rad AG1x8 to Eichrom AG1x8 and no change in elution characteristics was observed. The prefix AG signifies that the resin is an analytical grade and has been purified and size sorted to a greater degree than the technical grade. As stated earlier, the degree of cross-linking influences the ion exchange behaviour of the resin. Cross-linking is measured in the percentage of divinylbenzene (DVB) present in the resin. Resins are available in ranges of 2 to 12 % DVB, the most commonly used are 8 % and 10 %. Resins with low amounts of cross-linking (2 %) have a more open structure and swell to a larger wet diameter than higher cross-linked resins. This is

important if large molecules are required to be passed through the column but the use of low % DVB resins poses a risk of columns being split by swelling of the resin. The mesh size of the resin refers to the size of the resin beads. The smaller mesh sizes have a larger particle diameter which results in an increased flow rate. The most commonly used mesh size for the column method is 100 to 200 mesh.

The ionic form of the resin refers to the ion bound to the functional group. Resins generally come in one of two forms, anion exchange resins are normally purchased in the chloride (Cl^-) form and cation exchange resins in the hydrogen (H^+) form. Different ions have a different affinity for the functional groups. Generally, the resin should be in an ionic form that has lower selectivity than the sample ions to be sorbed. If the desired form is not the form in which the resins are purchased then they can be converted into the desired form by either adding an ion with a higher affinity for the resin or adding a higher concentration of an ion with a lower selectivity.

2.5.2 Development of ion exchange scheme for ^{210}Pb, ^{210}Bi and ^{210}Po

Before separation schemes were investigated, the final choice of pre-concentration method had to be decided. The optimum scheme will also allow the removal of any carrier ions from the separated aliquots of Pb, Bi and Po. The $Fe(OH)_3$ scavenging technique was previously chosen so the ion exchange behaviour of Fe^{3+} (as Fe^{3+} was purified from $Fe(NO_3)_3.9H_2O$) must also be investigated.

The elution schemes described in this following section are based on the relative recoveries of ^{210}Pb, ^{210}Bi and ^{210}Po. The absolute recoveries could not be established as the counting efficiencies had not been determined. The relative recoveries are based on 100 % counting efficiencies. The absolute counting efficiencies should be very close to 100 % for ^{210}Bi and ^{210}Po and around 95 % for ^{210}Pb.

2.5.2.1 Anion exchange behaviour of Pb

On strongly basic resins, Pb has its maximum adsorption in 1.2 M HCl solutions ($K_d = 25$). Adsorption decreased on both sides of this molarity and Pb passes through the column in solutions above 8 M HCl (Nelson and Kraus, 1954) (Fig. 2.15 a). In HNO_3 solutions, the adsorbability of Pb is low throughout the range of concentrations studied and maximum adsorption occurs in 2 M HNO_3 solutions (Fig. 2.15 b). Van Den Winkel *et al.* (1972) present data for the behaviour of Pb in acetic acid. The adsorbency of Pb is low up to around 10 M CH_3COOH, above which its adsorbency increases rapidly up to 18M CH_3COOH (Fig. 2.15 c). However, the literature concerning the behaviour of Pb on anion resins in HCl is often contradictory due to different resin types and cross-linking. Petrow *et al.* (1960) used a strongly basic anion exchange technique to remove ^{226}Ra from Pb, Bi and Po but the paper fails to reveal the elutants for Pb, Bi and Po. Ishimori (1955) used an Amberlite XE-98 resin to separate Pb, Bi and Po but Pacer (1983) found this resin to be no longer available.

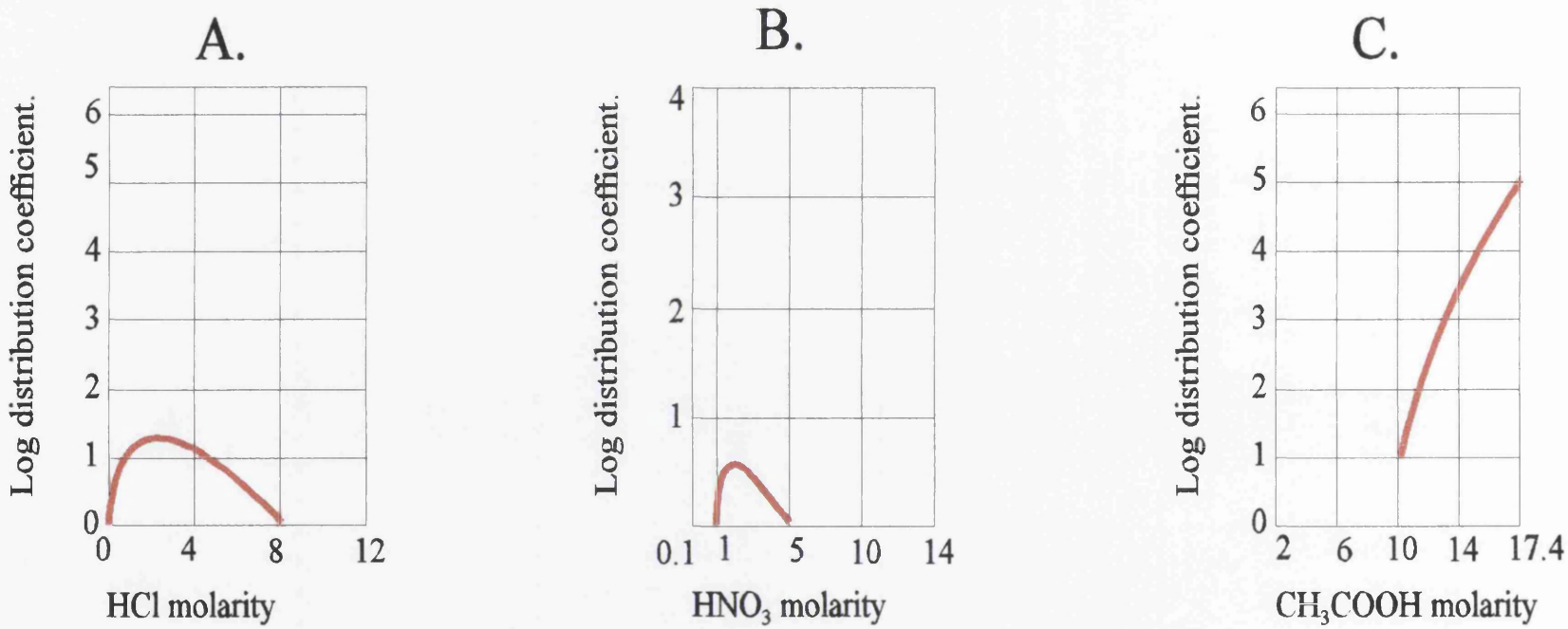

Figure 2.15: The anion exchange behaviour of Pb^{2+} in HCl (A), HNO_3 (B) and CH_3COOH (C) solutions on Dowex 1x10 (A & B) and Dowex 1x8 (C). Adapted from Kraus and Nelson (1956), Faris and Buchanan (1964) and Van Den Winkel *et al.* (1972).

2.5.2.2 Anion exchange behaviour of Bi

In HCl solutions, Bi is strongly held under all conditions, the maximum adsorption occurs in weak (0.25 M) HCl solutions ($K_d = 2x10^5$) and decreases to around 57 in 12M HCl (Fig. 2.16 a). Adsorption of Bi is low ($K_d = 1.6$) in 0.5 M HNO_3 solutions and increases to a maximum adsorption in 4 M HNO_3 ($K_d = 26$), it decreases to around 11 in 10 M HNO_3 (Fig. 2.16 b). However high HNO_3 concentrations can cause decomposition of the resin itself and this can be seen with the decolouration that occurs when high HNO_3 concentrations are passed through the column. In CH_3COOH solutions, Bi is well retained by the column, especially in high molarity solutions (Van Den Winkel *et al.*, 1972) (Fig. 2.16 c).

2.5.2.3 Anion exchange behaviour of Po

In HCl solutions, Po is strongly bound to the resin as $PoCl_4$ throughout the full range of HCl molarities (Fig.2.17 a). Its strong adsorption makes this resin suitable for the removal of ^{210}Po and this is the chosen technique of several authors for removal of any un-plated ^{210}Po from their original plating solution (Thomson and Turekian, 1976; Benninger, 1978; Joshi and Ku, 1979). The behaviour of Po in HNO_3 media is somewhat vague with some authors reporting 100 % removal of Po from the resin with 6 M HNO_3 (Ishimori, 1955), while Pacer (1983) was unable to resolve Bi from Po by using HNO_3. The ion exchange data from Saito (1984) does not display any information on the adsorbability of Po onto the column. In CH_3COOH solutions, Po is well held on the resin in the range of molarities studied (Fig. 2.17 b).

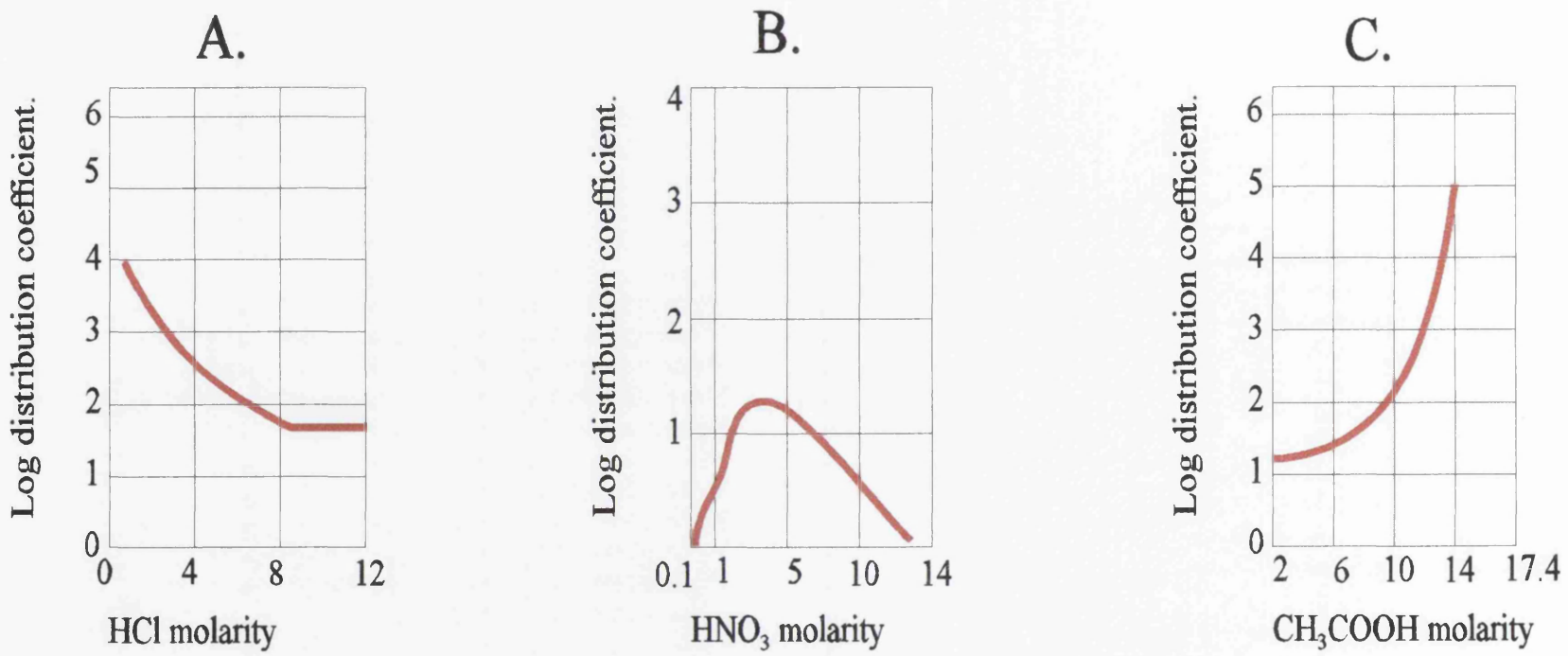

Figure 2.16: The anion exchange behaviour of Bi^{3+} in HCl (A), HNO_3 (A) and CH_3COOH (C) solutions on Dowex 1x10 (A & B) and Dowex 1x8 (C). Adapted from Kraus and Nelson (1956), Farisand Buchanan (1964) and Van Den Winkel *et al.* (1972).

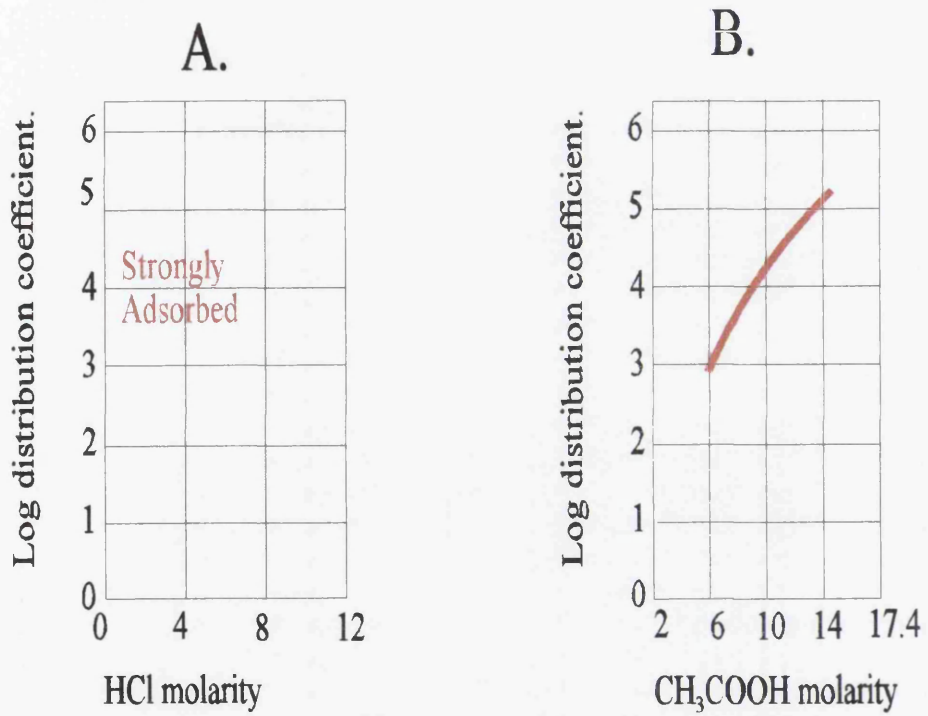

Figure 2.17: The anion exchange behaviour of Po^{4+} in HCl on Dowex 1x10 (A) and CH_3COOH on Dowex 1x8 (B) solutions. Adapted from Kraus and Nelson (1956) and Van Den Winkel *et al.* (1972).

2.5.2.4 Anion exchange behaviour of Fe

In HCl solutions, the adsorbency of Fe^{3+} increases with increasing molarity of HCl used and above approximately 9 M HCl, the adsorption of Fe^{3+} becomes constant (but still high) (Fig.2.18 a). The adsorption of Fe^{2+} is much lower in HCl solutions and this highlights the requirement of the iron carrier to be purified by DIPE before its use in this type of chemistry. In HNO_3 media, Fe^{3+} passes through the column in all concentrations (Fig. 2.18 b). While in CH_3COOH, Fe^{3+} retention was only observed in concentrated solutions (Fig. 2.18 c).

2.5.2.5 Cation exchange behaviour of sample ions

Although cation exchange would seem the obvious method for separating metal cations there are few methods which employ it. There is much less data on the cation exchange behaviour of metals although Nelson *et al.* (1964) provides relevant information (Fig. 2.19). The adsorbency of Fe^{3+} from HCl solutions first decreases with increasing HCl molarity. This reaches a minimum at around 4 M HCl where Fe^{3+} will pass through the column without any retention on the resin. Its adsorbency then increases rapidly up to around 10 M HCl. Pb adsorbency decreases with increasing HCl molarity and above 1.5 M HCl solutions it is reported to pass through the column. Similarly, Bi adsorbency above 0.5 M HCl is negligible and Po is reported to have minimum adsorbency in all HCl concentrations.

2.5.3 Ion exchange methodologies

2.5.3.1 Cation exchange experiments

The data presented by Nelson *et al.* (1964) suggest that cation exchange using strongly

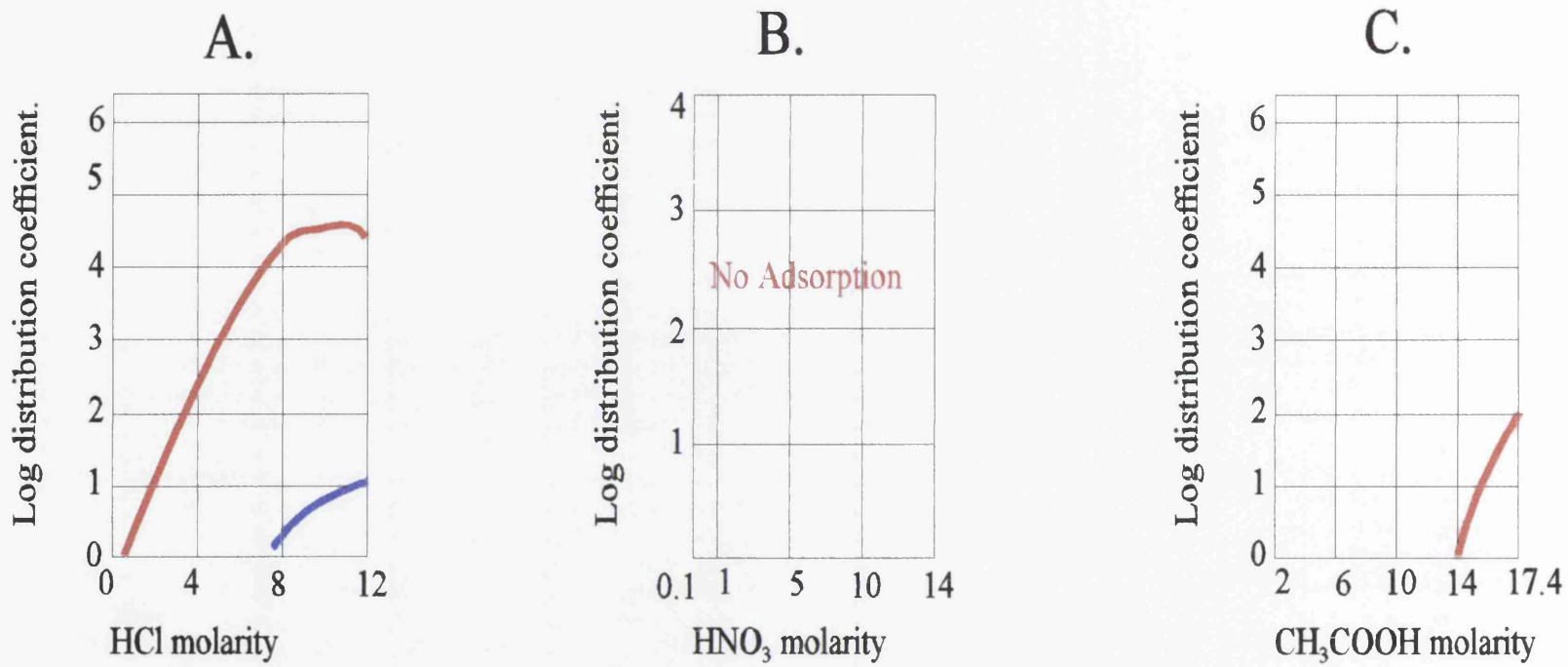

Figure 2.18: The anion exchange behaviour of Fe^{2+} (blue) and Fe^{3+} (red) in HCl (A), HNO_3 (B) and CH_3COOH (C) solutions on Dowex 1x10 (A & B) and Dowex 1x8 (C). Adapted from Kraus and Nelson (1956), Faris and Buchanan (1964) and Van Den Winkel *et al.* (1972).

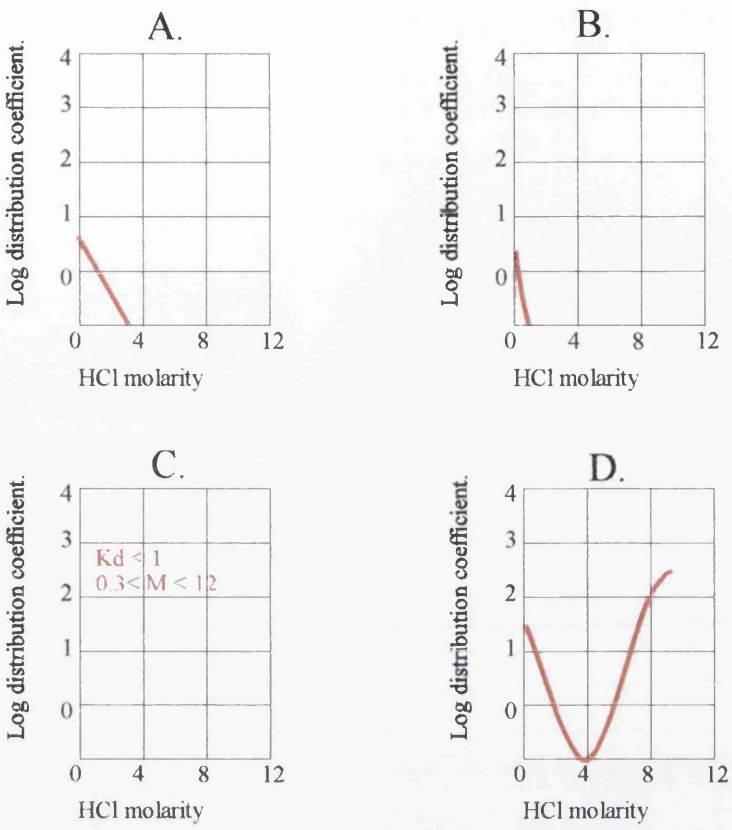

Figure 2.19: The cation exchange behaviour in HCl of Pb^{2+} (A), Bi^{3+} (B), Po^{4+} (C) and Fe^{3+} (D) on Dowex 50-X4.Adapted from Nelson *et al.* (1964).

acidic resins should provide a suitable method for the removal of the Fe^{3+} carrier from the sample ions. Furthermore, it should also be possible to separate U, Th and Ra from Pb, Bi and Po, thus making the method more widely applicable. Bojanowsli *et al.* (1983) used a Dowex AG 50Wx8 resin to separate Ra and Th from seawater as part of a multi-nuclide analysis method. They reported full elution of Pb and Po in the first 40 ml of 5 M HCl passed through the column. At this stage in the method development, the POLEX technique was still being employed for the separation of ^{210}Bi and ^{210}Po from ^{210}Pb as described by Wallner (1997). Problems were being encountered with removing Fe^{3+} from the nuclides of interest before counting (Section 2.3.4). If not removed, Fe^{3+} could be carried into the POLEX phase and cause serious quenching. The cation exchange behaviour of Fe^{3+} on AG 50Wx8 seemed ideal to separate Fe^{3+} from the analyte nuclides prior to extraction into POLEX. With this in mind the elution behaviour of Fe^{3+} on Dowex AG 50Wx8 was examined.

A 5 cm^3 column of resin was prepared and pre-conditioned with 9 M HCl. 3 ml of Fe^{3+} carrier (10 mg Fe^{3+} per ml) were added to 20 ml of 9 M HCl. This solution was added to the column, but the elution of Fe^{3+} with 9 M HCl was immediate. This finding contradicts the published data on this resin so the experiment was repeated using another bottle of the same cation exchanger, but Fe^{3+} was still not adsorbed. The experiment was also tried using the batch technique, it was hoped that using an excess of the resin may allow the adsorption of the Fe^{3+} carrier, but again it failed. The column experiment was again repeated, this time using 1.2 M HCl. The separation of Fe^{3+} again failed. Nelson *et al.* (1964) described the

cation exchange behaviour of iron to be "anomalous", and the work carried out here only confirms this finding.

2.5.3.2 Anion exchange experiments

When the initial experiments on anion exchange were carried out, the aim was primarily as a method of removal of the Fe^{3+} carrier. It was therefore imperative to look at the separation of Fe^{3+} from Pb, Bi and Po. To this end, an experiment was designed to examine two critical factors to this technique: (i) could Fe^{3+} be separated from Pb and Po? and (ii) could Pb and, more crucially, Po be easily eluted from the column?

An aliquot of Fe^{3+} carrier in 1.2 M HCl was spiked with an 8 Bq ^{210}Pb spike (with ^{210}Bi and ^{210}Po in equilibrium). This solution was added to a column of Bio-Rad AG 1x8 and 40 ml of 1.2 M HCl, 40 ml of 6 M HNO_3 and 40 ml of 15 M HNO_3 were eluted. The three portions were evaporated to dryness in 20 ml glass vials, re-dissolved in 1 ml of 0.1 M HCl, 5 g UG-LLT cocktail were added and the samples were counted by LSS (Section 2.1.3). At this point, the measurement of ^{210}Bi in conjunction with ^{210}Pb and ^{210}Po had not been considered. Stripping Bi from the sample would produced unsupported ^{210}Po for the initial POLEX extraction and ensure that no ^{210}Bi remained un-extracted. This is especially important if ^{210}Pb is to be determined by the ingrowth of its daughter ^{210}Bi. However, analysis of the spectrum produced for each aliquot revealed that no ^{210}Po was eluted in any aliquot. This effectively prohibits the use of anion exchange resins as a clean-up stage prior to POLEX extraction if ^{210}Po determination is required.

After the POLEX method had been abandoned, ion exchange techniques were re-examined. If ^{210}Po was removed before the column stage by spontaneous deposition (e.g. onto Cu foil), the purification of ^{210}Pb, and now ^{210}Bi, could be carried out using anion exchange techniques. Harada *et al.* (1989) described a similar method using a 12 cm^3 column of Bio-Rad AG 1x8 resin. After pre-conditioning the column, the sample was loaded in 8 M HCl and Pb eluted with two 40 ml aliquots of 8 M HCl, Bi could then be eluted by passing through 375 ml of 12 M HCl. An identical experiment was carried out.

2.5.3.2.1 HCl elutions

8 Bq of ^{210}Pb (with ^{210}Bi and ^{210}Po in equilibrium) was added to 20 ml of Fe^{3+} carrier (10 mg ml^{-1} Fe^{3+}). Addition of 18 M NH_4OH produced an $Fe(OH)_3$ precipitate which was centrifuged three times, washing the precipitate each time with reverse osmosis water and then finally the precipitate was re-dissolved in 15 ml of 8 M HCl. A 12 cm^3 column of Bio-Rad AG 1x8 resin was pre-conditioned with two 20 ml aliquots of 8 M HCl. The sample was loaded onto the column and four 20 ml aliquots of 8 M HCl were passed through the column to elute the Pb fraction. Eight 50 ml aliquots of 12 M HCl were then passed through the column to eluted ^{210}Bi. Each aliquot was collected in a separate beaker, gently evaporated to near dryness, transferred to a 20 ml scintillation vial and evaporated to dryness. The residue was re-dissolved in 1 ml of 0.1 M HCl and left for 1 hour. After this time 5 g UG-LLT were added and the vials counted by LSS (Section 2.1.3).

By calculating the net count rate and decay correcting for both ingrowth and decay of ^{210}Bi,

the percentage of the total activity of each isotope in each aliquot was derived, and an elution diagram constructed (Fig. 2.20).

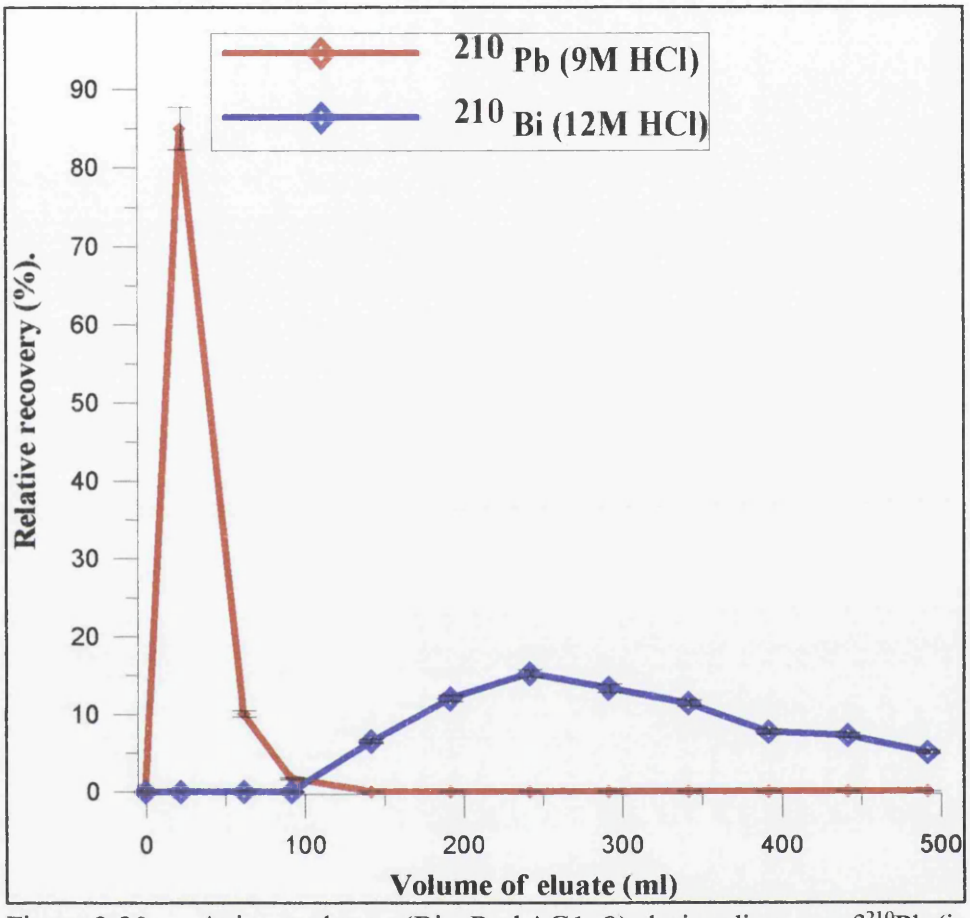

Figure 2.20: Anion exchange (Bio-Rad AG1x8) elution diagram of ^{210}Pb (in 9 M HCl) and ^{210}Bi (in 12 M HCl). Errors quoted at the 1σ significance.

The relative recovery of ^{210}Pb was 97 % ± 5 % while only 78 % ± 5 % of ^{210}Bi was recovered. The high relative recovery of ^{210}Pb implies that losses were not sustained during the $Fe(OH)_3$ precipitation step. Further, the shape of the elution curve implies that some ^{210}Bi was retained on the resin. The elution behaviour of Bi on AG 1x8 resin shows very severe tailing due to its affinity for the resin, even in high HCl concentrations. The Fe^{3+}

carrier was strongly held at the very top of the column during both the 8 M HCl and the 12 M HCl elutions. Also, very good recoveries of ^{210}Pb were achieved in a relatively small volume of eluent. Another elution technique for the removal of ^{210}Bi from the column is necessary due to the severe tailing. The time taken to elute 400 ml of 12 M HCl is also significant as the flow rate slowed when high molarity solutions were introduced to the column.

2.5.3.2.2 H_2SO_4 elutions

Kraus and Nelson (1958) presented an anion exchange scheme for the separation of Pb, Fe and Bi on an AG1x8 resin. Pb was eluted with 9 M HCl, Fe^{3+} with 0.5 M HCl and finally Bi was eluted with 1 M H_2SO_4. There is paucity of data concerning anion exchange behaviour in sulphate systems because most elements are not significantly adsorbed. This technique looked particularly promising and was investigated further.

A 6 cm^3 column of Bio-Rad AG 1x8 was prepared and pre-conditioned with 40 ml of 0.5 M HCl followed by 40 ml of 9 M HCl. 8 Bq of ^{210}Pb spike (with ^{210}Bi and ^{210}Po in equilibrium) was added to 20 ml of Fe^{3+} (10 mg ml^{-1} Fe^{3+}) carrier in 9 M HCl. After loading the column, eight 5 ml aliquots of 9 M HCl followed by one 50 ml aliquot were passed through the column for the elution of ^{210}Pb. Fe^{3+} was removed from the column with two 25 ml aliquots of 0.5M HCl. ^{210}Bi elution was achieved with ten 10 ml aliquots of 1 M H_2SO_4 followed by a final two aliquots of 50 ml 1 M H_2SO_4. The 5 ml and 10 ml aliquots were eluted into 20 ml scintillation vials and analysed directly after the addition of UG-LLT

(Section 2.1.3). The 25 and 50 ml aliquots were evaporated close to dryness, transferred to 20 ml scintillation vials and evaporated to dryness before the addition of 1 ml of 0.1 M HCl and 5 g UG-LLT and counted by LSS (Section 2.1.3). For the Fe^{3+} aliquots, the bulk of the Fe^{3+} was removed by DIPE extraction before proceeding as above for LSS analysis. Problems arose with the evaporation of the two 50 ml aliquots of 1 M H_2SO_4. The boiling point of H_2SO_4 is ~ 350 °C and therefore heating of the sample at 200 °C only removed the H_2O. This left concentrated H_2SO_4 in the vial which could not be removed by freeze-drying or evaporation. Addition of 20 g UG-LLT to this sample caused a black emulsion to form. The effect of concentrated H_2SO_4 is to cause sulphonation of the surfactants in the cocktail which leads to phase instability (Packard, 1996). The colour formation is due to sulphonation of minor impurities in the cocktail. Both these factors make the sample uncountable by LSS. The elution profile is displayed in Figure 2.21.

Again, Pb was eluted in a tight band free from Fe^{3+} interferences, the tailing observed in Figure 2.21 is due to the size of the last aliquot (50 ml) and the elution is likely to be tighter than shown. No activity was found in the Fe^{3+} aliquot. 100 % ^{210}Bi and around 50 % ^{210}Po recoveries were achieved. It would appear that ^{210}Po can be removed from strongly basic ion exchange resins, but because many elements are not adsorbed in H_2SO_4 systems, there is very little purification achieved by this step. Furthermore, the problems of trying to convert a large volume of H_2SO_4 into a suitable LSS matrix would appear to be a significant weakness, compared to any benefits of such an exchange scheme. If ion exchange is to be successfully employed as a purification method there must be suitable resolution of the

sample nuclides and they must be in a form which can be easily converted to a uniform sample matrix for LSS.

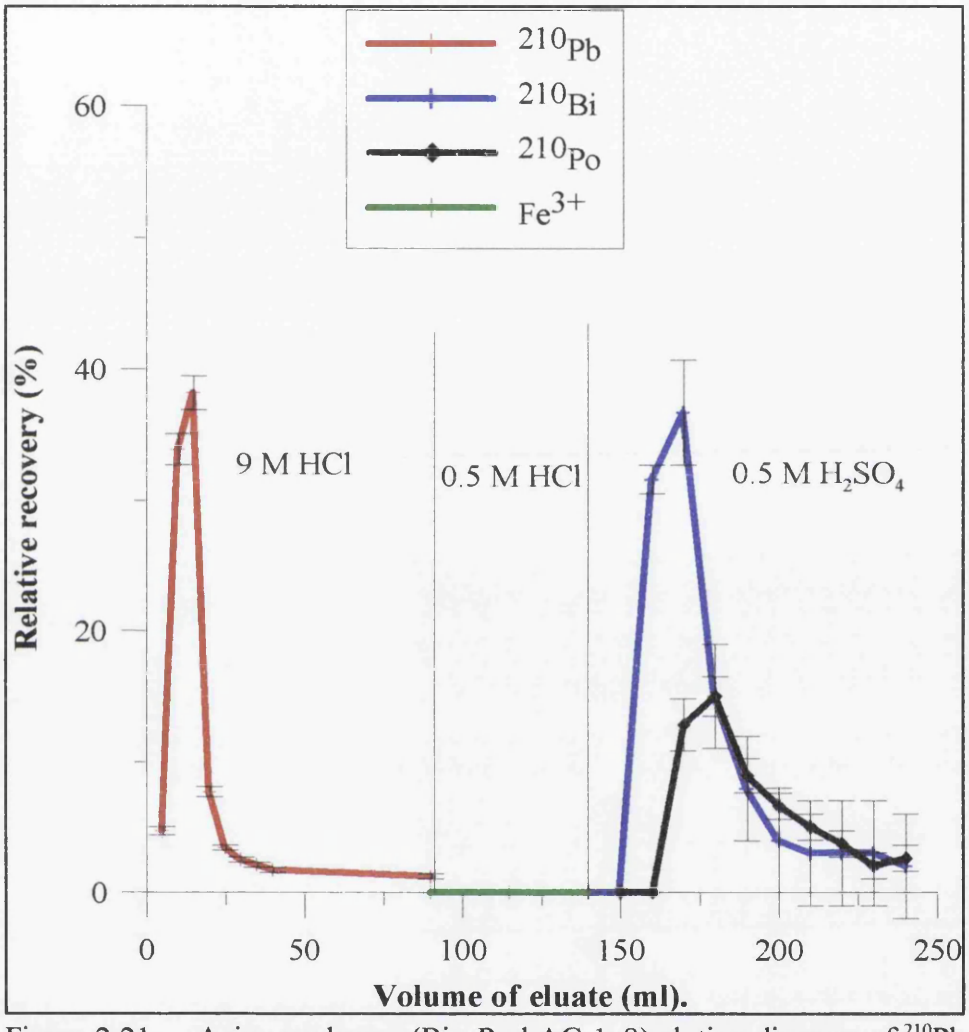

Figure 2.21: Anion exchange (Bio-Rad AG 1x8) elution diagram of ^{210}Pb (in 9 M HCl), Fe^{3+} (in 0.5 M HCl) and ^{210}Bi and ^{210}Po (in 1 M H_2SO_4). Elutions are successive and the elution of two nuclides with one elutant indicates contamination. Errors quoted at the 1σ significance.

So far, it has been demonstrated that Pb could be eluted without the presence of Fe^{3+}, if Po was removed by spontaneous deposition prior to ion exchange. Thus, the final hurdle would be the successful elution of Bi in a suitable matrix.

2.5.3.2.3 HNO_3 elutions

The ion exchange summary presented by Saito (1984) suggest that at low HNO_3 molarities, Bi elution may be possible in a smaller volume than achievable with HCl and in a more suitable matrix than H_2SO_4. An ion exchange procedure was set up to test this hypothesis. Once again, 8 Bq of ^{210}Pb spike (with ^{210}Bi and ^{210}Po in equilibrium) was added to 20 ml Fe^{3+} carrier (10 mg ml^{-1} Fe^{3+}). $Fe(OH)_3$ was precipitated by adding 18 M NH_4OH and the precipitate was re-dissolved in 20 ml of 9 M HCl. A 4 cm^3 column of Bio-Rad AG 1x8 was prepared and pre-conditioned with two 20 ml aliquots of 0.5 M HNO_3, two 20 ml aliquots of 0.5 M HCl and two 20 ml aliquots of 9 M HCl. Once the sample had been loaded in 9 M HCl, three 25 ml aliquots of 9 M HCl were added to elute ^{210}Pb. Three 25 ml aliquots of 0.5 M HCl were passed through the column to remove Fe^{3+}, before ten 10 ml aliquots, two 20 ml aliquots and two 50 ml aliquots of 0.5 M HNO_3 were added to elute ^{210}Bi. All aliquots were evaporated to near dryness, transferred to 20 ml glass vials before evaporation to dryness. The samples were re-dissolved in 1 ml 0.1 M HCl and 5 g UG-LLT added before counting by LSS (Section 2.1.3). Once again, the ^{210}Bi had 40 % of total ^{210}Po in the eluted fraction.

Despite the problem of partial Po elution, the experiment highlighted the fact that ^{210}Bi could

be successfully eluted with 0.5 M HNO_3 in a smaller volume than with HCl and in a more suitable matrix than H_2SO_4. Because Po would be spontaneously deposited onto copper foils before the column stage in a proper analytical scheme, it was decided that the ion exchange technique should be tested under realistic conditions.

With the elution data gained from the previous experiment it was decided that the experiment should be repeated but with ^{210}Po removed by spontaneous deposition onto Cu (Section 2.4.2). Firstly, an 8 Bq ^{210}Pb spike (with ^{210}Bi and ^{210}Po in equilibrium) and 20 ml Fe^{3+}(10 mg ml^{-1} Fe^{3+}) carrier were added to 50 ml of reverse osmosis water and 5 ml of 0.3 M $NH_2OH.HCl$. ^{210}Po was spontaneously plated for three hours onto a 1 cm^2 Cu foil with an epoxy resin backing. After this time, any co-deposited ^{210}Bi was removed from the Cu foil by rinsing the foil with reverse osmosis water back into the original plating solution. The plating solution was dried down and oxidised with 15 M HNO_3 and 12 M HCl, re-dried and dissolved several times in 9 M HCl to remove any last traces of 15 M HNO_3. The sample was loaded onto a 4 cm^3 column of Bio-Rad AG1x8 resin which had been pre-conditioned in the same manner as the previous experiment. After the sample had been loaded, five 15 ml aliquots of 9 M HCl were added to elute Pb. Fe^{3+} was removed with four 25 ml aliquots of 0.5 M HCl and finally Bi was eluted with ten 20 ml aliquots of 0.5 M HNO_3. All aliquots were evaporated to near dryness, transferred to 20 ml glass vials and taken to dryness. The residues were dissolved in 1 ml 0.1 M HCl before the addition of 5 g UG-LLT and the samples counted by LSS (Section 2.1.3). The elution diagram is shown in Figure 2.22.

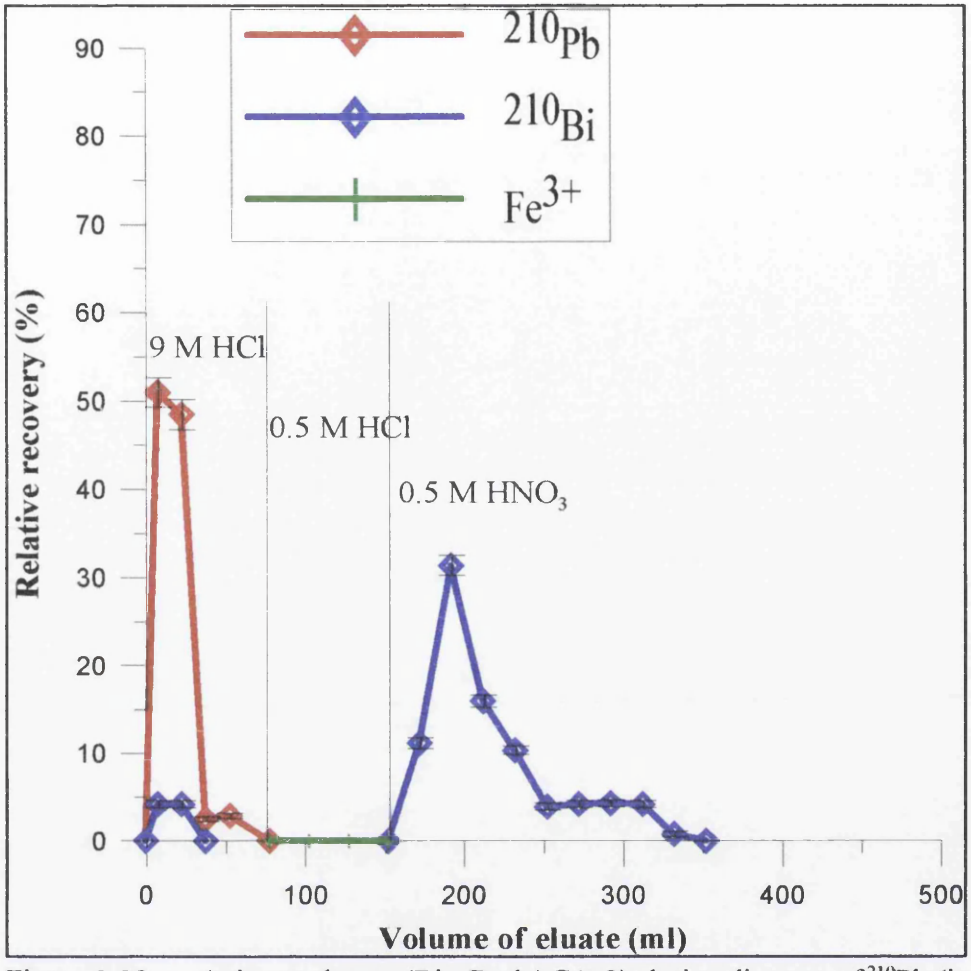

Figure 2.22: Anion exchange (Bio-Rad AG1x8) elution diagram of ^{210}Pb (in 9 M HCl), Fe^{3+} (in 0.5 M HCl) and ^{210}Bi (in 0.5 M HNO_3). Elutions are successive. Errors quoted at the 1σ significance.

It shows that using the HNO_3, 10 % of total ^{210}Bi activity will be carried through with the ^{210}Pb. This was detected after correcting the ^{210}Pb aliquots for ingrown ^{210}Bi when unsupported ^{210}Bi was observed. The recoveries of ^{210}Pb and ^{210}Bi are 100 % and 95 % respectively (the ^{210}Bi recovery includes ^{210}Bi eluted with ^{210}Pb). What this highlights is that the spontaneous deposition of ^{210}Po onto Cu foils is highly selective, and furthermore, any co-deposited ^{210}Bi can be removed from the foil by rinsing with reverse osmosis water. The

behaviour of Bi in 9 M HCl is unlike that seen in previous experiments and it is thought that the reducing agents added to the plating solution may be to blame. If any reducing agent is left un-oxidised then it may affect the ion exchange behaviour.

2.5.4 Other applications of ion exchange techniques

Further work on the behaviour of Pb on strongly basic resins was carried out as part of the purification scheme for ^{212}Pb from a $Th(NO_3)_4$ solution. Instead of investigating the removal of Pb, this work describes the procedures developed to maximise Pb retention on these columns while contaminants are removed. Full details of the experimental procedures can be found in Section 2.8. Similarly, the work carried out on ion exchange helped to improve the purification of Bi in marine samples. This work is presented in section 2.6.3.

2.5.5 Conclusions

The ion exchange behaviour of Pb Bi and Po on strongly basic resins has not been fully investigated and inconsistences between the literature and these experiments have been found. One possible cause of these variations is that application of LSS to the construction of these elution diagrams permits a visual interpretation of the spectra to be carried out. This process highlighted many of the anomalies and displays the power of LSS in modern radiochemical method development. Much of the original ion exchange data was derived from much less sophisticated instrumentation where no visual indicators were available. However, many of the differences in behaviour may be attributed to the oxidation state of the ion. For example, the removal of Pu from anion exchange columns requires the Pu to

be in the reduced 3+ state and not the oxidised 5+. Investigations into the anion exchange behaviour of Pb, Bi and Po in different oxidation states may provide useful methods for their purification. However, a full investigation was beyond the scope of this project.

Although ion exchange techniques could not fully resolve ^{210}Pb, ^{210}Bi and ^{210}Po to a sufficient degree, the behaviour observed in this series of experiments features later in the chapter. Anion exchange resins are utilized for purification of Bi and ^{212}Pb. In both these techniques, a highly selective procedure is required to remove contaminants. These applications of anion exchange techniques are described in the remaining sections of this chapter.

2.6 EiChrom Sr Spec column separation

At this stage in the research, a suitable separation scheme for the resolution of ^{210}Pb, ^{210}Bi and ^{210}Po from Fe^{3+}, and a range of NDS and anthropogenic radionuclides in seawater, was still sought. A highly selective technique for their purification was required which would also permit the application of chemical yield tracers. The activities of the particle reactive radionuclides ^{210}Pb, ^{210}Bi and ^{210}Po in seawater is usually much lower than their less particle reactive parents (e.g. ^{226}Ra, ^{234}U and ^{238}U). Furthermore, if the measurement of ^{210}Pb, ^{210}Bi and ^{210}Po is to be carried out in the Irish Sea, then it must be capable of removing the anthropogenic contaminants which may be present in much higher activities than the nuclides under investigation. During the course of investigating the ion exchange properties of Pb, Bi, Po and Fe^{3+}, a novel extraction method for the separation of Pb and Po was found in the literature. The method in question utilised an extractive chromatographic technique using crown ethers, which allows a highly selective purification of ^{210}Pb and ^{210}Po. Horwitz *et al.* (1992) present a summary of their experiments on the application of 4,4'(5')-bis(t-butylcyclohexano)-18-crown-6 (DtBuCH18C6) to the extraction of strontium in environmental analysis. They also observed a strong affinity between the resin and Pb, stronger even than the affinity of Sr for the resin. The commercial product is available from EiChrom Industries under the trade name Sr Spec (strontium specific). Application of Sr Spec resin in Sr analysis is a great improvement in both speed of analysis and safety compared to the classical fuming nitric acid method. Apart from Sr, only Pb, Np^{4+}, Po and Pu show significant affinity for the resin.

The Sr Spec resin is produced by impregnating Amberchrom resins with a 1 M solution of DtBuCH18C6 and is available as either bulk resin or in pre-packed columns. The selectivity of a crown ether is due to their ability to solvate metal cations by sequestering the metal in the centre of the polyether cavity (McMurray, 1992). Their selectivity for metal cations is a function of the cavity size and the ion size. The cavity size of the crown ether is determined by its size and structure, thus different crown ethers solvate different metal cations. The structure of the extractive agent is shown in Figure 2.23 and equation 2.2 represents the extraction process for Sr.

$$Sr^{2+} + 2NO_3^- + \underline{Cr} \rightarrow Sr(Cr)(NO_3)_2 \qquad (2.2)$$

where Cr represents 4,4'(5')-bis(t-butylcyclohexano)-18-crown-6

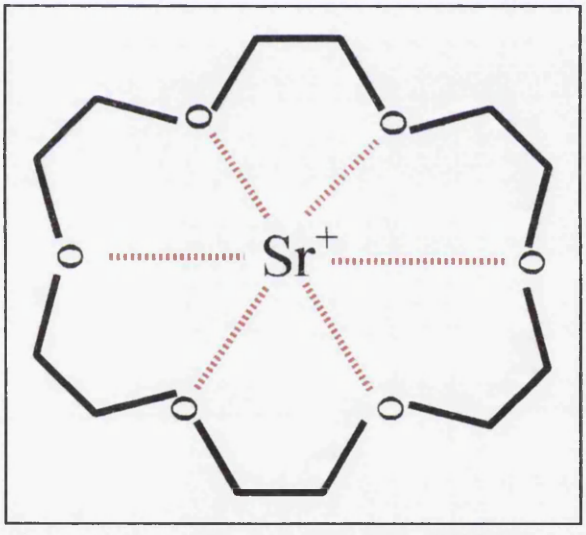

Figure 2.23: Structure of 4,4'(5')-bis(t-butylcyclohexano)-18-crown 6 extractant used in Sr Spec resin.

Only ions which exhibit an affinity for the crown ether (such as Sr, Pb, Po, Np^{4+} and Pu) can be held in this way and virtually every other ion will be removed from the column during the

washing process. The diameter of the inner cavity is 0.026 to 0.032 pm and the diameter of Sr^{2+} is 0.023 pm. Sr lodges in the crown ether cavity and is retained within by interaction with electronegative O_2 atoms within the crown ether structure. The selectivity of Pb and Po on Sr Spec resin is also based on the size of the Pb and Po ions.

2.6.1 Behaviour of Pb and Po on Sr Spec resin

Horwitz *et al.* (1992) characterised the affinity of many elements for this Sr Spec resin in HNO_3. Figure 2.24 highlights the selectivity of Sr Spec resin for Sr compared to the alkali and alkaline earth metals which would otherwise interfere with the purification of Sr. The affinity of Sr for this resin is higher than all these metals over virtually the whole HNO_3 concentration range that was studied (from 0.01 M to 10 M). Figure 2.25 shows the greater affinity of Pb and Po compared even to Sr. The retention of Pb on the column remains high throughout all HNO_3 concentrations (from 0.01 M to 10 M). In all HNO_3 concentrations studied, both Fe and Bi showed no affinity for the resin and passed through the column.

Vadja *et al.* (1997) present data concerning the behaviour of ^{210}Pb, ^{210}Bi and ^{210}Po in HCl solutions on Sr Spec resin. They found that in HNO_3 solutions, they were unable to resolve ^{210}Bi and ^{210}Po and so looked to HCl solutions. The behaviour of ^{210}Pb, ^{210}Bi and ^{210}Po in HCl was determined by LSS while ICP-AES was used to determine the behaviour of 16 stable elements. The results of the distribution coefficient experiments for ^{210}Pb, ^{210}Bi and ^{210}Po are presented in Figure 2.26. The affinity of Pb for Sr Spec resin decreases with increasing HCl concentration and at concentrations above 6 M HCl, Pb can easily be removed from the resin.

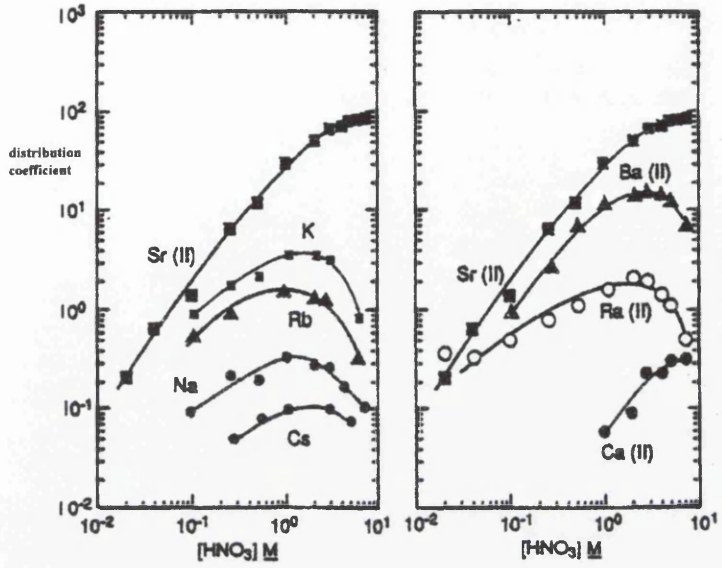

Figure 2.24: Distribution coefficients of Sr, alkali and alkaline earth metals in HNO_3 solutions on Sr Spec (after Horwitz *et al.*, 1992).

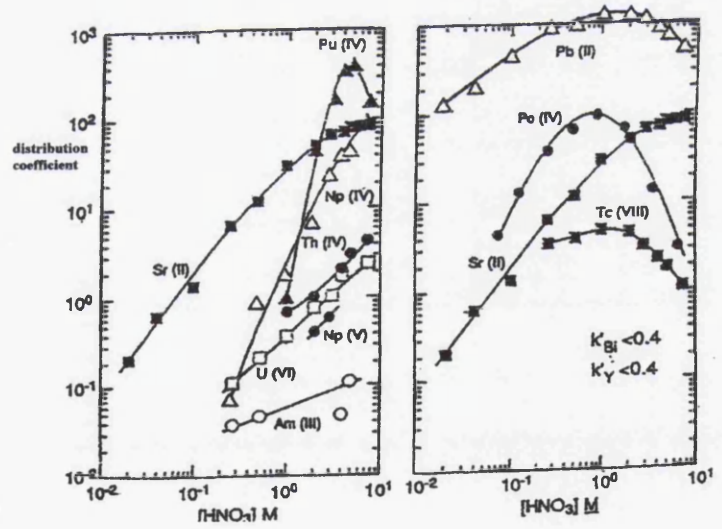

Figure 2.25: Distribution coefficient of Pb and Po in HNO_3 solutions on Sr Spec resin (after Horwitz *et al.*, 1992).

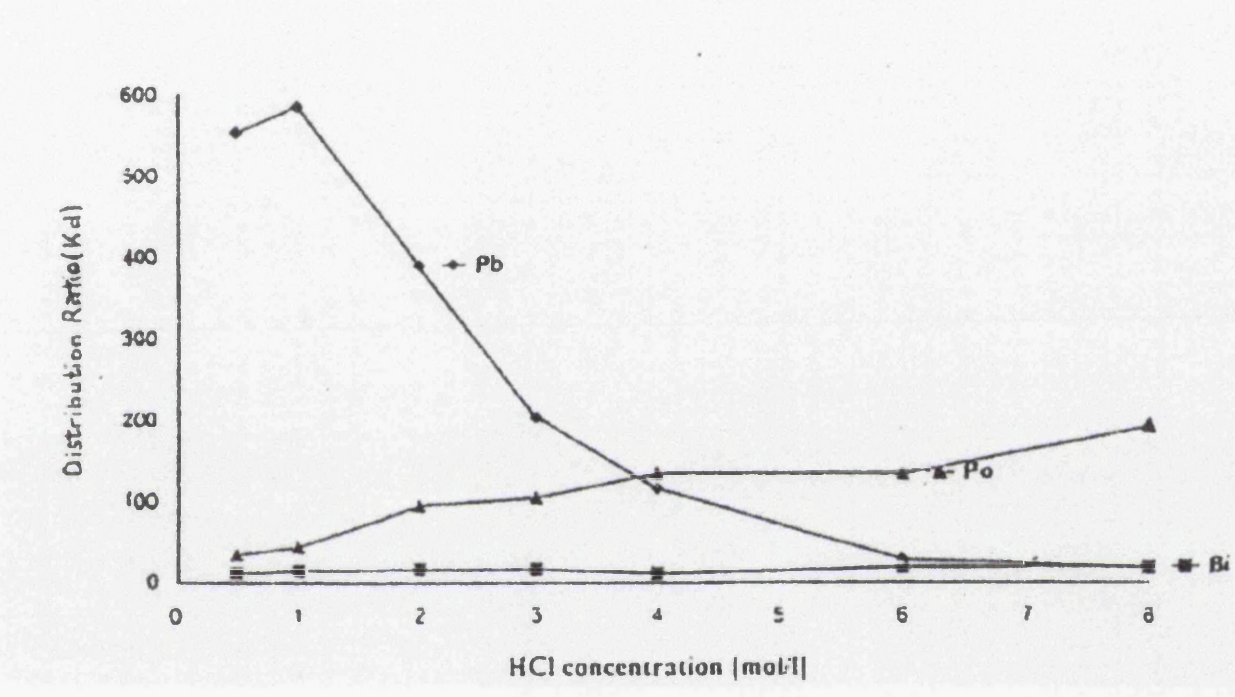

Figure 2.26: Distribution coefficients of Pb and Po in HCl solutions on Sr Spec resin (after Vadja *et al.*, 1997).

Bi was not retained by the column to any significant degree in all HCl concentrations that were investigated (0.5 M to 8 M HCl). The affinity of ^{210}Po for Sr Spec resin increases with increasing HCl molarity, although even at low HCl concentrations it is retained on the resin. The data on the behaviour of other selected elements highlights the selectivity of the resin for Pb and Po. All the elements studied can easily be stripped from the column with 2 M HCl. Included in this group of elements are Fe, Co and Mg, commonly used during co-precipitation stages in sample preparation of large water samples (Section 2.2).

There are clear advantages to the use of HCl with Sr Spec resin and by controlling the molarity of HCl passing through the column, Pb can either be retained or removed from the resin. In HNO_3 solutions, Pb is held tightly on the resin for the full range of concentrations studied (0.01 M to 10 M). It is this property that has led to Sr Spec resin being used to create ultra pure reagents for clean room work with Pb isotopes (R. Ellam, personal communication, 2000).

Vadja *et al.* (1997) have demonstrated a method for the purification of ^{210}Po by chromatographic methods which also allows Fe to be removed from both the ^{210}Pb and ^{210}Po aliquots. This technique therefore offers a range of possibilities for the successful resolution of ^{210}Pb and ^{210}Po from a wide range of possible contaminants.

2.6.2 Separation of ^{210}Pb, ^{210}Bi and ^{210}Po on Sr Spec resin

Vadja *et al.* (1997) continued their development with the Sr Spec resin to develop a robust

method for the determination of ^{210}Pb and ^{210}Po activities in sediment, soil, phosphate ore and biological samples. After loading the dissolved samples onto 3 g columns of bulk Sr Spec resin, they eluted with 100 ml 2 M HCl to remove interfering ions. ^{210}Po was then stripped from the resin with 85 ml of 6 M HNO_3, before removing ^{210}Pb with 60 ml of 6 M HCl. Po isotopes were spontaneously deposited onto Ag disks and counted by α-spectrometry. The recovery of Pb was determined by gravimetric analysis of a Pb-oxalate precipitate. Pb was then re-dissolved in HNO_3 and mixed with 15 ml Instagel, and the ^{210}Pb activity was determined by LSS. This technique permits a rapid determination of ^{210}Pb and ^{210}Po without the disadvantages of the traditional analysis (Section 2.1.2). Namely, ^{210}Po is separated prior to its spontaneous deposition, which prevents ingrowth of ^{210}Bi affecting the final results. The removal of Fe^{3+} in the 2 M HCl fraction makes for a more efficient plating of ^{210}Po and prevents Fe^{3+} having a quenching in the LSS determination of ^{210}Pb. Direct determination of ^{210}Pb can be achieved and this removes the long time delay present in the conventional analysis.

2.6.2.1 Spike experiments

The method of Vadja *et al.* (1997) was attempted but commercially available pre-packed columns of Sr Spec resin were used instead of 3 g of bulk resin. The pre-packed columns contain only 0.77 g of material but have the advantage of being uniformly constructed. 8 Bq of ^{210}Pb (with ^{210}Bi and ^{210}Po in equilibrium) spike in 0.1 M HCl was freeze dried and the residue dissolved in 2 ml of 2 M HCl. The pre-packed column was pre-conditioned with 100 ml aliquots of reverse osmosis water, 1 M HCl, 1 M HNO_3 and 2 M HCl. The ^{210}Pb spike

was added and the vial rinsed three times with 2 ml aliquots of 2 M HCl to ensure all the activity was added to the column (the transfer was checked by adding UG-LLT to the empty vial and counting by LSS). 100 ml of 2 M HCl (4 x 25 ml) were added to the column to remove ^{210}Bi, followed by 75 ml of 6 M HNO_3 (3 x 25 ml) to elute ^{210}Po, and finally 75 ml 6 M HCl (3 x 25 ml) was used to remove ^{210}Pb. The Pb, Bi and Po fractions were evaporated to near dryness, transferred to 20 ml scintillation vials and taken to dryness. The residues were re-dissolved in 1 ml of 0.1 M HCl before adding 5g UG-LLT and counting on a Packard 3170 TR/SL (Section 2.1.3). The spectra obtained from the Bi, Po and Pb elutions are shown in Figure 2.27.

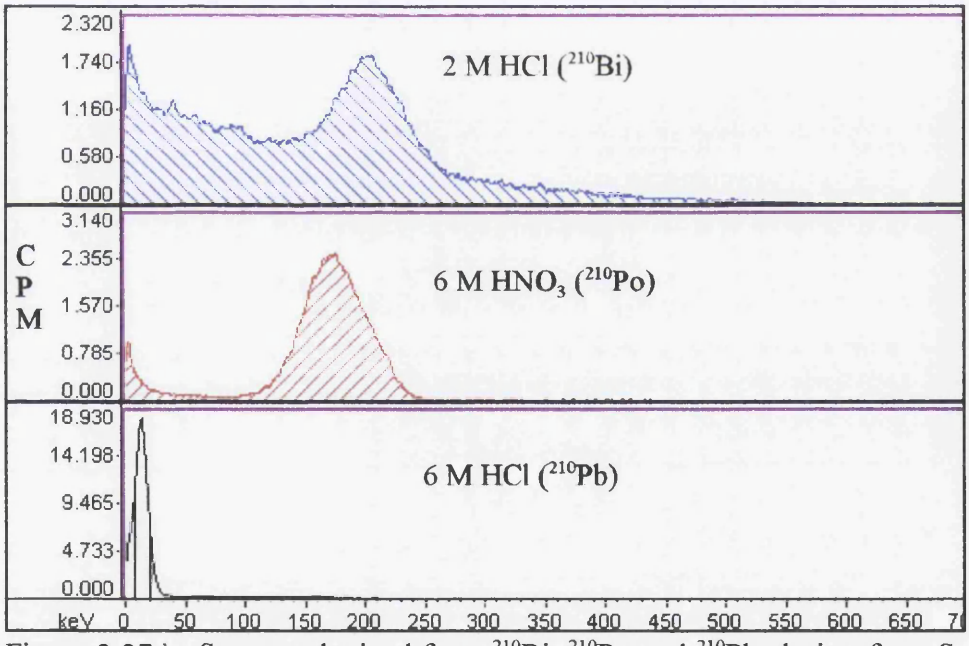

Figure 2.27: Spectra obtained from ^{210}Bi, ^{210}Po and ^{210}Pb elution from Sr Spec resin using the acid volumes suggested by Vadja *et al.* (1997).

It is clear that the volumes of acid used for the 3 g columns must be scaled down for the pre-packed columns. The main problem was the significant elution of ^{210}Po with ^{210}Bi in the 2 M HCl fraction. Success of this method required resolution of Bi and Po. To achieve this, the experiment was repeated and an elution profile was constructed by collecting small aliquots of the eluate and analysing each aliquot by LSS (as had been carried out in the ion exchange procedures). The elution was carried out as follows. The sample was loaded onto the column in 10 ml of 2 M HCl. Elution was carried out using one 20 ml aliquot of 2 M HCl followed by eight 10 ml aliquots. This was followed by three 20 ml aliquots of 6 M HNO_3 and two 10 ml aliquots, followed by eight 10 ml aliquots of 6 M HCl. The eluted fractions were evaporated to near dryness and transferred to 20 ml glass vials before being evaporated to dryness on a hot-plate. The residue was then re-dissolved in 1 ml of 0.1 M HCl before the addition of 5 g UG-LLT. The samples were then counted by LSS (Section 2.1.3) with appropriate blanks and the elution diagram is illustrated in Figure 2.28.

It was observed that Bi passes through the column and full recovery was achieved with 40 ml of 2 M HCl. At greater volumes of 2 M HCl, there is a small trace of ^{210}Po as breakthrough begins. Similarly, ^{210}Po is found in the first 40 ml of 6 M HNO_3. ^{210}Pb was fully recovered in 30 ml of 6 M HCl. The optimum acid volumes were 40 ml 2 M HCl, 40 ml 6 M HNO_3 and 30 ml 6 M HCl, which were then used for all subsequent work.

2.6.2.2 Seawater experiments

The results obtained prove that Pb and Po can be resolved successfully in simple spike

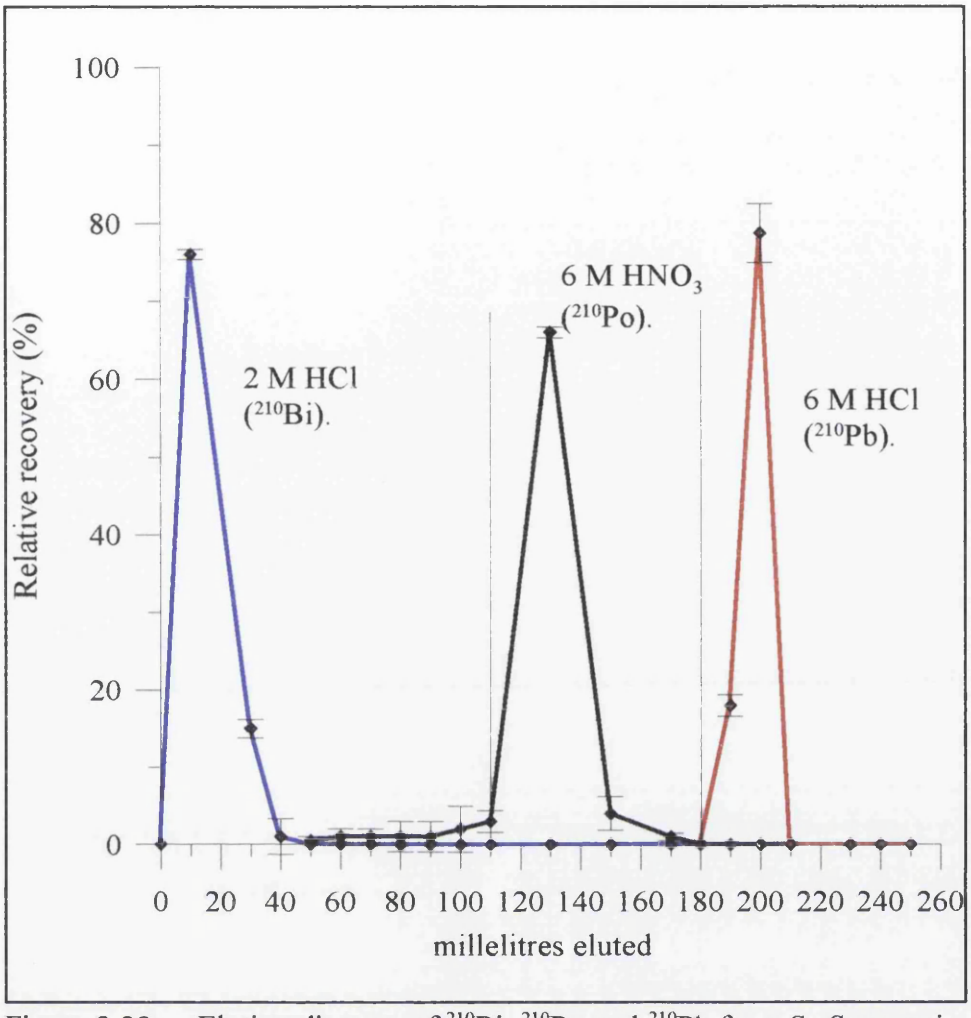

Figure 2.28: Elution diagram of ^{210}Bi, ^{210}Po and ^{210}Pb from Sr Spec resin. Errors quoted at the 1σ significance.

experiments. However, more complex matrices, such as seawater, may be more difficult to analyse and may interfere with the separation. To examine this, a "real" sample was created by spiking a 20 litre seawater sample (pre-filtered through 0.22 μm filter) with 8 Bq of ^{210}Pb spike (with ^{210}Bi and ^{210}Po in equilibrium) and 20 ml Fe^{3+} carrier (10 mg ml^{-1} Fe^{3+}). The surface seawater sample was collected from Dunure harbour in Ayrshire. In this environment, there should be virtually no dissolved ^{210}Pb, ^{210}Bi or ^{210}Po due to the enhanced

particle scavenging so close to shore. The activities of any ^{210}Pb, ^{210}Bi or ^{210}Po present naturally in the sample would be insignificant compared to the activity of spike added. The nuclides were co-precipitated with $Fe(OH)_3$ which was then washed with reverse osmosis water to remove any co-precipitated salts of major ions. To improve the column separation, the bulk of the Fe^{3+} carrier was removed by solvent extraction with DIPE prior to loading. This is recommended for several reasons:

1. The columns run much faster without the excess of Fe^{3+} in the sample.
2. It also prevents interference from Fe^{3+} which could swamp the column if present in too high a concentration (M. Langer, personal communication, 1999). In the application of these columns to Sr purification, no more than 10 mg $Sr(NO)_3$ carrier is recommended.
3. Evaporation of an Fe^{3+} rich solution creates problems of its own. It is difficult to remove the last tracers of acid without baking the sample onto the glassware.

It was also necessary to oxidise the concentrated sample prior to loading. If this stage is not carried out, the column can become blocked due to the presence of organic material in the sample. This was achieved by refluxing the sample in aqua regia for several hours. After the oxidation stage, the sample was evaporated and re-dissolved in 2 M HCl several times. The Bi, Po and Pb fractions were eluted using the optimised acid volumes (40 ml, 40 ml and 30 ml respectively) and prepared for LSS by the usual technique (Section 2.1.3). The recoveries obtained are presented in Table 2.10. The fractions were radiochemically pure and the yields were high, considering the size and complexity of the matrix.

Nuclide	Recovery
^{210}Pb	84.5 ± 2.0 %
^{210}Bi	84.1 ± 2.0 %
^{210}Po	69.2 ± 1.6 %

Table 2.10: Recoveries of ^{210}Pb, ^{210}Bi and ^{210}Po obtained from a spiked 20 litre seawater sample purified through a Sr Spec column. Errors quoted at the 1σ significance.

2.6.3 Elution behaviour of ^{210}Bi

Although this section should appear in the section on ion exchange techniques it has been included in the Sr Spec section for continuity. What the spike experiment did not show is that the removal of Bi from the Sr Spec resin does not "purify" the element. Many other elements are removed with the 2 M HCl fraction and a simple DIPE extraction to remove Fe^{3+} will not have any effect on the bulk of potential interferences present during ^{210}Bi determination. This includes both NDS nuclides (U, Th and Ra isotopes) and anthropogenic nuclides (^{60}Co, ^{90}Sr and ^{241}Pu, for example) This led to further development work with conventional anion exchange resins and picked up on previous techniques which had been less successful than the Sr Spec technique (Section 2.5). The speed of analysis is an important factor in ^{210}Bi determination due to the short half life of ^{210}Bi. The solvent extraction removal of Fe^{3+} initially appeared to be the quick and easy answer. When a 20 litre seawater sample was spiked with 8 Bq of ^{210}Pb, the DIPE extraction of Fe^{3+} was sufficient, but the activity used masked any interferences observed in real environmental samples. In reality, the activities of ^{210}Bi will be much lower than that of U, Th and Ra activities so a highly selective purification is required.

To address this problem, the ion exchange behaviour of ^{210}Bi was examined in more detail. U would be expected in measurable concentrations in seawater and would also be eluted from Sr Spec resin in 2 M HCl. Th isotopes may also interfere with the Bi determination if the sampling was carried out in open ocean locations. The highest activities would be expected from ^{238}U due to its conservative behaviour in the water column (Section 1.1.3). Oceanic ^{238}U activities have been reported around 0.042 Bq l^{-1} (Pates, 1995) which is far in excess of nearshore dissolved ^{210}Pb activities of 0.070 to 0.910 mBq l^{-1} reported for the Irish Sea (McCartney *et al.*, 1990). The ion exchange procedure was then designed to remove U and Th from the column before the elution of ^{210}Bi.

Drawing on the experienced gained previously with anion exchange separation allowed a robust purification technique to be developed. The highest retention of Bi occurs in low molarity HCl solutions (Fig. 2.16). Hence, it would be wise to use this feature to strip off the interferences if possible. Fortunately, both U and Th show negligible affinity for the column in such solutions and quantitative removal of Bi from AG1x8 resin in 0.5 M HNO_3 was demonstrated earlier (Section 2.5.3.2.3). A new experiment was devised to test the retention of Bi in 0.5 M HCl solutions. Instead of using an aliquot of ^{210}Pb spike, the Bi yield tracer, ^{207}Bi, was applied (Section 2.8.2). This offers several advantages over using the ^{210}Pb spike. Firstly, the spike is a pure Bi spike without radioactive parent or daughter nuclides to complicate the experiment. Its half life of 32.2 years (Lederer and Shirley, 1978) is much more suitable than ^{210}Bi for this type of experiment and finally, it is easily measurable by LSS or γ spectrometry.

A 1 ml aliquot of ^{207}Bi in 4 M HNO_3 was transferred to a 20 ml glass scintillation vial. The spike was then freeze dried in the vial, after which it was re-dissolved in 2 ml of 0.5 M HCl. A 4 cm^3 column of EiChrom AG1x8 was pre-conditioned with two 20 ml aliquots of 0.5 M HNO_3 and two 20 ml aliquots of 0.5 M HCl. The spike was loaded onto the column and five 10 ml aliquots of 1.2 M HCl were added. Bi was then eluted with ten 20 ml aliquots of 0.5 M HNO_3. Each aliquot was eluted directly into a 20 ml scintillation vial and it was evaporated to dryness on a hotplate. The residue was re-dissolved in 1 ml of 0.1 M HCl and 5 g UG-LLT were added. The activity of ^{207}Bi was determined by LSS (Section 2.1.3) and the results are shown in Figure 2.29.

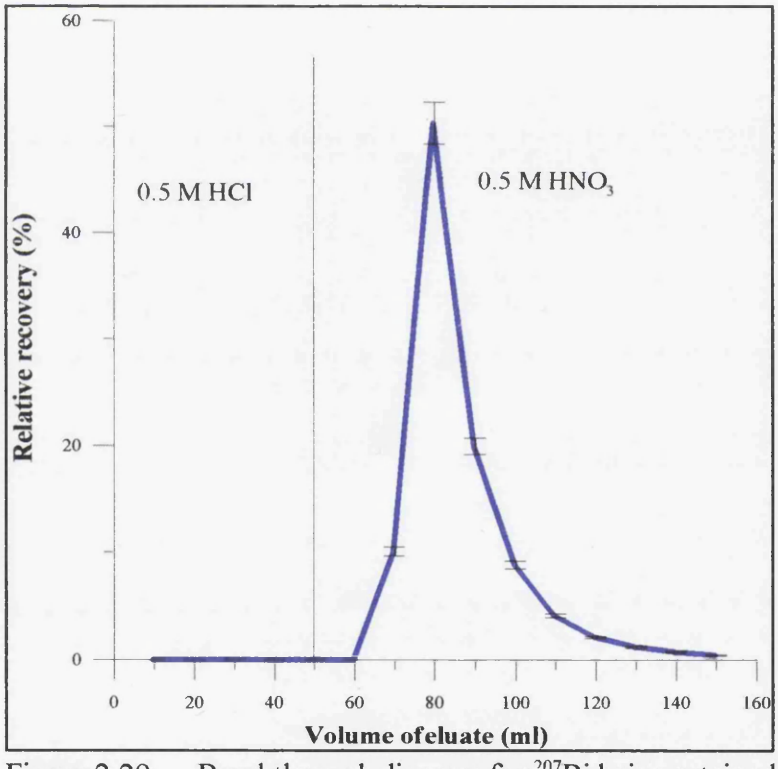

Figure 2.29: Breakthrough diagram for ^{207}Bi being retained in 0.5 M HCl (50 ml) and eluted with 0.5 M HNO_3 using a 4 cm^3 column of EiChrom AG1x8.

The recovery calculations were relative recoveries base don the LSS count rate from an identical aliquot of ^{207}Bi spike which was counted by LSS (Section 2.1.3) in conjunction with the samples.

The first 50 ml washing (0.5 M HCl) contained no Bi but full recovery of Bi was obtained with 100 ml of 0.5 M HNO_3. However, when this purification of Bi was applied to environmental samples it was found that there was still contamination of the Bi fraction with additional unknown activity. This was detected when the ^{210}Bi vial was re-counted after 20 days and residual activity was noted to be present in the vial. Two possible conclusions could be drawn. Either the volume of 0.5 M HCl was not sufficient to remove all the contamination before the elution of Bi with 0.5 M HNO_3 or the process itself was flawed due to another contaminant in the sample that was retained in 0.5 M HCl and eluted in 0.5 M HNO_3.

Work carried out previously with the extractive scintillator POLEX had shown that the extraction of Bi by TOPO was highly specific. Because Po isotopes had already been separated using the Sr Spec column, the extraction should be simple.

2.6.3.1 Purification of Bi by extractive scintillators

This idea was tested on the Bi fraction of a water sample collected from the Irish Sea (IS 6). The 2 M HCl fraction containing Bi was collected and Fe^{3+} was removed by solvent extraction with DIPE before being transferred to a 7 ml scintillation vial. This was taken to dryness and re-dissolved in 1 ml of 0.1 M HCl and 4 ml of 7 M H_3PO_4. 2 ml of the extractive

scintillator were added and the sample shaken for 30 minutes. A 1 ml aliquot of POLEX was removed to a 7 ml glass scintillation vial and counted on a 3170 TR/SL in NCM for 100 minutes. To determine the count rate of ^{207}Bi in POLEX, an extraction of pure ^{207}Bi corresponding to 100 % recovery of ^{207}Bi was also carried out. This allowed the chemical recovery of Bi to be determined by comparing the γ spectrum of both the sample vial and the spiked vial.

Despite the more specific extraction of Bi into an organic cocktail there was still contamination of the Bi fraction. According to the data on the extractive agent TOPO, the only other nuclide that could be extracted under these conditions is U (White and Ross, 1961; Case and McDowell, 1982). The data produced suggests that the contamination of the Bi fraction was indeed from U and hence the use of extractive scintillators would require scrubbing of the organic phase to remove this U (Case and McDowell, 1982). However, this stripping procedure is also shown to remove ^{210}Bi (Case and McDowell, 1982). The POLEX extraction had already been rejected because of instability of the toluene scintillator through time and the variable background. With the contaminant identified, the previous anion exchange method could be refined to ensure that all U was removed.

2.6.3.2 Re-assessment of anion exchange technique

To remove U from the column, the volume of 0.5 M HCl washings would have to be increased before the elution of Bi. A larger column length would allow Bi to be retained for a larger volume of 0.5 M HCl washings. A 1 ml aliquot of ^{207}Bi tracer was prepared as before

and was added to a pre-conditioned 5 cm^3 column of EiChrom AG1x8. Fifteen 10 ml aliquots of 0.5 M HCl were added, followed by four 25 ml aliquots of 0.5 M HNO_3. The samples were evaporated close to dryness, transferred to a 20 ml glass vial, evaporated to dryness, re-dissolved in 1 ml 0.1 M HCl and 5 g of UG-LLT added before counting by LSS (Section 2.1.3). The elution diagram observed in Figure 2.30 was constructed by comparing the net count rates from each fraction to an identical aliquot of ^{207}Bi. Figure 2.30 illustrates that Bi can be retained on the column even with the larger volume of 0.5 M HCl.

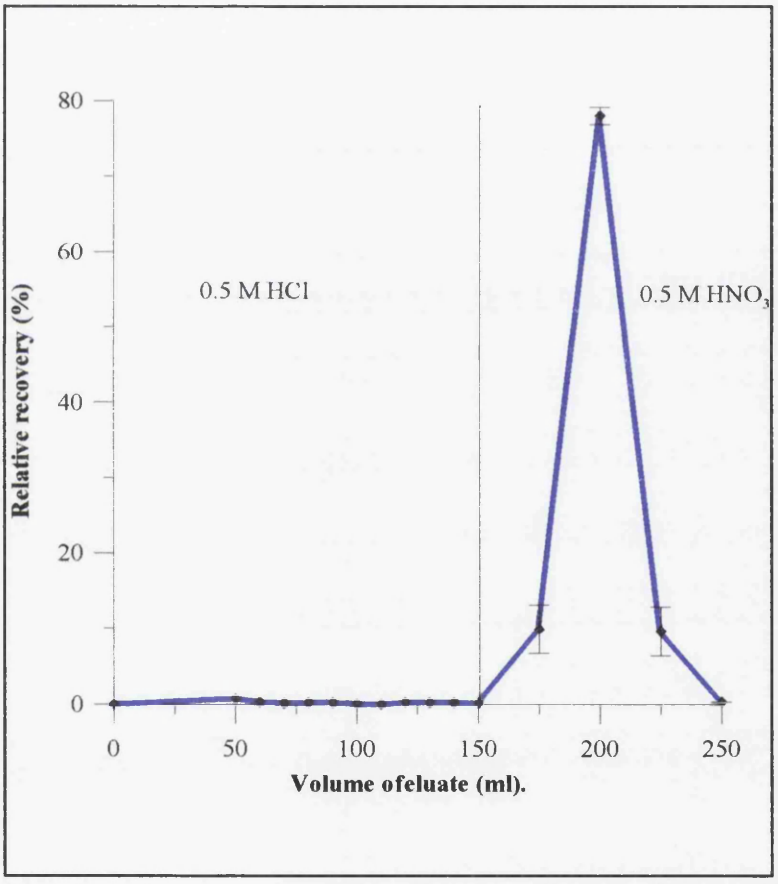

Figure 2.30: Breakthrough diagram for the improved retention of ^{207}Bi in 0.5 M HCl (150 ml) and its elution in 0.5 M HNO_3 using a 5 cm^3 column of EiChrom AG1x8.

2.6.4 Purification of ^{212}Pb

Another possible application of Sr Spec that could be of use in this study was the purification of ^{212}Pb from a $Th(NO_3)_4$ solution. ^{212}Pb was investigated as a possible yield tracer for the recovery of ^{210}Pb. After the successful application of Sr Spec resin to the resolution of ^{210}Pb and ^{210}Po it was decided that this route was worthy of investigation. This was especially relevant when anion exchange separation with AG1x8 resin was proving to be a challenge (Section 2.8). Horwitz *et al.* (1992) also presented data on such a scheme. ^{212}Pb could be successfully stripped from ^{224}Ra or ^{228}Th spikes. The strong affinity of Pb for the resin in HNO_3 solutions compared to virtually all other elements suggested that this may also prove to be fruitful.

In 0.1 M HNO_3, Pb is retained on Sr Spec resin while Th and Ra pass through the column. Horwitz *et al.* (1992) used an ammonium oxalate solution as a stripping agent for Pb. This allowed Pb to be removed easily from the column but its disadvantage lay in the low solubility of Pb in ammonium oxalate. Therefore, the Pb stripping agent was changed to 6 M HCl as the removal of Pb from pre-packed Sr Spec columns had been characterised earlier. A 1 ml solution containing approximately 1.2 g $Th(NO_3)_4$ in 0.1 M HNO_3 (equivalent to ~ 2000 Bq ^{212}Pb) was loaded onto a pre-conditioned Sr Spec column. Three 15 ml aliquots of 0.1 M HNO_3 were added to elute Ra and Th. Pb was then removed from the column with the addition of two 15 ml aliquots of 6 M HCl. The 6 M HCl aliquot was evaporated close to dryness and transferred to a 20 ml glass vial. The sample was then evaporated to dryness and re-dissolved in 1 ml 0.1 M HCl before the addition of 5 g UG-LLT. The vial was counted

for 1 hour on a HPGe γ photon detector to determine the presence of ^{212}Pb. The vial was then counted by LSS (Section 2.1.3) to monitor the decay of ^{212}Pb. The end result of these experiments was that ^{212}Pb could be purified from a $Th(NO_3)_4$ solution when conventional ion exchange techniques were, at this stage, unable to do so. However, there were several findings from this series of experiments which led to the selection of a conventional ion exchange technique over the Sr Spec technique.

1. The Sr Spec method was the first purification of ^{212}Pb that had been a success but it highlighted the fact that there was contamination of ^{212}Pb with ^{210}Pb. The contaminant ^{210}Pb could be observed in the LS spectrum after the decay of ^{212}Pb. At this stage, conventional ion exchange had not been developed far enough to see this.

2. When Pb is removed from Sr Spec there is a white residue found in the eluted Pb fraction, this has to be oxidised with strong acids and peroxide. The presence of this residue will interfere with the counting of the purified ^{212}Pb spike. The ^{212}Pb aliquot would require oxidation before γ spectroscopy and addition to the seawater sample. This makes its preparation time consuming and open to possible errors. The residue is also found in the 0.1 M HNO_3 eluate, which creates problems if the same 0.1 M HNO_3 fraction is to be continually milked as a source of ^{212}Pb.

3. Sr Spec columns can be regenerated to allow them to be used up to ten times (Vadja *et al.* 1997). However, this could not be achieved using the pre-packed Sr Spec

columns (this may be due to over-loading of the resin). Regeneration of the columns could not be achieved as there were memory effects when the columns were reused. This would require a new column for each purification and the cost of the columns was also a factor.

Although the experiments on ^{212}Pb purification were successful, these other factors suggested that the best results would be achieved by continued development of the anion exchange methodology. What it did highlight, however, was the presence of ^{210}Pb in the ^{212}Pb fraction. Knowledge of this contamination led to refinement of the anion exchange technique and the successful spike purification using anion exchange techniques (Section 2.8).

2.6.5 Regeneration of Sr Spec columns

It is possible to regenerate the Sr Spec resin so that the same column can be used again. Several authors (Vadja *et al.*, 1997; Jeter and Grob, 1994) have found that the columns can be re-used up to ten times before any degradation of the resin occurs. Regeneration is achieved by washing the column with distilled water (50 ml), 0.1 M ethylene di-amine tetra-acetic acid (EDTA) (100 ml), distilled water (50 ml) and finally 2 M HCl (100 ml). The columns are then stored in 2 M HCl. However, regeneration is only possible if the columns are not allowed to run dry during their use. Columns which have run dry will develop air pockets in the resin and this results in non-uniform distribution and these should be discarded. Re-using columns is an economic advantage of Sr Spec columns but frequently, the columns are discarded after a single use due to memory effects in the resin (Clark, 1995; Bricout,

1994). For these reasons columns used in this research were discarded after a single use.

2.6.6 Techniques for the successful application of Sr Spec

During the course of the investigations into Sr Spec resin, several features were noted which proved to be important for optimum use of these resins.

1. The resin should never be allowed to run dry. Not only does this dramatically slow down the elution process but it also prohibits the regeneration of the columns.

2. The speed of elution is greatly increased by removing large concentrations of interfering ions prior to loading. Fe^{3+} was removed by DIPE extraction before loading to prevent slow elution occurring. The removal does not need to be absolute for the effect to be noticed.

3. A white residue is often found when the eluted fractions are dried down. The residue does not dissolve in acidic solutions and requires oxidation with strong acids and peroxide. Vadja *et al.* (1997) placed the sample in a muffle furnace at 400 °C to destroy it but oxidation with strong acids is less likely to volatilise any of the nuclides.

4. Often, a white material was deposited onto the top frit of the column. This had been previously observed by Bricourt (1994) and the material can be carefully removed to allow the column to run. Analysis of this material by LSS showed that it contained no activity.

A wide range of radioanalytical separation schemes were investigated during this research but the use of extractive chromatography was by far the best technique. The separation of Pb, Bi and Po is relatively simple and does not require the use of any specialised chemicals or equipment. Furthermore, the elution behaviour of these elements could be further characterised to provide much tighter elution sequences in terms of volumes of acid required to elute each nuclide. In Sr application, Sr isotopes are fully removed with only 10 ml of 0.05 M HNO_3 (Goutelard *et al.*, 2000). Further research into determining the optimum pre-conditioning of the columns may also help to make the elution faster and may prevent the degradation of the columns that prohibited their re-use. The biggest advantage of theses columns is their selectivity for Pb and Po. This is especially important in this study where the activities of ^{210}Pb and ^{210}Po are very low and there is the presence of a number of NDS and anthropogenic radionuclides present in the sample. The techniques are now in place for the resolution of Pb, Bi and Po in marine water samples.

2.7 Analytical hardware

The theory behind LSS has been discussed in detail in chapter 1. The other detectors used in this work are high purity germanium (HPGe) detectors for γ spectrometry and passivated ion-implanted planar silicon (PIPS) detectors for α spectrometry. These will briefly be discussed below.

2.7.1 Semi-conductor detectors

The use of semi-conductor detectors is widespread today in almost all fields of radiochemistry. By definition, a semi-conductor will conduct at high temperatures and act as an insulator at low temperatures. A conductor such as copper (10^{-8} Ωm), will always have the conduction band occupied whereas an insulator such as Quartz (10^{12} Ωm) will only contain electrons in the valence band. Silicon (10^{3} Ωm) and germanium (0.6 Ωm) are semi-conductors, i.e. they act as conductors when thermal excitation of electrons causes a transition from the valence band to the conduction band. . There is a wide variety of semi-conductor detectors available but only these two systems will be described. More details on semi-conductor detectors can be found in any modern radiochemistry textbook (e.g. Choppin, 1994; Ehmann and Vance, 1991; L'Annunziata, 1998).

2.7.1.1 Alpha spectrometry

Two types of silicon are combined in an α spectrometer; p-type and n-type silicon. n-type silicon has phosphorous introduced as an electron donor and this introduces extra electrons which create an excess negative charge, thus, conduction occurs by electrons. If indium is

added as an impurity, the silicon will become an acceptor material and conduction is through the movement of positive holes. If these two materials are brought together, a p-n junction is formed. Some of the positive holes move to the n-type material and some of the negative electrons move to the p-type material. This creates a small depleted layer a few microns thick in the middle of the detector. As the holes are filled with electrons there are no charge carriers and the material is an insulator. If a voltage is applied across the detector in an arrangement termed *"reverse bias"*, then the p-type material is connected to the anode and the n-type to the cathode. This acts to draw the holes and electrons to their opposite charge and thus intensifies the size of the depleted layer such that no current flows. An α particle released by decay in a sample held close to the detector will cause the formation of ion pairs within the semi-conductor which are efficiently collected at the respective electrodes due to the high potential difference applied across the detector. The higher the specific ionization of the α particle, the greater the response at the electrodes. This feature allows the resolution of individual α energies, which is much more limited with LSS. Once the charge has been collected, the original conditions are restored in the silicon. In α spectrometry, these detectors must be operated under vacuum to prevent the attenuation of the α particles by air. The signals produced at the electrodes are amplified and sent to an ADC and then an MCA.

α spectrometry is a very sensitive method for α particle detection and offers FWHM of around 20 keV. Its insensitivity to β and γ radiation provides very low background count rates but its counting efficiency of around 20 % requires long count times for low activity

measurements. This technique is capable of resolving the α particles from ^{210}Po from those of ^{208}Po or ^{209}Po, added as a chemical yield tracer. The background over the course of 1,000,000 seconds can be as little as 10 counts (i.e. 0.0006 cpm-this study) which makes α spectrometry suitable for very low level activity determination.

2.7.1.2 Gamma spectrometry

For γ spectroscopy, germanium is the most commonly used detector material. Its advantage over silicon detectors is that the higher atomic number of germanium compared to silicon gives it a higher density (5.32 g cm^{-3} for Ge and 2.33 g cm^{-3} for Si). It therefore has a higher stopping power for γ photons which make it a more efficient detector. Today, HPGe detectors, available as either P-type or N-type, have almost completely replaced the Ge(Li) detectors once used for γ spectrometry. P-type γ spectrometers have a thicker entrance window and have a dead layer some 700 μm thick and this limits the detector to the measurement of γ photons above 40 keV. N-type detectors have an ion-implanted p+ contact which results in a dead layer of only 0.3 μm thick. This, combined with a thin Be or carbon-epoxy window, allows N-type detectors to measure γ photons greater than 3 keV. If an Al detector cap is used, N-type detectors can accurately determine γ emissions from about 15 keV upwards. As with α spectrometry, the reverse bias applied to a semiconductor causes a depleted region in the crystal. To allow this depleted layer to form in Ge detectors, the crystal must be cooled to around 77 °K. If a germanium crystal is cooled and a voltage applied in reverse bias, then no current will flow across the crystal. If

a γ photon interacts with the depleted region it raises electrons from the valence band to the conduction band. As with α spectrometry, the high potential difference across such a detector causes the charge to be drawn to the electrode. This produces an electrical pulse that is proportional to the incident radiation and this forms the basis of γ spectrometry. The additional hardware involved in γ spectrometry is typical of modern radioanalytical instrumentation and similar to α spectrometry. The detector is connected to a pre-amplifier, amplifier, ADC and MCA. Recent advances in γ spectrometry have seen the development of digital γ spectrometry which allows all the electronics to be integrated and controlled by a PC. Also, electrical cooling systems are now available. These use a He refrigerant gas to keep the detectors at the optimum temperature without the need for liquid nitrogen (LN_2). Further details about both γ and α spectrometry can be found in Gilmore and Hemingway (1995) and Choppin (1994) but it is beyond the scope of this work.

2.8 Yield tracers

A yield tracer is a known activity of an isotope of the desired element or a known concentration of a stable form of the radioactive species undergoing analysis. In addition, it must not interfere with the determination of the analyte itself.

At the outset of this research it was hoped that constant recoveries could be reached for ^{210}Pb, ^{210}Bi and ^{210}Po. If this could be achieved, the ratio of $^{210}Po/^{210}Pb$ and $^{210}Bi/^{210}Pb$ could be derived using LSS. This was especially attractive as determination of ^{210}Po currently requires a ^{208}Po or ^{209}Po tracer and determination by α spectrometry. This is a lengthy process due to the low α counting efficiency using this technique, which requires count times of up to 2 weeks. Application of LSS would allow a rapid determination of ^{210}Pb, ^{210}Bi and ^{210}Po due to the high counting efficiencies that can be achieved with LSS (~ 100 % for ^{210}Po and ^{210}Bi and ~ 95 % for ^{210}Pb).

Although a tracer free method for the determination of $^{210}Pb/^{210}Bi/^{210}Po$ is theoretically possible, the variable yields being obtained meant that yield tracers for each nuclide would have to be employed. The cause of the variations in the chemical recoveries most likely arose from the pre-concentration step. The tracer free methods reviewed in the literature (Section 2.3) were for less complex methods which did not require pre-concentration of the nuclides (e.g. Wallner, 1997). In aquatic samples, where the activities are very low and pre-concentration and purification are required, the chemistry involved in pre-concentrating the nuclides will often result in less than 100 % recovery and therefore chemical yield tracers

must be employed. This creates problems in the determination of ^{210}Po by LSS as the commonly used yield tracers (^{208}Po and ^{209}Po) have α energies similar to ^{210}Po. LSS cannot resolve these similar α energies and therefore α spectrometry must be applied for ^{210}Po determination. Ideally , the yield tracers applied to ^{210}Pb and ^{210}Bi determination could be measured alongside by LSS. In a novel method for the determination of ^{234}Th developed at SURRC, Pates *et al.* (1996) used ^{230}Th as the yield tracer. The novel aspect of the method is the application of an α emitting yield tracer to measure a β emitting nuclide and their simultaneous measurement using α/β LSS on a Packard 2550 TR/AB. This technique is attractive to the analyst as it only requires one instrument. If samples are collected during an oceanic cruise then it is vital to measure the short half-life nuclides (e.g. ^{234}Th) as soon as possible. This may involve transporting LS spectrometers on-board the ships themselves. Even for on-shore based measurements, it is an advantage to only require one instrument. If similar tracers could be found for ^{210}Pb, ^{210}Bi and ^{210}Po, the application of yield tracers to the method would not be a problem. The tracers would require to have minimal spectral overlap with the nuclide of interest or be differentiated using the α/β separation function on the LS spectrometer (Table 2.11).

Nuclide	Decay Mechanism	Ideal decay mechanism of tracer
^{210}Pb	combined β^-/γ	an α emitting Pb isotope
^{210}Bi	β^- decay	an α emitting Bi isotope
^{210}Po	α decay	a β^- emitting Po isotope

Table 2.11: Ideal decay mechanisms of radioactive yield tracers for ^{210}Pb, ^{210}Bi and ^{210}Po to allow their simultaneous determination by α/β LSS.

2.8.1 Lead tracers

Unfortunately there are no α emitting Pb isotopes with a half life greater than four minutes, so other tracers were investigated. In sediment analysis, unsupported ^{210}Pb is usually determined by γ spectrometry. In this case, a quantity of sediment containing no unsupported ^{210}Pb, usually from the base of the core, is spiked with a known activity of ^{210}Pb and the counting efficiency of ^{210}Pb determined. This technique works because minimal sample preparation is required before counting. In the traditional analysis of ^{210}Pb in aquatic matrices, the problems of variable Pb recovery is overcome by adding a known concentration of stable Pb to the sample and the recovery of the experiment calculated from the recovery of the stable tracer. The two main methods for determining the recovery of stable Pb are Atomic Absorption Spectrometry (AAS) (Fleer and Bacon, 1984) and gravimetric determination of Pb as $PbSO_4$ (Saito and Cunha, 1997), $PbCrO_4$ (Thomson *et al.*, 1993a) or as Pb-oxalate (Vadja *et al.*, 1997). However, these methods have their drawbacks. Determination by AAS requires the standards and samples to be in the same matrix but this can become complicated in seawater due to the presence of various concentrations of major and minor ions in the final sample solution. Gravimetric analysis also suffers from problems associated with co-precipitation of other ions (Joshi and Ku, 1979) and reproducible drying of the precipitate.

Radioactive tracers offer lower errors associated with counting compared to gravimetric analysis and can be non-destructive, unlike AAS. Of all the Pb isotopes there are only two that have sufficiently long half lives to be used as a tracer for ^{210}Pb. ^{203}Pb is produced by

nuclear bombardment reactions, is relatively expensive and not readily available. Its half life of 54 hours mean that its can only be used in laboratories with the capability to manufacture it on-site. ^{212}Pb has a half life of only 10.6 hours, but it is readily available as part of the ^{232}Th NDS (Fig. 1.1). With ^{212}Pb being present in natural thorium compounds it should be possible to have an inexpensive and almost inexhaustible supply of a tracer for ^{210}Pb analysis.

Sill and Willis (1965) devised a method for the preparation of ^{212}Pb as a yield tracer using $Th(NO_3)_4$ as the source of ^{212}Pb. Their method used a dithiocarbamate extraction which could not be employed in our laboratory because of the use of perchloric acid. $Th(NO_3)_4$ containing the full ^{232}Th decay chain in equilibrium was available at SURRC. The attraction of using a Th solution in which all the members of the decay chain are in equilibrium is that although ^{212}Pb is extracted from solution, it is rapidly regenerated from its parent nuclides remaining in solution, according to its 10.6 hour half life. This allows the same Th solution to be continually milked as source of ^{212}Pb with only one week of storage (Fig. 2.31). However, if the solution is to be reused as a source of ^{212}Pb then the $Th(NO_3)_4$ must be at least 4 years old and hence the ^{232}Th will be in equilibrium with ^{228}Ra and ^{228}Th. Figure 2.32 shows the decay of ^{228}Th after purification and the ingrowth of ^{228}Ra (produced from the decay of ^{232}Th). If the $Th(NO_3)_4$ has not been allowed time for ingrowth of ^{228}Ra ($t_{½} = 5.75$ y) then ^{228}Th will be unsupported by ^{232}Th and therefore decaying with a half life of 1.91 years. This will result in lower activities of ^{212}Pb being extracted and may affect the analytical accuracy of the final measurement.

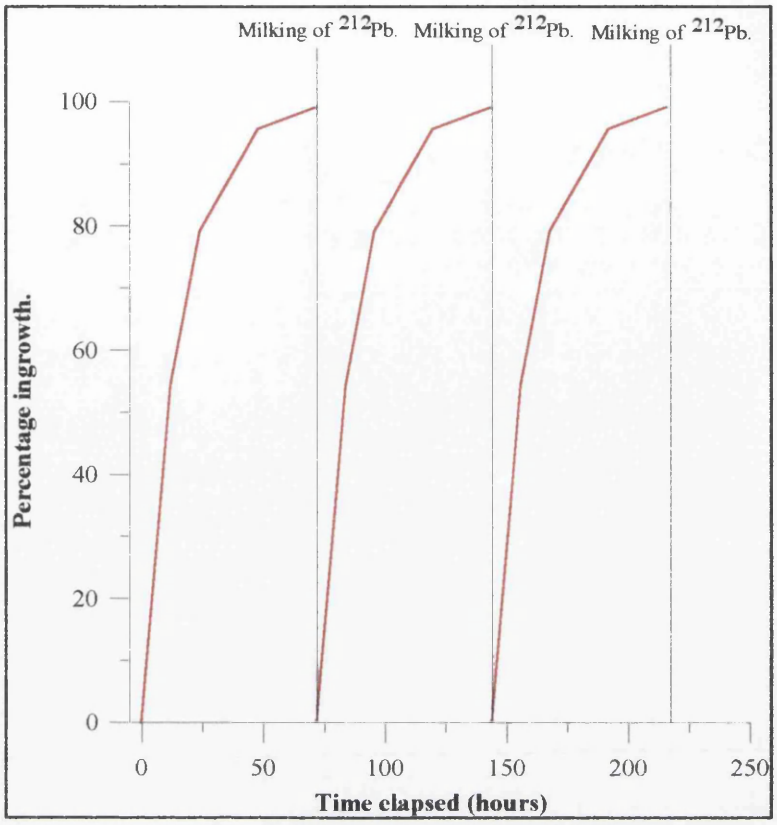

Figure 2.31: The ingrowth curve for ^{212}Pb showing its continual regeneration to around 99 % of its equilibrium value after 72 hours.

Using the previously obtained information on the behaviour of Pb on anion exchange resins allowed a purification method for ^{212}Pb to be developed. The behaviour of Pb had already be characterised on these resins (Section 2.5.2.1) so the behaviour of the other, potentially interfering, nuclides was examined. Ideally, the optimum scheme would allow Pb to be separated from Th, Ra and Ac in a single, simple elution procedure. Pb has its maximum adsorption onto a strongly basic anion exchange resin (e.g. AG1x8) in 1.2 M HCl solutions while Th, Ra, and Ac show no adsorption in HCl (Kraus and Nelson, 1956) and should not be retained on the column by 1.2 M HCl solutions. In addition, Pb can be stripped from the column in 9 M HCl. This technique appeared to be extremely efficient, as not only does it

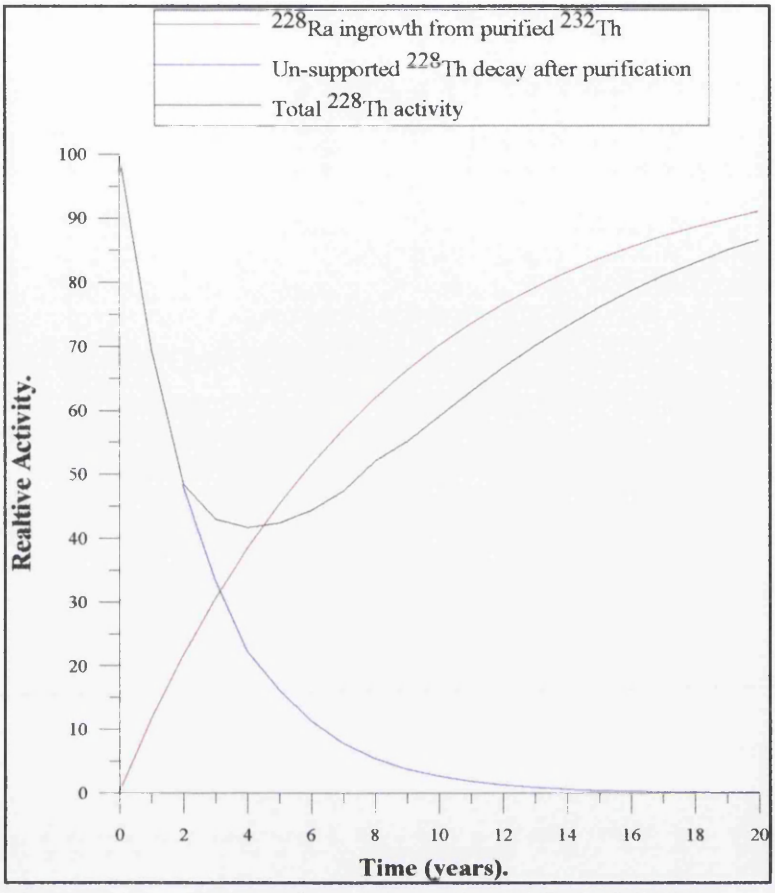

Figure 2.32: Ingrowth and decay in purified $Th(NO_3)_4$.

allow purification of ^{212}Pb from its parents but also allows Th, Ra and Ac to be eluted in one step, preventing any fractionation which could affect the ingrowth of ^{212}Pb. Also, there are no radioactive waste solutions to be disposed of as ^{212}Pb will decay to stable ^{208}Pb within one week.

^{210}Pb was used to examine the retention of Pb in 1.2 M HCl on columns of EiChrom AG1x8. ^{210}Pb was used in preference to ^{212}Pb because of its longer half life. There will be no interference from ^{210}Bi or ^{210}Po as they are both strongly held on the resin in this molarity of

HCl. Also, the ^{210}Pb was from a calibrated solution which allows the percentage recoveries in each fraction to be calculated. Due to the short half life of ^{212}Pb it would be beneficial to have as rapid a separation as possible. Therefore, the first "breakthrough" experiment was carried out using a 1 cm^3 column. However, no ^{210}Pb was retained on the column in 1.2 M HCl after adding 10 ml of 1.2 M HCl. The maximum retention of Pb occurs at 1.2 M HCl but the K_d is only 25. It seemed unlikely that all traces of Th, Ra and Ac would be removed in less than 10 ml of solution and therefore the focus moved to longer columns.

A 5 cm^3 column of EiChrom AG1x8 was pre-conditioned with 30 ml 9 M HCl and 30 ml 1.2 M HCl. 1 ml of ^{210}Pb solution (in 1.2 M HCl) was loaded onto the resin and five 10 ml aliquots of 1.2 M HCl were added, followed by six 5 ml aliquots of 9 M HCl. The fractions were eluted directly into 20 ml glass vials and evaporated to dryness. The residue was re-dissolved in 1 ml 0.1 M HCl before the addition of 5 g UG-LLT. The samples were counted with appropriate blanks as described in section 2.1.3. The results are shown in Figure 2.33. Although 12 % of the ^{210}Pb spike activity passing through after 50 ml of 1.2 M HCl, this is not necessarily a problem for the ^{212}Pb spike purification as the important factor is the removal of Th, Ra and Ac isotopes.

A bulk solution was prepared containing 1.2 g of $Th(NO_3)_4$ for each ml of 1.2 M HCl. This gave an initial ^{212}Pb activity of 2000 Bq and ensured that sufficient activity was present at the final stage of the experiment to obtain good counting statistics for the recovery of ^{212}Pb. Four 1 ml aliquots of Th solution were pipetted into individual beakers and evaporated to

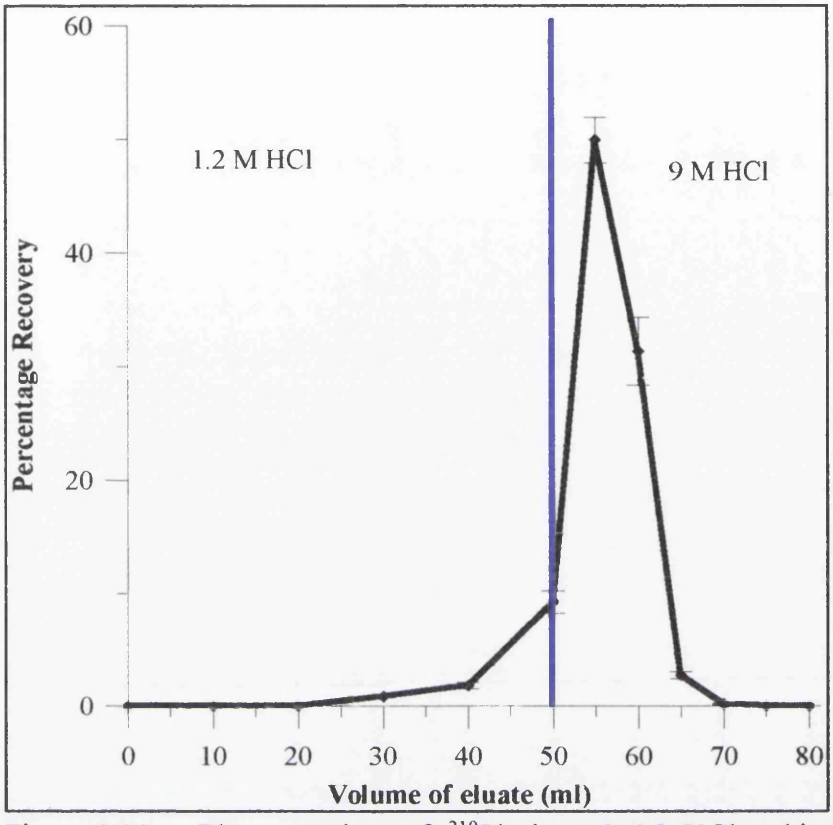

Figure 2.33: The retention of ^{210}Pb in 1.2 M HCl and its subsequent elution in 9 M HCl using a 5 cm^3 column of EiChrom AG1x8 anion exchange resin.

dryness. This process was carried out until no more NO_2 gas evolved which ensured that all traces of NO_3^- had been removed and that the thorium was present in solution as $ThCl_4$. The presence of any NO_3^- will cause the Th to be held on the column and contaminate the ^{212}Pb fraction when eluted with 9 M HCl. This new elution data obtained above was put to the test by then attempting a ^{212}Pb purification. The 5 cm^3 column was prepared exactly as described above. After loading 1 ml of $Th(NO_3)_4$ solution in 1.2 M HCl, four 10 ml aliquots of 1.2 M HCl were added to remove Th, Ra and Ac. Then ^{212}Pb was eluted with two 15 ml aliquots of 9 M HCl. The eluted 9 M HCl solution was reduced in volume and transferred

to a 20 ml vial where it was evaporated to dryness. The residue was re-dissolved in 1 ml of 0.1 M HCl, 5 g UG-LLT were added and the vial counted by γ spectrometry to confirm the presence of ^{212}Pb in the sample. The activity in the vial was also monitored by LSS (Section 2.1.3) and after two weeks, there was still 1000 cpm of activity, suggesting that ^{212}Pb was not totally purified and not all the Th was stripped from the column prior to ^{212}Pb elution. Therefore, further columns were prepared using 6 cm^3 and 7 cm^3 resin volumes and the retention of Pb with respect to increasing volumes of 1.2 M HCl was examined. Figure 2.34 shows the elution profile (prepared as for 5 cm^3 column) for ^{210}Pb from a 6 cm^3 column where 60 ml of 1.2 M HCl were eluted. Figure 2.35 is for a 7 cm^3 column (prepared as for 5 cm^3 column) using 80 ml of 1.2 M HCl. Increasing the length of the column allows Pb to be retained despite the larger volumes of 1.2 M HCl. This allows more washing of the column which provides an improved removal of Th, Ra and Ac.

The 6 cm^3 and 7 cm^3 columns were then tested using the $Th(NO_3)_4$ solution. The purified ^{212}Pb fraction from the 7 cm^3 column was found to decay to background levels after around one week. Initially it was thought that the elution through the 7 cm^3 column with 1.2 M HCl had given full removal of Th, Ra and Ac and hence only ^{212}Pb was eluted in 9 M HCl. However, it was only after the purification on Sr Spec resin that it was realised that some of the residual counts recorded from the 5 cm^3 column had been from ^{210}Pb "contamination" of the Th solution. When these experiments were carried out, the Th solution used for the 7 cm^3 column had already been used for the 5 cm^3 column previously run. The Pb aliquot was therefore the second generation of ^{212}Pb (insufficient time for ^{210}Pb ingrowth). Thus,

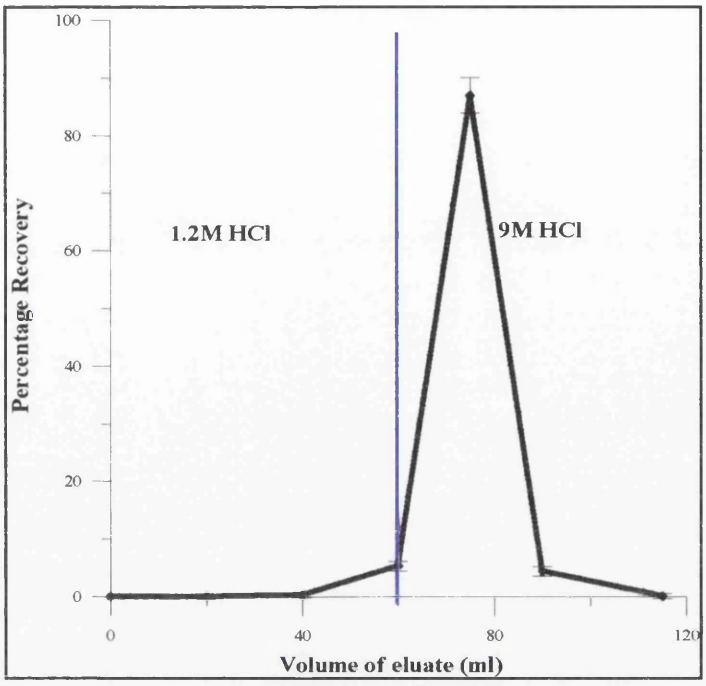

Figure 2.34: The retention of ^{210}Pb in 1.2 M HCl and its subsequent elution in 9 M HCl using a 6 cm^3 column of EiChrom AG1x8 anion exchange resin.

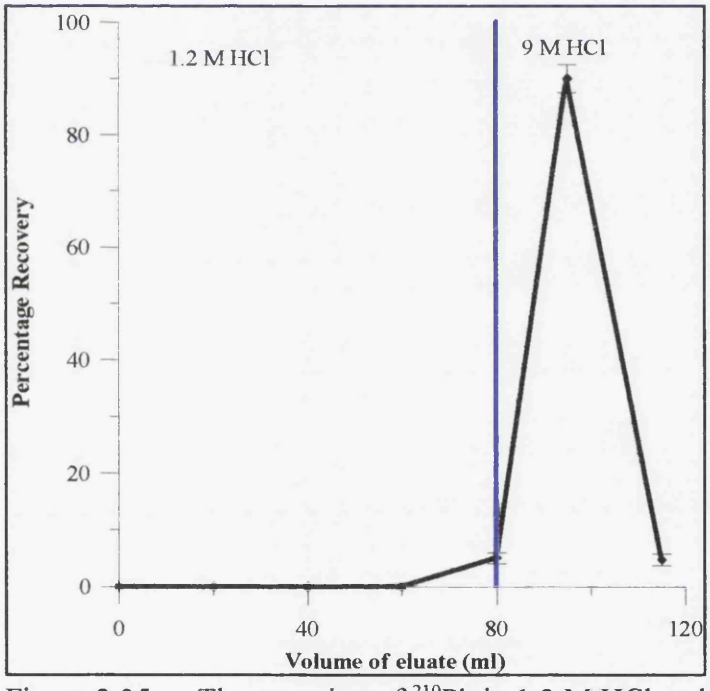

Figure 2.35: The retention of ^{210}Pb in 1.2 M HCl and its subsequent elution in 9 M HCl using a 7 cm^3 column of EiChrom AG1x8 anion exchange resin.

the initial problems with the purification had been due to two factors. Firstly, the smaller columns did not allow full removal of Th, Ra and Ac isotopes without also removing Pb, and secondly, there was also ^{210}Pb contamination interfering with the counting. Discarding the first generation of Pb allows the ^{210}Pb contamination to be removed.

The $Th(NO_3)_4$ used at SURRC was found to have approximately 0.1 % contamination with ^{210}Pb, which could be observed after the decay of ^{212}Pb in the 6 M HCl fraction eluted from the Sr Spec column (Section 2.6.4) (Fig. 2.36).

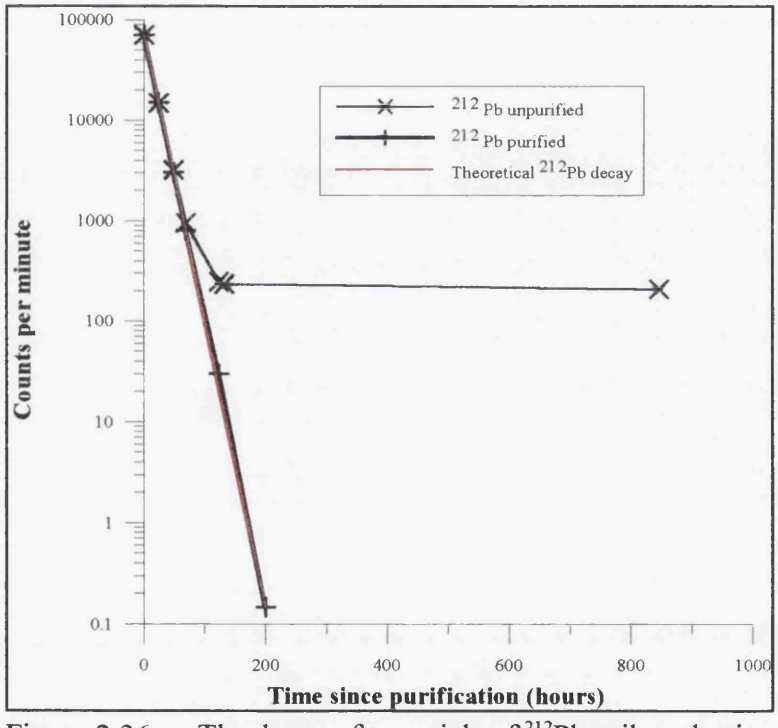

Figure 2.36: The decay of two vials of ^{212}Pb spike, plotting net cpm against time. The unpurified spike fails to decay to background due to the presence of ^{210}Pb contamination. Also plotted is the theoretical decay curve of ^{212}Pb which highlights the lack of contamination in the purified spike.

The contaminant ^{210}Pb must originate from ^{230}Th in the original $Th(NO_3)_4$ as it can contain ^{232}Th, ^{228}Th, and ^{230}Th. Because over 30 years had elapsed since the manufacture of the $Th(NO_3)_4$, this was sufficient time for ^{210}Pb to ingrow from the decay of ^{230}Th. Obviously, if the tracer itself contains ^{210}Pb then it is of little use as a tracer for ^{210}Pb. Therefore, an initial clean up of the $Th(NO_3)_4$ was necessary to remove the contaminant ^{210}Pb from the spike. With these problems overcome, a protocol could be established for the production of ^{212}Pb spikes.

2.8.1.1 Procedure for production of ^{212}Pb spikes

The first column is run to ensure full removal of ^{210}Pb contamination. A 5 cm^3 column of EiChrom AG1x8 was pre-conditioned with two 20 ml aliquots of 9 M HCl followed by two 20 ml aliquots of 1.2 M HCl. 1 ml of the Th solution in 1.2 M HCl was carefully added ensuring that the spike was applied drop-wise to the resin bed, to avoid adsorption onto the glass column. Two 20 ml aliquots of 1.2 M HCl were added to the column to elute Th, Ra and Ac. This fraction was labelled and stored with the date of purification and would be used for ^{212}Pb spike production. The ^{210}Pb and ^{212}Pb were eluted with two 15 ml aliquots of 9 M HCl. After storage for 1 week this fraction could be discarded. By storing the 1.2 M HCl fraction (containing Th, Ra and Ac) for one week, sufficient time has elapsed for ^{212}Pb to have grown back from its parents (Fig. 2.37). The second column is then used to purify the ^{212}Pb before addition to a sample, a 7 cm^3 column of Eichrom AG1x8 was pre-conditioned with two 20 ml aliquots of 9 M HCl followed by two 20 ml aliquots of 1.2 M HCl. The Th solution was evaporated to dryness and re-dissolved several times in 2 to 3 ml

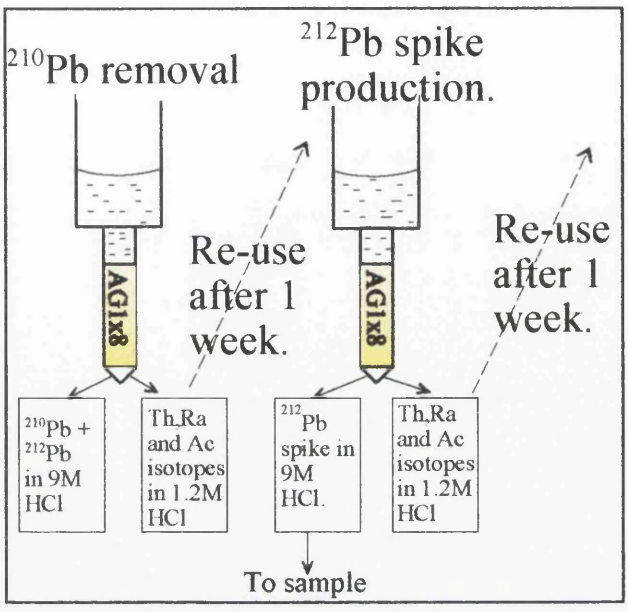

Figure 2.37: Schematic of the "milking" process used to regenerate ^{212}Pb spike.

of 1.2 M HCl. This again ensured that the Th was applied to the column as $ThCl_4$, a neutral species that will pass through the column and allowed the sample to be loaded in the correct molarity of HCl. The Th solution is the "cow" from which ^{212}Pb can be "milked" ready for the column purification process. The Th solution was carefully added drop-wise to the resin bed, to avoid absorption onto the glass column. Four 20 ml aliquots of 1.2 M HCl were eluted into the same beaker which was then stored for another "milking". ^{212}Pb was then removed from the column by elution with two 15 ml aliquots of 9 M HCl.

2.8.1.2 Detection of ^{212}Pb

^{212}Pb is most easily and characteristically detected by its γ emissions, the most intense occurring at 238 keV. Although the peaks at 74.8 keV and 77.1 keV have intensities of 11% and 18% respectively , the peak at 238 keV has a 45% intensity and does not suffer

from interferences from Pb X-rays. Once the two 15 ml aliquots of 9 M HCl had completely passed through the column, eluting ^{212}Pb, a 1 ml aliquot was carefully removed from the 9 M HCl fraction and pipetted into a 20 ml scintillation vial marked $^{212}Pb_{control}$. The remaining 29 ml were added to the seawater sample ($^{212}Pb_{sample}$).

The determination of Pb recovery is a relative yield determination so changes in ^{212}Pb activity between spikes is not important. Furthermore, this method does not require the absolute efficiencies of the γ spectrometer to be determined for ^{212}Pb determination. It is important to ensure that the milked ^{212}Pb aliquot has finished its elution from the ion exchange column before removing the $^{212}Pb_{control}$ aliquot. The technique relies on the 1 ml aliquot being representative of the whole 30 ml spike. Therefore the 30 ml addition must be measured accurately and the 9 M eluate must be homogeneously mixed before any aliquot is removed or the calculated yield will be incorrect. The 1 ml aliquot of ^{212}Pb was removed with a pipette calibrated before each set of spikes was prepared.

Both the ^{212}Pb control vial and the ^{212}Pb sample vial were counted in exactly the same conditions on a HPGe γ photon detector. The count time for both samples was a preset live time of 3600 seconds and the vials were counted in the centre of the detector using a specially designed holder for a 20 ml vial (Fig. 2.38). The vial holder was designed such that the sleeve of the holder fits tightly over the detector head to allow accurate positioning of the vial to be achieved. This is necessary due to the variation in counting efficiency across the section of the detector head. The vial is held one millimetre above the detector head to

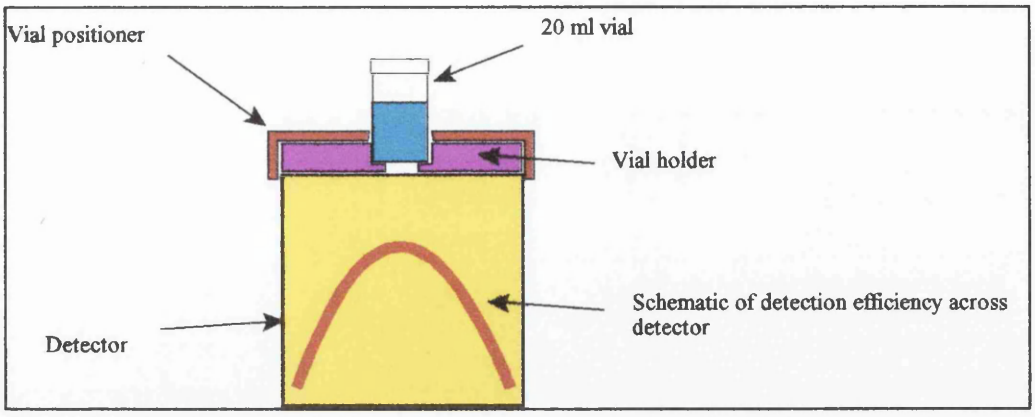

Figure 2.38: The vial holder designed to allow 20 ml scintillation vials to be counted by γ spectrometry at constant efficiency. The changes in counting efficiency across the detector are also shown.

prevent any possible transfer of contamination from the vial to the detector. Although this slightly lowers the detection efficiency of ^{212}Pb, the use of the vial holder keeps the counting efficiency constant for all measurements. The vials used for the measurement of ^{212}Pb were 20 ml low K borosilicate glass vials (Packard Instrument Company). The advantage of 20 ml vials compared to 7 ml vials is in the counting geometry, as they have a larger diameter. Glass was chosen over plastic as the counting of the sample itself would be carried out in glass vials as they have the advantage of allowing the sample to be dried down on a hotplate.

The calculation of Pb recovery is as follows:

The recovery of ^{212}Pb was calculated by decay correcting the activities of both the 1 ml aliquot and the 29 ml aliquot to the start of the original 9 M HCl elution. Thus, the activity of ^{212}Pb in the 1ml aliquot can be calculated using equation 2.3:

$$A_{0_{spike}} = At_{spike} e^{\lambda t_1} \times 29 \qquad (2.3)$$

wheret_1 = time between start of 9 M HCl elution end of 1 ml $^{212}Pb_{control}$ γ count. A_{0spike}=decay correct counts per second (cps) of ^{212}Pb in 1 ml aliquot and At_{spike} = cps measured by γ spectrometry of ^{212}Pb in 1 ml aliquot.

A similar calculation is used to calculate the original ^{212}Pb activity in the sample (equation 2.4):

$$A_{0sample} = At_{sample} e^{\lambda t_2} \quad (2.4)$$

where t_2 = time between start of 9 M HCl elution and end of $^{212}Pb_{sample}$ γ count, $A_{0sample}$ = decay correct counts per second (cps) of ^{212}Pb in sample and At_{sample} =cps measured by γ spectrometry of ^{212}Pb in sample.

The recovery of the ^{212}Pb tracer is calculated by comparing the two decay corrected count rates (equation 2.5):

$$\text{Recovery of Pb (\%)} = \frac{A_{0sample}}{A_{0spike}} \times \frac{100}{1} \quad (2.5)$$

2.8.1.3 Advantages of ^{212}Pb

Although little use has been made of ^{212}Pb as a tracer for ^{210}Pb in the past it offers several advantages over more conventional Pb tracers.

1. There is no requirement for any portion of the sample to be removed for analysis of

the tracer, either by ICP-MS or AAS. This is especially important in the measurement of very small activities such as this application.

2. The ^{212}Pb does not interfere with the counting of the ^{210}Pb as all the ^{212}Pb activity will have decayed within one week, leaving only the ^{210}Pb which can then be analysed.

3. This technique avoids the use of gravimetric determination of Pb which would require the sample to be re-dissolved prior to its determination by LSS or the use of gelling based cocktails which only holds the sample suspended for a few days.

4. The ^{212}Pb is an inexpensive and virtually inexhaustible spike which can be milked from the $Th(NO_3)_4$ solution without the production of radioactive waste.

5. A ^{232}U spike could also be used as a source of ^{212}Pb but the high activity required would introduce a significant cost into the analysis.

6. The ion exchange procedure does not require changing of acid types (e.g. HCl to HNO_3). Keeping the solutions as Cl^- prevents any adsorption of Th, Ra or Ac onto the resin.

2.8.2 Bismuth tracers

At the outset of this research the aim was to develop a more time efficient method for

determination of ^{210}Pb and ^{210}Po activities in seawater. Once it became clear that the method being developed could also be used to measure ^{210}Bi in the same sample, without significantly increasing the time of analysis, a yield tracer for Bi was also needed. There have been few measurements of ^{210}Bi in the aquatic environment (Harada *et al.*, 1989), its main (although limited) application has been in atmospheric studies (Poet *et al.*, 1972; Moore *et al.*, 1972; Wallner, 1997). If suitable tracers and detection methods were developed, the measurement of ^{210}Bi ($t_{½}$ = 5.013 days), in conjunction with ^{210}Po/^{210}Pb measurements, would allow processes occurring on very short time scales to be modelled (in the order of days to weeks instead of months to years). Because the uptake of particle reactive pollutants in the marine system is thought to occur on such time scales this concept was investigated fully.

Stable Bi has been used previously by Nevissi (1991) to determine the chemical yield for ^{210}Bi alongside Pb and Po. However, the method requires eight precipitation stages, an anion exchange column and a final precipitation of Bi as $BiPO_4$. Although the procedure could be carried out in a day it is labour intensive and time consuming for the analyst. Narita *et al.* (1989) used an electrochemical method for separation of ^{210}Pb, ^{210}Bi and ^{210}Po whereby Bi was electroplated onto a platinum gauze. Stable Bi was added as bismuth nitrate pentahydrate and Bi was precipitated as bismuth oxychloride and the yield determined gravimetrically. Although this method is faster than that of Nevissi (1991), it is again labour intensive and still takes up to six hours to purify the Bi. Church *et al.* (1994) realised that the applications of stable Bi as a tracer for ^{210}Bi would complicate the recovery and limit the

number of analyses that could be carried out. They highlighted the use that could be made of a radioactive Bi spike, namely ^{207}Bi ($t_{½}$ = 32.2 years) (Lederer and Shirley, 1978).

^{207}Bi is available from several sources in the United Kingdom (National Physics Laboratory and AEA Technologies) and from the United States (Los Alamos National Laboratories). It is relatively inexpensive to purchase as the measurements do not require a calibrated/certified source, as a relative yield determination can be easily carried out by the analyst.

^{207}Bi decays by electron capture to stable ^{206}Pb, producing characteristic γ emissions, the most intense of which are found at 72.8 keV (21.8 %), 75 keV (36.8 %), 569 keV (98 %) and 1064 keV (74.9 %). Its usefulness as a tracer is that it is commercially available, has a long half life and decays straight to its stable nuclide without any radioactive daughters which could complicate its measurement.

2.8.2.1 Detection of ^{207}Bi

^{207}Bi can be measured by LSS and γ spectrometry. It was hoped that the LSS response of ^{207}Bi would be confined to the very low energy end of the spectrum (0 to 15 keV) while ^{210}Bi (E_{max} = 1161 keV) would be covering a much larger portion of the spectrum. This would allow ^{207}Bi recovery and ^{210}Bi activity to be determined simultaneously by LSS in a similar technique to dual label counting of ^{3}H and ^{14}C.

The ^{207}Bi was counted on two LS spectrometers, a Packard 2250 CA and a Packard 3170 TR/SL both on LLCM and NCM. Both counters are capable of counting in Low Level (i.e. low background) mode but the 3170 TR/SL features programable DBB and a BGO guard (Section 1.3). The 2250 CA has a preset DBB of 75 ns while the 3170 TR/SL can be set from 75 to 800 ns. The same vial of ^{207}Bi was counted on both these counters for the same count time after leaving the vial in the counter bed for 1 hour prior to counting. Because the spike does not have an absolute activity it is impossible to assess the true counting efficiency. However, relative counting efficiencies provide a useful tool to optimise the tracer with regard to activity required and optimal conditions for counting. The spectrum of the ^{207}Bi spike is not limited just to the low end of the energy range but continues up to around 1000 keV (Fig. 2.39).

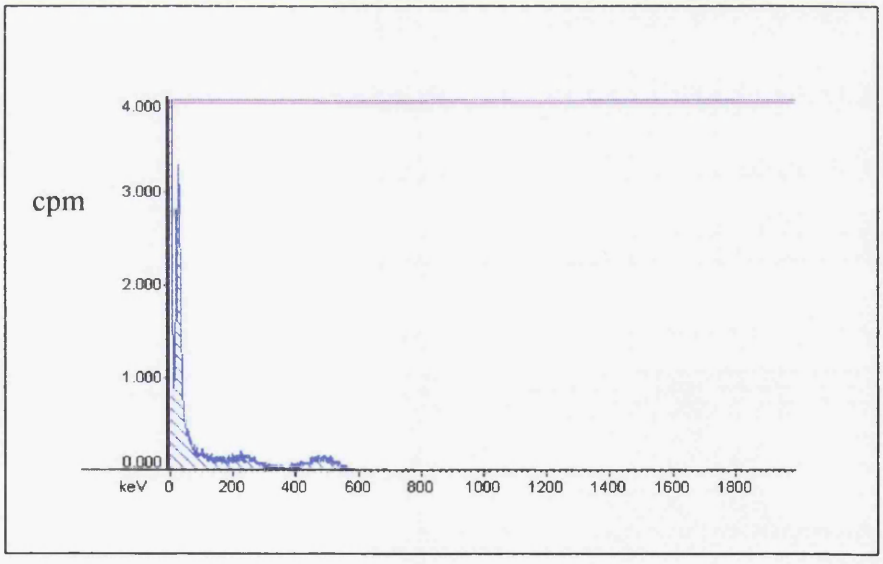

Figure 2.39: LS spectrum of ^{207}Bi, much of the activity is found at low energy (0 to 15 keV).

The low counting efficiency of the 3170 TR/SL relative to the 2250 CA in NCM indicates that a degree of PSA is in use (Table 2.12). The γ photons produced from the decay of ^{207}Bi induce Compton electrons in the cocktail. They produce photons of light virtually identical to those produced by β^- interaction with the cocktail. However, the γ photons (with reduced energy) may also interact with the BGO guard on the 3170 TR/SL. This will produce a long pulse that is rejected by the PSA circuitry. The interaction in the vial and in the BGO guard are virtually co-incident and therefore the decay event may be rejected as a background event. The substantial reduction (>50 %) in^{207}Bi counting efficiency of the 3170 TR/SL results from the high percentage of events accompanied by high energy γ photons.

2.8.2.2 Calibration of LSS against gamma spectrometry

The concept behind the calibration was to be able to predict the LSS count rate of ^{207}Bi from the γ spectrum obtained from a HPGe detector. The BGO guard on the 3170 TR/SL will cause a reduction in the counting efficiency due to the γ emissions interacting with it. This makes it important to test the linearity of the responses of the LSS with respect to its γ spectrometry response. If the activities of ^{207}Bi were too high, the response of the BGO guard could introduce a significant dead time causing a non-linear relationship between the γ spectrometer and the LSS. As with the counting of the ^{212}Pb spike by γ spectrometry, the ^{207}Bi vial was also counted in a specialised vial holder. The response of the four main γ photon peaks relative to the LSS response were examined separately as follows.

Count Mode	2250CA Gross cpm	background	Net cpm	Relative Efficiency	3170TR/SL Gross cpm	background	Net cpm	Relative Efficiency
NCM	4779	30	4749	100 %	2311	13	2298	48.4 %
LLCM DBB @ 800 ns	*	*	*	*	1901	8	1893	39.9 %
LLCM DBB @ 400 ns	*	*	*	*	1809	7	1802	37.9 %
LLCM DBB @ 200 ns	*	*	*	*	1665	5	1660	35.0 %
LLCM DBB @ 75 ns	3336	12	3324	70.0 %	1305	3	1302	27.4 %

Table 2.12: The variation of the LS response of ^{207}Bi between a Packard 2250CA and a Packard 3170 TR/SL which features a BGO guard. The counting efficiency relative to 2250 CA NCM is also shown for comparison. For the 2250 CA spectrometer the LLCM DBB setting is preset at 75 ns.

A series of spiked vials were prepared containing 1 ml, 0.9 ml, 0.8 ml, 0.6 ml, 0.4 ml, 0.2 ml and 0.1 ml of ^{207}Bi. The spike was freeze dried in the vials and the residues were re-dissolved in 1 ml of 0.1 M HCl before the addition of 5 g UG-LLT. The spikes were counted for 100 minutes by LSS on a 3170 TR/SL LS spectrometer in NCM and then counted on a HPGe γ photon detector. The results are plotted in Figure 2.40, and show clearly the linear response between the LSS response and the γ spectrometer.

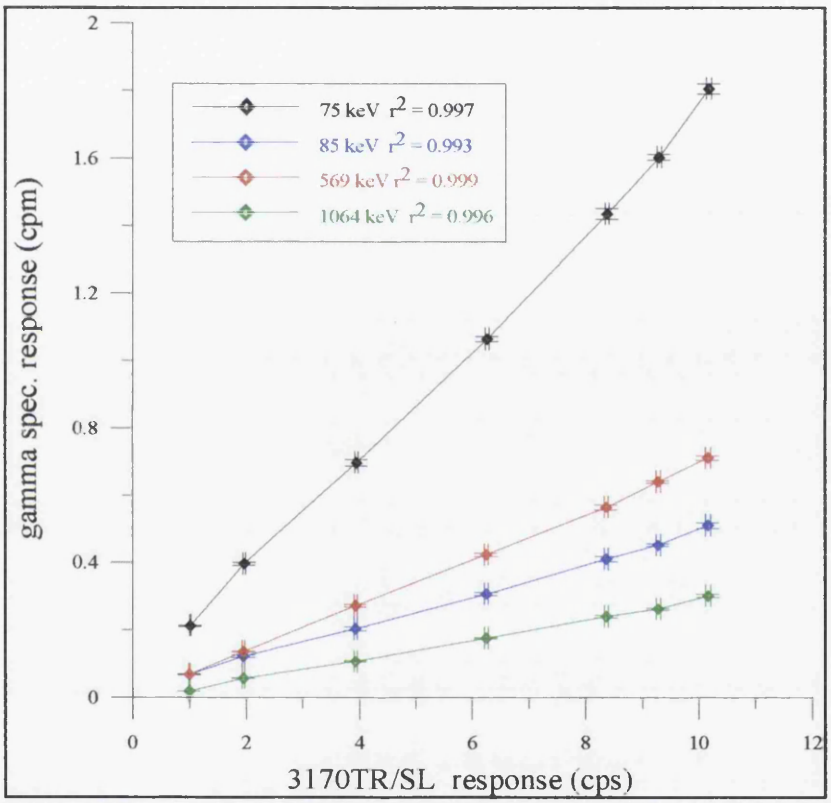

Figure 2.40 The linear response observed between a Packard 3170 TR/SL LS spectrometer and γ spectrometry for the four main photo-peaks of ^{207}Bi for a range of activities. The γ count rate for each peak was converted into cpm. The r^2 values were obtained from a standard regression analysis.

Above 8 cps the calibration appears to lose its linearity but the most likely cause is of this is an error in pipetting. The problem with this method is that it relied on using the same γ spectrometer for the calibration to hold, furthermore, if there were any changes to the activity of the original spike then the calibration would need to be carried out again. Both these problems arose during the method development so a technique that was independent of specific detectors had to be investigated.

The ^{207}Bi spike was diluted such that the count rate of a 1 ml aliquot on a Packard 3170 TR/SL (in LLCM with DBB@ 600 ns) was around 35 cpm. Reducing the activity of the spike required a much longer count by γ spectrometry but this was unavoidable. Also, only the peak at 569 keV would be used as the peaks at 75 and 85 keV suffered from interferences from the Pb X-rays and the peak at 1064 keV would not have a sufficiently high count rate to be useful.

2.8.2.3 Procedure for utilisation of ^{207}Bi as a tracer for ^{210}Bi

When the seawater sample was being spiked, an identical aliquot of spike was pipetted into a 20 ml scintillation vial. To ensure that the chemical conditions in the spiked vial were identical to the sample, the spike was evaporated to dryness on a hotplate, re-dissolved in 1 ml of 0.1 M HCl and 5 g UG-LLT were added. This was then counted by γ spectrometry while the sample was processed and the count rate of the 569 keV photopeak recorded ($\gamma_{control}$). This control vial (containing only ^{207}Bi) was counted using the same LSS protocol as the eventual Bi sample (containing both ^{207}Bi and ^{210}Bi). These will be referred to as

$LS_{control}$ and LS_{sample} respectively. Finally, the Bi sample vial was counted by γ spectrometry for 10 hours and the count rate of the 569 keV photopeak recorded ($\gamma_{control}$). Thus, the recovery of Bi can be calculated using equation 2.6:

$$\text{Bi recovery (\%)} = \frac{\gamma_{sample}}{\gamma_{control}} \times \frac{100}{1} \qquad (2.6)$$

where γ_{sample} = count rate obtained by γ spectrometry of sample vial and $\gamma_{control}$ = count rate obtained by γ spectrometry of the ^{207}Bi control vial.

The counts resulting from ^{210}Bi in the sample can be calculated using equation 2.7:

$$^{210}\text{Bi (cpm)} = LS_{sample} - \left(\frac{\text{Recovery of Bi (\%)}}{100} \times LS_{control} \right) \qquad (2.7)$$

where LS_{sample} = count rate of sample vial by LSS (containing both ^{210}Bi and ^{207}Bi) and $LS_{control}$ = count rate of control vial by LSS (contains only ^{207}Bi)

2.8.3 Polonium tracers

Traditionally, ^{208}Po or ^{209}Po are used as yield tracers in ^{210}Po determination. Despite Po having 19 isotopes, only ^{208}Po and ^{209}Po have suitable half lives to be employed. Unfortunately both ^{208}Po and ^{209}Po are pure α emitters and a limiting factor in the application of LSS to this study is its inability to provide suitable resolution of the α peaks. The advantage of the tracer free method was that ^{210}Po would have been determined by LSS.

The only solution to this problem lay in the measurement of Po by α spectrometry which can resolve the peaks. Unlike Bi and Pb, there is no stable form of Po so one of these α emitting tracers must be used. The technique involving α spectrometry requires a known activity of ^{208}Po or ^{209}Po to be added to the sample. Once sufficient counts have been recorded in both peaks, the background is subtracted. ^{208}Po has a half life of 2.93 years and emits a 5.11 MeV α particle, ^{209}Po has a 102 year half life and emits a 4.88 MeV α particle. ^{209}Po is often favoured as it is easier to resolve from the 5.3 MeV α particle from ^{210}Po although ^{208}Po is more readily available (Holtzman, 1987).

A calibrated ^{208}Po tracer was used to determine ^{210}Po recovery. Initially, the activity added to the sample was ~ 0.1 Bq, but this created problems due to the excess of ^{208}Po counts compared to ^{210}Po counts from the sample. When this was realised, the ^{208}Po activity was reduced to ~ 0.01 Bq and this allowed the sample to be counted for sufficient time to ensure good counting statistics for the ^{210}Po.

2.9 Finalisation of method

This research has now enabled the pre-concentration and purification of the nuclides to be optimised (Fig. 2.2). The final stage of the methodology is now counting of the samples to determine their activity. This final section will discuss the development of the counting procedures before introducing the method in its entirety and finally suggesting future developments of the method.

2.9.1 Instrumentation

γ spectrometry was carried out using a Canberra Industries 35 % relative efficiency, N–type high purity germanium (HPGe) γ photon detector with a beryllium thin window. α spectrometry utilized a Canberra Industries Quad-Alpha Spectrometer Model 7404 with four 450 mm^2 passivated implanted planar silicon (PIPS) detectors. LSS was carried out on a Packard 3170 TR/SL spectrometer.

2.9.2 Optimisation of counting procedures

The DBB settings for the 3170 TR/SL were chosen by counting purified aliquots of ^{210}Pb and ^{210}Bi at a range of DBB settings. A high activity ^{210}Pb spike (activity = 858 ± 19 Bq) was utilised. This allowed short (5 minute) count times at each setting which therefore minimised ingrowth and decay corrections. Furthermore, it allowed precise calculation of ^{210}Bi underlying the ^{210}Pb peak (0-40 keV). ^{210}Pb and ^{210}Bi were purified on a 2 ml pre-packed column of Sr Spec resin and the eluted fractions were evaporated close to dryness and transferred to 20 ml glass vials before being evaporated to dryness. The residue was re-

dissolved in 1 ml 0.1 M HCl before the addition of 5 g UG-LLT. This ensured that the degree of quenching and the counting geometry was the same for the spiked samples as it would be for environmental samples. Background vials composed of 1 ml of 0.1 M HCl and 5 g of UG-LLT cocktail were also counted over the range of DBB settings but were counted for 800 minutes. The optimum DBB is a compromise between low background count rates (on a low DBB setting) and high counting efficiency (on a high DBB setting). To find the best resolution of signal to noise ratio, the figure of merit (E^2/B where E = efficiency and B = background) was also calculated for the same DBB settings. The optimum DBB setting was therefore chosen as 600 ns which gave the highest E^2/B for both ^{210}Pb and ^{210}Bi (Table 2.13).

2.9.2.1 Determination of ^{210}Pb counting efficiency

To determine accurately the absolute counting efficiency of ^{210}Pb requires the recovery from the column separation procedure, described above, to be determined. To achieve this, an identical aliquot of ^{210}Pb (activity = 858 ± 19 Bq, with ^{210}Bi and ^{210}Po in equilibrium) was added to a glass scintillation vial and 5 g UG-LLT added to create an identical counting geometry to the separated ^{210}Pb. Once the vial containing the separated ^{210}Pb had been counted by LSS at the range of DBB settings, it was then counted by γ spectrometry. The unseparated ^{210}Pb spike was counted on the same γ spectrometer. By comparing the count rate of the 46.5 keV photo-peak of the separated and unseparated vials allowed the activity of ^{210}Pb used in the LSS optimisation procedures to be accurately determined and an absolute ^{210}Pb counting efficiency to be derived. The counting efficiency of ^{210}Pb by γ

Count mode	^{210}Pb counting efficiency (%)	Background 0-40 keV (cpm)	E^2/B	^{210}Bi counting efficiency	Background 15-2000 keV (cpm)	E^2/B
Normal Count Mode	96.8 ± 2.8 %	9.11	1030 ± 30	92.7 ± 0.3 %	6.02	1430 ± 20
LLCM DBB @ 800 ns	93.7 ± 2.8 %	3.76	2330 ± 80	90.2 ± 0.3 %	3.95	2060 ± 40
LLCM DBB @ 700 ns	93.1 ± 2.8 %	3.50	2480 ± 90	89.9 ± 0.3 %	3.77	2140 ± 50
LLCM DBB @ 600 ns	91.9 ± 2.8 %	3.35	2520 ± 90	88.8 ± 0.3 %	3.65	2160 ± 50
LLCM DBB @ 500 ns	90.4 ± 2.8 %	3.31	2470 ± 90	87.3 ± 0.3 %	3.61	2110 ± 50
LLCM DBB @ 400 ns	87.9 ± 2.8 %	3.23	2390 ± 90	84.6 ± 0.3 %	3.45	2080 ± 50
LLCM DBB @ 300 ns	83.3 ± 2.8 %	2.91	2380 ± 90	78.8 ± 0.3 %	2.92	2130 ± 50
LLCM DBB @ 200 ns	76.1 ± 2.8 %	2.57	2250 ± 80	68.2 ± 0.3 %	2.37	1960 ± 50
LLCM DBB @ 100 ns	61.3 ± 2.8 %	2.25	1670 ± 60	52.5 ± 0.3%	1.73	1600 ± 50
LLCM DBB @ 75 ns	54.2 ± 2.8 %	2.10	1400 ± 60	31.3 ± 0.3 %	0.98	1000 ± 40

Table 2.13: Variations in counting efficiency, background and E^2/B for ^{210}Pb and ^{210}Bi over a range of Delay Before Burst (DBB) settings using a Packard 3170 TR/SL LS spectrometer. The counting efficiency of ^{210}Pb is an absolute counting efficiency. The ^{210}Bi counting efficiency is approximately 100 % on a 0-2000 keV window in NCM. The error on the E^2/B figures includes the 1σ error on the background count rate.

spectrometry was observed to be 0.504 ± 0.013 %. This corresponded to a ^{210}Pb counting efficiency of 96.8 ± 2.8 % by LSS on NCM in a 0 - 40 keV counting window. The counting efficiency of ^{210}Bi in NCM (0 - 2000 keV) was assumed to be 100 % (or very close to) which would be expected for a high energy β^- emitter with a tSIE of ~440 units.

2.9.2.2 Quenching

The degree of quenching in samples was constant throughout (average tSIE = 448 units, standard deviation = 7). This was achieved by ensuring the sample was fully oxidised and evaporated to complete dryness prior to re-dissolution in acid and the addition of scintillation cocktail. When the vials are being taken to dryness on a hotplate it is important that the temperature is sufficiently high enough to evaporate the acid. However, it is vital that the temperature is not too high, otherwise the nuclides may "bake" onto the vial. The presence of any residual acids prior to re-dissolution of the sample in 1 ml 0.1 M HCl and 5 g UG-LLT will induce serious quenching. If any residue remained undissolved in the 0.1 M HCl, the contents of the vial were repeatedly oxidised with 12 M HCl, 15 M HNO_3 and 35 % H_2O_2 until the sample was totally colourless and fully dissolved in 0.1 M HCl.

2.9.2.3 Detection limits

It is also important to establish the Minimum Detectable Activity (MDA), also referred to as the lower limit of detection (LLD). This has been comprehensively described by Currie (1968) (equation 2.8):

$$LLD = 2.71 + 4.65\sqrt{\mu}_B \qquad (2.8)$$

where μ_B is the mean background expressed as counts.

This can be expressed as an activity concentration or Minimum Detectable Activity (MDA) by dividing by factors specific for each nuclide (equation 2.9):

$$\text{MDA (Bq l}^{-1}) = \frac{2.71 + 4.65\sqrt{\mu_B}}{\text{E.V.T.60}} \qquad (2.9)$$

where E = fractional counting efficiency, V = sample volume (litres), T = count time (minutes) and 60 = dpm to Bq conversion factor.

The background values in the Pb and Bi counting windows are shown in Table 2.13 (DBB = 600 ns). Using the sample volume of 20 litres and counting efficiencies of 91.91 %, 88.8 % and 20 % for ^{210}Pb, ^{210}Bi and ^{210}Po respectively, this produced MDAs of 0.324 mBq l^{-1}, 0.345 mBq l^{-1} and 0.07 mBq l^{-1} for ^{210}Pb, ^{210}Bi and ^{210}Po.

2.9.2.4 Blanks

A blank sample was run to check the purity of each fraction and to determine the background levels of ^{210}Pb, ^{210}Bi and ^{210}Po that may be introduced by the reagents. This was achieved by following the analytical protocol as shown in Figure 2.41. 20 litres reverse osmosis water replaced the seawater sample for dissolved analysis and a cellulose nitrate filter was used in the particulate blank analysis. The blank values found are given in Table 2.14.

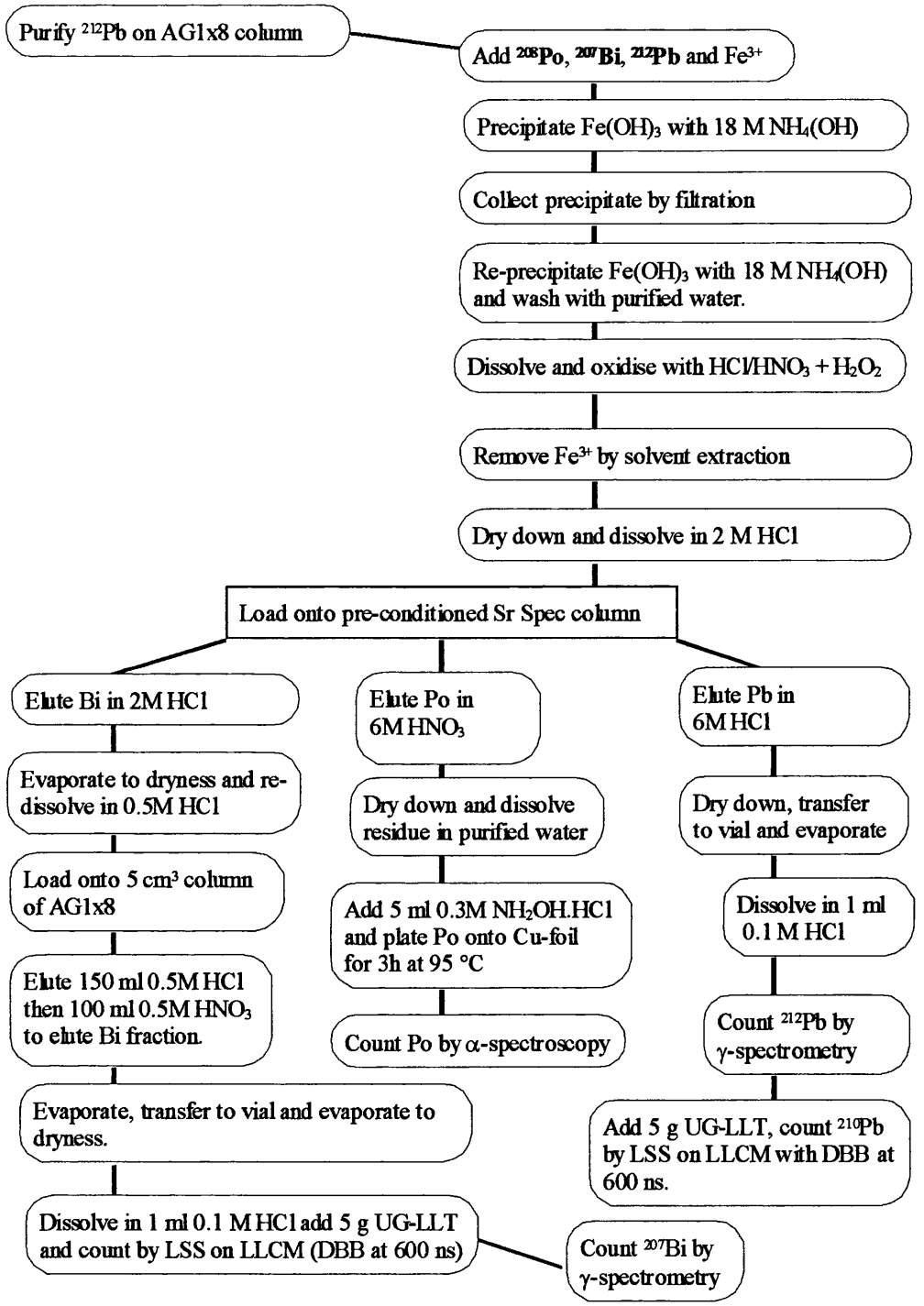

Figure 2.41: Flowchart of the analytical procedure developed to determine the dissolved and particle-associated activities of ^{210}Pb, ^{210}Bi and ^{210}Po in seawater.

	Dissolved	Particulate
^{210}Pb	0.013	0.040
^{210}Bi	0.060	0.023
^{210}Po	0.021	0.013

Table 2.14: Reagent blank activities (mBq l^{-1}) for dissolved (20 litres reverse osmosis water) and particle-associated (293 mm Whatmans cellulose nitrate filter paper) ^{210}Pb, ^{210}Bi and ^{210}Po.

2.9.3 Methodology

2.9.3.1 Sample reception

On return to the laboratory the samples were immediately filtered using a 0.22 μm pore size cellulose nitrate filter (Whatman) to differentiate between dissolved and particle-associated phases. Filtering was carried out using a diaphragm pump powered by compressed air with a filter rig that accepted 293 mm diameter filter papers. The apparatus is shown in Figure 2.42. The diaphragm pump was placed behind the filter to minimise any contamination and to prevent any particulate material becoming entrained inside the pump. Filtering of a 20 litre sample using this system could carried out in around 20 minutes.

2.9.3.2 Particle-associated nuclides

The 0.22 μm cellulose nitrate filter was removed from the filtering rig and placed in a one litre Teflon beaker. It was then spiked with 29 ml of ^{212}Pb solution (~69 Bq ml^{-1}), 0.1 ml ^{207}Bi (~8 Bq ml^{-1}) and 0.1 ml ^{208}Po (activity = 0.1 Bq ml^{-1}). Care was taken to ensure that the spikes covered the filter paper. Much of the filter was oxidised by refluxing the sample overnight in a solution of 50 ml 12 M HCl and 50 ml 15 M HNO_3. The following day, the solution was evaporated to dryness on a hotplate and any residual siliceous material was

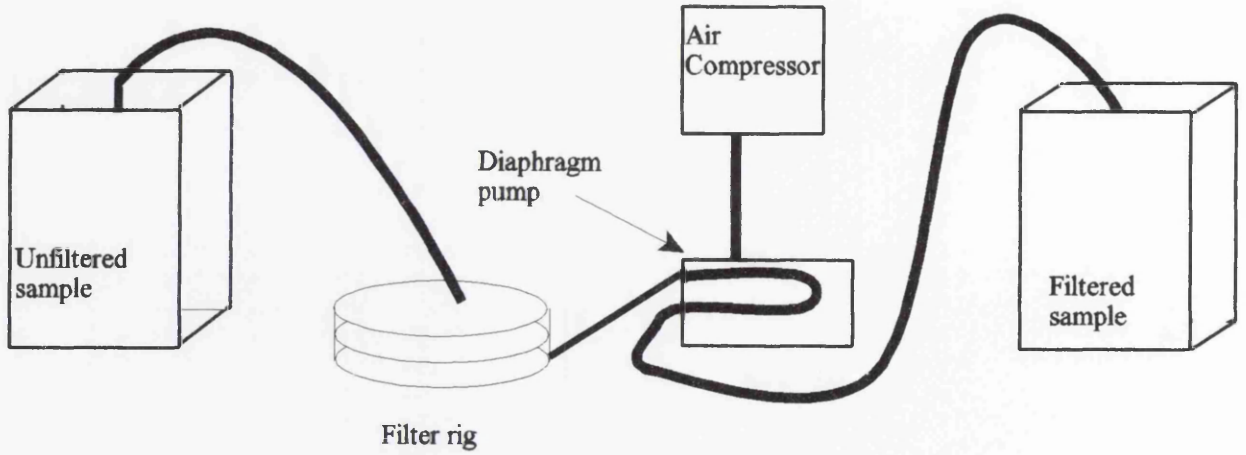

Figure 2.42: Diagram of the filtering apparatus used for both separating the dissolved and particle-associated (>0.22 μm) fractions and collection of $Fe(OH)_3$ precipitate.

destroyed with two 20 ml aliquots of 37 M HF. This was carefully evaporated to ensure that all traces of HF were removed before proceeding. After the HF digestion there was very little residue remaining in the beaker. 30 ml of 9 M HCl were added to the beaker and it was gently heated to re-dissolve the nuclides. A further 10 ml of 9 M HCl was used to wash down the sides of the Teflon beaker to remove any nuclides bound onto the sides. After the addition of 5 ml of Fe^{3+} carrier (10 mg ml^{-1} Fe^{3+}), $Fe(OH)_3$ was precipitated with 18 M NH_4OH. The precipitate was transferred to a 50 ml plastic centrifuge tube. After centrifuging at 3500 rpm for 5 minutes, the $Fe(OH)_3$ precipitate was washed with reverse osmosis water as described in Section.2.3.4.1 to remove any salts that had become entrained. The precipitate was then dissolved in 2 M HCl ready for Sr Spec purification. There is no need for a solvent extraction of the Fe^{3+} carrier prior to the Sr Spec column because the concentrations were not sufficiently high to cause problems.

2.9.3.3 Dissolved phase (< 0.22 μm) analysis

The filtered 20 l sample was immediately acidified with 50 ml of 15 M HNO_3 and 29 ml ^{212}Pb (~69 Bq ml^{-1}), 0.1 ml ^{207}Bi (~8 Bq ml^{-1}), 0.1 ml ^{208}Po (activity = 0.1 Bq ml^{-1}) and 20 ml Fe^{3+} carrier (10 mg ml^{-1} Fe^{3+}) were added. The lid was replaced and the container shaken for 2 minutes. It was then left overnight to allow full equilibration of the spikes and carrier with the sample.

The following morning, the pH of the sample was raised to 9 with the addition of ~ 65 ml of 18 M NH_4OH (the pH of the solution was monitored with pH sticks). The lid was

replaced and the sample shaken for 2 minutes before bubbling the sample with air for 20 minutes via an air pump and leaving the sample for 2 hours to allow the precipitate to fully form. The $Fe(OH)_3$ precipitate was then collected by filtration using Whatman 0.45 μm cellulose nitrate filter papers through the filtering apparatus shown in Figure 2.42. The precipitate was then dissolved off the filter papers with 20 ml 2 M HCl washes in a large evaporation dish as described in Section 2.2.3.2. $Fe(OH)_3$ was subsequently re-precipitated with 18 M NH_4OH and transferred to a 50 ml plastic centrifuge tube where the precipitate was centrifuged and washed with reverse osmosis water as described in Section 2.2.3. The sample was re-dissolved in 9 M HCl and the bulk of the Fe^{3+} carrier removed by solvent extraction using DIPE. The sample was then heated for one hour to oxidise any dissolved organic material still present in the sample. It was then evaporated to dryness on a hotplate and re-dissolved in 2 M HCl. This was repeated twice to ensure the sample was in the correct molarity for the Sr Spec separation.

2.9.3.4 Purification of ^{210}Po and ^{210}Pb on Sr Spec columns

A pre-packed column of EiChrom Sr Spec resin (100 - 150 mm particle diameter) was conditioned with 50 ml of reverse osmosis water, 50 ml of 6 M HNO_3, 25 ml of 6 M HCl and 25 ml of 2 M HCl. The sample was then loaded onto the column and two 20 ml aliquots of 2 M HCl were passed through to elute Bi and Fe. Two 20 ml aliquots of 6 M HNO_3 were used to elute the Po fraction, and then two 15 ml aliquots of 6 M HCl were passed through the column to elute the Pb fraction.

2.9.3.5 Purification of ^{210}Bi

The 2 M HCl fraction containing the Bi also contained other nuclides of both anthropogenic and natural series origins that are present in the seawater. Bi was separated from the interfering nuclides by anion exchange on a 5 cm^3 column of EiChrom AG1x8 using the procedures described in Section 2.6.3.2. Thus, the Bi fraction in 2 M HCl was evaporated to dryness and re-dissolved in 0.5 M HCl. The drying and re-dissolution steps were repeated twice to ensure the correct molarity of the sample. The column was pre-conditioned with 40 ml of 0.5 M HNO_3 followed by 40 ml of 0.5 M HCl. The sample was then loaded onto the column and any residual Fe, together with U and Th were eluted with three 50 ml aliquots of 0.5 M HCl. Bi was eluted with four 25 ml aliquots of 0.5 M HNO_3.

2.9.3.6 Preparation of the counting sources

The Bi fraction, contained in approximately 100 ml of 0.5 M HNO_3, was reduced in volume, transferred to a 20 ml scintillation vial and taken to dryness. The residue was re-dissolved in 1 ml of 0.1 M HCl, 5 g of UG-LLT were added and the sample shaken vigorously.

The Po fraction, in 6 M HNO_3, was heated until almost dry, taken up in 50 ml of reverse osmosis water and then 5 ml of 0.3 M $NH_2OH.HCl$ were added. ^{208}Po and ^{210}Po were spontaneously deposited onto copper foils at 95 °C for a period of three hours. The plating solution was maintained at a constant volume by adding reverse osmosis water of the same temperature. After plating, the foil was dried and analysed by α spectrometry.

The Pb fraction was dried down as quickly as possible and transferred to a 20 ml scintillation vial. The sample was taken to dryness and the residue dissolved in 1 ml of 0.1 M HCl. The recovery of the ^{212}Pb tracer was determined immediately by γ spectrometry. 5 g UG-LLT were subsequently added to the vial, which was stored for around 10 days to allow the ^{212}Pb yield tracer to decay, after which the ^{210}Pb activity was determined by LSS. The times of all elutions were noted so that the ingrowth of ^{210}Bi could be determined.

2.9.4 LS counting procedures

2.9.4.1 Lead

The activity of ^{210}Pb is calculated as described below.

If the activity of ^{210}Pb (0-40 keV) at time of elution from Sr Spec (t_0) = x, the counting efficiency of ^{210}Bi (0-40 keV) = 17.1 % and the both the decay of ^{210}Pb and ingrowth of ^{210}Po is assumed to be negligible. Then the count rate at the mid-point of LSS determination (t_1) in the 0-40 keV consists of the ^{210}Pb activity (x) plus the fraction of ^{210}Bi in a 0 to 40 keV window produced from ingrowth from ^{210}Pb (y'). This can be written as (equation 2.10):

$$y' = x + 0.171x\left(1 - e^{-\lambda_{Bi}t}\right) \qquad (2.10)$$

So the fraction of ^{210}Bi after time t can be expressed as (equation 2.11):

$$= \frac{0.171x(1 - e^{-\lambda_{Bi}t})}{x + 0.171x(1 - e^{-\lambda_{Bi}t})} \qquad (2.11)$$

Thus the counts of ^{210}Bi in a 0-40 keV window can be determined by multiplying the fraction of ^{210}Bi counts (equation 2.11) by the total counts in a 0-40 keV window (y') (equation 2.12):

$$\text{Counts of } ^{210}\text{Bi (0-40 keV) in y'} = y'\left(\frac{0.171x(1-e^{-\lambda_{Bi}t})}{x+0.171x(1-e^{-\lambda_{Bi}t})}\right) \quad (2.12)$$

where y' = counts of ^{210}Pb and ^{210}Bi (0-40 keV) after time t.

Therefore the activity of ^{210}Bi in y' can be obtained by multiplying the above expression by the counting efficiency of ^{210}Bi in a 0-40 keV window (equation 2.13):

$$\text{Activity}\left(^{210}\text{Bi in y'}\right) = \frac{y'}{0.171}\cdot\left(\frac{0.171x(1-e^{-\lambda_{Bi}t})}{x+0.171x(1-e^{-\lambda_{Bi}t})}\right) \quad (2.13)$$

Which allows the ^{210}Pb (cpm) in y' to be written as (equation 2.14):

$$^{210}\text{Pb}\left(\text{cpm}\right) = y'-\left(\frac{y'}{0.171}\right).\left(\frac{0.171x(1-e^{-\lambda_{Bi}t})}{x+0.171x(1-e^{-\lambda_{Bi}t})}\right) \quad (2.14)$$

This then allows the ^{210}Pb activity to be calculated by equation 2.15:

$$^{210}\text{Pb}\left(\text{m Bq l}^{-1}\right)=^{210}\text{Pb (cpm)}.\frac{100}{R}.\frac{100}{E}.\frac{1}{V}.\frac{1000}{60}. \quad (2.15)$$

where R = recovery of Pb, E = counting efficiency of Pb and V= sample volume (litres).

2.9.4.2 Bismuth

The vial containing the purified Bi fraction was placed in a Packard LSS for at least one hour prior to counting to dark adapt the sample. The sample was then counted together with background vials comprising 1 ml of 0.1 M HCl and 5 g UG-LLT, and "spiked" samples consisting of the ^{207}Bi yield tracer taken to dryness and re-dissolved in 1 ml 0.1 M HCl and 5 g UG-LLT. This allowed any changes in the activity of the spike to be monitored. The sample was counted three times, each for 200 minutes, with the LLCM activated and the DBB set to 600 ns. The techniques for determination of Bi yield are described in 2.8.2.3. The determination of ^{210}Bi requires the ingrowth of ^{210}Po from the final anion exchange column to the ^{210}Bi count by LSS to be determined.

At t_0 the purified ^{210}Bi vial contains only ^{210}Bi (y). After time t, the ^{210}Bi sample contains counts from decaying ^{210}Bi and ingrowing ^{210}Po (z). This can be written as (equation 2.16):

$$z = ye^{-\lambda_{Bi}t} + \frac{\lambda_{Po}}{\lambda_{Po} - \lambda_{Bi}} . y(e^{-\lambda_{Bi}t} - e^{-\lambda_{Po}t}) \qquad (2.16)$$

Thus the fraction of ^{210}Po after time t can be expressed as (equation 2.17):

$$= \frac{\frac{\lambda_{Po}}{\lambda_{Po} - \lambda_{Bi}} . y(e^{-\lambda_{Bi}t} - e^{-\lambda_{Po}t})}{ye^{-\lambda_{Bi}t} + y\frac{\lambda_{Po}}{\lambda_{Po} - \lambda_{Bi}}(e^{-\lambda_{Bi}t} - e^{-\lambda_{Po}t})} \qquad (2.17)$$

Which can be simplified to (equation 2.18):

$$= \frac{\frac{\lambda_{Po}}{\lambda_{Po} - \lambda_{Bi}} . (e^{-\lambda_{Bi}t} - e^{-\lambda_{Po}t})}{e^{-\lambda_{Bi}t} + \frac{\lambda_{Po}}{\lambda_{Po} - \lambda_{Bi}} (e^{-\lambda_{Bi}t} - e^{-\lambda_{Po}t})} \qquad (2.18)$$

Thus knowing the fraction of ^{210}Po that has ingrown after time t allows the ^{210}Bi count rate to be calculated my multiplying the counts after time t (z) by the fraction of ^{210}Po counts in z after time t (equation 2.19):

$$^{210}\text{Bi (cpm)} = Z. \left(\frac{\frac{\lambda_{Po}}{\lambda_{Po} - \lambda_{Bi}} . (e^{-\lambda_{Bi}t} - e^{-\lambda_{Po}t})}{e^{-\lambda_{Bi}t} + \frac{\lambda_{Po}}{\lambda_{Po} - \lambda_{Bi}} (e^{-\lambda_{Bi}t} - e^{-\lambda_{Po}t})} \right) \qquad (2.19)$$

The ^{210}Bi (cpm) requires further correction for the ingrowth of ^{210}Bi from ^{210}Pb between time of filtration and time of Sr Spec separation (t_4) (equation 2.20):

$$\text{Decay Corrected } ^{210}\text{Bi} = ^{210}\text{Bi (cpm)} . A_{Pb}\left(1 - e^{-\lambda_{Bi}t}\right) \qquad (2.20)$$

The ^{210}Bi (cpm) value is the calculated as ^{210}Bi (m Bq l^{-1}) by correcting for counting efficiency (E), Bi recovery (R), Sample volume in litres (V) and converted from cpm to mBq

l^{-1} (equation 2.21):

$$^{210}Bi\left(m\ Bq\ l^{-1}\right) = {}^{210}Bi(cpm).\frac{100}{R}.\frac{100}{E}.\frac{1}{V}.\frac{1000}{60} \qquad (2.21)$$

2.9.4.3 Polonium

The ^{208}Po spike was a certified yield tracer, therefore, the net counts of ^{208}Po measured by α spectrometry are related to the recovery of Po. ^{208}Po and ^{210}Po recoveries will be identical, therefore, the activity of ^{210}Po in the sample could be calculated from the count rate of the ^{208}Po tracer using equation 2.22:

$$^{210}Po\ (mBq\ l^{-1}) = \frac{\text{Net } ^{210}Po \text{ counts}}{\text{Net } ^{208}Po \text{ counts}} \text{ x A x } \frac{1000}{V} \qquad (2.22)$$

where A = decay corrected activity of ^{208}Po spike (Bq).

The ingrowth of ^{210}Po has been ignored in this calculation as its influence will be insignificant in the short time scale of this method.

2.9.5 Calculation of errors

Throughout this research, errors have been calculated at the 1σ level of significance. Errors include the errors associated with counting, chemical recovery, counting efficiency, certified

spike errors (in the case of Po determination) and errors in pipetting.

2.9.6 Future development of method

This method still has further scope for development, which could allow more data to be produced from a single sample. The high selectivity of the Sr Spec resin results in many nuclides passing through the column in 2 M HCl with Bi. The time constraints at the end of this research did not allow the further developments to be tested but the philosophical challenge was addressed and the possibility of studying further members of the NDS would lead to a greater understanding of the oceanic processes affecting particle reactive nuclides. As stated in Section 1.1, the parent-daughter pairs $^{234}Th/^{238}U$ are often used to calculated rates of particle scavenging in the nearshore environment. The potential of this method was realised when the 0.5 M HCl solution from the Bi purification (Section 2.6.3.2) was examined and found to contain significant activity. By changing the Bi purification scheme it would be possible to separate Bi, U and Th from the sample. This would allow the determination of $^{234}Th/^{238}U$ using the LSS method of Pates *et al.* (1995).

If the Bi fraction is re-dissolved in 9 M HCl instead of 0.5 M HCl, a number of separations become possible. Th can be eluted with 9 M HCl while both Bi and U isotopes are retained on EiChrom AG1x8. U can be eluted with 0.5 M HCl before the elution of Bi with 0.5 M HNO_3. Pates *et al.* (1995) used a ^{230}Th tracer to determine the ^{234}Th recovery and simultaneously determined these nuclides (α and β^- emitting respectively) using α/β LSS. ^{238}U can be determined by its relationship to salinity (Ku *et al.*, 1977), by ICP-MS after the

addition of a suitable tracer or by α spectrometry. It should be pointed out that a ^{232}U yield tracer should be avoided as its decay will introduce ^{228}Th into the sample which may interfere with the Pb recovery calculation. ^{232}U would require a purification stage prior to its addition to remove its daughter products. Other uranium yield tracers are available (e.g. ^{236}U), but not without significant costs which would tend to favour the salinity measurements for marine samples.

NDS nuclides are suitable for measuring processes on timescales up to around four half lifes. Thus a method to determine ^{210}Pb ($t_{½}$ = 22 years), ^{210}Po ($t_{½}$ = 138 days), ^{234}Th ($t_{½}$ = 24 days) and ^{210}Bi ($t_{½}$ = 5 days) on a single sample, would allow rates of processes occurring on 100 year, 1 to 2 year, 3 month and monthly timescales to be examined. Not only does this method allow the measurement of ^{210}Pb, ^{210}Bi and ^{210}Po, but it allows them to be measured within two weeks of sampling, a large time saving over the traditional method.

Chapter Three: Irish Sea water column studies

3.1 Introduction and aims

A sampling campaign was undertaken between spring and autumn 2000 in the Irish Sea, the aims of which were to apply the recently developed method to the measurement of ^{210}Pb, ^{210}Bi and ^{210}Po activities in the dissolved and particulate phases of seawater in the nearshore environment. The objectives of this study were: firstly, to identify problems with the methodology when applied to environmental samples and to make any necessary modifications; secondly, to generate data that would provide primary indications to the biogeochemical cycling of ^{210}Pb, ^{210}Bi and ^{210}Po in the nearshore environment.

As discussed below, the radiological significance of waste discharged to the Irish Sea has initiated several studies on the rates of particle scavenging of radionuclides (Pentreath *et al.*, 1984; Hamilton-Taylor *et al.*, 1987). Much of the radioactive discharge in this region is into the marine environment and model predictions are required to assess the behaviour of these nuclides in this environment. Modelling of transuranic nuclide (Pu and Am) removal from the aqueous to the solid phase in the Irish Sea has previously relied on $^{234}Th/^{238}U$ disequilibrium studies, which provide information of the rate of particle removal over a timescale of 6 months to 1 year. Successful application of the $^{210}Pb/^{210}Bi/^{210}Po$ method developed during the course of this research would allow different rates of processes to be observed, by utilising the different half lives of the nuclides. Furthermore, precise modelling of the $^{210}Pb/^{210}Bi/^{210}Po$ system would also provide more data on the fate of NDS nuclides previously released from the Marchon plant in Whitehaven as discussed below.

Finally, testing the method in such an environment would allow any contamination from both natural and anthropogenic nuclides to be observed and the methodology altered to account for a wide range of potential contaminants.

3.1.1 Setting

The Irish Sea is a body of water which separates Ireland from Britain. It is connected to the Atlantic Ocean by St. Georges Channel in the south and by the North Channel in the north. The predominant water flow is northwards although the circulation patterns vary. Between spring and autumn the water column is homogeneously mixed (McKinley *et al.*, 1976).

Radioactive inputs to the Irish Sea are dominated by BNFL's nuclear fuel reprocessing plant at Sellafield which discharges low level liquid radioactive waste directly to the Irish Sea (Table 3.1). Sellafield is by far the largest contributor to radioactivity in the Irish Sea, although there are several other sources, i.e. defence establishments (Barrow), nuclear electricity generation (Heysham and Chapelcross), radioactive waste repositories (Drigg) and nuclear fuel fabrication and processing plants (Springfields and Capenhurst).

Non-nuclear industries have also contributed significant radioactive inputs. Processing of phosphate ore for the production of phosphoric acid took place at the Albright and Wilson (now Rhodia Consumer Specialities) Marchon plant in Whitehaven from 1954 to 1992. During this time, around 11.4 and 11.5 TBq of ^{210}Pb and ^{210}Po, respectively, were released under license to the Irish Sea (McCartney *et al.*, 2000). Phosphate ores are rich in ^{238}U

	TBq	
Alpha	0.133	
Beta	110	
^{3}H	2520	
^{14}C	5.76	
^{60}Co	0.89	
^{90}Sr	31.2	
$^{95}Zr + ^{95}Nb$	0.182	
^{99}Tc	68.8	
^{106}Ru	2.72	
^{129}I	0.485	
^{134}Cs	0.34	
^{137}Cs	9.12	
^{144}Ce	0.602	
Pu alpha	0.115	
^{241}Pu	2.87	
^{241}Am	0.035	
U	536	(kg)

Table 3.1: Liquid discharges from Sellafield's pipelines to the Irish Sea in 1999. From Environment Agency/SEPA (2000).

decay series nuclides and significant activities of ^{226}Ra, ^{210}Pb and ^{210}Po have been discharged from the Marchon plant to the Irish Sea. In 1992, changes in waste treatment practices and cessation of the use of phosphate ore virtually eliminated discharge of NDS nuclides to the Irish Sea (McCartney *et al.*, 2000). The high removal rates onto particulate material of ^{210}Pb and ^{210}Po in the nearshore environment have been discussed earlier (Section 1.1.6). Thus 8 years after the cessation of discharges from the plant, the activities of ^{210}Pb and ^{210}Po in the marine water column will now be present only from the processes discussed in Section 1.1.2, namely, in-situ production from ^{226}Ra (supported ^{210}Pb), atmospheric inputs (unsupported ^{210}Pb and ^{210}Po) and in-situ production of ^{210}Bi and ^{210}Po from ^{210}Pb. The other

sources of radioactivity in the Irish Sea result from Chernobyl and weapons testing fallout (i.e. ^{137}Cs and ^{241}Am, Brown *et al.*, 1999).

3.1.2 Previous work

The enhancement of NDS nuclides in the Irish Sea was first observed by McCartney *et al.* (1990) who observed a much larger unsupported ^{210}Pb inventory in the sediments than could be accounted for by the overlying water column. Although lateral advection of dissolved ^{210}Pb may occur in these region, $^{230}Th/^{210}Pb$ ratios close to unity in these sediments suggested anthropogenic sources. ^{230}Th is more particle reactive than ^{210}Pb (Sarin *et al.*, 1992) and fluxes resulting from lateral advection would have lower ^{230}Th activities than ^{210}Pb, thus the $^{230}Th/^{210}Pb$ ratio would be expected to be less than unity, as a larger proportion of ^{230}Th had already been scavenged from the advecting waters. The technological enhancement of ^{210}Pb and ^{210}Po was observed in the biota and sediments around the Whitehaven area. Later work (Keating *et al.*, 1996; McCartney *et al.*, 2000) monitored the effect of the cessation of NDS discharge from the plant on the biota and sediments in the vicinity. The observed activities indeed decreased to close to background levels in most matrices, although the sediments still contain enhanced activities of ^{210}Pb and ^{210}Po.

3.2 Sampling and processing

Duplicate 20 litre surface water samples were collected 2.4 km west of St Bees Head at a water depth of 20 metres (Fig. 3.1). Samples were collected in 25 litre plastic carboys, which had been soaked in 0.25 % HNO_3 solution for 1 month prior to sampling. They were

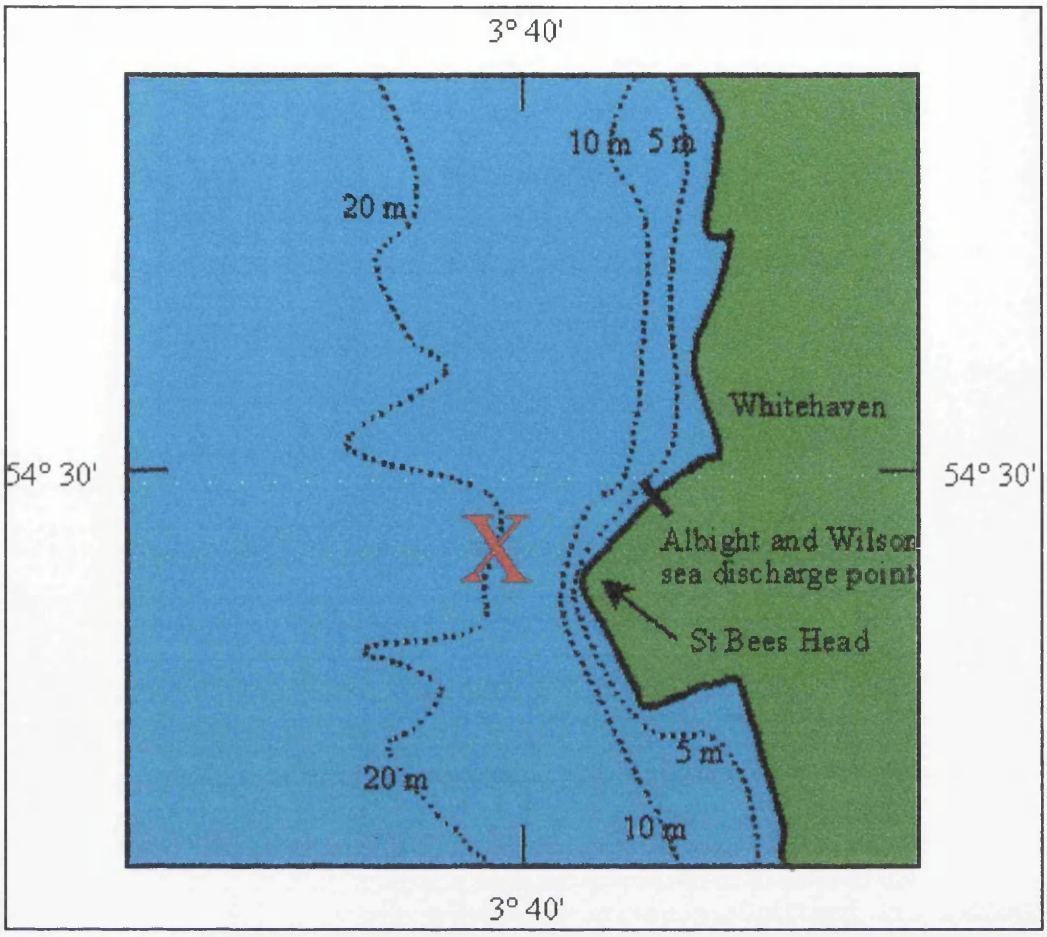

Figure 3.1: Location of the sampling site and bathymetry (m) in the Irish Sea (from Poole *et al.*, 1995).

then thoroughly washed with reverse osmosis water to remove the final traces of acid. Samples were transported back to SURRC on the day of collection and were immediately filtered and the filtrate acidified to pH 2 with 15 M HNO_3, as described in Section 2.9.3.1. While the samples were being collected, ^{212}Pb spike purification was carried out at SURRC. This allowed the samples to be filtered, acidified and spiked on the day of sampling, permitting the shortest time delay prior to the purification and separation of ^{210}Pb, ^{210}Bi and ^{210}Po.

3.3 Results

The results obtained from this study are shown in Table 3.2.

3.4 Discussion of values

Much of the earlier research on $^{210}Po/^{210}Pb$ was carried out on unfiltered samples or samples filtered through a 0.45 μm filter. The convention for defining "dissolved" phase has now changed to 0.22 μm, therefore, the results presented in Table 3.2 used a 0.22 μm filter to discriminate between dissolved and particulate material. The effect of the smaller pore size filter is that additional particles between 0.22 μm and 0.45 μm, and associated nuclides, will be collected in the solid phase. A slight bias in the particulate activities may therefore be present relative to older work, but this bias will reflect a closer approximation of *dissolved* and *particulate* activities. Bacon *et al.* (1988) observed dissolved $^{210}Po/^{210}Pb$ ratios of 0.26 and 0.67 in the coastal waters off New England (Stations 1 and 36, water depth = 80 and 45 metres respectively). Sarin *et al.* (1992) observed ranges of 0.19 to 0.45 (average = 0.30) in the eastern Arabian Sea. Both these data sets were constructed using 0.45 μm to discriminate between dissolved and particulate. The dissolved $^{210}Po/^{210}Pb$ ratios for the Irish Sea samples, given in Table 3.3, vary between 0.04 and 0.29 with an average ratio of 0.14. This indicates the faster rates of particle scavenging of ^{210}Po relative to ^{210}Pb and a subsequent enrichment of particle bound ^{210}Po can be observed in Table 3.3. Bacon *et al.* (1988) found the particulate $^{210}Po/^{210}Pb$ ratio to be 2.50 (Station 1) The lower ratio of particulate $^{210}Po/^{210}Pb$ in the Irish Sea (average = 1.18) suggests that the rates of particle removal are faster in this setting, which is to be expected in this nearshore location.

Sample ID	Sample date	Dissolved ^{210}Pb	±	Particulate ^{210}Pb	±	Dissolved ^{210}Bi	±	Particulate ^{210}Bi	±	Dissolved ^{210}Po	±	Particulate ^{210}Po	±
IS3	31 May	**1.431**	**0.102**	ND		ND		ND		0.144	0.011	ND	
		1.518	0.074										
		1.344	0.070										
IS4	19 June	**1.783**	**0.140**	ND		ND		ND		**0.064**	**0.007**	ND	
		1.783	0.140							0.064	0.007		
		SL	SL							SL	SL		
IS5	7th Aug	**0.533**	**0.059**	**0.861**	**0.110**	ND		ND		**0.073**	**0.007**	**0.541**	**0.030**
		0.533	0.059	0.920	0.074					0.073	0.007	0.541	0.030
		SL	SL	0.802	0.083					SL	SL	SL	SL
IS6	29th Aug	**0.416**	**0.066**	SL	SL	ND		ND		**0.121**	**0.011**	**0.410**	**0.024**
		0.453	0.054							0.109	0.009	0.259	0.013
		0.379	0.038							0.131	0.007	0.561	0.020
IS7	11th Sept	**0.641**	**0.094**	**0.296**	**0.040**	**0.093**	**0.032**	**0.874**	**0.099**	**0.102**	**0.013**	**0.512**	**0.027**
		0.729	0.072	0.283	0.030	0.102	0.025	0.845	0.069	0.098	0.010	0.555	0.022
		0.553	0.061	0.309	0.027	0.084	0.020	0.903	0.071	0.106	0.009	0.469	0.015

Table 3.2: Results obtained for duplicate 20 litre water samples collected 2.4 km west of St Bee's Head in the Irish Sea between May and September 2000. All activities are expressed in mBq l^{-1}. SL indicates where a sample was lost during processing. ND indicates activity not determined. The average of the duplicates is displayed in bold

Sample	$^{210}Po/^{210}Pb$ (dissolved)	$^{210}Po/^{210}Pb$ (particulate)
IS 3	0.10	ND
IS 4	0.04	ND
IS 5	0.14	0.63
IS 6	0.29	ND
IS 7	0.16	1.73

Table 3.3: $^{210}Po/^{210}Pb$ activity ratios observed in the Irish Sea sampling using 0.22 μm filters to discriminate between dissolved and particulate phases. ND indicates activity not determined. The activity ratios are calculated from the average values (in bold) displayed in Table 3.2.

By summing the dissolved and particulate values for ^{210}Pb and ^{210}Po it is possible to observe total $^{210}Po/^{210}Pb$ activity ratios between 0.44 and 0.65. Similar surface $^{210}Po/^{210}Pb$ activity ratios have been observed in the Pacific and Indian Oceans (Nozaki and Tsunogai, 1976; Cochran *et al.*, 1983), and in the nearshore environment (Tanaka *et al.*, 1983). The lower activities of ^{210}Po being due to preferential removal of ^{210}Po by primary production and its higher scavenging effectiveness (Sarin *et al.*, 1992).

In the mid 1980s McCartney *et al.* (1990) measured dissolved (< 0.45 μm) ^{210}Pb activities in the eastern Irish Sea. During this time there was still significant input of NDS nuclides from the Albright and Wilson plant in Whitehaven. However, the reported values did not show significant enhancement due to high rates of particle scavenging in this environment resulting in rapid removal of ^{210}Pb from the water column. Between November 1986 and January 1988 the range of dissolved ^{210}Pb activities observed by McCartney *et al.* (1990) was 0.070 to 0.910 mBq l^{-1}, similar to the range of results obtained during the present

research. Furthermore, Bacon *et al.* (1988) reported similar ^{210}Pb activities in the waters off the eastern coast of the United States. A summary of the ranges of ^{210}Po and ^{210}Po activities obtained for seawater in the present work and other studies is displayed in Table 3.4. Overall, the values observed in this nearshore location reflect the more intense particle flux in this region resulting in lower concentrations of ^{210}Po and ^{210}Pb in the water column. These data allow estimates of the residence times of ^{210}Po and ^{210}Pb in this environment. Several different models will be applied and the results compared to observe the effects of different model constraints on the removal rates.

3.5 Modelling of data

3.5.1 ^{210}Po/^{210}Pb disequilibria

The first two models presented are steady-state models which are often applied to calculating the residence times of ^{210}Po and ^{210}Pb in the SML of the oceans. The assumption in the steady-state models are that there is no change in the total activity (i.e. dN/dt = 0). In the open ocean this may be a valid assumption. However in the nearshore environment this may not occur due to the rapid nature of nearshore processes (tidal movements and currents), biological activity and re-suspension of particles. However, the well mixed water column of the Irish Sea may allow a simple steady-state box model to be utilised.

Residence times for dissolved ^{210}Pb and ^{210}Po were calculated for the Irish Sea using the steady-state box model applied by Carvalho (1997) which assumed a ^{226}Ra activity of 2 mBq l^{-1} (A_{Ra}) (Poole *et al.*, 1995), an atmospheric input (Ia_{Pb}) of 86 Bq m^{-2} y^{-1} of ^{210}Pb

Author	Location	Pore size (μm)	Average water depth	Dissolved			Particulate			Total		
				^{210}Pb	^{210}Po	^{210}Po/^{210}Pb (mean)	^{210}Pb	^{210}Po	^{210}Po/^{210}Pb (mean)	^{210}Pb	^{210}Po	^{210}Po/^{210}Pb (mean)
This study	Irish Sea	0.22	20m	0.42 to 1.43	0.064 to 0.19	0.14	0.30 to 0.86	0.41 to 0.54	1.18	0.94 to 1.39	0.53 to 0.61	0.50
McCartney *et al.* (1990)	Irish Sea	0.45	10 to 30 m	0.07 to 0.91								
Bacon *et al.* (1988)	New England coast	0.45	45 to 80 m	0.26 to 0.67	0.17 to 0.24	0.47	0.13	0.31	2.50	0.80	0.55	0.68
Tanaka *et al.* (1983)	Funka Bay	UF	92 m							0.75 to 2.3	0.23 to 1.32	0.46
Nozaki *et al.* (1998)	Off Mexico	UF								2.20	0.90	0.41
	Caribbean/Gulf of Mexico	UF								1.72	1.10	0.64
	Mediterranean	UF								2.60	1.17	0.45
	Red Sea	UF								1.70	0.47	0.27
	Arabian Sea	UF								1.30	0.48	0.37
	Bay of Bengal	UF								2.35	1.42	0.60
	S China Sea	UF								0.78	0.57	0.72
Shannon *et al.* (1970)	South African coast	UF	> 1 km							1.4	0.73	0.52
Sarin *et al.* (1992)	Arabian Sea	0.45	> 1 km	1.07 to 2.54	0.43 to 0.76	0.29						
Krishnaswami and Somayajulu (1975)	Santa Barbara Basin	UF	570 m							1.00		
Benninger (1978)	Long Island Sound		20 m							0.7		

Table 3.4: Comparison of results obtained from this study with surface ^{210}Po and ^{210}Pb concentrations (mBq l^{-1}) in similar environmental settings. UF indicates un-filtered samples, the dissolved and particulate phases have been summed to allow Total activities to be compared.

(McCartney *et al.*, 1990) with the atmospheric input of ^{210}Po (Ia_{Po}) being 1/10th that of ^{210}Pb (Shannon *et al.*, 1970, Carvalho, 1997). Conversion of these factors into the units used in the model gives A_{Ra} = 2 Bq m^{-3}, Ia_{Pb} = 8.6 Bq m^{-2} y^{-1}, Ia_{Po} = 0.86 Bq m^{-2} y^{-1}. The model applied by Carvalho (1997) includes factors accounting for riverine input and output of water, but in the present case, these factors were removed from the model as they are not applicable to the Irish Sea. Advection of water masses has been ignored since this application is a one-dimensional model which assumes steady-state advective movement. The advective removal of water is slow relative to the rates of scavenging process under investigation. The atmospheric inputs are assumed to be in the dissolved phase which would seem likely as the pH of rain water is around 5 (Talbot and Andren, 1984). Dry deposition of ^{222}Rn progenies may occur but the significant input will occur during wet deposition in a moist marine climate.

The activity of dissolved ^{210}Pb in the Irish Sea will depend on several factors; (1) the atmospheric input of ^{210}Pb to the water column (Ia_{Pb}), (2) ^{210}Pb produced from radioactive decay of ^{226}Ra (λ_{Pb} x A_{Ra}), (3) radioactive decay of ^{210}Pb (λ_{Pb} x A_{Pb}) and (4) the rate of removal to the solid phase, which is assumed to follow first order kinetics and is characterised by a rate constant (λ_S). Thus the balance of ^{210}Pb can be written as:

$$\lambda_{Pb}A_{Ra} + Ia_{Pb} = \lambda_{Pb}A_{Pb} + \lambda_S A_{Pb} \qquad (3.1)$$

Equation 3.1 can be solved for λ_S, which allows calculation of the mean dissolved residence time τPb (days) (equation 3.2):

$$\tau Pb = \frac{1}{\lambda_S} = \frac{\lambda_{Pb}A_{Ra} + Ia_{Pb} - \lambda_{Pb}A_{Pb}}{A_{Pb}} \qquad (3.2)$$

A similar calculation can be carried out for ^{210}Po, and in this case, the in-situ production becomes more significant, and the residence time of dissolved ^{210}Po (τPo) can be calculated by equation 3.3:

$$\tau Po = \frac{1}{\lambda_S} = \frac{\lambda_{Po}A_{Pb} + Ia_{Po} - \lambda_{Po}A_{Po}}{A_{Po}} \qquad (3.3)$$

The data obtained from the Irish Sea samples were used to calculated the residence times of dissolved ^{210}Pb and ^{210}Po, the results are shown in Table 3.5.

Sample	Sample date	λ_S Po	τPo (days)	λ_S Pb	τPb (days)
IS 3	31st May	22.23	**16**	6.01	**61**
IS 4	19th June	62.59	**6**	4.82	**76**
IS 5	7th August	23.31	**16**	16.20	**23**
IS 6	29th August	11.57	**32**	20.76	**18**
IS 7	11th September	18.10	**20**	13.46	**27**

Table 3.5: The dissolved residence times of ^{210}Pb and ^{210}Po in the water column of the Irish Sea using the steady state model (after Carvalho, 1997).

Carvalho (1997) observed dissolved residence times of ^{210}Po and ^{210}Pb of 18 days and 30 days respectively in the Tagus Estuary near Lisbon, similar to the calculated residence times for the Irish Sea. Moreover, the Irish Sea results show pronounced temporal variations in

both ^{210}Po and ^{210}Pb residence times, possibly indicative of seasonal effects (e.g. variations in plankton levels). The residence times of dissolved ^{210}Po and ^{210}Pb highlight the intense particle scavenging that takes place in the nearshore environment. Furthermore, the data clearly confirms the higher particle reactivity of ^{210}Po than ^{210}Pb. This is consistent with the strong affinity of ^{210}Po for uptake by biota (Wildgust *et al.*, 1998) and the high level of biological activity in nearshore waters. This model assumes that there is no re-dissolution back into the dissolved phase which is not the case for ^{210}Po. Thomson and Turekian (1976), Bacon *et al.* (1976), Sarin *et al.* (1992) have all shown that ^{210}Po can be released from particles by dissolution of biological particles.

Another type of model has been applied to calculate residence times of ^{210}Po and ^{210}Pb in the oceanic water column (Bacon *et al.*, 1976, Ritchie and Shimmield, 1991). Bacon *et al.* (1976) assumed atmospheric input of ^{210}Po is negligible due to escape of ^{210}Po into the marine aerosol. This may be valid in open ocean environments but atmospheric ^{210}Po inputs may be important in the nearshore environment due to the proximity of land. ^{222}Rn/^{226}Ra disequilibrium is also ignored (although a 25 % deficiency may exist) as the atmospheric input of ^{210}Pb is far greater than in-situ decay from ^{226}Ra. In this approximation, the dissolved residence time of ^{210}Po can be derived by stating that the production of ^{210}Po by decay of ^{210}Pb is balanced by radioactive decay of ^{210}Po and its transfer onto particles (equation 3.4):

$$\lambda_{Po} A^{d}_{Pb} + J_{Po} = \lambda_{Po} A^{d}_{Po} \qquad (3.4)$$

where J_{Po} represents the transfer between the dissolved and particulate phases. A positive J value indicates a transfer from particulate to dissolved phase. When J is negative it indicates removal from the dissolved phase to the particulate phase. The residence time of dissolved ^{210}Po can then be calculated by equation 3.5:

$$\tau_{Po}^{d} = \frac{A_{Po}^{d}}{-J_{Po}} \tag{3.5}$$

For particulate ^{210}Po it is assumed that the supply of particulate ^{210}Po by decay of particulate ^{210}Pb and transfer from solution is balanced by radioactive decay of ^{210}Po and settling of particles from the water column, this is expressed in equation 3.6:

$$\lambda_{Po} A_{Pb}^{p} - J_{Po} = \lambda_{Po} A_{Po}^{p} + P_{Po} \tag{3.6}$$

where P represents the removal in the particulate phase. This allows the particulate ^{210}Po residence time to be calculated using equation 3.7:

$$\tau_{Po}^{p} = \frac{A_{Po}^{p}}{P_{Po}} \tag{3.7}$$

It is then assumed the same particles responsible for removal of ^{210}Po will also remove ^{210}Pb from solution. This allows the flux of particulate ^{210}Pb (P_{Pb}) to be determined using equation 3.8:

$$P_{Pb} = \left(\frac{A_{Pb}^{p}}{A_{Po}^{p}} \right) \times P_{Po} \tag{3.8}$$

This allows the flux of dissolved ^{210}Pb to be calculated (equation 3.9):

$$-J_{Pb} = \lambda_{Pb} A^{p}_{Pb} + P_{Pb} \qquad (3.9)$$

Having thus derived the net flux of dissolved ^{210}Pb, its residence time can be determined (equation 3.10):

$$\tau^{d}_{Pb} = \frac{A^{d}_{Pb}}{-J_{Pb}} \qquad (3.10)$$

Finally, the atmospheric input (*I*a) of ^{210}Pb can be derived using equation 3.11.

$$\lambda_{Pb} A_{Ra} + I_{a} + J_{Pb} = \lambda_{Pb} A^{d}_{Pb} \qquad (3.11)$$

The results obtained are given in Table 3.6. The residence time of dissolved ^{210}Po calculated by this model follows a similar pattern to the change in removal rates using the box model applied by Carvalho (1997). The values are not significantly different to those obtained in the previous model which included an atmospheric input of ^{210}Po. The difference in dissolved ^{210}Po residence times between the two models is greatest when the residence times are longest. This may suggest that the atmospheric input of ^{210}Po becomes significant when the rate of scavenging is slower. The residence time of particulate ^{210}Po is longer than that found in the dissolved phase. This could suggest several processes: (1) that there is significant recycling of ^{210}Po between dissolved and particulate phases in this productive environment; (2) that the particles are not removed from the water column as quickly as anticipated; or (3) that there is significant resuspension of particles in this shallow environment.

Sample	Sample date	J Po (dpm cm^{-2} yr^{-1})	τ Po (dissolved) (days)	P Po (dpm cm^{-2} yr^{-1})	τ Po (particulate) (days)	P Pb (dpm cm^{-2} yr^{-1})	J Pb (dpm cm^{-2} yr^{-1})	τ Pb (dissolved) (days)	Ia Pb (dpm cm^{-2} yr^{-1})
IS 3	31st May 00	-0.283	**22**	ND	ND	ND	ND	ND	ND
IS 4	19th June 00	-0.377	**7**	ND	ND	ND	ND	ND	ND
IS 5	7th Aug 00	-0.101	**32**	0.1713	**138**	0.2726	-0.2694	**87**	0.264
IS 6	29th Aug 00	-0.065	**82**	ND	ND	ND	ND	**ND**	ND
IS 7	11th Sept 00	-0.118	**38**	0.0709	**316**	0.0410	-0.0399	**704**	0.035

Table 3.6: Application of the model calculations from Bacon *et al.* (1976) to the data obtained from the Irish Sea sampling. J denotes a net flux between dissolved and particulate phases (a negative value indicating a net transfer from dissolved to particulate phase). P indicates the net flux of particulate-associated activity from the water column. ND indicates activity not determined. The model calculation of dissolved ^{210}Pb residence time (τPb dissolved) and atmospheric input (IaPb) requires particulate data for both ^{210}Pb and ^{210}Powhich was not available for IS 3,4 and 6.

The residence time of dissolved Pb is much longer than the values obtained from the Carvalho model and the two values obtained are significantly different (0.24 years and 1.92 years). This model has been applied by Bacon *et al.* (1976) and Ritchie and Shimmield (1991) to modelling residence times in Atlantic surface mixed layer water. In these conditions the steady-state model is more valid than in the coastal environment. One problem in the application of this model in the nearshore environment is that it assumes that the same particles are responsible for removal of ^{210}Pb and ^{210}Po from the dissolved phase. The differences in geochemistry of ^{210}Po and ^{210}Pb discussed in Section 1 would suggest otherwise. Furthermore, the greater significance of atmospheric inputs close to land, changes in fluxes of particles and re-suspension of bottom sediments in this shallow setting may invalidate this model.

Tanaka *et al.* (1983) applied a non-steady-state model to examine temporal variations in the residence time of ^{210}Po and ^{210}Pb in the waters of Funka Bay as the water column inventories of these nuclides changed from month to month. The residence time of ^{210}Po can be calculated as (equation 3.12):

$$\tau Po = \frac{1}{k} = \lambda_{Po}\left[\frac{A_{Pb}}{A_{Po\,1}} - 1\right] + \frac{I_{Po}}{A_{Po\,1}} + \frac{1}{t}\left[1 - \frac{A_{Po\,2}}{A_{Po\,1}}\right] \qquad (3.12)$$

Where $A_{Po\,1}$ and $A_{Po\,2}$ refer to the activities of total ^{210}Po in subsequent measurements and t represents the time (in days) between the measurements. The decay constant (λ_{Po}) is also calculated in days. A similar calculation for ^{210}Pb can be written as (equation 3.13):

$$\tau Pb = \frac{1}{k} = \lambda_{Po}\left[\frac{A_{Ra}}{A_{Pb\,1}} - 1\right] + \frac{I_{Pb}}{A_{Pb\,1}} + \frac{1}{t}\left[1 - \frac{A_{Pb\,2}}{A_{Pb\,1}}\right] \qquad (3.13)$$

The residence times of total ^{210}Po and ^{210}Pb were calculated as 121 and 56 days respectively using the non-steady-state model. At first it may seem odd that the more particle reactive nuclide has a longer residence time in the water column but similar results were obtained by Tanaka *et al.* (1983). This would suggest that different particle types are responsible for the removal of these nuclides and that the particles which remove ^{210}Po remain in the water column longer, possibly a result of more effective re-cycling of ^{210}Po by biological processes. Tanaka *et al.* (1983) also highlight that the calculated residence times are shorter when the non-steady-state model is applied. If the results from IS 5 and IS 7 are applied to a steady-state model (equations 3.2 and 3.3), the average total ^{210}Po and ^{210}Pb residence times would be 126 and 50 days respectively. Tanaka *et al.* (1983) do not report if their steady-state model takes atmospheric input of ^{210}Po into account. Without accounting for atmospheric ^{210}Po input, the total residence times would increase to 157 and 380 days for IS 5 and 7. This highlights the importance of atmospheric input of ^{210}Po in nearshore scavenging models. In the nearshore environment the activities of ^{210}Po are lower than would be found in the surface ocean. It is therefore crucial to include atmospheric inputs in the ^{210}Po scavenging model to gain as true an estimation of the geochemical behaviour of particle reactive pollutants.

3.5.2 Summary of ^{210}Pb and ^{210}Po modelling

Carvalho (1997) obtained dissolved ^{210}Po and ^{210}Pb residence times of 18 and 30 days respectively in the Tagus estuary. Using the same model, the data from the present study produced average residence times of 18 days and 40 days for ^{210}Po and ^{210}Pb respectively, in excellent agreement with Carvalho's data. Applying the model of Tanaka *et al.* (1983) to the Irish Sea data gives total residence times of 121 and 56 days for ^{210}Po and ^{210}Pb, respectively, again in good agreement with the results of Tanaka *et al.* (1983) who observed average residence times of 137 and 86 days for total ^{210}Po and ^{210}Pb, respectively, in Funka Bay. There is less agreement with the model of Bacon *et al.* (1976) as this model was designed for oceanic studies while the setting for this work was the nearshore environment and the influence of re-suspension of bottom sediments may account for some of the discrepancies. Also, there is little difference between the figures obtained from the non-steady-state and steady-state-models. This suggests that the simple box model which includes atmospheric inputs of ^{210}Po holds well in this setting.

It would appear that the model applied by Carvalho (1997) is valid for the setting of this study and that the data generated from the model can be used to characterise temporal changes in the behaviour of ^{210}Pb and ^{210}Po in the Irish Sea. The sampling protocol began on the 31st May 2000 and the final sample was collected on the 11th of September. The variation in dissolved ^{210}Pb and ^{210}Po residence times over the course of this 103 day period is displayed in Figure 3.2. Dissolved ^{210}Pb and ^{210}Po both display strong temporal changes in their dissolved residence times which may be related to changes in primary production and

particle fluxes. Higher dissolved ^{210}Pb residence times were found in early summer than in the autumn. Dissolved ^{210}Po residence times are lower in early summer than in autumn and this may suggest a link to productivity. An inverse correlation (-0.80) was found between the dissolved residence times of ^{210}Po and ^{210}Pb which would suggest different biogeochemical behaviour in the water column.

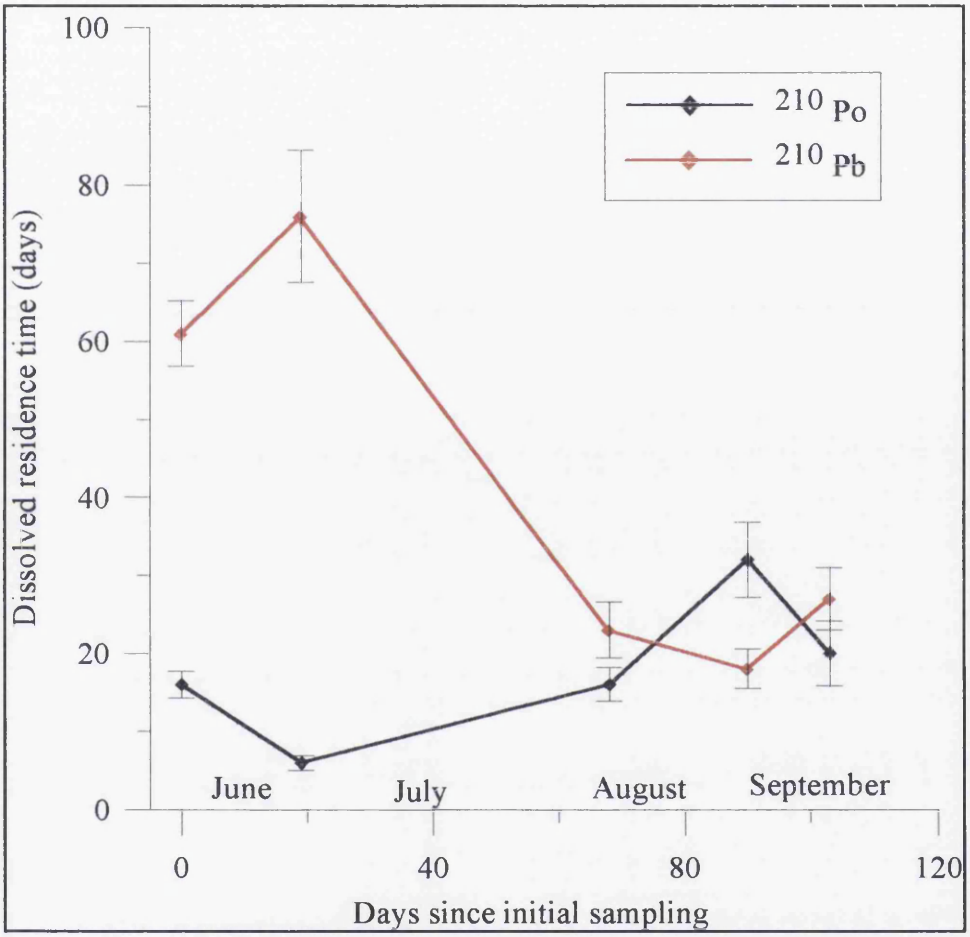

Figure 3.2: Temporal changes in the residence time of dissolved ^{210}Pb and ^{210}Po observed in the Irish Sea.

3.5.3 Modelling the behaviour of ^{210}Bi

A simple box model which accounts for atmospheric inputs has been shown to be suitable

for the determination of dissolved ^{210}Po residence times. This model will now be applied to the determination of dissolved ^{210}Bi residence times in the same environment. For the determination of ^{210}Bi the ingrowth from ^{210}Pb may be significant due to its shorter half life compared to ^{210}Po. Furthermore, the atmospheric input of ^{210}Bi will be more significant as the residence time of ^{210}Pb in the atmosphere is long enough for significant ingrowth of ^{210}Bi from its parent. Assuming a ^{210}Pb residence time of 10 days (Francis *et al.*, 1970), the ^{210}Bi/^{210}Po activity ratio in rainwater would be 0.5. The calculation to determine dissolved ^{210}Bi residence time based on the model of Carvalho (1997) is:

$$\tau Bi = \frac{1}{\lambda_S} = \frac{\lambda_{Bi} A_{Pb} + Ia_{Bi} - \lambda_{Bi} A_{Bi}}{A_{Bi}} \qquad (3.14)$$

The residence time of dissolved ^{210}Bi in the Irish Sea was calculated as 0.82 days. This extremely short residence time would suggest that uptake of particle reactive species in the nearshore environment may be occurring on very rapid timescales. Application of ^{210}Bi to marine tracer studies will require further work to examine the temporal changes of this nuclide in the coastal environment. Accurate determination of the atmospheric input is not as important in the calculation of the residence time as the activity of ^{210}Pb and the decay correction calculations. Table 3.7 displays the residence time of ^{210}Bi over a range of atmospheric inputs values, from $Ia_{Bi} = Ia_{Pb}$ to $Ia_{Bi} = 0.1\ Ia_{Pb}$ (the assumed atmospheric input of ^{210}Po). If removal of ^{210}Bi does occur on such timescales it draws questions as to the origins of ^{210}Po in the water column and the re-cycling of ^{210}Bi. Alternatively, the rapid

Ia_{Bi} (% of ^{210}Pb input)	τ^{210}Bi (days)
100 %	0.744
80 %	0.773
60 %	0.804
50 %	0.821
40 %	0.839
30 %	0.857
20 %	0.876
10 %	0.896

Table 3.7: The effect of variation in the atmospheric input of ^{210}Bi on the residence time of dissolved ^{210}Bi. At 100 % $Ia_{Pb} = Ia_{Bi}$.

removal processes suggested for ^{210}Bi may not be suitable for box model calculation. Further studies into the biogeochemical behaviour of ^{210}Bi are warranted.

The development of this method offers the opportunity to study the dynamics of rapid transfer of radionuclides onto particles. No references to the activities of ^{210}Bi in marine systems were found during the course of this research. It is possible that scavenging processes may be occurring on much faster timescales than previously thought. It would be unwise to make these conjectures based upon one measurement of ^{210}Bi in this system but the method is now in place for high resolution determination of a range of removal processes via the ^{210}Pb-^{210}Bi-^{210}Po system.

3.6 Further refinement

The detection limits of this method are based on a 20 litre sample size. The low activities

found in the nearshore environment require a larger sample size to ensure suitable activities of ^{210}Bi are present. If the sample size is increased the limits of detection will be reduced. The effect of increasing sample size on detection limits is shown in Table 3.8. Clearly the larger sample size offers improved detection limits, something which was admittedly not anticipated during the sampling protocol. The dissolved ^{210}Bi residence time is therefore quite speculative.

Volume (litres)	^{210}Bi MDA (mBq l^{-1})	^{210}Pb MDA (mBq l^{-1})
20	0.341	0.316
40	0.171	0.158
60	0.114	0.105
80	0.085	0.079
100	0.068	0.063

Table 3.8: The effect of increasing the sample volume on the minimum detectable activity (MDA) of ^{210}Bi and ^{210}Pb.

3.7 Conclusions

The method developed during this research has been successfully applied to real samples in a complex environment containing high levels of anthropogenic contaminants. The results of both the analytical and modelling components are generally in very good agreement with each other. This indicates, despite the presence of anthropogenic nuclides in the sample matrix, that the methodology is sensitive to the very low activities of particle reactive NDS radionuclides present. Different models were applied to the data and a steady-state

scavenging model which accounts for atmospheric inputs appears to be suitable for the nearshore environment. The results from modelling of the data can be used (by analogy) to predict the behaviour of anthropogenic radionuclides in the nearshore environment of the Irish Sea.

Chapter Four: Loch Etive sediments study

4.1 Introduction

The original aims of this research were (a) to develop a time efficient method for the determination of ^{210}Po and ^{210}Pb in seawater, and, (b) to apply this method in a study of temporal variations in ^{210}Po and ^{210}Pb activities in seawater and suspended particles in Loch Etive. However, problems in the method development stage meant that there was insufficient time for the Loch Etive water column studies to be completed and the sample site selected for initial testing of the method was, therefore, changed to the Irish Sea (Chapter 3). A full annual cycle would have been required for the Loch Etive study which would have evaluated organic versus inorganic scavenging during periods of contrasting productivity. However, at the start of the research, a suite of sediment cores was collected from Loch Etive to provide information on the fate of ^{210}Pb and ^{210}Po in this setting. These were analyzed for both anthropogenic (^{137}Cs) and NDS radionuclides (^{210}Po, ^{210}Pb and ^{226}Ra).

4.1.1 Setting

Loch Etive is a fjordic sea loch on the west coast of Scotland close to Oban (Fig. 4.1). The loch is around 28 km long and features two distinct basins separated by a shallow sill at Bonawe. The outer basin has a maximum depth of 60 m, while the inner basin has a maximum depth of 170 m. The outer basin has a well mixed oxygenated water column. The sill at Bonawe creates different conditions in the inner basin where circulation is more

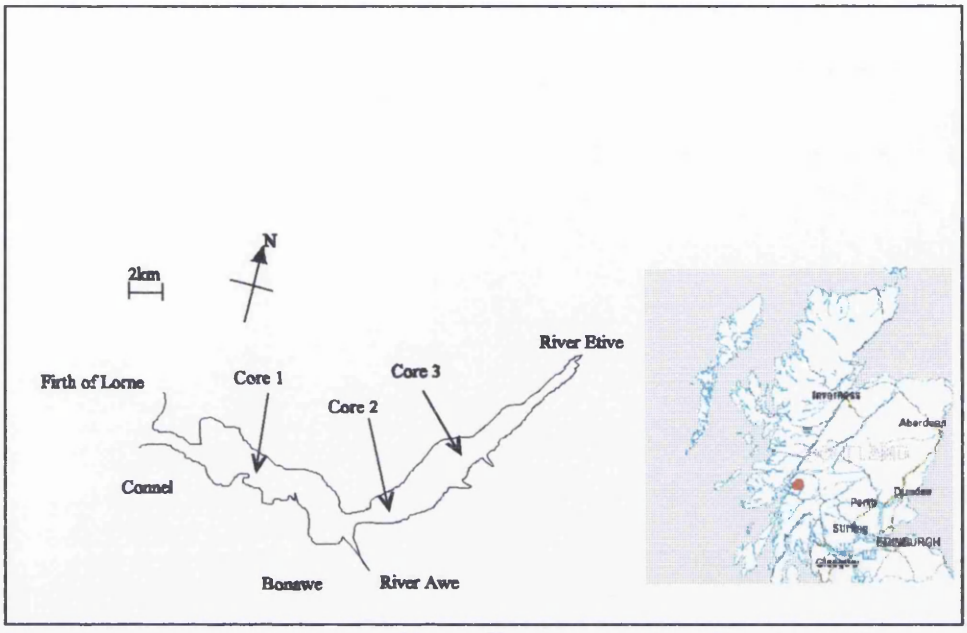

Figure 4.1: Location map of Loch Etive illustrating the sample sites for the sediment cores.

restricted and seasonal stratification of the water column occurs (Ridgway and Price, 1987). This stratification is greatest in the summer and leads to anoxic conditions in the deeper waters (Shimmield, 1993). The surface waters of the inner basin have a larger freshwater input from the Rivers Etive and Awe. During periods of anoxia, the redox front in the inner basin frequently occurs above the sediment water interface and leads to strong seasonal cycling of redox sensitive metals (Fig. 4.2). Wei and Murray (1994) have shown anoxic basins to be important sites for boundary scavenging of ^{210}Pb and suggest that the distribution of ^{210}Pb may be controlled by redox cycling of Fe and Mn. Benoit and Hemmond (1987) observed enhanced ^{210}Pb and ^{210}Po activities in the bottom waters of Bickford Pond, Massachusetts, during a brief period of anoxic conditions. They attributed these high values to reductive dissolution of Fe and Mn oxyhydroxides resulting in the

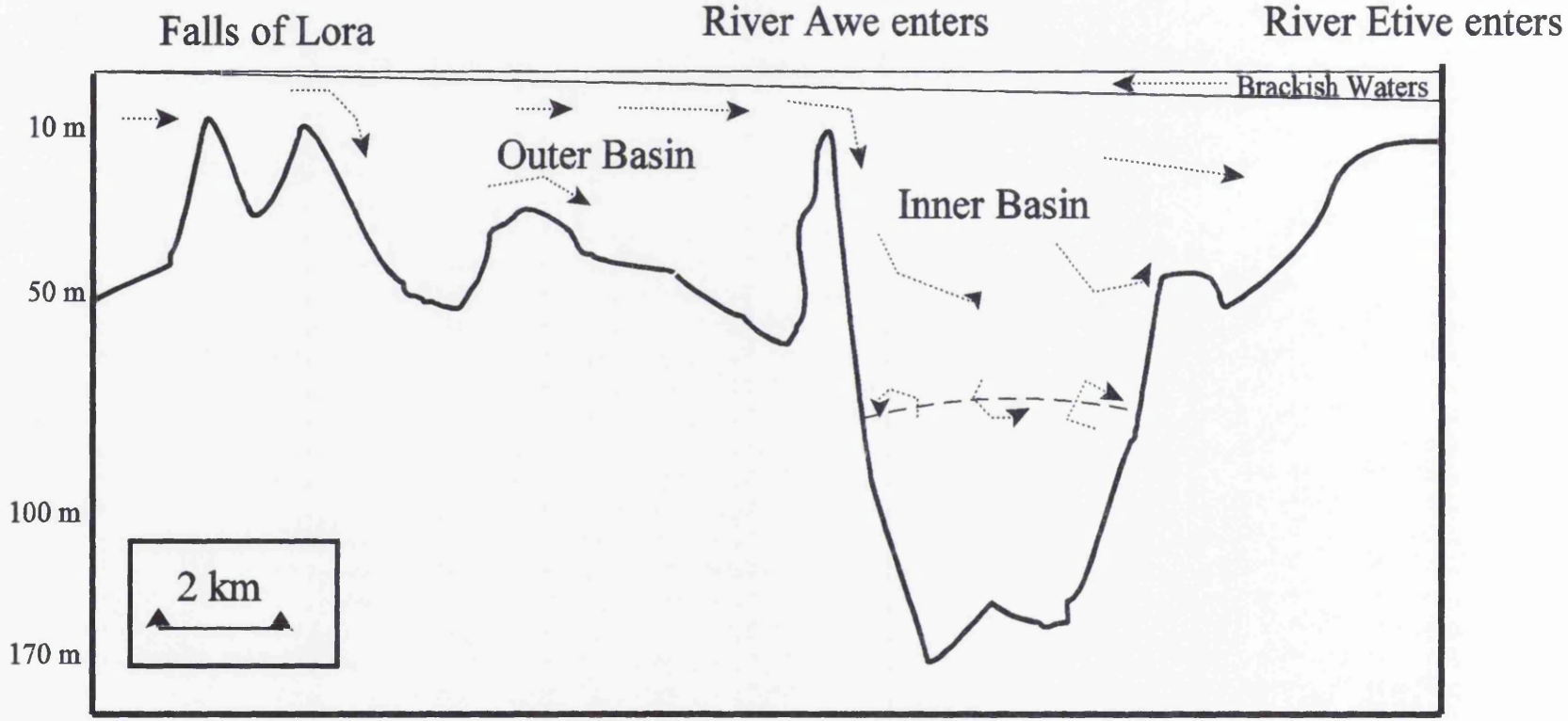

Figure 4.2: Cross section of Loch Etive (from Shimmield, 1993).

release of ^{210}Po and ^{210}Pb into the water column. Swarzenki *et al.* (1999) found an enrichment of ^{210}Pb and ^{210}Po at the O_2/H_2S boundary in an anoxic fjord and suggested that the behavior of both these nuclides is strongly influenced by biological process.

As the measurements of ^{210}Po/^{210}Pb disequilibria have shown (Chapter 3), the nearshore environment is a very important region in terms of removal of particle reactive pollutants from the marine system. The rationale of this part of the study is thus:

It will allow determination of the fluxes of ^{210}Pb to the sediment in contrasting geochemical environments and highlight the wide ranging application of NDS radionuclides.

It will allow a comparison ^{210}Po/^{210}Pb activities in the surface sediments of two distinct basin and may provide clues to the fate of particle reactive pollutants in anoxic conditions.

4.2 Methodology

4.2.1 Sample Collection

Three sediment cores were collected from Loch Etive on the 7 th November 1997 on board the RV "*Seol Mara*". The locations and lengths of the cores can be observed in Table 4.1. The cores were collected using a Sholkovitz gravity corer and care was taken to preserve the sediment water interface. All three cores were extruded onboard ship and placed into pre-weighed and labeled plastic bags. The top 10 cm of each core was sampled at a 1 cm resolution. From 10 to 30 cm the sample resolution was 2 cm and the remainder of the core

was then sampled at 5 cm increments apart from the final 15 cm sample in core 1.

Identification	Latitude	Longitude	Water depth (m)	Length of core (cm)
Core 1	56° 27' 110 N	05° 14' 875 W	60	95
Core 2	56° 27' 401 N	05° 10 997 W	145	80
Core 3	58° 28' 877 N	05° 09 212 W	107	80

Table 4.1: The location of the sediment cores, the depth of the overlying water column and the length of sediment core collected.

4.2.2 Sample preparation

On return to the laboratory, the individual sections were logged before being placed into pre-washed and weighed plastic bowls. After recording the wet weight of the sediment, the samples were placed in a drying oven at 40 °C and dried until constant weight was achieved. The samples were dried at 40 °C to minimize any volatilization of ^{210}Po that may occur at higher temperatures. The weights of the dried samples were recorded before the samples were ground with a mortar and pestle until a homogeneous powder was achieved.

4.2.3 Analysis of ^{210}Po in sediment

Approximately 1 g of the dried and ground sediment was weighed accurately on a four figure balance and transferred to a 250 ml Pyrex beaker. 1 ml of ^{208}Po spike (activity = 0.25 Bq ml^{-1}) was added to the beaker, followed by 50 ml of 6 M HCl. This was then left overnight to allow the spike to equilibrate with the sample. The sample was evaporated to dryness and the residue digested in 50 ml of Aqua-Regia solution (50 % 15 M HNO_3 and

50 % 6 M HCl). The sample was again evaporated to dryness before the addition of 25 to 50 ml of 35 % H_2O_2. This was heated gently to allow H_2O_2 to react with organic matter in the sediment. Once the reaction had finished, the sample was again taken to dryness. The residue was then dissolved in 40 ml of 6 M HCl and heated gently prior to filtration through a Whatman 541 filter paper. Fe^{3+} was removed from the sample by solvent extraction with DIPE. The extraction of Fe^{3+} was required to prevent Fe^{3+} interfering with the subsequent polonium plating stage. The removal of Fe^{3+} was not always totally successful with a single extraction, but slight heating of the solution prior to the solvent extraction stage meant that virtually all Fe^{3+} was removed after three extractions. The remaining solution was then taken close to dryness on a hotplate and the residue was taken up in 50 ml of reverse osmosis water. Care must be taken to ensure that all the acid has been boiled off but also that the residue is not over-dried. If either of these situations occurs it can affect the plating of polonium. 5 ml of 30 % hydroxyl ammonium chloride solution ($NH_2OH.HCl$) was added to the plating solution. Po isotopes were then spontaneously deposited onto 1 cm^2 copper foils and counted by α spectrometry (Section 2.4.3.2).

4.2.4 Gamma spectrometry

Samples were prepared for analysis of the NDS nuclides, ^{210}Pb and ^{226}Ra and the anthropogenic nuclide ^{137}Cs. This was achieved by preparing pellets of sediment from each section. The higher sample resolution at the top of the core required three different sample geometries to be used, with weights of 5 g, 10 g and 20 g respectively. The pellets were prepared by adding the sediment to a hydraulic press and compressing at 10 tonnes pressure

for 60 seconds. The pellets were placed in polycarbonate containers which were then sealed with epoxy resin before being stored for 4 weeks to allow ^{222}Rn (and progeny) to ingrow from the decay of ^{226}Ra. Each pellet was inspected to ensure the seal was complete.

The energy-channel number calibration of the γ spectrometers was carried out with a ^{155}Eu source. The efficiency calibration was preformed by creating spiked standards using the sediment collected from the bottom of the core which had previously been analysed by γ spectroscopy to establish background levels. 5, 10 and 20 g samples of this sediment were individually spiked with 35 Bq ^{137}Cs, 23 Bq ^{226}Ra and 100 Bq ^{210}Pb and prepared in the same manner as samples. Although this technique is more time consuming than using mixed γ standard sources, it accounts for self-adsorption of the γ photons by the sample. This is especially important for the low energy γ photons of ^{210}Pb ($E\gamma = 46.5$ keV).

4.3 Results

The results for the three cores are presented in Tables 4.2, 4.3 and 4.4. The results are quoted as Bq kg^{-1} (dry) and have been corrected for the presence of salt (Swan *et al.*, 1982). Errors are quoted at the 1 sigma (1σ) level of significance. The sediment profiles are illustrated in Figures 4.3 to 4.8. The cumulative dry mass (g cm^{-2}) has been used for the horizontal scale. This compensates for sediment compaction when sedimentation rates are derived (Huh *et al.* 1987).

Core 1 Depth	^{210}Po (Bq kg^{-1})	±	^{210}Pb (Bq kg^{-1})	±	^{226}Ra (Bq kg^{-1})	±	^{137}Cs (Bq kg^{-1})	±
0 - 1	408.3	18.6	390.2	0.8	61.6	9.4	85.2	1.9
1 - 2	446.2	17.5	437.9	0.7	47.1	7.8	94.7	2.2
2 - 3	403.8	18.3	431.9	0.7	65.6	9.4	98.1	2.0
3 - 4	461.3	24.0	450.0	1.0	66.7	8.1	103.8	2.6
4 - 5	424.9	21.8	430.0	1.2	48.0	7.4	92.2	2.9
5 - 6	390.0	24.4	400.0	1.3	44.9	9.3	98.0	2.9
6 - 7	378.1	16.8	375.2	1.0	60.6	12.2	95.1	2.9
7 - 8	378.5	12.8	364.1	1.0	45.3	10.3	109.8	3.1
8 - 9	336.0	11.6	342.4	1.1	43.2	7.6	120.5	3.4
9 - 10	338.9	13.7	340.1	1.1	41.8	6.4	134.4	3.3
10 - 12	323.0	12.3	315.4	2.0	32.5	4.0	169.1	2.4
12 - 14	275.4	11.5	282.7	2.0	32.8	5.1	195.1	2.6
14 - 16	255.5	9.4	265.1	2.7	30.1	3.9	192.4	2.6
16 - 18	212.3	8.7	217.0	6.0	30.7	3.7	171.8	2.4
18 - 20	180.0	12.2	185.4	4.2	57.7	7.8	141.8	2.6
20 - 22	156.8	7.9	157.6	6.1	63.5	7.5	125.9	2.3
22 - 24	193.2	10.8	142.3	6.0	66.4	10.2	105.8	2.7
24 - 26	135.0	8.5	130.1	6.1	64.9	8.1	68.5	2.0
26 - 28	129.4	7.3	122.5	18.6	62.1	6.9	55.9	1.9
28 - 30	119.3	8.5	123.5	39.2	60.1	5.8	45.6	0.9
30 - 35	90.8	4.8	81.0	40.0	59.3	7.2	22.7	1.1
35 - 40	26.8	1.5			59.2	10.5	10.3	1.3
40 - 45	13.1	1.3			59.5	5.9		
45 - 50	16.6	1.2			62.0	7.4	6.2	1.7
50 - 55	24.2	1.7			61.4	7.3	4.1	1.0
55 - 60					58.7	7.3		
60 - 65					30.8	3.3	1.7	0.6
65 - 70					31.6	4.4		
70 - 75					60.5	4.2		
75 - 80					56.8	9.2		
80 - 95					56.9	4.0		

Table 4.2: Specific activities observed in Loch Etive Core One. All activities are in Bq kg^{-1} dry and errors quoted at the 1σ level of significance.

Core 2 Depth	^{210}Po (Bq kg^{-1})	±	^{210}Pb (Bq kg^{-1})	±	^{226}Ra (Bq kg^{-1})	±	^{137}Cs (Bq kg^{-1})	±
0 - 1	290.3	12.4	245.2	3.0	200.3	19.2	72.7	2.0
1 - 2	466.6	37.6	266.3	1.7	130.9	12.4	81.7	3.2
2 - 3	304.5	14.2	206.4	3.4	99.8	14.1	80.7	2.9
3 - 4	291.3	10.0	211.1	3.0	115.0	18.6	91.3	3.1
4 - 5	265.3	12.9	238.9	2.5	88.3	12.7	93.8	3.0
5 - 6	287.9	12.3	218.4	2.7	110.6	21.3	100.0	2.7
6 - 7	270.4	15.9	269.7	2.1	116.0	12.9	95.6	2.8
7 - 8	263.3	12.6	266.3	1.9	109.7	13.2	106.9	2.8
8 - 9	251.7	15.8	205.0	2.4	106.4	10.2	114.4	2.3
9 - 10	203.3	11.8	187.4	3.6	129.1	18.5	128.5	3.6
10 - 12	311.4	16.2	134.4	4.7	78.0	10.3	131.5	2.5
12 - 14	160.2	9.3	126.5	5.8	69.9	9.6	125.7	2.3
14 - 16	145.3	8.1	130.0	3.6	70.9	7.4	126.4	2.0
16 - 18	146.3	5.5	150.0	5.2	79.7	16.7	131.0	3.0
18 - 20	137.2	6.4	128.3	5.6	79.3	10.3	130.4	1.9
20 - 22	114.6	6.1	114.2	6.9	75.3	11.0	113.6	1.9
22 - 24	108.9	4.7	78.9	12.7	77.8	10.9	103.5	2.0
24 - 26	36.1	2.9	97.0	9.7	80.4	12.0	102.4	1.7
26 - 28	96.7	4.6	85.2	12.6	72.1	10.7	87.8	2.6
28 - 30	76.5	4.6	69.1	14.6	70.5	7.2	60.2	1.5
30 - 35	48.0	3.0	44.9	33.3	63.6	9.5	45.4	1.7
35 - 40	107.0	5.8			63.4	5.7	14.4	1.2
40 - 45	41.9	2.7			67.6	8.2	24.7	1.1
45 - 50	23.3	2.4			72.9	11.3		
50 - 55					76.7	11.7		
55 - 60					74.0	11.0		
60 - 65					33.3	4.7		
65 - 70					34.5	4.5		
70 - 75					36.2	7.6		
75 - 80					68.2	7.1		

Table 4.3: Specific activities observed in Loch Etive Core Two. All activities are in Bq kg^{-1} dry and errors quoted at the 1σ level of significance.

Core 3 Depth	^{210}Po (Bq kg^{-1})	±	^{210}Pb (Bq kg^{-1})	±	^{226}Ra (Bq kg^{-1})	±	^{137}Cs (Bq kg^{-1})	±
0 - 1	377.7	19.2	468.6	5.0	332.9	27.0	130.1	6.0
1 - 2	412.5	20.4	503.8	5.1	409.7	28.5	113.5	5.7
2 - 3	453.2	27.9	471.1	3.1	307.5	14.7	100.4	2.2
3 - 4	387.0	17.3	389.0	3.2	276.8	23.7	116.7	3.5
4 - 5	375.7	22.4	348.8	4.8	173.2	17.0	134.9	4.5
5 - 6	292.8	18.6	305.8	5.3	135.4	23.4	133.9	4.6
6 - 7	295.2	16.9	291.4	4.6	123.3	18.3	115.4	4.0
7 - 8	216.7	13.1	256.8	5.1	120.9	18.4	107.9	3.6
8 - 9	191.7	11.2	225.6	6.8	134.1	21.9	100.1	3.4
9 - 10	201.6	10.2	176.9	7.7	130.5	17.8	93.2	3.3
10 - 12	166.3	10.0	127.6	7.8	78.4	7.3	75.1	2.1
12 - 14	139.2	8.4	171.8	5.0	79.5	7.5	57.8	2.0
14 - 16	82.4	7.6	65.9	15.0	83.2	10.7	47.0	2.1
16 - 18	93.6	4.6	85.2	11.2	84.4	11.5	47.0	1.8
18 - 20	74.1	9.0	50.6	20.0	83.1	12.4	44.9	1.8
20 - 22	81.1	4.1	44.0	19.1	84.5	9.8	40.7	1.7
22 - 24	135.1	9.4	59.9	14.1	76.4	9.4	38.5	1.8
24 - 26	80.9	4.9	79.1	10.4	80.9	11.1	40.5	2.2
26 - 28	63.7	3.3	40.6	15.2	87.3	4.9	33.9	1.7
28 - 30	65.2	3.5	30.8	18.4	87.3	8.8	33.7	1.5
30 - 35	55.5	3.1			89.7	5.1		
35 - 40	42.1	2.8			69.0	5.7		
40 - 45	43.7	3.1			110.6	8.1		
45 - 50	37.0	2.9			99.5	8.5		
50 - 55					96.8	5.0		
55 - 60					84.2	5.0		
60 - 65					69.1	8.9		
65 - 70					69.8	6.9		
70 - 75					47.0	6.4		
75 - 80					128.4	7.5		

Table 4.4: Specific activities observed in Loch Etive Core Three. All activities are in Bq kg^{-1} dry and errors quoted at the 1σ level of significance.

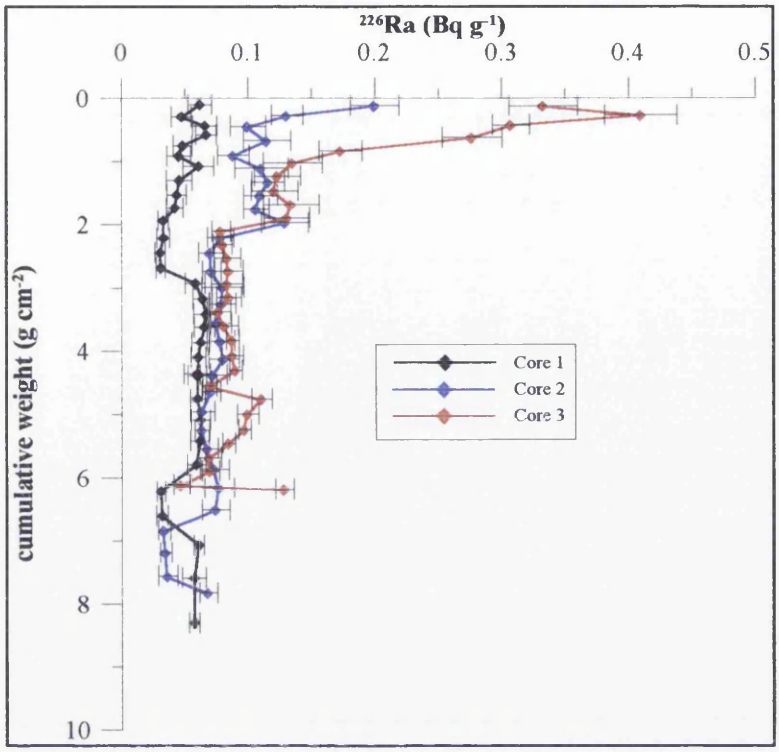

Figure 4.3: ^{226}Ra activities in Loch Etive sediment cores.

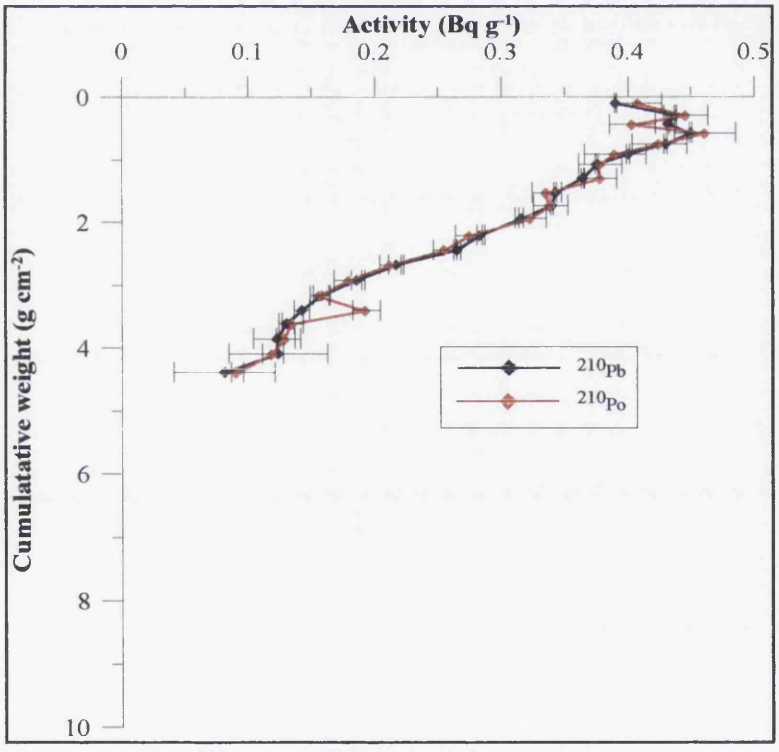

Figure 4.4: ^{210}Po and ^{210}Pb activities in core 1.

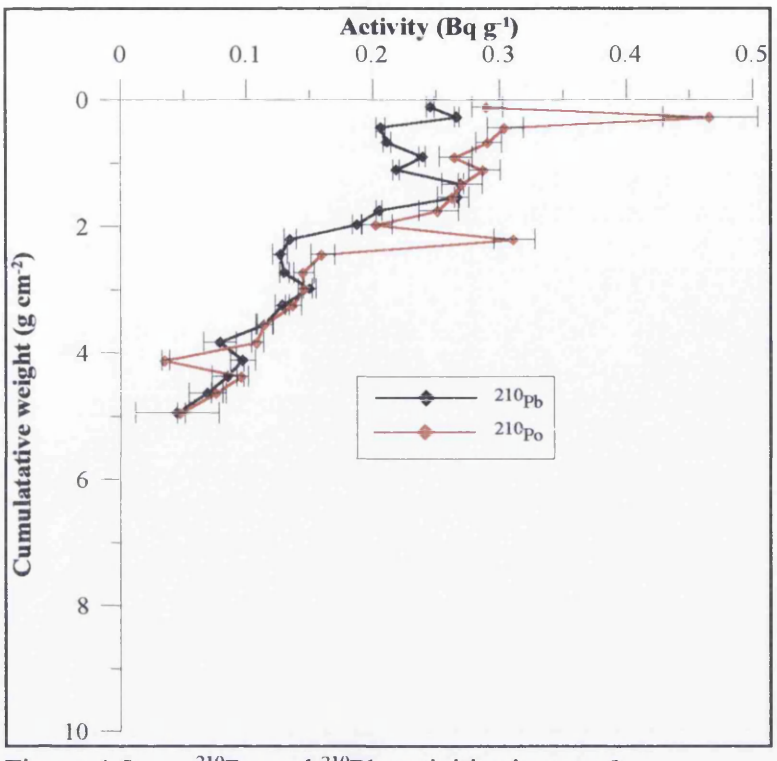

Figure 4.5: ^{210}Po and ^{210}Pb activities in core 2.

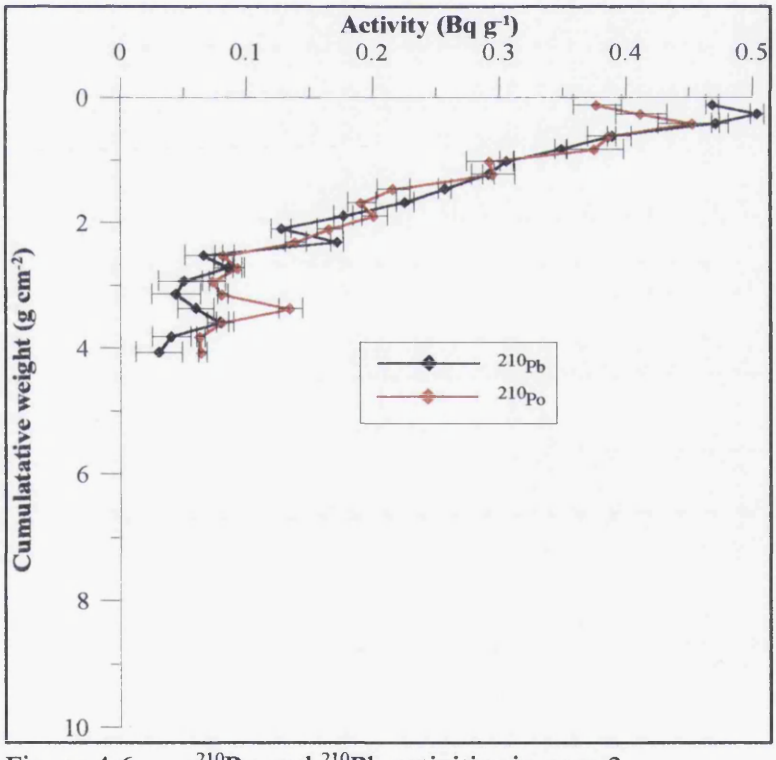

Figure 4.6: ^{210}Po and ^{210}Pb activities in core 3.

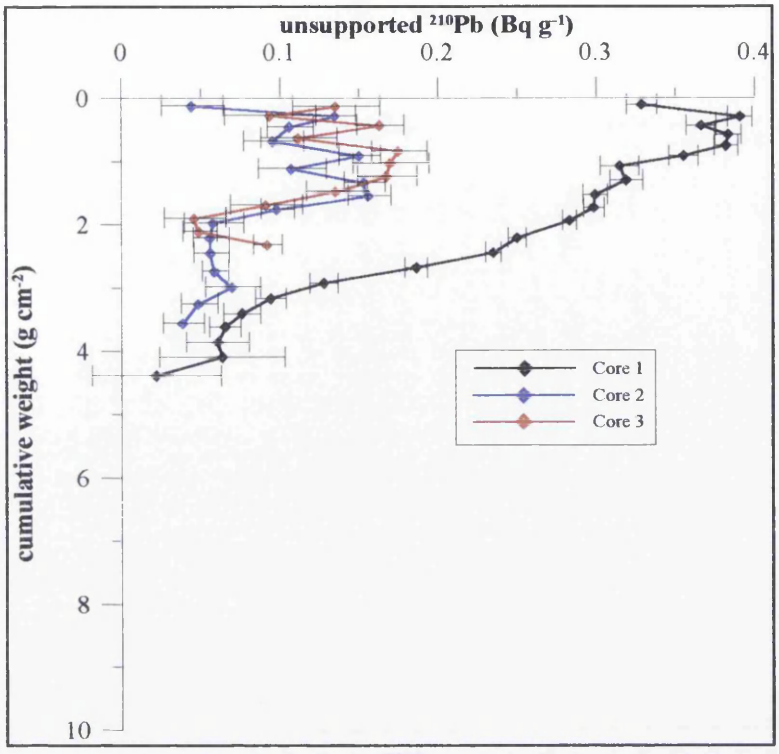

Figure 4.7: Unsupported ^{210}Pb activities in Loch Etive sediment cores.

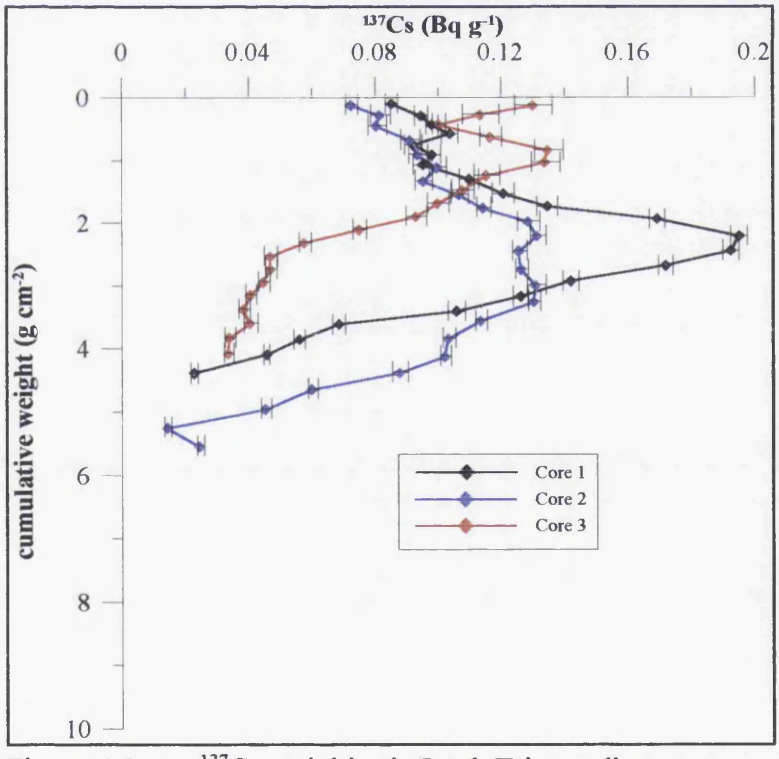

Figure 4.8: ^{137}Cs activities in Loch Etive sediment cores.

4.4 Discussion

4.4.1 ^{226}Ra

Measurements of ^{226}Ra were carried out to determine the supported fraction of ^{210}Pb and subtraction of the supported ^{210}Pb from the total ^{210}Pb yields the unsupported ^{210}Pb in the sediment. The unsupported ^{210}Pb results from: (i) atmospherically introduced ^{210}Pb; (ii) produced by decay of ^{226}Ra in solution in seawater; (iii) advective movement of dissolved ^{210}Pb in seawater; or (iv) added by introduction of suspended particulate matter in seawater or river water. ^{210}Pb is then is scavenged in the water column and removed to the sediment by sinking particles. The ^{226}Ra inventories (Table 4.5) do not show any major differences, indicating that the supply from the water column is fairly constant for the two basins. However, the surface enrichment of ^{226}Ra in core 3 (and to a lesser extent in core 2) may indicate redox driven cycling of metals in the inner basin, resulting from the anoxic conditions at this location. Similar ^{226}Ra surface enrichment in anoxic sediments has been observed by Kadko *et al.* (1987) who suggested that such enrichment is a result of Mn re-mobilization in anoxic sediments. Williams *et al.* (1987) observed up to 4 % Mn in the surface sediments. Core 3 receives a larger input of organic matter, Fe and Mn from the River Etive than core 2 (Overnell *et al.*, 1996) which may result in stronger redox conditions at this site and could explain the larger surface enrichment of ^{226}Ra in core 3. Thus the high sediment Mn concentrations, combined with anoxic conditions, would result in the observed profile. The ^{226}Ra profile of core 2 is intermediate between core 1 (oxic) and core 3 (anoxic). Metal analysis of the cores would provide more evidence for the redox driven redistribution of ^{226}Ra but this work was beyond the timescale of this research. However,

similar ^{226}Ra profiles were observed by Shimmield (1993) for sediment cores collected in close proximity to this study.

Location	Unsupported ^{210}Pb (Bq cm^{-2})	^{226}Ra (Bq cm^{-2})	^{137}Cs (Bq cm^{-2})
Core 1	1.303	1.869	0.841
Core 2	0.413	1.557	0.914
Core 3	0.303	1.615	0.414

Table 4.5: Sediment inventories (Bq cm^{-2}) for the three cores collected from Loch Etive.

4.4.2 ^{210}Po and ^{210}Pb

The profiles of total ^{210}Pb and ^{210}Po for the three cores are shown in Figures 4.4, 4.5 and 4.6. In core 1 the profiles of ^{210}Po and ^{210}Pb are virtually identical. This would be expected in an oxic sediment where sufficient time has elapsed for secular equilibrium to be established. On this basis, ^{210}Po has been measured as a proxy for ^{210}Pb activity (Carpenter *et al.*, 1981; Smoak *et al.*, 1996; Sanchez-Cabeza *et al.*, 1999). The profiles obtained from cores 2 and 3 show a degree of disequilibria between ^{210}Po and ^{210}Pb. The top 5 cm of core 2 shows an excess of ^{210}Po compared to its parent ^{210}Pb, while in core 3 there is an excess of ^{210}Pb over ^{210}Po. This may suggest that the anoxic conditions which can exist in both the water column and the sediment of this basin have led to re-mobilization of ^{210}Po and/or ^{210}Pb from the sediments into the water column (Benoit and Hemmond, 1987; Wei and Murray, 1994; Balistrieri *et al.*, 1995; Nozaki *et al.*, 1997; Swarzenski *et al.*, 1999). In oxic conditions, Balistrieri *et al.* 1995 observed Pb and Po to be linked to the cycling of Fe and Mn, respectively, in a seasonally anoxic lake (Lake Sammamish, USA). During times of anoxia

the behavior of Pb (and possibly Po) was influenced by the sulphur cycle. The variation between ^{210}Pb and ^{210}Po profiles between cores 2 and 3 may also be a result of the variation in degree of anoxia between the two core sites (Overnell *et al.*, 1996) although more study is required to interpret these profiles. Measurements of ^{210}Po, ^{210}Bi and ^{210}Pb in the bottom waters in conjunction with sediment studies, as had initially been intended, might allow a better understanding of these redox driven distributions. Application of the methods described in Chapter 3 would allow further insights to the dynamics of the ^{210}Pb/^{210}Bi/^{210}Po geochemical system in anoxic basins. What can be drawn from these data is that relying on measurements of ^{210}Po to infer the ^{210}Pb activity in oxic sediments may be valid, but these profiles suggest that this methodology is not suitable for anoxic sediments.

4.4.2.1 Unsupported ^{210}Pb

Sediment accumulation rates are often derived from ^{210}Pb derived chronologies (Koide *et al.*, 1972; Robbins and Edginton, 1975; Appleby and Oldfield, 1978). The unsupported ^{210}Pb profiles for the three sediment cores are shown in Figure 4.7. The striking feature of the unsupported ^{210}Pb activity profiles is the similarity between cores 2 and 3 and their contrast to core 1. The inventories of un-supported ^{210}Pb are shown in Table 4.5. The larger inventory of core 1 may be a result of lateral advection of dissolved ^{210}Pb into the outer basin from the open sea (Krishnaswami *et al.*, 1975; Carpenter *et al.*, 1981; DeMaster *et al.*, 1986). The sill at Bonawe restricts the water movement into the inner basin which may result in much of the ^{210}Pb being removed in the outer basin. Another possible cause of this distribution may be sediment focusing. Williams *et al.* (1987) observed a decrease

in surface sediment organic matter from landward to seaward end of Loch Etive and found a correlation (r^2 = 0.85) between ^{210}Pb and the sediment organic content. There was considerable variation of both ^{210}Pb and organic carbon in the surface sediments and the area of sediment high in organic carbon may act as sites of preferential ^{210}Pb scavenging.

The unsupported ^{210}Pb data were used to calculate sediment accumulation rates. The assumptions in this technique are that the supply of ^{210}Pb is constant, that there is no post-depositional mobilization of ^{210}Pb and that bioturbation is minimal (Swan *et al.*, 1982). The sediment accumulation rates were calculated below the zone of mixed sediment (below ~ 1.5 g cm^{-2}). The sedimentation rates and the coefficient of determination (r^2) are shown in Table 4.6.

Location	**^{210}Pb derived sedimentation rate (g cm^{-2})**	**Coefficient of determination r^2**
Core 1	0.034	0.93
Core 2	0.038	0.83
Core 3	0.014	0.68

Table 4.6: ^{210}Pb derived sedimentation rates calculated for Loch Etive sediment cores.

Ridgway and Price (1987) calculated ^{210}Pb sediment chronologies for the inner and outer basins of Loch Etive. To compare their values with those obtained during this research the ^{210}Pb sedimentation rates were also calculated as cm y^{-1} (i.e. without accounting for compaction of the sediment) and are displayed in Table 4.7. The oxic sediments of core 1

agrees with previous estimates of sedimentation rates in the outer basin of Loch Etive. The sedimentation rate for the inner basin shows a much larger variation. This may be attributed to variation in sediment mineralogy (Baskaran and Naidu, 1995) or sediment focusing (Shimmield, 1993) resulting in variation in the unsupported ^{210}Pb distribution.

	This study (cm y^{-1})	**Coefficient of determination (r^2)**	**Ridgway and Price (1987) (cm y^{-1})**
Core 1	0.29	0.95	0.33
Core 2	0.26	0.81	0.86
Core 3	0.08	0.57	

Table 4.7: Sedimentation rates based on ^{210}Pb chronology for Loch Etive sediment cores and the coefficient of determination for each value.

4.4.3 ^{137}Cs

^{137}Cs is an anthropogenic radionuclide released to the environment from weapons testing in the 1950s and more recently from nuclear fuel reprocessing plants and, to a lesser extent, from nuclear reactors. ^{137}Cs input to the environment also occurred from the Chernobyl incident in 1986. ^{137}Cs exists in the aquatic environment as a monovalent cation and exhibits conservative behavior in seawater (Livingston and Bowen, 1979; Swan *et al.*, 1982). The dominant ^{137}Cs input to Loch Etive is from the liquid effluent discharges to the Irish Sea from BNFL's Sellafield plant. McKinley *et al.* (1981) observed a plume of ^{137}Cs contaminated seawater migrating northwards from the Irish Sea close to the West coast of Scotland. Loch Etive sediments can therefore be expected to display measurable activities of ^{137}Cs. Current ^{137}Cs discharge from Sellafield are 9.12 TBq y^{-1} and the maximum

discharge was around 1974 when approximately 5000 TBq y^{-1} was discharged to sea (Shimmield, 1993). In a previous study of Loch Etive sediments, Ridgway and Price (1987) used the onset of ^{137}Cs to derive their sediment chronology. Their assumption that the first observation of ^{137}Cs indicated the first discharges from Sellafield requires no mobility of ^{137}Cs in the sediment. However, Sholkovitz *et al.* (1983) suggest that ^{137}Cs may be significantly mobile in marine sediments. Thus the first observation of ^{137}Cs may represent diffusion of ^{137}Cs down the core and thus result in an over-estimation of ^{137}Cs derived sedimentation rates.

The sediment accumulation rates calculated for this study are therefore based on the sub-surface maximum in ^{137}Cs activity representing the peak Sellafield discharge. Assuming a 1 year transit time from discharge at Sellafield to removal to Loch Etive sediment (Livingston and Bowen, 1977; McKinley *et al.*, 1981) then the peak ^{137}Cs input would occur at around 1975. The profiles of ^{137}Cs activity in the sediments of Loch Etive are presented in Figure 4.8. If sediment accumulation rates are based on ^{137}Cs, the mixed layer that occurs down to depths of ~ 1.5 g cm^{-2} should be ignored as Shimmield (1993) observed Chernobyl derived ^{137}Cs to become mixed to several cm in a few months. Cores 1 and 2 have a sedimentation rate of around 0.3 g cm^2 y^{-1} which is in excellent agreement with the ^{210}Pb derived chronologies (Table 4.8). The ^{210}Pb derived chronology for core three was 0.014 g cm^{-2} and therefore the slower sedimentation rate results in Sellafield derived ^{137}Cs subsurface peak occurring in the mixed zone. Shimmield (1993) obtained sediment cores from similar locations to this study and the ^{137}Cs derived chronologies are similar for the

inner basin.

	^{137}Cs derived sedimentation rate (g cm^{-2})		^{210}Pb derived sedimentation rate (g cm^{-2})
	This study	**Shimmield (1993)**	**This study**
Core 1	0.032-0.041	0.1	0.034
Core 2	0.032-0.067	0.04-0.07	0.038
Core 3	ND	0.06	0.014

Table 4.8: ^{137}Cs derived chronologies for Loch Etive sediment cores from this study and from Shimmield (1993). The locations of Shimmield's cores are almost identical to those of the cores this study. Chronology based on salt corrected cumulative weight assuming peak Sellafield discharge in 1974 and a 1 year transit time.

4.5 Conclusions

In the surface sediments of the inner basin there is disequilibrium between ^{210}Pb and ^{210}Po which suggests recycling of ^{210}Po and/or ^{210}Pb into the water column. In core two, an excess of ^{210}Po was found in the top layers of sediment which may suggest that Pb is re-mobilized from anoxic sediments while in core 3 an excess of ^{210}Pb (over ^{210}Po) exists. The strong redox chemistry of the inner basin results in a modified ^{226}Ra profile.

There is excellent agreement between ^{210}Pb and ^{137}Cs derived chronologies for the sediment cores. Using an independent time-stratigraphic marker, such as ^{137}Cs, confirms the accuracy of the ^{210}Pb derived chronology (Smith, 2001).

These sediment cores highlight the usefulness of NDS and anthropogenic radionuclide in the study of natural processes. Analysis of the ^{210}Pb and ^{210}Po distribution of the bottom waters may help to gain a fuller understanding of the biogeochemical cycling of Loch Etive. If the method developed during the course of this research is applied to such a setting it will allow ^{210}Pb, ^{210}Bi and ^{210}Po to be determined. Not only will this improve the understanding of the biogeochemistry of metal cycling in seasonally anoxic basins but may also provide information on the rates of processes occurring on a range of timescales and have implications on the fate of pollutants in such a region. Such a study would also provide information on organic versus inorganic scavenging over periods of variable biological production.

Chapter Five: Conclusions

A new method for the determination of ^{210}Pb and ^{210}Po in the dissolved and particle-associated phases of seawater has been successfully developed. It allows determination of ^{210}Po and ^{210}Pb in around 10 days compared up to one year using ingrowth of ^{210}Po, or six weeks using ingrowth of ^{210}Bi, to determine ^{210}Pb activity. The method also allows determination of ^{210}Bi activities in the same sample which allows rates of processes occurring on short (up to 20 days) timescales to determined.

Different methods were examined to find the best technique to determine ^{210}Pb and ^{210}Po activities in seawater. The complexity of the sample matrix and the very low activities of ^{210}Po and ^{210}Pb in seawater require pre-concentration and a high degree of purification before counting. To achieve this, the best techniques were found to be via an $Fe(OH)_3$ pre-concentration stage and purification on Sr Spec resin.

The requirement of a pre-concentration step results in variable recovery and as a result yield tracers must be applied in the determination. The only Po isotopes suitable as yield tracers had α energies too close to that of ^{210}Po to be suitably resolved by LSS. Therefore ^{210}Po determination utilised α spectrometry to count both ^{210}Po and its yield tracer, ^{208}Po. ^{212}Pb was utilised as a tracer for ^{210}Pb. ^{212}Pb is a useful Pb yield tracer as it is readily available as part of the ^{232}Th decay series and can be milked from a Th solution to provide an inexpensive and virtually inexhaustible source of ^{212}Pb tracer. Furthermore, its short half life ($t_{½}$ = 10.6

hours) causes its complete decay from the Pb fraction after around 10 days. ^{207}Bi was utilised as a tracer for ^{210}Bi. Future development of this method will allow ^{234}Th and ^{238}U to be determined simultaneously with ^{210}Pb, ^{210}Bi and ^{210}Po. This will allow rates of processes occurring on a range of timescales to be determined.

The application of the new method to a study of nearshore scavenging processes in the Irish Sea allowed final changes to be made to the method to further purify Pb, Bi and Po from both anthropogenic and NDS radionuclides present in the sample. The results of this sampling showed that the method could be successfully applied to studies of nearshore marine scavenging and produced similar values of ^{210}Pb and ^{210}Po to those already reported for the nearshore environment. Model calculation for the residence times of dissolved ^{210}Pb, ^{210}Bi and ^{210}Po were carried out and the steady-state box model which accounts for atmospheric ^{210}Po inputs was found to be most suitable. This produced dissolved residence times of 18 to 76 days for ^{210}Pb, 0.82 days for ^{210}Bi and 6 to 32 days for ^{210}Po.

The methodology provides a high degree of selectivity for Pb, Bi and Po and is therefore suitable for application in areas where there is considerable contamination from anthropogenic radionuclides which makes it a useful method for determination of removal times of particle reactive radionuclides resulting from the nuclear fuel cycle. However, the application of larger samples volumes in future studies would allow lower limits of detection than those obtained with 20 litre samples. This is especially important in the nearshore environment where the observed activities are much lower than the open ocean.

A series of sediment cores from Loch Etive were also analysed for NDS and anthropogenic radionuclides. This study highlighted the possible mobilization of ^{210}Pb and ^{210}Po in seasonally anoxic basins. Application of the new methodology to this location may provide information on the rates of particle scavenging in such locations which has implications on the fate of particle reactive pollutants.

Finally, this research highlights the usefulness of liquid scintillation spectrometry in radiochemical method development. By producing a spectra for each sample allows the analyst to observe any contamination from α, β^- or γ emitting radionuclides. This was especially important in the purification of ^{210}Bi and ^{212}Pb.

References

Adu, J. K. and Oades, J. M. 1974. Suspension counting of ^{14}C in soil, soil extracts and plant materials by liquid scintillation counting. In: Stanley, P. E. and Scroggins, B. A., eds., *Liquid Scintillation Counting: Recent Developments.* New York. Academic Press: 207-221.

Ageno, M., Chiozzotto, M. and Querzolii, R. 1950. Scintillations in liquids and solutions. *Physical Review* **79**: 720.

Alessio, M., Allegri, L., Bella, F. and Improta, S. 1976. Study of background characteristics by means of high efficiency liquid scintillation counter. *Nuclear Instruments and Methods* **137**: 537-543.

Aller, R. C. and DeMaster, D. J. 1984. Estimates of particle flux and reworking at the deep sea floor using $^{234}Th/^{238}U$ disequilibrium. *Earth and Planetary Science Letters* **67**: 308-318.

Appleby, P. G. and Oldfield, F. 1978. The calculation of ^{210}Pb dates assuming a constant rate of supply of unsupported ^{210}Pb to the sediment. *Catena* **5**: 1-8.

Bacon, M. P., Spencer, D. W. and Brewer, P.G. 1976. $^{210}Pb/^{226}Ra$ and $^{210}Po/^{210}Pb$ disequilibria in seawater and suspended particulate matter. *Earth and Planetary Science Letters* **32**: 277-296.

Bacon, M. P. and Elzerman, A. M. 1980. Enrichment of ^{210}Po and ^{210}Pb in the sea-surface micro-layer. *Nature* **284**: 332-334.

Bacon, M. P. and Anderson, R. F. 1982. Distribution of thorium isotopes between dissolved and particulate forms in the deep sea. *Journal of Geophysical Research* **87**: 2045-2056.

Bacon, M. P., Belastock, R. A., Tecotsky, M., Turekian, K. K. and Spencer, D. W. 1988. Lead-210 and polonium-210 in the ocean water profiles of the continental shelf and slope south of New England. *Continental Shelf Research* **8**: 841-853.

Bagnall, K. W. 1957. *Chemistry of the Rare Radioelements.* Academic Press Inc. New York: 94p.

Balistrieri, L., Murray, J. W. and Paul, B. 1995. The geochemical cycling of stable Pb, ^{210}Pb and ^{210}Po in seasonally anoxic Lake Sammamish, Washington, USA. *Geochimica et Cosmochimica Acta* **59** (23): 4845-4861.

Baskaran, M. and Naidu, A, S. 1995. ^{210}Pb-derived chronology and the fluxes of ^{210}Pb and ^{137}Cs isotopes into continental shelf sediments, East Chukchi Sea, Alaskan Arctic. *Geochimica et Cosmochimica Acta* **59** (21): 4435-4448.

BEIR (1990). *Health Effects of Exposure to Low Levels of Ionizing Radiation.* Committee on the Biological Effects of Ionising Radiation. BEIR-V. National Research Council. National Academy Press. Washington, D.C: 128 p.

Benitez-Nelson, C. R. and Buesseler, K. O. 1997. Measurement of cosmogenic ^{32}P and ^{33}P activities in rainwater and seawater. *Analytical Chemistry* **70**: 64-72.

Benninger, L. K. 1978. ^{210}Pb balance in Long Island Sound. *Geochimica et Cosmochimica Acta* **42**: 1165-1174.

Benoit, G. and Hemmond, H. F. 1987. A biogeochemical mass balance of ^{210}Po and ^{210}Pb in an oligotrophic lake with seasonally anoxic hypolimnion. *Geochimica et Cosmochimica Acta* **51**: 1445-1456.

Blanchard, R. L. 1966. Rapid determination of Lead-210 and Polonium-210 in environmental samples by deposition onto Nickel. *Analytical Chemistry* **38**: 189-197.

Bojanowski, R., Fukai, R., Ballestra, S. and Asari, H. 1983. Determination of natural radioactive elements in marine environmental materials by ion-exchange and alpha spectrometry. Proceedings of the 4th Symposium on Determination of Radionuclides in Environmental and Biological Materials, Laboratory of the Government Chemist, London, Paper No 9.

Boyle, E. A. and Edmund, J. M. 1975. Determination of trace metals in aqueous solution by APDC chelate co-precipitation. In: Gibbs, T. R. P., ed., *Analytical Methods in Oceanography.* Am. Chem. Soc. Adv. Chem. Ser. 147: 44-45.

Bricout, R. 1994. Amelioration du dosage du strontium90 dans les vegeaux, le lait et les sols. DCE-S/UGSP/SRSE/94-291/SB: 37p.

Broecker, W. S., Li, Y. H. and Cromwell, J. 1967. Radium-226 and radon-222 concentrations in Atlantic and Pacific Oceans. *Science* **158**: 1307-1310.

Brown, L., Cook, G. T., MacKenzie, A. B., Thomson, J. and Nixon, S. 1999. Radionuclide tracers of contaminant fate in the N.E. Atlantic. *Environmental Geochemistry and Health* **21** (4): 323-329.

Buessler, K. O. 1991. Do upper-ocean sediment traps provide an accurate record of particle flux? *Nature* **353**: 420-423.

Buesseler, K. O., Andrews, J., Hartman, M., Belastock, R. and Chai, F. 1995. Regional estimated of the export flux of particulate organic carbon derived from thorium-^{234} during the JGOFS EqPaC program. *Deep-Sea Research II* **42**: 777-804.

Burnett, W. C. and Tai, W.-C. 1992. Determination of radium in natural waters by alpha liquid scintillation. *Analytical Chemistry* **64**: 1691-1697.

Carpenter, R., Bennett, J. T. and Peterson, M. L. 1981. ^{210}Pb activities in and fluxes to sediments off the Washington continental slope and shelf. *Geochimica et Cosmochimica Acta* **45**: 1155-1172.

Carvalho, F. P. 1995. ^{210}Pb and ^{210}Po in sediments and suspended matter in the Tagus estuary, Portugal. Local enhancements of natural levels by wastes from phosphate ore processing industry. *The Science of the Total Environment* **159**: 201-214.

Carvalho, F. P. 1997. Distribution, cycling and mean residence time of ^{226}Ra, ^{210}Pb and ^{210}Po in the Tagus estuary. *The Science of the Total Environment* **196**: 151-161.

Case, G. N. and McDowell, W. J. 1982. An improved sensitive assay for polonium-210 by use of a background rejecting extractive liquid scintillation method. *Talanta* **29**: 845-848.

Chakravarty, R. and Van Grieken, R. 1982. Concentration of trace metals with $Fe(OH)_3$. *Journal of Environmental Analytical Chemistry* **11**: 67-76.

Chalupnik, S. and Lebecka, J. M. 1990. Determination of radium isotopes in water samples by means of a low background liquid scintillation spectrometer. Quantulus. In: Povince, P., ed., *Rare Nuclear Processes.* World Scientific. Singapore: 327-335.

Chalupnik, S. and Lebecka, J. M. 1993. Determination of ^{226}Ra, ^{228}Ra and ^{224}Ra in water and aqueous solutions by liquid scintillation counting. In: Noakes, J. E., Schönhofer, F. and Polach, H. A., eds., *Liquid Scintillation Spectrometry 1992.* Radiocarbon. Arizona: 397-403.

Chester, R. 1990. *Marine Chemistry.* Unwin Hyman. London: 698p

Choppin, G. R. 1994. *Radiochemistry and Nuclear Chemistry.* Pergamon Press. New York: 693p.

Chung, Y., Finkel, R., Bacon, M. P., Cochran, J. K. and Krishnaswami, S. 1983. Intercomparision of ^{210}Pb measurements at GEOSECS station 500 in the northeast Pacific. *Earth and Planetary Science Letters* **65**: 393-405.

Chung, Y. and Craig, H. 1983. ^{210}Pb in the Pacific: the GEOSECS measurements of particulate and dissolved concentrations. *Earth and Planetary Science Letters* **65**: 406-432.

Church, T .M., Hussain, N., Ferdelman, T. G. and Fowler, S. W. 1994. An efficient quantitative technique for the simultaneous analysis of radon daughters ^{210}Pb, ^{210}Bi and ^{210}Po. *Talanta* **41** (2): 243-249.

Clark, S. B. 1995. Separation and determination of radiostrontium in calcium carbonate matrices of biological origin. *Journal of Radioanalytical and Nuclear Chemistry Articles* **194** (2): 297-302.

Coale, K. H. and Bruland, K. W. 1985. ^{234}Th/^{238}U disequilibrium within the California Current. *Limnology and Oceanography* **32** (1): 189-200.

Cochran, J. K. and Krishnaswami, S. 1980. Radium, thorium, uranium and ^{210}Pb in deep-sea sediments and sediment porewaters from the north equatorial Pacific. *American Journal of Science* **9**: 739-747.

Cochran, J. K., Bacon, M. P., Krishnaswami, S. and Turekian, K. K. 1983. ^{210}Po and ^{210}Pb distributions in the central and eastern Indian Ocean. *Earth and Planetary Science Letters* **65**: 433-452.

Cochran, J. K. 1992. The oceanic chemistry of the uranium- and thorium- series nuclides. In: Ivanovitch, M. and Harmon, R. S., eds., *Uranium-series disequilibrium: Application to Earth, Marine and Environmental Sciences, 2nd ed.* Clarendon Press. Oxford: 384-430.

Cook, G. T. and Anderson, R. A. 1991. The determination of ^{241}Pu by liquid scintillation spectrometry using the Packard 2250CA. *Journal of Radioanalytical and Nuclear Chemistry, Letters* **154** (5): 319-330.

Cook, G. T., Harkness, D. D. and Anderson, R. 1991. Performance of the Packard 2000CA/LL and 2250 CA/XL liquid scintillation counters for ^{14}C dating. *Radiocarbon* **31** (3): 352-358.

Cooper, E. L., Cox, J. M. and Workman, W. J. 1998. Analysis of ^{90}Sr and alpha-particle emitters on air filters and swipe samples using a liquid scintillation counters with alpha/beta discrimination. *Radioactivity and Radiochemistry* **9** (3): 25-40.

Cotton, F. A., Wilkinson, G. and Gaus, P. L. 1987. *Basic Inorganic Chemistry.* John Wiley and Sons. Canada: 697p.

Cowan, J. P., Hodge, V. F. and Folsom, T. R. 1977. Coprecipitation and electrodeposition of polonium from seawater. *Analytical Chemistry* **49**: 494-496.

Craig, H., Krishnaswami, S. and Somayajulu, B.L.K. 1973. ^{210}Pb-^{226}Ra: radioactive disequilibrium in the deep sea. *Earth and Planetary Science Letters* **17**: 295-305.

CRC Handbook of Chemistry and Physics, 69th Edition. 1988-89. F164.

Crompton, T. R. 1993. The analysis of natural waters, volume 2. *Direct Preconcentration Techniques.* Oxford University Press. Oxford: 249p.

Curie, M. and Debierne, A. 1910. C. R. Acad. Sci. Paris: 150: 386p.

Currie, L. A. 1968. Limits for qualitative detection and quantitative determination. *Analytical Chemistry* **40** (3): 586-593.

Dazhu, Y., Yongjun, Z. and Möbius, S. 1991. Rapid method for alpha counting with extractive scintillators and pulse shape analysis. *Journal of Radioanalytical and Nuclear Chemistry, Articles* **147** (1): 177-189.

DeFilippis, S. J. and Van Cauter, S. C. 1985. A novel approach to external standardisation in liquid scintillation counting. *Transactions of the American Nuclear Society* **50**: 22-23.

DeMaster, D. J., Kuehl, S. A. and Nittrouer, C. A. 1986. Effects of suspended sediments on geochemical processes near the mouth of the Amazon River: examination of biological silica uptake and the fate of particle-reactive elements. *Continental Shelf Research* **6**: 107-125.

Desideri, D., Guerra, F., Meli, M. A. and Testa, C. 1995. Determination of ^{210}Pb in sediments by extraction chromatography. *Journal of Radioanalytical and Nuclear Chemistry (Letters)* **200** (5): 385-396.

Dunne, J. P., Murray, J. W., Young, J., Balistrieri, L. S. and Bishop, J. 1997. ^{234}Th and particle cycling in the central equatorial Pacific. *Deep-Sea Research II* **44** (9): 2049-2083.

Ehinger, S. C., Pacer, R. A. and Romines, F.L. 1986. Separation of the radioelements ^{210}Pb-^{210}Bi-^{210}Po by spontaneous deposition onto noble metals and verification by liquid scintillation counting. *Journal of Radioanalytical and Nuclear Chemistry, Articles* **98** (1): 39-48.

Ehmann, W. D. and Vance, D. E. 1991. *Radiochemistry and Nuclear Methods of Analysis.* John Wiley and Sons. United States of America: 531p.

Erbacher, O. and Philip, K. 1928. Z. Physik, 51: 309.

Farris, J. P. and Buchanan, R. F. 1964. Anion exchange characteristics of elements in nitric acid medium. *Analytical Chemistry* **36** (6): 1157-1158.

Feldman. I. and Frisch. M. 1956. Precision plating of polonium. *Analytical Chemistry* **28**: 2024.

Figgins, P. E. 1961. *The Radiochemistry of Polonium.* NAS-NS 3037. Office of Technical Services, Department of Commerce, Washington, D.C: 68p.

Fleer, A. P. and Bacon, M. P. 1984. Determination of ^{210}Po and ^{210}Pb in seawater and particulate matter. *Nuclear Instruments and Methods in Physics Research* **223**: 243-249.

Flynn, W. W. 1968. The determination of low levels of ^{210}Po in environmental materials. *Analytica Chimica Acta* **43**: 221-227.

Francis, C. W., Chester, G. and Haskin, L. A. 1970. Determination of lead-210 mean residence time in the atmosphere. *Environmental Science and Technology* **4**: 586-589.

Friedrich, M. and Schönhoffer, F. 1996. ^{90}Sr in Austrian food after the Chernobyl accident. In: Cook, G. T., Harkness, D. D., McKenzie, A. B., Millar, B. F. and Scott, E. M., eds., *Advances in Liquid Scintillation Spectrometry, 1994.* Radiocarbon. Arizona: 141-148.

Gascoyne, M. 1992. Geochemistry of the actinides and their daughters. In: Ivanovitch, M. and Harmon, R. S., eds., *Uranium-series disequilibrium: Application to Earth, Marine and Environmental Sciences, 2nd ed.* Clarendon Press. Oxford: 34-61.

Gibbs, J. A., Everett, L. J. and Moore, D. 1976. *Sample Preparation for Liquid Scintillation Counting.* Packard Instrument Company. Connecticut: 69p.

Gilmore, G. and Hemmingway, J. D. 1995. *Practical Gamma Ray Spectrometry.* John Wiley and Sons. England: 314p.

Goutelard, F., Nazard, R., Bocquet, C., Coquenlorge, N., Letessier, P. and Calmet. D. 2000. Improvement in ^{90}Sr measurements at very low levels in environmental samples. *Applied Radiation and Isotopes* **53**: 145-151.

Hamilton-Taylor, J., Kelly, M., Mudge, S. and Bradshaw, K. 1987. Rapid remobilization of plutonium from estuarine sediments. *Journal of Environmental Radioactivity* **5**: 409-423.

Harada, K., Burnett, W. C., LaRock, P. A. and Cowart, J. B. 1989. Polonium in Florida groundwater and its possible relationship to the sulphur cycle and bacteria. *Geochimica et Cosmochimica Acta* **53**: 143-150.

Hayes, F. N. 1956. Liquid Scintillators: attributes and applications. *International Journal of Applied Radiation and Isotopes* **1**: 46-56.

Hogg, A. G. 1993. Performance and design of 0.3 ml to 10 ml synthetic silica liquid scintillation vials for low level ^{14}C determination. In: Noakes, J. E., Schönhofer, F. and Polach, H. A., eds., *Liquid Scintillation Spectrometry 1992*. Radiocarbon. Arizona: 135-142.

Holtzman, R. B. 1987. The determination of ^{210}Pb and ^{210}Po in biological and environmental materials. *Journal of Radioanalytical and Nuclear Chemistry, Articles* **115** (1): 59-70.

Horrocks, D. L. 1974. *Applications of Liquid Scintillation Counting.* Academic Press. New York: 346p.

Horrocks, D. L. 1976. Absolute disintegration rate pulse determination of beta-emitting radionuclides by pulse height-extrapolation method. In: Noujaim, A. A., Ediss, C. and Weibe, L. I., eds., *Liquid Scintillation Science and Technology*. Academic Press. New York: 185-198.

Horrocks, D. 1985. Studies of background sources in liquid scintillation counting. *International Journal of Applied Radiation and Isotopes* **36**: 609-617.

Horwitz, E. P., Chiariza, R. and Dietz, M. L. 1992. A novel strontium selective extraction chromatographic resin. *Solvent Extraction and Ion Exchange* **10** (2): 313-336

Huh, C. A., Zahnle, D. L. and Small, L. F. 1987. Budgets and behaviours of uranium and thorium series isotopes in Santa Monica Basin sediments. *Geochimica et Cosmochimica Acta* **51**: 1743-1754.

Hussain, N. and Krishnaswami, S. 1980. U-238 series radioactive disequilibrium in groundwaters: implications to the origin of excess U-234 and fate of reactive pollutants. *Geochimica et Cosmochimica Acta* **44**: 1287-1291.

Hussain, N. and Krishnaswami, S. 1982. The behaviour of short-lived radiogenic lead isotopes (^{214}Pb and ^{212}Pb) in groundwaters and laboratory leaching experiments. *Earth and Planetary Science Letters* **58**: 430-438.

Ishimori, I. T. 1955. Separation of RaD, RaE and RaF by ion exchange. *Bull. Chem. Soc. Japan* **28** (6): 432-435.

Jenson, M. L. and Bateman, A. M. 1979. *Economic Mineral Deposits.* 3rd Edition. John Wiley and Sons. New York: 351p.

Jeter, H. W. and Grob, B. 1994. Determination of radiostrontium in milk using an extraction chromatography column. *Radioactivity and Radiochemistry* **5** (3): 8-17.

Jia, G., Belli, M., Blasi, M., Marchetti, A., Rosamilia, S. and Sansone, U. 2000. ^{210}Pb and ^{210}Po determination in environmental samples. *Applied Radiation and Isotopes* **53**: 115-120.

Jiang, H., Lu, S., Fu, S., Zhang, T., Ye. Y., Li, M., Fu, P., Wang, S., Peng, C. and Jiang, P. 1983. Model DYS low level liquid scintillation counter. In:

McQuarrie, S. A., Ediss, C. and Wiebe, L. I., eds., *Advances in Scintillation Counting.* Alberta Press, University of Alberta: 478-493.

Joshi, L. U. and Ku, T. L. 1979. Measurement of ^{210}Pb from a sediment core off the coast of California. *Journal of Radioanalytical Chemistry* **52** (2): 329-334.

Joshi, S. R. 1987. Nondestructive determination of lead-210 and radium-226 by direct photon analysis. *Journal of Radioanalytical and Nuclear Chemistry, Articles* **116** (1): 169-182.

Kadko, D. 1980. ^{230}Th, ^{226}Ra and ^{222}Rn in abyssal sediments. *Earth and Planetary Science Letters* **49**: 360-380.

Kadko, D., Cochran, J. K. and Lyle, M. 1987. The effect of bioturbation and adsorption gradients on solid and dissolved radium profiles in sediments from the eastern equatorial Pacific. *Geochimica et Cosmochimica Acta* **51**: 1613-1623.

Kadko, D. 1993. Excess ^{210}Po and nutrient cycling within the California coastal transition zone. *Journal of Geophysical Research* **98**: 857- 864.

Kaihola, L. and Oikari, T. 1991. Some factors affecting the alpha particle detection in liquid scintillation spectrometry. In: Ross, H. H., Noakes, J. E. and Spaulding, J. D., eds., *Liquid Scintillation Counting and Organic Scintillators.* Lewis Publishers. Michigan: 211-218.

Keating, G. E., McCartney, M. and Davidson, C. M. 1996. Investigation of the technological enhancement of natural decay series radionuclides by the manufacture of phosphates on the Cumbrian coast. *Journal of Environmental Radioactivity* **32** (1): 53-56.

Kershaw, P. J. and Young, A. 1988. Scavenging of ^{234}Th in the eastern Irish Sea. *Journal of Environmental Radioactivity* **6**: 1-23.

Kessler, M. J., ed. 1989. *Liquid Scintillation Analysis. Science and Technology.* Packard Instrument Company. Connecticut: 178 p.

Kim, G., Hussain, N., Church, T. M. and Yang, H-S. 1999. A practical and accurate method for the determination of ^{234}Th simultaneously with ^{210}Po and ^{210}Pb in seawater. *Talanta* **49**: 851-858.

Kim, G., Hussain, N. and Church, T. M. 2000. Excess ^{210}Po in the coastal environment. *Tellus B* **52** (1): 74-80.

Kimura, K. and Ishimori, T. 1958. Some studies on the tracer chemistry of polonium. In: *Proceedings of the Second U.N. International Conference on Peaceful Uses of Atomic Energy*, Geneva, **28**: 151-153.

Koide, M., Soutar, A. and Goldberg, E. D. 1972. Marine geochronology with Pb-210. *Earth and Planetary Science Letters* **14**: 442-446.

Kraus, K. A. and Nelson, F. 1956. Anion exchange studies of the fission products. In: *Proceedings of the International Conference on Peaceful Uses of Atomic Energy*, Geneva **7:** 113-125.

Kraus, K. A. and Nelson, F. 1958. Symposium on Ion Exchange and Chromatography in Analytical Chemistry. ASTM special technical publication. **195:** 27-57.

Krishnaswami, S., Somayajulu, B. L. K. and Chung, Y. 1975. ^{210}Pb/^{226}Ra disequilibrium in the Santa Barbara Basin. *Earth and Planetary Science Letters* **27**: 388-392.

Ku, T-L., Knauss, K. G. and Mathieu, G. G. 1977. Uranium in open ocean: concentration and isotopic composition. *Deep-Sea Research* **24**: 1005-1017.

L'Annunziata, M. F. and Kessler, M. J. 1998 Radiotracer Liquid Scintillation Analysis. In: M. F. L'Annunziata., ed., *Handbook of Radioactivity Analysis.* Academic Press. London: 210-321.

Lederer, C. M. and Shirley, V. S., eds. 1978. *Table of Isotopes*, 7th ed. John Wiley and Sons. New York: 1599 p.

Livingston, H. D. and Bowen, V. G. 1977. Windscale effluents in the waters and sediments of the Minch. *Nature* **269**: 586-588.

MacKenzie, A. B. and Scott, R. D. 1979. Separation of bismuth-210 and polonium-210 from aqueous solutions by spontaneous adsorption on copper foils. *Analyst* **104**: 1151-1158.

McCartney, M., Kershaw, P. J. and Allington, D. J. 1990. The behaviour of ^{210}Pb and ^{226}Ra in the Eastern Irish Sea. *Journal of Environmental Radioactivity* **12**: 243-265.

McCarntney, M., Davidson, C, M., Howe, S. E. and Keating, G. E. 2000. Temporal Changes in the distribution of natural radionuclides along the Cumbrian coast following the reduction of discharges from a phosphoric acid production plant. *Journal of Environmental Radioactivity* **49**: 279-291.

McDowell, W. J. and Coleman, C. F. 1974. Combined solvent extraction-liquid scintillation method for radio-assay of alpha emitters. In: Proceedings of international solvent extraction conference. Society of Chemical Industry. London: 2123-2135.

McDowell, W. J., Bouwer, E. J., McKleeven, J. W. and Case, G. N. 1980. Application of the combined solvent extraction-high resolution liquid scintillation method to the determination of ^{230}Th and $^{234\text{-}238}$U in phosphotic materials. In: Peng, C. T., Horrocks, D. L. and Alpen, E. L., eds., *Liquid Scintillation Counting, Recent Applications and Developments.* Volume 1, physical aspects. Academic Press. New York: 333-346.

McDowell, W. J. and Case, G. N. 1986. A procedure for the determination of uranium on cellulose air sampling filters by photon-electron rejecting alpha liquid scintillation spectrometry. ORNL/TM 10175.

McDowell, W. J. 1986. Alpha counting and spectrometry using liquid scintillation methods. National Academy of Sciences-National Research Council: Nuclear Science series on Radiochemical Techniques. Oak Ridge, Tennessee. Technical Information Centre, Office of Scientific and Technical Information. US Department of Energy: 108p.

McDowell, W. J. and McDowell, B. L. 1991. Liquid Scintillation Alpha Spectrometry: a method for today and tomorrow. In: Ross, H. H., Noakes, J. E. and Spaulding, J. D., eds., *Liquid Scintillation Counting and Organic Scintillators.* Lewis Publishers. Michigan: 105-123.

McDowell, W. J. and McDowell, B. L. 1994. *Alpha Liquid Scintillation Spectrometry.* CRC Press. Florida: 184p.

McKinley, I. G., Baxter, M. S., Ellet, D. J. and Jack, W. 1981. Tracer application of radiocaesium in the Sea of the Hebrides. *Estuarine, Coastal and Shelf Science* **13**: 69-82.

McKlveen, J. W. and Johnson, W. R. 1975. Simultaneous alpha and beta particle assay using liquid scintillation counting with pulse shape discrimination. *Health Physics* **28**: 5-11.

McKlveen, J. W. and McDowell, W. J. 1984. Liquid scintillation alpha spectrometry techniques. *Nuclear Instrument and Methods in Physics Research* **223**: 372-376.

McMurray, J. 1992. *Organic Chemistry 3rd Edition.* Brooks Cole. California: 1212p.

Marckwald, W. 1905. Ber., 38: 591.

Möbius, S., Kamolchote, P. and Roeksbutr, W. 1993. Use of extractive scintillation and pulse shape analysis for environmental alpha assay. *The Science of the Total Environment* **130**: 467-471.

Momoshima, N., Takashima, Y., Koike, M., Imaizumi, Y. and Harada, T. 1994. Simultaneous determination of ^{210}Bi and ^{210}Po on pine needles by solvent extraction and liquid scintillation counting. *Journal of Radioanalytical and Nuclear Chemistry, Articles* **177** (2): 219-228.

Moore, H. E., Poet, S. E. and Martell, E. A. 1972. Lead-210, bismuth-210 and polonium-210 in the atmosphere: accurate ratio measurements and application to aerosol residence time determination. *Journal of Geophysical Research* **77**: 6515-6527.

Moore, W. S. 1969. Oceanic concentrations of ^{228}Ra. *Earth and Planetary Science Letters* **6**: 437-446.

Moore, W. S. 1976. Sampling radium-228 in the deep ocean. *Deep-Sea Research* **23**: 647-651.

Moore, W. S., Ku, T-L., MacDougall, J. D., Burns, V. M., Burns, R., Dymond, J., Lyle, M. W. and Piper, D. Z. 1981. Fluxes of metals to a manganese nodule: radiochemical, chemical structural and mineralogical studies. *Earth and Planetary Science Letters* **52**: 151-171.

Moore, W. S. and Dymond, J. 1988. Correlation of ^{210}Pb removal with organic carbon fluxes in the Pacific Ocean. *Nature* **331**: 339-341.

Murray, J. W., Young, J., Newton, J., Dunne, J. P., Chapin, T. and Paul, B. 1996. Export production determined using ^{234}Th/^{238}U disequilibria. *Deep-Sea Research II* **43**: 1095-1132.

Narita, H., Harada, K., Burnett, W. C., Tsunogai, S. and McCabe, W. J. 1989. Determination of ^{210}Pb, ^{210}Bi and ^{210}Po in natural waters and other materials by electrochemical separation. *Talanta* **36** (9): 925-929.

Nelson, F. and Kraus, K. A. 1954. Anion exchange studies. XI, Pb (II) and Bi (III) in chloride and nitrate solutions. *Journal of the American Chemical Society* **76**: 5916-5920.

Nelson, F., Murase, T. and Kraus, K. A. 1964. Ion exchange procedures 1. Cation exchange in concentrated HCl and $HClO_4$ solutions. *Journal of Chromatography* **13**: 501-535.

Nevissi, A. E. 1991. Measurement of lead-210, bismuth-210 and polonium-210, in environmental samples. *Journal of Radioanalytical and Nuclear Chemistry, Articles* **148** (1): 121-131.

Nibeck, J. I., Bares, S. L. and Williams, E. S. 1980. New scintillation cocktails in response to present and future trends in liquid scintillation counting. In: Peng, C. T., Horrocks, D. L. and Alpen, E. L., eds., *Liquid Scintillation Counting, Recent Applications and Developments.* Volume 1, Physical Aspects. Academic Press Inc. New York: 59-72.

Niven, S. E. H. and Moore, R. M. 1988. Effect of natural colloidal matter on the equilibrium adsorption of thorium in seawater. In: Guary, J. –C., Guegueniat, P. and Pentreath, R. J., eds., *Radionuclides: A Tool for Oceanography.* Elsevier Applied Science. Amsterdam: 111-120.

Noakes, J. E. and Valenta, P. J. 1996. The role of $Bi_4Ge_3O_{12}$ as an auxiliary scintillator for $\alpha/\beta/\gamma$ liquid scintillation counting and low level counting. In: Cook, G. T., Harkness, D. D., McKenzie, A. B., Millar, B. F. and Scott, E. M., eds., *Advances in Liquid Scintillation Spectrometry, 1994.* Radiocarbon Publishing. University of Arizona: 43-58

Nozaki, Y., Thomson, J. and Turekian, K. K. 1976. The distribution of ^{210}Pb and ^{210}Po in the surface waters of the Pacific Ocean. *Earth and Planetary Science Letters* **32**: 304-312

Nozaki, Y. and Tsunogai, S. 1976. ^{226}Ra, ^{210}Pb and ^{210}Po disequilibrium in the western North Pacific. *Earth and Planetary Science Letters* **32**: 313-321.

Nozaki, Y., Zhang, J. and Takeda, A. 1997. ^{210}Pb and ^{210}Po in the equatorial Pacific and the Bering Sea: the effects of biological productivity and boundary scavenging. *Deep-Sea Research II* **44** (9): 2203-2220.

Nozaki, Y., Dobashi, F., Kato, Y. and Yamamoto, Y. 1998. Distribution of Ra isotopes and the ^{210}Pb balance in the surface seawaters of the mid Northern Hemisphere. *Deep-Sea Research I* **45**: 1263-1284.

Oikari, T., Kojola, H., Nurmi, J. and Kaihola, L. 1987. Simultaneous counting of low alpha and beta particle activities with liquid scintillation spectrometry and pulse shape analysis. *Journal of Applied Radiation and Isotopes* **38**: 875-878.

Othman, I., Yassine, T. and Bhat, I. S. 1994. The measurement of some radionuclides in the marine coastal environment of Syria. *The Science of the Total Environment* **153**: 57-60.

Overnell, J., Harvey, S. M. and Parkes, R. J. 1996. A biogeochemical comparison of sea loch sediments. Manganese and iron contents, sulphate reduction and oxygen uptake rates. *Oceanographic Literature Review* **43** (11): 110-117.

Packard Instrument Company. 1996. Counting Solutions 5*: Counting aqueous samples by LSC*: PAN0091. USA

Pacer, R. A. 1983. The role of Cherenkov and liquid scintillation counting in evaluating the anion exchange separation of ^{210}Pb-^{210}Bi-^{210}Po. *Journal of Radioanalyitcal Chemistry* **77** (1): 19-28.

Passo Jr, C. J. and Kessler, M. J. 1992. *The Essentials of α/β Discrimination.* Packard Instrument Co. Connecticut: 24 p.

Passo Jr, C. J. and Cook, G. T. 1994. *Handbook of Environmental Liquid Scintillation Spectrometry. A Compilation of Theory and Methods.* Packard Instrument Co. Connecticut: 121 p.

Passo Jr, C. J. and Roberts, D. J. 1996. Expanded energy range for time-resolved liquid scintillation counting: an enhancement for programmable TR-LSC®. In: Cook, G. T., Harkness, D. D., MacKenzie, A. B., Millar, B. F. and Scott, E. M., eds., *Advances in Liquid Scintillation Spectrometry, 1994.* Radiocarbon Publishing. University of Arizona: 67-74.

Pates, J. M. *The Use Of Alpha Beta Liquid Scintillation Spectrometry In Marine Tracer Studies.* Ph.D thesis. University of Glasgow 1995.

Pates, J. M., Cook, G. T., MacKenzie, A. B., Anderson, R. and Bury, S. J. 1996. Determination of ^{234}Th in marine samples by liquid scintillation spectrometry. *Analytical Chemistry* **68**: 3783-3788.

Pates, J. M., Cook, G. T., MacKenzie, A. B. and Passo Jr, C. J. 1998. Implications of beta energy and quench level for alpha/beta liquid scintillation spectrometry calibration. *The Analyst* **123**: 2201-2207.

Peck, G. A. and Smith, J. D. 2000. Determination of ^{210}Po and ^{210}Pb in rainwater using measurement of ^{210}Po and ^{210}Bi. *Analytica Chimica Acta* **422**: 113-120.

Pentreath, R. J., Lovett, M. B., Jefferies, D. F., Woodhead, D. S., Talbot, J. W. and Mitchell, N. T. 1984. The impact on public radiation exposures of transuranium nuclides discharged in liquid wastes from fuel element reprocessing at Sellafield, UK. In: *Radioactive Waste Disposal*, Proceedings of an IAEA Conference, Seattle, Volume 5. IAEA. Vienna: 315-329.

Petrow, H. G., Nietzel, O. A. and DeDesa, M. A. 1960. Radiochemical determination of radium in uranium milling process samples. *Analytical Chemistry* **32**: 926-927.

Plummer, C. C. and McGeary, D. 1991. *Physical Geology 5th Edition.* WCB publishers. USA: 543p

Poet, S. E., Moore, H. E. and Martell, E. A. 1972. Tropospheric aerosol residence times indicated by radon and radon-daughter concentrations. In: Adams, J. A. S., Lowder, W. M. and Gessel, T. F., eds., *Natural Radiation Environment II.* US Energy Research and Development Administration. Washington D.C.: 775-786.

Polach, H., Gower, J. and Heinonen, A. 1983. An ideal vial and cocktail for low-level scintillation counting. In: McQuarrie, S. A., Ediss, C., and Wielbe, L. I., eds., *Advances in Scintillation Counting.* University of Alberta. Canada: 508-525.

Polach, H., Calf, G., Harkness, D., Hogg, A., Kaihole, L. and Robertson, S. 1988. Performance of new technology liquid scintillation counters for ^{14}C dating. *Nuclear Geophysics* **2** (2): 75-79.

Poole, A.J., Allington, D. J. and Denoon, D.C. 1995(a). Temporal and spatial survey of dissolved ^{226}Ra in coastal waters of the eastern Irish Sea. *The Science of the Total Environment* **168**: 233-247.

Poole, A. J., Allington, D. J., Baxter, A. J. and Young, A. K. 1995(b). The natural radioactivity of phosphate ore and associated waste products discharged in into the eastern Irish Sea from a phosphoric acid production plant. *The Science of the Total Environment* **173**: 137-149.

Radakovitch, O., Cherry, R. D., Heyraud, M. and Heussner, S. 1998. Unusual $^{210}Po/^{210}Pb$ ratios in the surface water of the Gulf of Lions. *Oceanologica Acta* **21** (3): 459-468.

Radakovitch, O., Cherry, R. D. and Heyraud, M. 1999. ^{210}Pb and ^{210}Po: tracers of particle transfer on the Rhône continental margin (NW Mediterranean). *Deep-Sea Research I* **46** (9): 1539-1563.

Radioactivity in Food and the Environment. 1999. (RIFE –5) Food Standards Agency and Scottish Environmental Protection Agency. London.

Rama, M., Koide, M. and Goldberg, E. D. 1961. Lead-210 in natural waters. *Science* **134**: 98-99.

Rapkin, E. 1970. Development of the modern liquid scintillation counter. In: Bransome, E. D., ed., *The Current State of Liquid Scintillation Counting.* Grune and Stratton. New York: 45p

Ridgeway, I. M. and Price, N. B. 1987. Geochemical associations and post-depositional mobility of heavy metals in coastal sediments: Loch Etive, Scotland. *Marine Chemistry* **21**: 229-248.

Ritchie, G. D. and Shimmield, G. B. 1991. The use of ^{210}Pb/^{210}Po disequilibria in the study of the fate of marine particulate matter. In: Kershaw, P. J and Woodhead, D. S., eds,. *Radionuclides in the Study of Marine Processes.* Elsevier Applied Science. UK: 142-153.

Robbins, J. A. and Edington, D. N. 1975. Determination of recent sedimentation rates in Lake Michigan using ^{210}Pb and ^{137}Cs. *Geochimica et Cosmochimica Acta* **39**: 285-304.

Roodenberg, S., Kroondijk, R. and Verhuel, H. 1972. Cerenkov radiation in photomultiplier windows and the resulting time shift in delayed coincidence time spectra. *Nuclear Instruments and Methods in Physics Research* **105**: 551-555.

Ryan, T. P., Mitchell, P. I., Vives i Battle, J., Sanchez-Cabeza, J. A., McGarry, A. T. and Schell, W. R. 1993. Low-level ^{241}Pu analysis by supported-disk liquid scintillation counting. In: Noakes, J. E., Schönhofer, F. and Polach, H. A., eds., *Liquid Scintillation Spectrometry 1992.* Radiocarbon. Arizona: 75-82.

Saito, N. 1984. Selected data on ion exchange separations in radioanalytical radiochemistry. *Pure and Applied Chemistry* **56** (4): 523-539.

Saito, R. T. and Cunha, I. I. L. 1997. Analysis of ^{210}Po in marine samples. *Journal of Radioanalytical and Nuclear Chemistry* **220** (1): 117-119.

Sanchez-Cabeza, J. A. and Pujol, L. 1996. Gross alpha and beta activities in natural waters using low- background liquid scintillation: Study of the Ebro river (Spain). In: Cook, G. T., Harkness, D. D., MacKenzie, A. B., Millar, B. F. and Scott, E. M., eds., *Advances in Liquid Scintillation Spectrometry, 1994.* Radiocarbon Publishing. University of Arizona: 307-316.

Sanchez-Cabeza, J. A., Masque, P., Martinez-Alfonzo, M., Mir, J. and Esteve, I. 1999. ^{210}Pb atmospheric flux and growth rates of a microbial mat from the northwestern Mediterranean Sea (Ebro River delta). *Environmental Science and Technology* **33**: 3711-3715.

Sarin, M. M., Bhushan, R., Rengarajan, R. and Yadav, D. N. 1992. Simultaneous determination of ^{238}U series nuclides in waters of Arabian Sea and Bay of Bengal. *Indian Journal of Marine Science* **21**: 121-127.

Sarin, M. M., Krishnaswami, S., Ramesh, R. and Somayajula, B. L. K. 1994. ^{238}U decay series nuclides in the northeastern Arabian Sea: scavenging rate and cycling processes. *Continental Shelf Research* **14**: 251-265.

Sarin, M. M., Kim, G. and Church, T. M. 1999. ^{210}Po and ^{210}Pb in the South-equatorial Atlantic: distribution and disequilibrium in the upper 500 m. *Deep-Sea Research II* **46** (5): 907-917.

Schell, W. R. 1977. Concentrations and physico-chemical states and mean residence times of ^{210}Pb and ^{210}Po in marine and estuarine waters. *Geochimica et Cosmochimica Acta* **41**: 1019-1031.

Senior, J. E. 1998. *Marie and Pierre Curie.* Sutton Publishing. Channel Islands: 117p.

Shannon, L. V., Cherry, R. D. and Orren, M. J. 1970. Polonium-210 and lead-210 in the marine environment. *Geochimica et Cosmochimica Acta* **34**: 701-711.

Shannon, L. V. and Orren, M. J. 1970. A rapid method for the determination of polonium-210 and lead-210 in seawater. *Analytica Chimica Acta* **52**: 166-169.

Shaw, P. G. 1991. Rapid determination of Pu content on filters and smears using alpha liquid scintillation. In: Ross, H., Noakes, J. E. and Spaulding, J. D., eds., *Liquid Scintillation Counting and Organic Scintillators.* Lewis Publishers. Michigan: 435-457.

Shimmield, G. B., Ritchie, G. D. and Fileman, T. W. 1995. The impact of marginal ice zone processes on the distribution of ^{210}Pb, ^{210}Po and ^{234}Th and implications for new production in the Bellinghausen Sea, Antarctica. *Deep-Sea Research II* **42**: 1313-1335.

Shimmield, T. M. 1993. *A Study of Radionuclides, Lead and Lead Isotopes Ratios in Scottish Loch Sediments.* PhD thesis. University of Edinburgh.

Sholkovitz, E. R., Cochran, J. K. and Carey, A. E. 1983. Laboratory studies of the diagenesis and mobility of $^{239,240}Pu$ and ^{137}Cs in nearshore sediments. *Geochimica et Cosmochimica Acta* **47**: 1369-1379.

Sill, S. W. and Willis, C. P. 1965. Preparation and use of Lead-212 tracer. *Analytical Chemistry* **37** (9): 1176-1178.

Skwarzec, B. 1997. Radiochemical methods for the determination of polonium, radiolead, uranium and plutonium in environmental samples. *Chimica Analyticzna* **42**:107-115.

Smith, J. N. and Ellis, K. M. 1995. Radionuclide tracer profiles at the CESAR ice station and Canadian Ice Island in the western Arctic Ocean. *Deep-Sea Research II* **42** (6): 1449-1470.

Smith, J. N. 2001. Why should we believe ^{210}Pb sediment geochronologies. Journal of Environmental Radioactivity **55**: 121-123.

Smoak, J. M., DeMaster, D. J., Kuehl, S. A., Pope, R. H. and McKee, B. A. 1996. The behaviour of particle-reactive tracers in a high turbidity environment: ^{234}Th and ^{210}Pb on the Amazon continental shelf. *Geochimica et Cosmochimica Acta* **60** (12): 2123-2137.

Spencer, D. W., Bacon, M. P. and Brewer, P. G. 1981. Models of the distribution of ^{210}Pb in a section across the North Equatorial Atlantic Ocean. *Journal of Marine Research* **39**: 119-138.

Spinks, J. W. T. and Woods, R.J. 1964. *An Introduction to Radiation Chemistry.* John Wiley and Sons. London: 477p.

Stavrakakis, S., Chronis, G., Tselepides, A., Heussner, S., Monaco, A. and Abassi, A. 2000. Downward fluxes of settling particles in the deep Cretan Sea (NE Mediterranean). *Processes in Oceanography* **46**: 217-240.

Swan, D. S., Baxter, M. S., McInley, I. G. and Jack W. 1982. Radiocaesium and ^{210}Pb in Clyde Loch Sediments. *Coastal and Shelf Science* **15**: 515-536.

Swank, R. K., Buck, W. L., Hayes, F. N. and Ott, D. G. 1958. Comparison of scintillator solvents by relative photon yield. *Review of Scientific Instruments* 29: 279-285.

Swarzenski, P. W., McKee, B. A., Sørensen, K. and Todd, J. F. 1999. ^{210}Pb and ^{210}Po, manganese and iron cycling across the O_2/H_2S interface of a permanently anoxic fjord: Framvaren, Norway. *Marine Chemistry* **67**: 199-217.

Talbot, R. W. and Andren, A. W. 1984. Seasonal variations of ^{210}Pb and ^{210}Po concentrations in an oligotrophic lake. *Geochimica et Cosmochimica Acta* **48**: 2053-2063.

Tanaka, N., Takeda, Y. and Tsunogai, S. 1983. Biological effect of removal on ^{234}Th, ^{210}Po and ^{210}Pb from the surface water in Funka Bay, Japan. *Geochimica et Cosmochimica Acta* **47**: 1783-1790.

Thomson, J. and Turekian, K. K. 1976. ^{210}Po and ^{210}Pb distributions in the ocean water profiles from the Eastern South Pacific. *Earth and Planetary Science Letters* **32**: 297-303.

Thomson, J. 1991. Di-isopropylnaphthalene- a new solvent for liquid scintillation counting. In: Ross, H. H., Noakes, J. E. and Spaulding, J.D., eds., *Liquid Scintillation Counting and Organic Scintillators.* Lewis Publishers. Michigan: 19-34.

Thomson, J., Colley, S., Anderson, R., Cook, G. T., MacKenzie, A. B. and Harkness, D. D. 1993(a). Holocene sediment fluxes in the Northeast Atlantic Ocean from ^{230}Th excess and radiocarbon measurements. *Palaeoceanography* **8**: 631-650.

Thomson, J., Colley, S., Anderson, R., Cook, G. T. and MacKenzie, A. B. 1993(b). ^{210}Pb in the sediments and water column of the Northeast Atlantic from 47 to 59°N along 20°W. *Earth and Planetary Science Letters* **115**: 75-87.

Thorngate, J. H., McDowell, W. J. and Christian, D. J. 1974. An application of pulse shape discrimination to liquid scintillation counting. *Health Physics* **27**: 123-126.

Turekian, K. K., Kharkar, D. P. and Thomson, J. 1974. The fate of ^{210}Pb and ^{210}Po in the ocean surface. *Journal of Atmospheric Research* **8**: 639-649.

Turekian, K. K. and Nozaki, Y. 1980. ^{210}Po and ^{210}Pb in the eastern South Pacific-the role of upwelling on their distributions in the water column. In: *Isotope Marine Chemistry*: 157-164.

Vadja, N., LaRosa, J., Zeisler, R., Danesi, P. and Kis-Benedek, Gy. 1997. A novel technique for the simultaneous determination of ^{210}Pb and ^{210}Po using a crown ether. *Journal of Environmental Radioactivity* **37** (3): 355-372.

Van Cauter, S. 1986. Three dimensional spectrum analysis: a new approach to reduce background of liquid scintillation counters. Application Bulletin 006. Packard Instrument Co. Illinois: 8p.

Van Den Winkel, P., De Corte, F. and Hoste, J. 1972. Distribution coefficients for 65 elements in acetic acid medium on Dowex 1X8. *Journal of Radioanalytical Chemistry* **10**: 139-143.

Van Loon, G. W. and Duffy, S. J. 2000. Environmental Chemistry: A global perspective. Oxford University Press. Bath: 669p.

Vladimirova, M. V. 1998. Centennial anniversary of discovery of polonium. *Radiochemistry* **40** (4): 299-301.

Wallner, G. and Irlweck, K. 1997. Determination of Lead-210 and its progenies in aerosol fractions of different particles sizes. *Radiochemica Acta* **78**: 173-176.

Wallner, G. 1998. ^{210}Pb and its progenies in phosphoric acid: Significance for low level determinations using liquid scintillation counting with extractive

cocktails. *Journal of Radioanalytical and Nuclear Chemistry* **227** (1): 121-122.

Wallner, G. 1997. Simultaneous determination of ^{210}Pb and ^{212}Pb progenies by liquid scintillation counting. *Applied Radiation and Isotopes* **48** (4): 511-514.

Wei, C.-L. and Murray, J. W. 1994. The behaviour of scavenged isotopes in marine anoxic environments: ^{210}Pb and ^{210}Po in the water column of the Black Sea. *Geochimica et Cosmochimica Acta* **58** (7): 1795-1811.

Wildgust, M. A., McDonald, P. and White, K. N. 1998. Temporal changes of ^{210}Po in temperate coastal waters. *The Science of the Total Environment* **214**: 1-10.

Williams, T. M., MacKenzie, A. B., Scott, R. D., Price, N. B. and Ridgway, I. M. 1988. Radionuclide distributions in the surface sediments of Loch Etive. In: Guary, J. –C., Guegueniat, P. and Pentreath, R. J., eds., *Radionuclides: A Tool for Oceanography*. Elsevier Applied Science. Amsterdam: 340-350.

White, J. C. and Ross, W. J. 1961. Separations by solvent extraction with Tri-n-octylphosphine oxide. NAS-NS 3102, National Academy of Sciences, National Research Council: 56p.

Wu, J. and Boyle, E. A. 1997. Lead in the western North Atlantic Ocean: Completed response to leaded gasoline phaseout. *Geochimica et Cosmochimica Acta* **61** (15): 3279-3283.

Young, S. A. 1996. *A Radionuclide Tracer Study Of Heavy Metal Cycling In Loch Etive, Scotland.* PhD thesis. University of Edinburgh.

Zuo, Z. Z. and Eisma, D. 1993. ^{210}Pb and ^{210}Po distributions and disequilibrium in the coastal and shelf waters of the Southern North Sea. *Continental Shelf Research* **13** (8): 999-1022.